Aston University

Some pages of this thesis may have been removed for copyright restrictions.

If you have discovered material in AURA which is unlawful e.g. breaches copyright, (either yours or that of a third party) or any other law, including but not limited to those relating to patent, trademark, confidentiality, data protection, obscenity, defamation, libel, then please read our Takedown Policy and contact the service immediately

Effect of Pulsed Current on the Electrodeposition of Chromium and Copper.

Trevor Pearson.

Doctor of Philosophy.

The University of Aston in Birmingham.

November 1989.

This copy of the thesis has been supplied on condition that anyone who consults it is understood to recognise that its copywright rests with the author and that no quotation from the thesis and no information derived from it may be published without the author's prior, written consent.

The University of Aston in Birmingham.
Thesis Summary.

Title: Effect of Pulsed Current on the Electrodeposition of Chromium and Copper.
Author: Trevor Pearson.
Degree: Doctor of Philosophy (Ph.D.)
Date: November, 1989.

This research was concerned with the effects of pulsed current on the electrodeposition of chromium and copper. In the case of the latter metal, a novel application has been studied and a theory proposed for the ability to improve throwing power by the joint use of organic additives and pulsed reverse current. During the course of the research, several improvements were made to the pulse plating unit.

Chromium.

A study was made of the effect of square wave pulsed current on various physical properties of deposits from three hard chromium plating electrolytes. The effect of varying frequency at a duty cycle of 50% on the mean bulk internal stress, visual appearance, hardness, crack characteristics and surface topography of the electrodeposits was determined. X-ray diffraction techniques were used to study the phases present in the deposits. The effect of varying frequency on the cathodic efficiencies of the electrolytes was also determined.

It was found that pulsed current reduced the internal stress of deposits from the sulphate catalysed electrolyte. It also reduced or eliminated cracking of deposits and reduced deposit brightness. Under certain conditions, pulsed current was found to induce the co-deposition of hydrides of chromium. Deposit hardness was found to be reduced by the use of pulsed current. Cathodic efficiencies of the high efficiency electrolytes were reduced by the use of pulsed current although this effect was minimised at high frequencies. The sulphate catalysed electrolyte showed an increase in efficiency over the frequency range where hydrides were co-deposited.

Copper.

The polarisation behaviour of acid copper solutions containing polyethers, sulphopropyl sulphides and chloride ions was studied using both direct and pulse reverse current. The effect of these additives on the rest potentials of copper deposits immersed in the electrolyte was also studied. Hole Throwing Power on printed circuit boards was determined using a specially designed test cell. The effect of pulsed reverse current on the hole throwing power of commercially produced printed circuit boards was also studied.

Polyethers were found to have an inhibiting effect on the deposition of copper whereas the sulphopropyl sulphides produced a stimulating (i.e. depolarising) effect. Studies of rest potentials made when both additives were present indicated that the sulphopropyl sulphide was preferentially adsorbed.The use of pulsed reverse current with solutions containing both polyether and sulphopropyl sulphide was found to cause desorption of the sulphopropyl sulphide at the cathode surface. Thus, at higher current densities, the inhibiting effect of the polyether produced an increase in the cathodic polarisation potential. At lower current densities, the depolarisation effect of the sulphopropyl sulphide could still occur. On printed circuit boards, this effect was found to produce an increase in the "hole throwing power" due to depolarisation of the holes relative to the surface of the boards. Typically, using direct current, hole/surface thickness ratios of 40% were obtained when plating 0.6 mm holes in a 3.2 mm thick board at a current density of 3 A/dm^2 whereas using pulsed reverse current, ratios of 80% could be obtained at an equivalent rate of deposition. This was observed both in laboratory tests and on commercially plated boards.

Keywords : Pulse Plating, Chromium Plating, Printed Circuits, Organic Additives, Copper Plating.

Acknowledgements.

I would like to thank the University of Aston for providing a studentship and financial support for the research work undertaken in this thesis. Also thanks to J.C.T. Controls Ltd. for additional financial support, supplying the pulse plating hardware and providing the commercial results reported in the thesis.

I would also like to thank Mr. S.J. Wake and W.Canning Ltd. for the supply of the commercial chromium plating electrolytes, the organosulphur compounds used as additives in the acid copper electrolytes and the use of their polarograph.

Thanks also to my supervisor, Dr. J.K. Dennis for his valuable guidance and assistance and to Mr. J. Foden for his advice and help with metallographic preparation. Additionally, thanks to Mr. R.Howell for his assistance with the electron microscopy and to Dr. M. Durman for his assistance with preparation of samples for T.E.M.

Finally, I would like to thank my wife, Judith for her tolerance and support during the preparation of this thesis.

List of Contents.

		Page
	Title Page.	1
	Thesis Summary.	2
	Acknowledgements.	3
	List of Contents.	4
	List of Tables.	13
	List of Figures.	15
	List of Symbols.	23
Chapter 1.	Introduction.	25
Chapter 2.	The Theory of the Application of Pulsed Current.	29
2.1.	The Characterisation of Pulsed Current Waveforms.	29
2.1.1.	Characterisation of Pulsed Current.	31
	i. Duty Cycle.	
	ii. Average Current Density.	
	iii. Frequency.	
2.1.2.	Characterisation of Pulsed Reverse Current.	32
2.2.	The Effect of Charge and Discharge of the Double Layer.	33
2.2.1.	Calculation of Charge and Discharge Times for Unipolar Pulses.	37
	i. Calculation of Charge Time for the Double Layer.	
	ii. Calculation of Discharge Time for the Double Layer.	
2.2.2.	Calculation of Degree of Flattening.	41
2.3.	Mass Transport in Pulse Plating.	44
2.3.1.	Mass Transport in Non Steady State Diffusion.	46
2.3.2.	Practical Aspects of Mass Transport in Pulse Plating.	52
	i. The Effect of Pulsed Current on the Maximum Practical Current Density.	
	ii. The Effect of Pulsed Current on Current Efficiency.	
	iii. The Effect of Pulsed Current on the Throwing Power of Electrolytes.	

2.4.	Current Distribution in Pulse Plating.	55
	i. Primary Current Distribution.	
	ii. Secondary Current Distribution.	
	iii. Tertiary Current Distribution.	
2.4.1.	The Effect of Pulsed Current on the Primary Current Distribution.	56
2.4.2.	The Effect of Pulsed Current on the Secondary Current Distribution.	57
2.4.3.	The Effect of Pulsed Current on the Tertiary Current Distribution.	59
2.4.4.	Current Distribution Using Pulse Reverse Current.	63
2.5.	The Effect of Pulsed Current on Electrocrystallisation.	63
2.5.1.	The Effect of Pulsed Current on the Deposit Grain Size.	64
2.5.2.	The Effect of the Off Time on Deposit Grain Size.	65
Chapter 3.	**The Effect of Pulsed Current on the Properties of Electrodeposited Metals.**	66
3.1.	Electrochemical Properties.	66
3.1.1.	Effect of Pulsed Current on Power Consumption.	66
3.1.2.	Effect of Pulsed Current on Deposit Metal Distribution.	67
3.2.	Physical Properties of Metals Deposited by Pulsed Current.	68
3.2.1.	The Effect of Pulsed Current on the Porosity of Deposits.	68
	i. Bulk Porosity.	
	ii. Transverse Porosity.	
3.2.2.	The Effect of Pulsed current on the Incorporation of Impurities.	69
	i. Inclusion of Hydrogen.	
	ii. Inclusion of Organic Impurities.	
3.2.3.	Effect of Pulsed Current on Grain Size and Deposit Morphology.	73
	i. Grain Size.	
	ii. Deposit Morphology.	
3.2.4.	The Effect of Pulsed Current on the Hardness of Electrodeposits.	77

3.2.5. The Effect of Pulsed current on the Ductility and Internal Stress of Deposits. 80
i. Ductility.
ii. Internal Stress.
3.2.6. The Effect of Pulsed Current on the Properties of Electrodeposited Alloys. 86

Chapter 4. The Electrodeposition of Chromium. 88

4.1. Introduction. 88

4.2. The Mechanism of Chromium Plating. 90

4.3. Operating Parameters for the Deposition of Chromium. 91
4.3.1. Electrolyte Constituents. 91
4.3.2. Operating Conditions. 93
i. Chromic Acid Concentration and Catalyst Ratio.
ii. Temperature and Current Density.

4.4. Physical Properties of Electrodeposited Chromium. 95

4.5. The Effect of Pulsed Current on Electrodeposited Chromium. 96
4.5.1. The Effect of Pulsed Current on the Hydrogen Content of Chromium Deposits. 97
4.5.2. The Effect of Pulsed Current on Crack Formation and Visual Appearance of Chromium Deposits. 99
4.5.3. The Effect of Pulsed Current on the Cathodic Efficiency of Chromium Plating Electrolytes. 100
4.5.4. The Effect of Pulsed Current on the Corrosion Resistance, Wear Resistance and Fatigue Properties of Hard Chromium Deposits. 101

Chapter 5. The Electrodeposition of Copper From Acidic Electrolytes. 103

5.1. Introduction. 103
5.2. The Mechanism of Deposition from the Acid Copper Electrolyte. 105
5.2.1. Electrochemical Reduction of the Cupric Ion. 105
5.2.2. Anodic Reactions. 106
5.2.3. Conductivity, Cathodic Polarisation and Throwing Power. 107
5.2.4. Current Density and Temperature. 108
5.2.5. Addition Agents. 109

5.3. The Structure and Properties of Electrodeposited Copper. 110
5.3.1. Grain Structure of Electrodeposited Copper from Acidic Electrolytes. 111

5.4. The Effect of Pulsed Current on Electrodeposited Copper from Acidic Electrolytes. 112
5.4.1. The Effect of Pulsed Current on the Efficiency of Copper Deposition from the Acid Copper Electrolyte. 112
5.4.2. The Effect of Pulsed Current on the Throwing Power of Acid Copper Electrolytes. 114
5.4.3. The Effect of Pulsed Current on the Structure and Properties of Copper Deposits. 116

Chapter 6. Selection of Pulse Parameters for Experimental Work. 117

6.1. Introduction 117

6.2. A Computer Model of Degree of Flattening. 117

6.3. Selection of Duty Cycle. 128

6.4. Selection of Pulse Parameters for Pulsed Reverse Current 129

Chapter 7. Experimental Procedure. 131

7.1. Introduction. 131

7.2. Pulse Plating Equipment. 132

7.3. Selection of Plating Electrolytes. 133
7.3.1. Electrolytes for the Deposition of Chromium. 133
7.3.2. Electrolytes for the Deposition of Copper. 134

7.4. Pretreatment. 136

7.5. Measurement of Internal Stress. 137

7.6. Determination of Electrolyte Covering Power. 141

7.7. Determination of Deposit Thickness. 142
7.7.1. Determination of Thickness by Microsection. 142
7.7.2. Determination of Thickness by Coulometric Methods. 142

7.8. Determination of Throwing Power. 143
7.8.1. Determination of Macro Throwing Power. 143
7.8.2. Determination of "Hole Throwing Power". 144

7.9. Determination of Cathodic Efficiency. 148

7.10. Determination of Cathode Potential. 149

7.11. Potentiodynamic Scans. 151

7.12. Polarographic Studies. 153

7.13. Hardness Testing. 154

7.14. Microscopy. 154
7.14.1. Surface Examination. 154
7.14.2. Examination of Grain Structure. 155

7.15.	X-Ray Diffraction Studies.	156
7.16.	Determination of Sulphur Incorporation in Copper Deposits.	157
Chapter 8.	**Experimental Results - Chromium.**	158
8.1.	Coating Properties.	158
8.1.1.	Hardness of Coatings.	158
8.1.2.	Internal Stress of Deposits.	159
8.1.3.	Visual Appearance, Crack Formation and Surface Topography of Deposits.	162
8.1.3.1.	Visual Appearance.	162
8.1.3.2.	Crack Characteristics of Deposits.	163
8.1.3.3.	Surface Topography of the Deposits.	164
8.1.4.	Anodic Behaviour of the Coatings.	169
8.1.5.	Composition and Orientation of Deposits.	172
8.2.	Electrochemical Properties.	179
8.2.1.	Cathodic Efficiencies.	179
8.2.2.	Covering Power.	180
Chapter 9.	**Discussion of Results - Chromium.**	182
9.1.	Hardness and Internal Stress.	182
9.2.	Crack Formation and Anodic Behaviour.	184
9.3.	Deposit Composition.	186
9.4.	Cathodic Efficiency.	188
9.5.	Covering Power.	190
Chapter 10.	**Conclusions - Chromium.**	192

Chapter 11. Experimental Results - Copper. 194

11.1 Results of Polarisation Studies. 194

11.1.1. The Effect of Direct and Pulsed Reverse Current on Electrodeposition from the Base Electrolyte. 194

11.1.2. The Effect of Direct and Pulsed Reverse Current on Electrodeposition from Electrolytes Containing Single Additives. 194

11.1.3. The Effect of Direct and Pulsed Reverse Current on Electrodeposition from Electrolytes Containing Sulphopropyl Sulphides and Polyether in Combination. 197

11.1.4. The Effect of Varying Polyether Concentration on Electrolyte Polarisation Characteristics. 201

11.1.5. The Effect of Direct and Pulsed Reverse Current on Electrolyte Polarisation Characteristics: Electrolyte Containing Polyether Plus Varying Concentration of MPS. 202

11.1.6. The Effect of Polyether Molecular Weight on the Polarisation Characteristics with Direct and Pulsed Reverse Current. 203

11.2. Results of Rest Potential Studies. 206

11.3. Throwing Power Studies. 209

11.4. Metal Distribution on Boards Produced Under Commercial Conditions. 215

11.5. Surface Topography Studies. 218

11.6. Transmission Electron Microscope Studies. 223

11.7. Hardness Values. 227

11.8. Polarographic Studies. 228

Chapter 12. Discussion of Results - Copper. 229

12.1. Introduction. 229

12.2. The Effect of Pulsed Reverse Current on an Additive Free Acid Copper Electrolyte. 229

12.3. Factors Affecting the Incorporation of Organic Additives in Deposits Plated from Acid Copper Electrolytes. 231
12.3.1. Adsorption of Polyether Molecules. 232
12.3.2. Adsorption of Sulphopropyl Sulphides. 234
12.3.3. Adsorption of Chloride Ions. 237

12.4. The Effect of Pulsed Reverse Current on the Adsorption of Organic Additives. 237
12.4.1. The Effect of Pulsed Reverse Current on the Adsorption of Polyethers. 237
12.4.2. The Effect of Pulsed Reverse Current on the Adsorption of Sulphopropyl Sulphides. 238

12.5. The Effect of Additives on the Structure of Deposits. 241

12.6. Factors Affecting the Chemical Stability of Additives in Acid Copper Electrolytes. 242
12.6.1. The Sulphopropyl Sulphides. 242
12.6.2. The Polyethers. 244

Chapter 13. Conclusions - Copper. 245

Chapter 14. Concluding Comments on General Aspects of Deposition by Pulsed Current. 249

14.1. Introduction. 249

14.2 Effect of Pulsed Current on Current Density Distribution. 249

14.3. Effect of Pulsed Current on Maximum Rate of Deposition. 250

14.4. Effect of Pulsed Current on Power Consumption. 251

14.5. Effect of Pulsed Current on Deposit Properties. 251

14.6. Other Aspects of Deposition with Pulsed Current. 252

Chapter 15. Suggestions for Further Work. 253

15.1. Chromium. 253

15.2. Copper. 254

15.3. Other Work. 255

References 256

List of Tables.

		Page
Table 1.	Effect of Pulsed Reverse Current on the Microhardness of Nickel Deposits from an All Chloride Electrolyte. (After Kendrick et. al. [79]).	79
Table 2.	Effect of Pulsed Current on the Hardness of Deposits from a Gold-Cobalt Alloy Electrolyte. (After Knodler. [67]).	80
Table 3.	Operating Conditions for Various Chromium Plating Processes. (After Dennis and Such. [101]).	94
Table 4.	Hydrogen Contents of Chromium Deposits. (After Knodler [61]).	97
Table 5.	Efficiency of Sulphate Catalysed Electrolyte with Pulsed Current. (After Nesnidal. [118]).	100
Table 6.	Typical Formulations for Acid Copper Electrolytes.	108
Table 7.	Program to Calculate Charge Parameters.	118
Table 8.	Computer Calculated Charge and Discharge Parameters for Various Duty Cycles.	121
Table 9.	Comparison of Methods of Calculation of Degree of Flattening.	124
Table 10.	Pulse Conditions used on the Commercial Test Boards. (Average Current Density 3 A/dm^2)	147
Table 11.	Effect of Frequency on the Hardness of Deposits Obtained from Three Different Chromium Electrolytes.	159
Table 12.	The Effect of Varying Frequency on the Visual Appearance of Three Different Chromium Deposits.	163

Table 13.	The Effect of Varying Frequency on the Crack Characteristics of Deposits from Three Different Electrolytes	163
Table 14.	Expected Diffraction Angles for Chromium Phases using Copper Kα Radiation.	174
Table 15.	The Effect of Varying Frequency on the Phases Present in Deposits from Three Different Chromium Electrolytes	174
Table 16.	The Effect of Varying Frequency on the Cathodic Efficiencies of Three Different Chromium Plating Electrolytes.	179
Table 17.	The Effect of Varying Frequency on the Covering Power of Three Different Chromium Plating Electrolytes on a Brass Substrate.	181
Table 18.	The Effect of Additions of Polyether on Rest Potentials and Exchange Current Densities.	206
Table 19.	The Effect of Sulphopropyl Sulphides on Rest Potentials and Exchange Current Densities.	207
Table 20.	The Effect of Combined Additives on Rest Potentials and Exchange Current Densities.	208
Table 21.	Hole/Land Thickness Ratios 10ms Cathodic, 2ms Anodic	212
Table 22.	Hardness of Copper Deposits.	227

List of Figures.

Figure 1.	Characterisation of Pulsed Current Waveforms. (After Puippe.(2)).	30
Figure 2.	Representation of the Equivalent Circuit of an Electrode.	35
Figure 3.	Illustration of the Smoothing Effect of the Double Layer Capacitance. (After Puippe. (4)).	36
Figure 4.	Illustration of Current Recovery at the end of a Pulse. (After Puippe. (4)).	37
Figure 5.	Plot of Degree of Flattening against Ratio of On Time : Charge Time. (After Puippe. (4)).	42
Figure 6.	a) Mass Transport to a Sawtooth Profile. - Macroprofile. b) Mass Transport to a Sawtooth Profile. - Microprofile.	60
Figure 7.	Hardness vs. Pulse Current Density of Nickel Deposited from a Watt's Electrolyte (After Sutter. et al. (78)).	78
Figure 8.	Hardness vs. Pulse Current Density of Nickel Deposited from a Sulphamate Electrolyte (After Sutter. et al. (78))	78
Figure 9.	Mean Internal Stress vs Duty Cycle at Two Different Frequencies of Nickel Deposited from Watts Electrolyte.	83
Figure 10.	Internal Stress of D.C. and P.C. Plated Gold/Cobalt and Gold/Nickel Alloy Deposits vs. Temperature. (After Knodler.(67)).	85
Figure 11.	Current Efficiency vs Various Pulse Parameters for an Acid Copper Electrolyte. (After Cheh et al. (145)).	[illegible]

Figure 12.	Frequency vs Degree of Flattening (After Ibl[5]) for Various Duty Cycles.	125
Figure 13.	Frequency vs Degree of Flattening (After Maksimovic[7]) for Various Duty Cycles.	126
Figure 14.	T_{on}/T_c vs Degree of Flattening (After Ibl[5]) for Various Duty Cycles.	126
Figure 15.	T_{on}/T_c vs Degree of Flattening (After Maksimovic[7]) for Various Duty Cycles.	127
Figure 16.	Pulse Current Density vs Duty Cycle at a Fixed Average Current Density (40 A/dm^2).	129
Figure 17.	Schematic Diagram of Hoar and Arrowsmith[153] Apparatus.	140
Figure 18.	Schematic Diagram of Test Cell used for Throwing Power Determinations.	146
Figure 19.	Schematic Diagram of Apparatus used for Cathode Potential Measurement.	150
Figure 20.	Diagram of Equipment for Polarisation Studies using Pulsed Reverse Current.	152
Figure 21.	Effect of Frequency on the Hardness of Deposits Obtained from Three Different Chromium Electrolytes.	159
Figure 22.	Coil Calibration Graph for Hoar and Arrowsmith Apparatus.	160
Figure 23.	The Effect of Pulsed Current on the Mean Internal Stress of Deposits Obtained from the Sulphate Catalysed Electrolyte at a Frequency of 100 Hz and Duty Cycles of 50 and 70%.	161

Figure 24. The Effect of Pulsed current on the Mean Internal Stress of Deposits at a Frequency of 2500 Hz and Duty Cycles of 50 and 70%. 161

Figure 25. The Effect of Pulsed Current on the Surface Topography of Chromium Deposits at 100 Hz, 50% Duty Cycle at 40 A/dm^2 54 ^oC. 165

25a) Deposit from Sulphate Catalysed Electrolyte.

25b) Deposit from Chromefast C Electrolyte.

25c) Deposit from Mach 1 Electrolyte.

Figure 26. The Effect of Pulsed Current on the Surface Topography of Chromium Deposits at 3000 Hz, 50% Duty Cycle at 40 A/dm^2 , 54 ^oC. 166

26a) Deposit from Sulphate Catalysed Electrolyte.

26b) Deposit from Chromefast C Electrolyte.

26c) Deposit from Mach 1 Electrolyte.

Figure 27. Surface Topographies of Three Different Chromium Deposits Plated with Direct Current at 40 A/dm^2, 54 ^oC. 167

27a) Deposit from Sulphate Catalysed Electrolyte.

27b) Deposit from Chromefast C Electrolyte.

27c) Deposit from Mach 1 Electrolyte.

Figure 28. Deposits Produced from a Sulphate Catalysed Electrolyte After 20 second Etch in 10% Chromic Acid. 168

28a) Deposit Produced by Direct Current at 40 A/dm^2, 54 ^oC.

28b) Deposit Produced by Pulsed Current at 3000 Hz, 50% Duty Cycle.

28c) Deposit Produced by Pulsed Current at 100 Hz, 50% Duty Cycle.

Figure 29. Potentiodynamic Scan of Deposit Produced by Direct Current from Sulphate Catalysed Electrolyte. 171

Figure 30. Potentiodynamic Scan of Deposit Produced at 3000 Hz, 50% Duty Cycle from Sulphate Catalysed Electrolyte. 171

Figure 31. Potentiodynamic Scan of Deposit Produced at 100 Hz, 50% Duty Cycle from Sulphate Catalysed Electrolyte. 172

Figure 32. X-ray Diffraction Spectra of Deposits Produced from a Sulphate Catalysed Electrolyte. 176

32a) Deposit Produced by Direct Current.

32b) Deposit Produced at 2500 Hz, 50% Duty Cycle.

32c) Deposit Produced at 1000 Hz, 50% Duty Cycle.

32d) Deposit Produced at 500 Hz, 50% Duty Cycle.

32e) Deposit Produced at 100 Hz, 50% Duty Cycle.

32f) Deposit Produced at 16 Hz, 50% Duty Cycle.

Figure 33. The Effect of varying Frequency on the Cathodic Efficiencies of Three Different Chromium Plating Electrolytes. 180

Figure 34. Frequency vs Covering Power (A/dm^2) on a Brass Substrate. 181

Figure 35. The Effect of Pulsed Reverse and Direct Current on the Electrolyte Polarisation Characteristics: Base Electrolyte. 195

Figure 36. The Effect of Single Additives on Electrolyte Polarisation Characteristics: Direct Current. 196

Figure 37. The Effect of Single Additives on Electrolyte Polarisation Characteristics: Pulsed Reverse Current. 196

Figure 38. The Effect of Combined Additives on Electrolyte Polarisation Characteristics at Three Different Chloride Concentrations: Direct Current. 198

- 40 ppm MPS, 75 ppm Oxilube 50,000.

Figure 39. The Effect of Combined Additives on Electrolyte Polarisation Characteristics at Three Different Chloride Concentrations: Direct Current. 199

- 40 ppm SSP, 75 ppm Oxilube 50,000.

Figure 40. The Effect of Combined Additives on Electrolyte Polarisation Characteristics at Three Different Chloride Concentrations: Pulsed Reverse Current.
- 40 ppm MPS, 75 ppm Oxilube 50,000. 200

Figure 41. The Effect of Combined Additives on Electrolyte Polarisation Characteristics at Three Different Chloride Concentrations: Pulsed Reverse Current.
- 40 ppm SSP, 75 ppm Oxilube 50,000. 200

Figure 42. The Effect on Electrolyte Polarisation Characteristics of Varying Concentration of Oxilube: Direct Current (Cl^- 100 ppm). 201

Figure 43. The Effect of Varying MPS Concentration on Electrolyte Polarisation Characteristics: Direct Current
- Electrolyte Containing 75 ppm of Oxilube 50,000. 202

Figure 44. The Effect of Varying MPS Concentration on Electrolyte Polarisation Characteristics: Pulsed Reverse Current
- Electrolyte Containing 75 ppm of Oxilube 50,000. 203

Figure 45. The Effect of Molecular Weight of Polyether on Electrolyte Polarisation Characteristics: Direct Current. 204

Figure 46. The Effect of Molecular Weight of Polyether on Electrolyte Polarisation Characteristics: Direct Current.
- Electrolyte Containing MPS (20 ppm) and Polyether (75 ppm). 205

Figure 47. The Effect of Molecular Weight of Polyether on Electrolyte Polarisation Characteristics: Pulsed Reverse Current.
- Electrolyte Containing MPS (20 ppm) and Polyether (75 ppm). 206

Figure 48. The Effect of Pulsed reverse Current on the Metal Distribution on a Hull Cell Panel. 209

Figure 49. Hole/Land Thickness Ratio Obtained using Different Additive Combinations with Direct Current. 210

Figure 50. Hole/Land Thickness Ratio Obtained using Different Additive Combinations with Pulsed Reverse Current. 211

Figure 51. Hole/Land Thickness Ratios Obtained using 10ms Cathodic 0.5 ms Anodic Pulse Times. Electrolyte Containing SSP and Oxilube. 211

Figure 52. Hole/Land Thickness Ratios Obtained using 10ms Cathodic 1 ms Anodic Pulse Times. Electrolyte Containing SSP and Oxilube. 212

Figure 53. Hole/Land Thickness Ratios Obtained using 10ms Cathodic 0.5 ms Anodic Pulse Times in P.C.81 Bright Acid Copper. 214

Figure 54. Hole/Land Thickness Ratios Obtained using 10ms Cathodic 1 ms Anodic Pulse Times in P.C.81 Bright Acid Copper. 214

Figure 55. Hole/Land Thickness Ratios Obtained using Different Cathodic Pulse Times. 215

Figure 56. Hole/Land Thickness Ratios Obtained on Commercially Plated Boards. (10 ms Cathodic 0.5 ms Anodic). 216

Figure 57. Hole/Land Thickness Ratios Obtained on Commercially Plated Boards. (10 ms Cathodic 1.0 ms Anodic). 217

Figure 58. Ground Plane/Isolated Pad Thickness Ratio using Pulsed Reverse Current on Commercially Produced Boards. 218

Figure 59.	Surface Topography of Deposits Produced by Direct Current.	220
59a)	Additive Free Electrolyte.	
59b)	Electrolyte + 75 ppm Oxilube 50,000.	
Figure 60.	Surface Topography of Deposits Produced by Pulsed Reverse Current. Cathodic time 10ms. Anodic time 0.5 ms Anodic/Cathodic Current Density Ratio 3:1.	221
60a)	Additive Free Electrolyte.	
60b)	Electrolyte + 75 ppm Oxilube 50,000.	
60c)	Electrolyte + 75 ppm Oxilube + 20 ppm SSP.	
Figure 61.	Surface Topography of Deposits Produced at Various Anodic/Cathodic Current Density Ratios (10 ms Cathodic, 1 ms Anodic)	222
61a)	2:1 Ratio.	
61b)	3:1 Ratio.	
61c)	4:1 Ratio.	
Figure 62.	Surface Topography of Deposit Produced using Cathodic Pulse time 10ms, Anodic Pulse time 2 ms.	223
Figure 63.	T.E.M. Photographs Showing Grain Structure of Copper Deposits Produced by Direct Current.	224
63a)	Additive Free Electrolyte.	
63b)	Electrolyte + 75 ppm Oxilube 50,000.	
63c)	Electrolyte + 75 ppm Oxilube + 20 ppm SSP.	
Figure 64.	T.E.M. Photographs Showing Grain Structure of Copper Deposits Produced by Pulsed Reverse Current. (10:0.5ms, 3:1)	226
64a)	Additive Free Electrolyte.	
64b)	Electrolyte + 75 ppm Oxilube 50,000.	
64c)	Electrolyte + 75 ppm Oxilube + 20 ppm SSP.	

Figure 65. Mechanism Proposed by Yokoi et al [163] for the Adsorption of Polyether Molecules. 233

Figure 66. Log Potential vs Log Oxilube Concentration at 2 A/dm^2 22 ^oC. 233

Figure 67. 236

67a) Proposed Mechanism for Adsorption and Complex Formation of Sulphopropyl Sulphide.

67b) Final Stage of Reduction.

Figure 68. Proposed Mechanism for Adsorption of Sulphopropyl Sulphide with Pulsed Reverse Current. 240

List of Symbols.

j_m	Average current density.
j_l	Limiting current density.
j_p	Pulse current density.
j_{pl}	Pulse limiting current density.
j_{ca}	Cathodic current density.
j_a	Anodic current density.
j_t	Total current density.
j_f	Faradaic current density.
j_c	Capacitative current density.
j_o	Exchange current density.
t_{on}	On time. (seconds)
t_{off}	Off time. (seconds)
$t_{on(c)}$	Cathodic on time. (seconds)
$t_{on(a)}$	Anodic on time. (seconds)
t_c	Charge time for double layer. (seconds)
t_d	Discharge time for double layer. (seconds)
T	Transition time.(seconds)
α	Transfer coefficient.
z	Ionic charge of discharging species.
F	Faraday constant.
R	Gas constant.
T	Temperature (K).
Q	Charge (Coulombs)
C_{dl}	Double layer capacitance (Farads)
η	Overpotential (volts).
η_a	Activation overpotential (volts).
λ	Frequency. (Hz)
Δ	Degree of Flattening (After Puippe & Ibl).

Δ^*	Degree of Flattening (After Maksimovic et al.)
C	Concentration (moles/litre)
x	Distance from cathode surface.
D	Diffusion coefficient of diffusing species.
δ	Thickness of diffusion layer.
δ_p	Thickness of pulsating diffusion layer.
ω	Duty Cycle.
Wa	Wagner number.

Chapter 1.

Introduction.

The use of pulsed or modulated current in the electroplating industry is not new and was employed as early as 1893 for the deposition of zinc (1). Early applications of modulated current involved fairly long cathodic pulses usually of several seconds in length followed by anodic pulses. Examples of the use of this technique include the use of periodic reverse (P.R.) plating in cyanide copper solutions where an improved plating rate and metal distribution can be obtained under suitable conditions.

Developments in modern electronics led to the production of pulse generators which were capable of switching currents at a rapid rate and the use of very short pulses (in some cases in the microsecond range) became possible. This use of short pulses means that the diffusion layer does not fully disperse between pulses and this is what distinguishes pulsed reverse plating from periodic reverse plating. However, these pulse rectifiers were not capable of switching very large currents and were relatively expensive. Because of these limitations, early applications of these pulse rectifiers were limited to uses in the deposition of precious metals where currents tended to be small and the cost of the rectifiers could be justified.

Research into the application of pulsed current to many electrochemical systems was undertaken but due to a lack of basic understanding of the theory of the application of modulated current to electroplating systems, many claims were made regarding the advantages of pulse plating which were false. Some workers claimed that plating rates could be improved by several orders of magnitude and it has also been claimed that pulsed current can save power. As will be discussed in later chapters these claims are

generally false. Other claims for the applications of pulsed current included improved throwing power, reduced porosity, increased hardness and better ductility. All of these effects are found in specific electrochemical systems but the nature of the effect of pulsed current on an electrochemical system is specific to that system and not generally applicable.

The introduction of microprocessor control and fast switching solid state rectifiers which were capable of switching much larger currents than the first generation pulse rectifiers meant that greater flexibility and control of the applied waveform could be achieved; virtually any waveform could be generated. Typical waveforms can be subdivided into two groups. Unipolar pulses are pulses which all have the same polarity; bipolar pulses have forward and reverse pulses. These can be further subdivided into superimposed pulse, pulse on pulse etc. These waveforms will be described more fully in later chapters.

Because of the larger switching capabilities of these rectifiers, they became available for a wide range of applications. Unfortunately, the manufacturers of the pulse plating rectifiers who were keen to maximise sales assumed that the advantages reported in the literature for specific processes were generally applicable and sold pulse rectifiers as a universal remedy for plating problems. This combined with the very large number of variables in the waveform led to pulse plating generally getting a bad reputation since it rarely lived up to the claims of the rectifier manufacturers when applied in commercial practice.

Research on the use of pulsed current continued and the major limitations of the process were identified. The capacitance of the double layer at the electrode/electrolyte interface was found to exert a smoothing effect on high frequency pulses due to the charge and

discharge of the double layer. Models for mass transport by the use of pulsed current and studies of the effect of pulsed current on the electrocrystallisation of deposits added to knowledge of the effect of pulsed current. This increase in the understanding of the use of modulated current has lead to the acceptance of pulse plating as a useful technique and it has found uses in alloy plating where alloy composition can be adjusted by the current waveform. Pulsed current is also still used for the deposition of precious metals.

Although some work has been carried out on the application of modulated current to commonly deposited metals, there are no major general applications of pulsed current for the deposition of these commonly deposited metals.

Most electroplating solutions also contain one or more organic compounds which modify the electrocrystallisation of the deposit and give brightening, levelling or grain refining properties and may also modify deposit metal distributions. No work has been carried out on the effect of pulsed current on the mechanism of incorporation of these additives. As pulsed current can produce grain refining effects, it has been suggested that it can be used as a brightener substitute since the applied waveform is more controllable than additive concentrations. However, the effect of pulsed current is generally much less than that of organic additives so the use of pulsed current is unlikely to replace the use of organic additives especially as small grain size does not guarantee the production of a bright deposit.

Aims.

The aim of the research work presented in this thesis was to evaluate the application of pulsed current to two commonly deposited metals. Chromium was chosen for one of the metals since a considerable amount of attention has been directed to the use of pulsed current to produce crack free chromium deposits. However, while the production of crack free deposits has already been studied, there are many aspects of this which have not been investigated. For example, the co-deposition of chromium hydrides in certain cases has been noted but no explanation has been given as to the cause of this phenomenon.

The other metal investigated was copper as deposited from an acid copper electrolyte. Here, the effect of modulated current on acid copper solutions containing organic additives was studied in order to investigate the way modulated current can affect the mechanism of co-deposition of organic additives. Copper was chosen for this purpose because the electrolyte is very simple as are brightener systems for acid copper electrolytes. Acid copper electrolytes have a wide application in the printed circuit industry to deposit copper in plated through holes. With new developments in surface mount technology, holes are becoming smaller so it is important to maximise the metal thickness distribution within the holes on printed circuit boards. Across the board distribution is also important. It has been found that the use of pulsed reverse current can improve the throwing power of acid copper electrolytes which contain organic additives. A major part of the research was to determine the reason for this observed phenomenon.

Chapter 2.

The Theory of the Application of Pulsed Current.

2.1. The Characterisation of Pulsed Current Waveforms.

Pulse plating is the application of modulated current to an electrochemical system. Thus any deviation of the current waveform from a direct current is a form of pulse plating. In any electrochemical reaction, the rate of the reaction is controlled by the current density and the driving force of the reaction is controlled by the potential of the electrode at which the reaction is occurring. By the use of modulated current, it is possible to produce deposits at electrode potentials and current densities which would not be possible with the use of continuous current due to mass transport limitations. This makes it feasible to produce electrodeposits with different physical and mechanical properties from those produced by direct current. The use of pulsed current is also beneficial for the deposition of alloys where deposit compositions can be altered by selecting the correct pulse parameters since deposit composition is affected by the electrode potential.

The advent of modern electronics and microprocessor control has meant that great flexibility over the programming of the applied waveform can be achieved. Modern pulse plating rectifiers or switches allow very short or very long pulses to be applied of either cathodic or anodic polarity. Trains of pulses can be programmed to give very complex waveforms. Puippe (2) has characterised these waveforms and some examples are given in figure 1. All of the illustrated waveforms are square waves since this is the easiest waveform to produce because it requires only a simple switching arrangement. Most commercial pulse plating rectifiers operate using square wave current. It can be

Figure 1. Characterisation of Pulsed Current Waveforms.

(After Puippe.[2]).

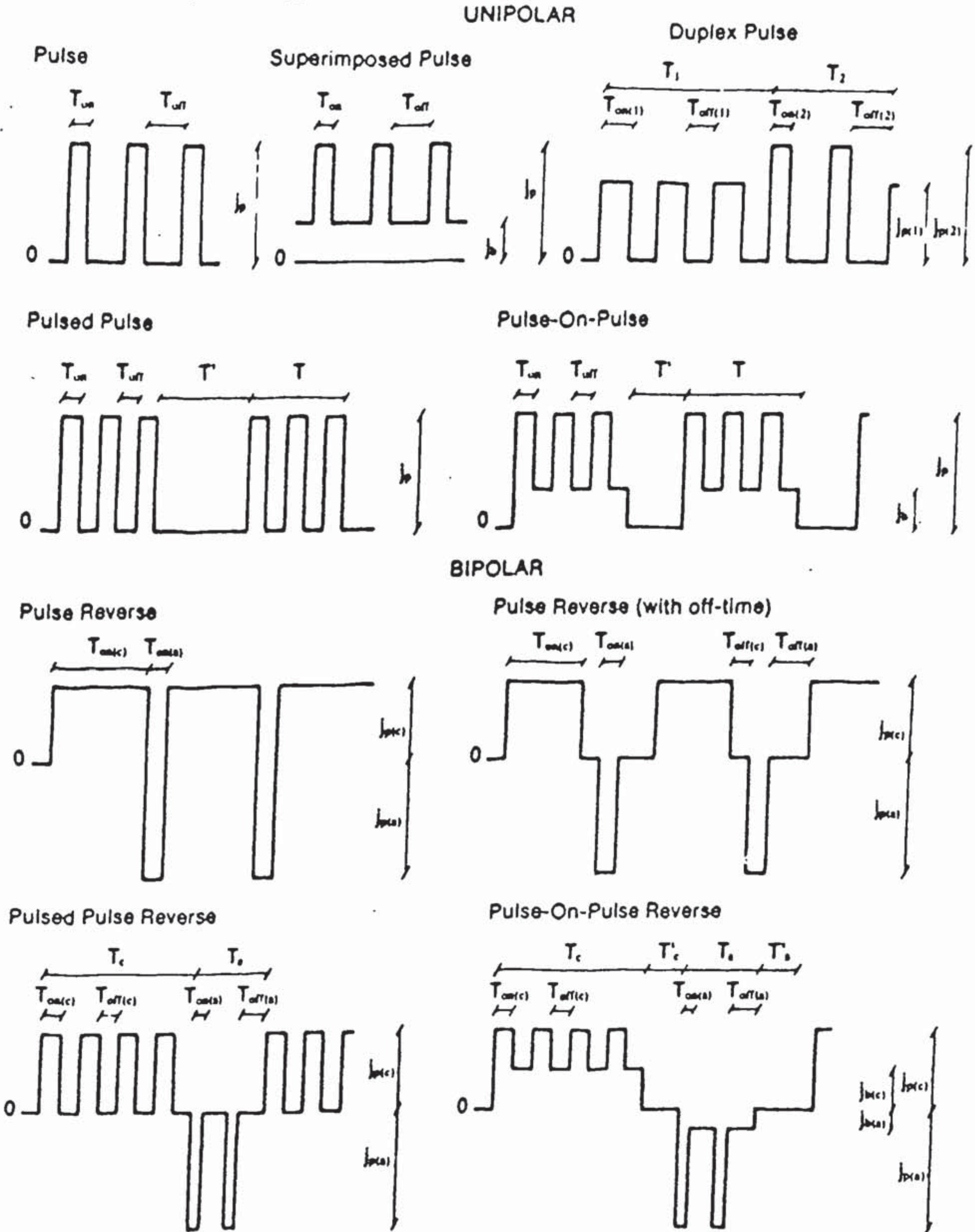

The parameters shown in this figure are independent. The average current density, j_m, dependent parameter, can be calculated from the above mentioned parameters. Pulse reverse is characterized by three different average current densities:

j_m, $j_{m(c)}$, $j_{m(a)}$, with $j_m = j_{m(c)} + j_{m(a)}$

seen from figure 1 that current waveforms can be subdivided into two major groups, unipolar pulses, where all of the pulses are in one direction, and bipolar pulses where anodic and cathodic pulses are mixed. These two major groups can be further divided into superimposed pulses, duplex pulses etc. However, as the complexity of the applied waveform increases, so the number of parameters required to characterise the waveform also increases. This means that the number of variables involved also increases and this can make it difficult to understand how a particular waveform is affecting the electrodeposition process. For this reason the waveforms used in the research reported in this thesis are either simple unipolar square wave pulses or simple pulse reverse bipolar pulses. These are characterised as follows :-

2.1.1. Characterisation of Pulsed Current.

In order to characterise a direct current, it is sufficient to know the current density (j). The characterisation of a train of current pulses requires three parameters to be known. These are the pulse current density (j_p), the pulse length (t_{on}) and the interval between the pulses (t_{off}) [3]. Each of these parameters can influence the properties of the electrodeposited metal. The three parameters listed above are sometimes expressed in different ways. These are as follows :-

i) Duty Cycle

This quantity is most usually expressed as a percentage value. It represents the percentage time in each cycle when the current is on. It can be expressed mathematically as follows :-

$$\text{Duty cycle } \% = \frac{t_{on} \times 100}{(t_{on} + t_{off})} \quad (1)$$

ii) Average current density.

This quantity (j_m) is important as it represents the same quantity (j) as the current density in direct current plating. It is this variable which determines the overall plating rate and so can be used to calculate plating thicknesses provided that the efficiency of the electrolyte is known. Average current density and pulse current density are connected by the following relationship :-

$$j_m = \frac{j_p \cdot t_{on}}{(t_{on} + t_{off})} \quad (2)$$

iii) Frequency.

Frequency is simply the reciprocal of the total cycle time expressed as follows :-

$$\text{Frequency (Hz)} = \frac{1}{(t_{on} + t_{off})} \quad (3)$$

2.1.2. Characterisation of Pulsed Reverse Current.

Whereas three parameters are sufficient to characterise a train of unipolar pulses, four parameters are required to characterise a pulsed reverse waveform. The on time for the cathodic pulse ($t_{on(c)}$), the on time for the anodic pulse ($t_{on(a)}$), the cathodic current density (j_c) and the anodic current density (j_a) all need to be known. Calculation of average current density (j_m) is as follows [2]:-

The average current density is given by the sum of the anodic and cathodic current densities, i.e.

$$j_m = j_{m(c)} + j_{m(a)} \tag{4}$$

and :-

$$j_m = \frac{\left(j_c \cdot t_{on(c)}\right) + \left(j_a \cdot t_{on(a)}\right)}{\left(t_{on(c)} + t_{on(a)}\right)} \tag{5}$$

It should be noted here that the anodic and cathodic current densities have opposite polarities so care must be taken when using this formula to take this factor into account. It can be seen from this equation that calculation of average current density from even a simple pulse reverse waveform can be much less straightforward than for simple unipolar pulses.

2.2. The Effect of Charge and Discharge of the Double Layer.

The electrical double layer is present at any electrode/electrolyte interface and consists of charged layers separated by a few Angstroms. The electrical behaviour of this layer when a current or series of current pulses is applied can be equated to that of a capacitor with an interplate distance corresponding to the thickness of the double layer. Because the thickness of the double layer is so small, a relatively high capacitance results and a typical value of the double layer capacitance for electroplating solutions is of the order of 50 $\mu F/cm^2$.

When current is applied to this double layer, either when the current is switched on or at the beginning of a current pulse, charge must be applied to the double layer in order to raise its potential to a value corresponding to the steady state potential. The electrode as a whole behaves like a capacitor with a resistance connected in parallel to it where the

resistance is the charge transfer resistance for the electrode reaction occurring at the potential applied (4). This situation is shown in figure 2 and represents the simplest situation which can occur. In practice, the equivalent circuit of an electrode may be much more complicated than this in that more than one electrode reaction may occur at any given potential and additional capacitances can be introduced by the adsorption of molecules or ions at the electrode surface.

When selecting parameters for pulse plating applications, it is important that the pulse length chosen must be considerably longer than the charging time for the double layer or the waveform of the applied Faradaic current will be smoothed by the capacitative effect of the double layer (4). This is illustrated in figure 3. It is also important in the case of unipolar pulses that the off time after the pulse has finished is longer than the discharge time for the double layer. In the case of bipolar pulses, both cathodic and anodic pulse times should ideally be longer than the charge times.

The current used to charge the double layer is not lost but is recovered at the end of a pulse during the discharge of the double layer as shown in figure 4. Thus it has been found that the efficiency of metal deposition with pulsed current is generally similar to that obtained with direct current in electrolytes where only one major cathodic reaction occurs. In electrolytes where more than one reaction occurs (such as the combined discharge of hydrogen and copper in cyanide copper electrolytes) the relative efficiencies of the electrode processes may be altered. Because plating occurs by discharge of the stored charge in the double layer through the charge transfer resistance, it is important when designing pulse generators that the electroplating bath is left in an open circuit condition at the end of each pulse. If the pulse generator leaves the bath in a

Figure 2. Representation of the Equivalent Circuit of an Electrode.

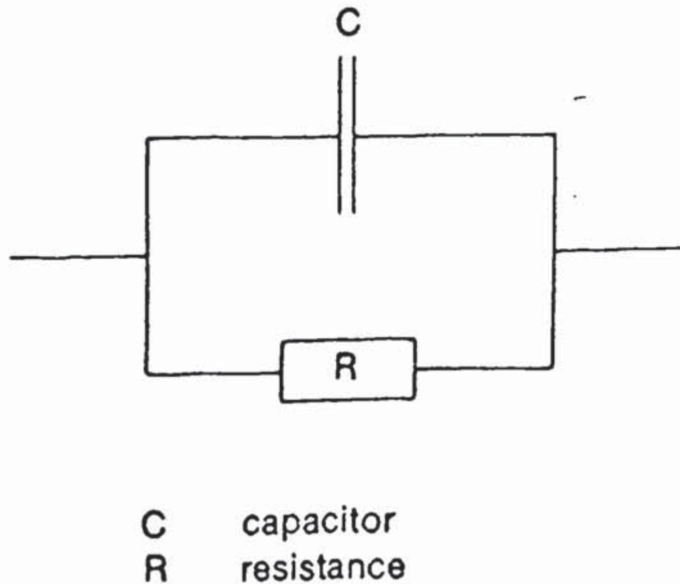

C capacitor
R resistance

short circuit condition, the double layer can discharge through the pulse generator rather than the charge transfer resistance. This can cause a large reduction in the apparent cathodic efficiency of an electrolyte. Some commercial equipment suppliers have not been aware of this problem.

In order to select pulse parameters so that "flattening" of the Faradaic waveform does not occur, it is necessary to be able to calculate or measure charge and discharge times. This problem has been approached in several ways which will be discussed in the following sections.

Figure 3. Illustration of the Smoothing Effect of the Double Layer Capacitance on the Waveform of the Faradaic Current. (After Puippe.[4]).

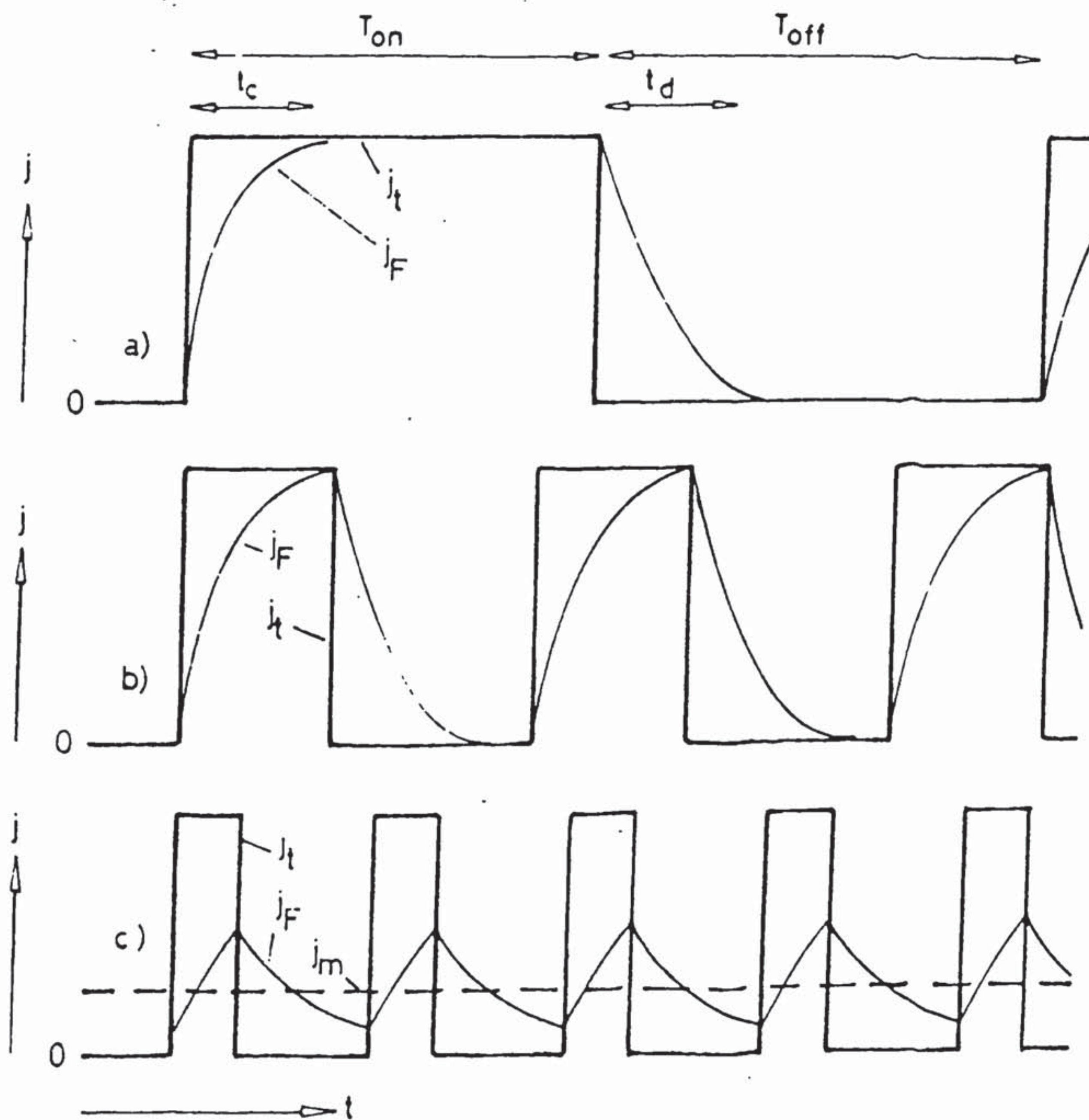

a) $T_{on} > t_c$, $T_{off} > t_d$: small damping

b) $T_{on} = t_c$, $T_{off} = t_d$: medium damping

c) $T_{on} < t_c$, $T_{off} < t_d$: strong damping

Figure 4. Illustration of Current Recovery at the end of a Pulse. (After Puippe.[4]).

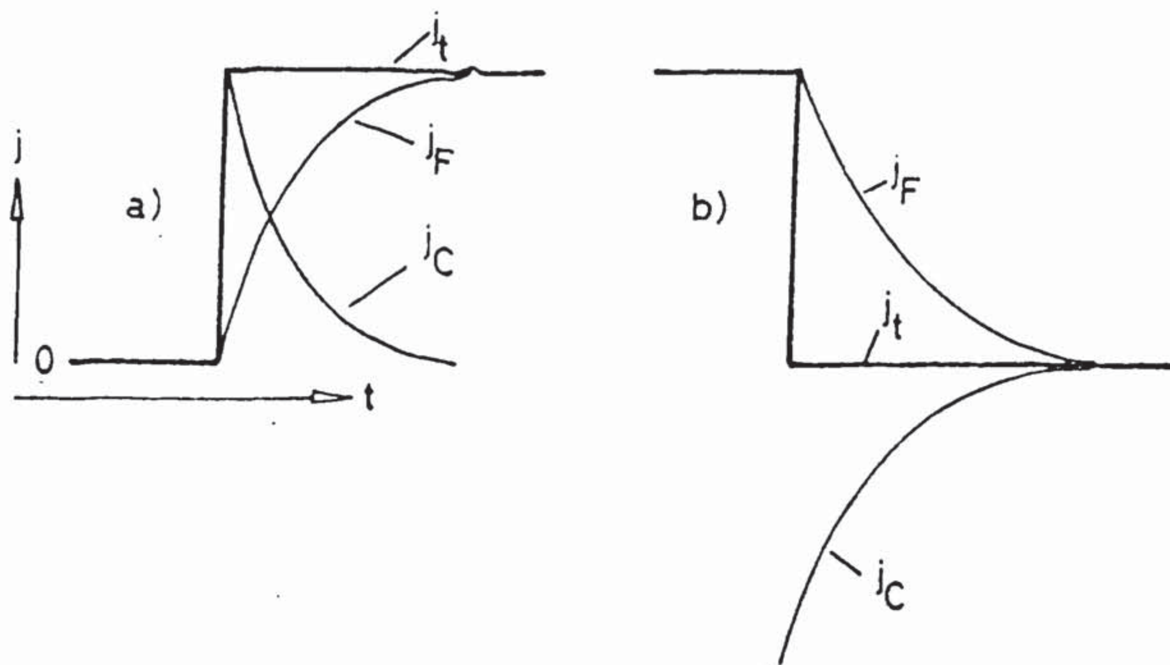

a) beginning of a pulse b) end of a pulse

2.2.1. Calculation of Charge and Discharge Times for Unipolar Pulses.

The method of calculating charge and discharge times using an integration procedure was developed by Puippe and Ibl [5]. The method is based on the calculation of charge quantities and is as follows :-

Any current density for metal deposition corresponds to a particular overpotential. When a train of pulses is applied, at the beginning of each pulse the potential of the cathode must be raised to this potential. This process takes time because the double

layer represents a capacitance which must be charged.

At the beginning of a pulse, the total current supplied by the pulse generator (j_t) is split into two components. These are the capacitative current density (j_c) which charges the double layer and the Faradaic current density (j_f) which corresponds to the rate of metal deposition.

It is assumed that the simple electrode equivalent circuit as shown in fig 2 applies and that only one electrode reaction occurs. It is also assumed that the system is controlled by activation overpotential and that the effects of concentration overpotential are negligible. If these assumptions are made, then the overpotential is linked with the Faradaic current density by the Volmer-Butler equation [6]:-

$$j_f = j_0 \left[\exp\left(\frac{\alpha z F \eta_a}{RT}\right) - \exp - \left(\frac{(1-\alpha) z F \eta_a}{RT}\right) \right] \qquad (6)$$

To visualise the system, the electrode/electrolyte interface is represented as a capacitance and a resistance in parallel. The capacitance is due entirely to the capacitance of the double layer and the total Faradaic current is assumed to be due entirely to the charge transfer reaction. Thus the resistance in the equivalent circuit is due solely to the charge transfer reaction. Charge transfer resistance is not constant but is dependent upon the magnitude of the applied Faradaic current.

The capacitative current density is given by the equation :-

$$j_c = \frac{dQ}{dt} = C_{dl} \frac{d\eta}{dt} \qquad (7)$$

The total current density is the sum of the capacitative and Faradaic current densities and is equal to the pulse current density (j_p) :-

$$j_t = j_p = j_f + j_c \qquad (8)$$

If a galvanostatic pulse is considered, there is no change in the magnitude of the applied pulse so the following relationship applies :-

$$dj_t = 0 \quad \text{so} \quad dj_f = -dj_c \qquad (9)$$

If very small increments in potential are taken, the variation of the Faradaic current can be regarded as linear in the interval considered. In the nth interval :-

$$j_f = \frac{1}{A_n}\eta_a + B \qquad (10)$$

where A_n is a proportionality factor between the current and the potential in the nth interval and B is a constant. A_n is given by the equation :-

$$A_n = \frac{\eta_{a(n)} - \eta_{a(n-1)}}{j_{f(n)} - j_{f(n-1)}} \qquad (11)$$

and so :-

$$d\eta_a = A_n dj_f \qquad (12)$$

combining equations 7,9 and 12 gives the expression :-

$$j_c = -C_{dl} A_n \left(\frac{dj_c}{dt}\right) \qquad (13)$$

Substituting the right hand side of equation 11 for A_n, rearranging the equation, and integrating with respect to time, an equation can be derived which gives the time needed

to change the potential for the nth interval, this equation is as follows :-

$$t_n = C_{dl} \frac{\eta_{a(n)} - \eta_{a(n-1)}}{j_{f(n)} - j_{f(n-1)}} \ln \frac{j_{c(n-1)}}{j_{c(n)}} \quad (14)$$

where t_n is the time to change the potential for the nth interval. This equation can be used in conjunction with equation 6 to calculate charge and discharge times. The method is based on using a computer to sum times calculated from equation 14.

i) Calculation of Charge Time for the Double Layer.

During the Pulse :-

$$j_t = j_p \quad (15)$$

$$j_f = j_p - j_c \quad (16)$$

Theoretically, the double layer takes an infinite time to charge but charge times can be calculated by setting arbitrary limits. Puippe and Ibl [5,6] defined the charge time as the time elapsing until the Faradaic current reached a value of 99% of the total pulse current. In order to calculate charge time, the sum of the times t_n as defined in equation 14 using incremental steps in potential of 1mV is calculated by computer until the Faradaic current reaches a value of 99% of the total applied current. The Faradaic current for each step in potential is calculated from equation 6.

ii) Calculation of Discharge Time for the Double Layer.

After the pulse :-

$$j_t = 0 \quad (17)$$

$$j_f = -j_c \quad (18)$$

At the end of a pulse, the accumulated charge in the double layer discharges through the charge transfer resistance. Puippe and Ibl (5,6) defined the discharge time as the time elapsing for the Faradaic current to fall to a value of 0.1% of the Faradaic current applied during the pulse. The computation is performed in the same way as for calculation of charge time.

It should be noted that although this method theoretically allows the computation of charge and discharge times, values for transfer coefficients, double layer capacitance values and exchange current densities are rarely known accurately and values have to be assumed. However, the method can give a good indication of charge and discharge times.

2.2.2. Calculation of Degree of Flattening.

The concept of degree of flattening was first introduced by Puippe and Ibl (5,6) to describe quantitatively the degree of departure of the Faradaic waveform from that of the applied waveform. Degree of flattening was defined as a dimensionless variable which varied between 0 and 1. It was defined as follows :-

$$\Delta = \frac{\int_{t(on)}^{t(off)} j_f \, dt}{j_m t_{off}} = \frac{j_p t_{on} - \int_0^{t(on)} j_f \, dt}{j_m t_{off}} \qquad (19)$$

The numerator of this expression represents the amount of metal deposited during the off time. The denominator represents the amount of metal which would be deposited if a current equal to the average current were flowing in the interval between the pulses. Thus a degree of flattening of 1 represents direct current and a degree of flattening of 0 represents a situation where the effects of the double layer capacitance are negligible.

Puippe and Ibl (5) produced a plot of degree of flattening against the ratio of on time to charge time. This is reproduced in figure 5. From this plot, it can be seen that the degree of flattening becomes negligible when the pulse time is more than 6 times the length of the charge time. This dimensionless plot has the advantage of being independent of the exchange current density and the double layer capacitance.

The main disadvantage of defining degree of flattening in this way is that is is not possible directly to measure this degree of flattening since it is based on charge

Figure 5. Plot of Degree of Flattening against Ratio of On Time : Charge Time. (After Puippe. (4)).

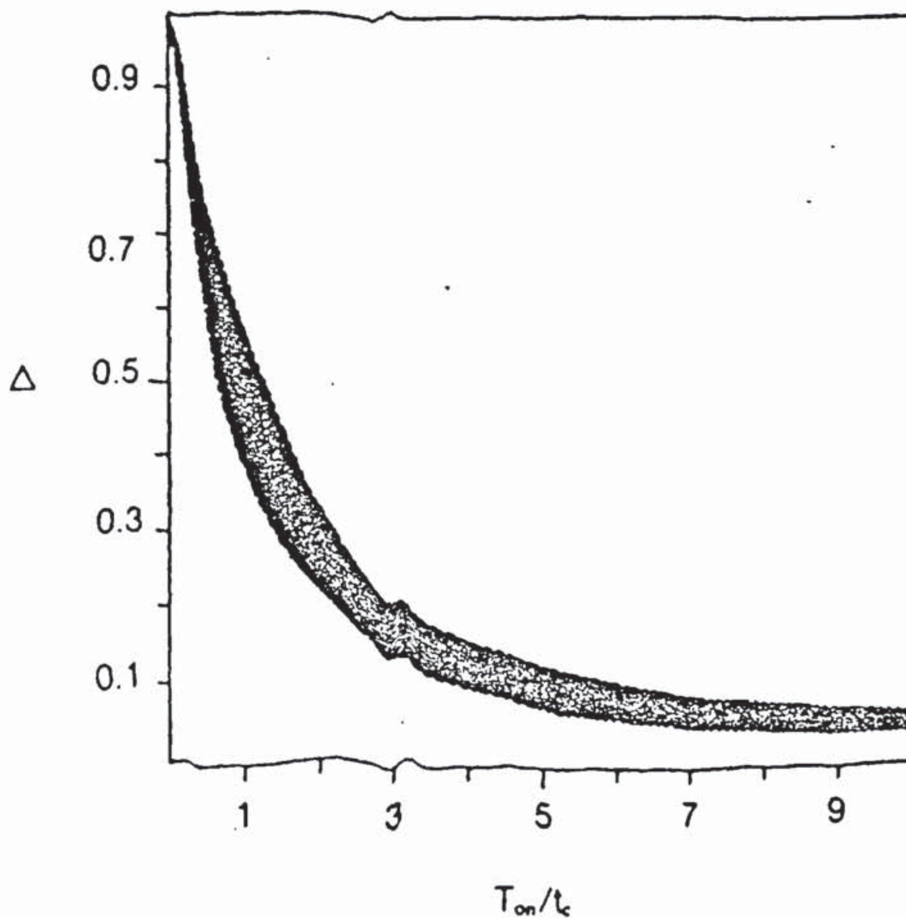

quantities. Maksimovic et al. [7] stated that there was no significant difference between the degree of flattening of the Faradaic current amplitude and that of the overpotential amplitude and suggested an alternative way of defining degree of flattening based on the flattening of potential rather than current. This makes it possible to make measurements of this since average overpotentials are easily measured by the use of reference electrodes and Luggin capillaries.

When a train of pulses is applied to an electrochemical system, because there is a time in the cycle when the current is off, a higher current needs to be applied during the pulses in order to maintain the same average current density as the equivalent direct current. The potential which needs to be applied in order to maintain a particular current density depends on the charge transfer resistance (provided that the effects of concentration are negligible). Charge transfer resistance is lowered as current density is increased so in the case of pulsed current, deposition during the pulse occurs at a lower resistance than for direct current at the same average rate of deposition. This means that for a given average current density, the average overpotential is lower for pulsed current than for direct current [8]. This reduction in average overpotential can be measured by the use of suitable electrodes. As the frequency of the pulses increases, flattening of the waveform will occur and the measured overpotential will rise to approach that of direct current. Using this observed effect, Maksimovic et al. suggested that degree of flattening could be defined as follows [7] :-

$$\Delta^{*} = 1 - \frac{\Delta\eta_{(\lambda)}}{\Delta\eta_{(0)}} \qquad (20)$$

The denominator of the expression represents the change in the average overpotential between direct current and pulsed current of a given duty cycle when no flattening occurs and the numerator is the measured change in overpotential from that of direct current at a given frequency.

The equation may be thus be written as follows :-

$$\Delta^{*} = \frac{\eta_{(d.c.)} - \eta_{(\lambda)}}{\eta_{(d.c.)} - \eta_{(0)}} \quad (21)$$

A detailed comparison of calculation of degree of flattening using both current and potential methods is given in the experimental procedure section since these methods were assessed for practical use. Comparison of the two methods shows that they do not yield the same values for delta under the same conditions. Degrees of flattening obtained by Maksimovic's method (7) show a strong dependence on duty cycle whereas using Puippe and Ibl's (5,6) method, degree of flattening is almost independent of duty cycle.

2.3. Mass Transport in Pulse Plating.

Mass transport plays an important role in electroplating since this defines the rate at which the metal ions are supplied to the electrode surface (9). The rate of mass transport is governed by convection produced by the concentration gradient present in the diffusion layer. If the electrolyte is agitated, forced convection becomes the determining factor. As current density is increased, the rate of consumption of metal ions increases. If the rate of consumption is greater than the rate of renewal by convection, a situation is reached where the concentration of metal ions at the cathode surface becomes zero. This imposes a limit on the maximum rate of deposition for a system which is termed the limiting current density. In practical plating, the maximum practical current density is much less than the theoretical limiting current density. This is because as the concentration of metal ions at the cathode becomes smaller, the diffusion gradient becomes steeper. Even on a polished cathode, surface roughness exists (or is generated by the nucleation of the growing electrodeposit). Peaks on the

cathode surface are privileged from a viewpoint of diffusion and so more metal is deposited on these. This causes the formation of a rough or dendritic deposit (known as a "burnt" deposit by platers) at current densities well below the theoretical limiting current density. Because of this, most plating solutions are operated at current densities which are only 10 to 20% of the theoretical maximum.

When pulsed current is used for the production of electrodeposits, the mass transport of ions to the electrode surface can be strongly influenced by the pulsating current [(6)]. During the pulse, the concentration of metal ions at the cathode surface falls and if the pulse is very long, will reach a steady state value which is determined by the hydrodynamic factors which prevail. At the end of the pulse, the diffusion layer generated during the current pulse will begin to disperse and if the off time is long enough, will disperse completely. However, most practical pulse plating is carried out at pulse frequencies which are much too high to allow dispersion of the diffusion layer between pulses. In this situation, large concentration fluctuations occur only in the electrolyte very close to the cathode surface. Further away from the cathode surface, a stationary diffusion layer is produced which corresponds to the slope of the diffusion gradient which would be obtained using direct current of the same average current density. This formation of a duplex diffusion layer occurs because the pulsed current is too rapid to allow complete dispersion of the diffusion layer between pulses. Various models have been applied to the mass transport situation using pulsed current. Cheh [(10)] used a simple diffusion model to calculate the limiting current density in pulse plating. Ibl [(6)] . used a similar duplex diffusion layer model as outlined above to calculate the thickness of the pulsating diffusion layer. This model was later modified on a semi-empirical basis by Datta and Landolt [(11)]. Viswanthan et al. [(12)] calculated both the rate of mass transfer and the pulsating diffusion layer thickness by taking into account both diffusion and convection. Here, the thickness of the pulsating diffusion

layer was found to depend upon the pulse characteristics and also the hydrodynamic conditions prevailing.

2.3.1. Mass Transport in Non Steady State Diffusion.

In this theoretical consideration, the effects of Faradaic flattening are assumed to be negligible.

Non steady state diffusion is governed by Fick's second law [9]:-

$$\frac{dC}{dt} = \frac{d^2C}{dx^2} \qquad (22)$$

For constant applied current and in the absence of convection the boundary conditions which can be applied to this equation are as follows :-

$$C = C_b \quad \text{at } x >= 0 \text{ and } t = 0 \qquad (23)$$

$$C = C_b \quad \text{at } x = \text{infinity and } t > 0 \qquad (24)$$

$$\frac{dC}{dx} = \frac{j}{zFD} \quad \text{at } x = 0 \text{ and } t > 0 \qquad (25)$$

The subscript b refers to bulk properties.

Integration of equation 22 with boundary conditions 23, 24 and 25 yields Sand's Equation [13] :-

$$C_s = C_b - \frac{2j}{zF}\sqrt{\left(\frac{t}{\pi D}\right)} \qquad (26)$$

Here, C_s is the concentration of the diffusing species at the electrode surface at any time t.

The time at which the surface concentration reaches zero is the transition time T :-

$$T = \frac{\pi D z^2 F^2 C_b^2}{4 j^2} \qquad (27)$$

Non steady state diffusion in convective systems can be treated analogously by assuming the existence at the cathode surface of a diffusion layer of finite thickness δ, the value of which depends upon the convection conditions. The boundary condition 24 is then replaced by :-

$$C = C_b \qquad \text{at} \quad x >= \delta \ \text{and} \ t > 0 \qquad (28)$$

Rosebrugh and Miller [14] obtained a solution to equation 22 subject to the boundary conditions 23, 28 and 25 by the use of a Fourier transformation. The surface concentration for electrolytes where both convection and diffusion occurs can be written thus :-

$$C_s = C_b - \frac{j\delta}{zFD} k \qquad (29)$$

Where k is a constant and is given by the following equation :-

$$k = 1 - \frac{8}{\pi^2} \sum_{n=1}^{n=\text{inf.}} \frac{1}{(2n-1)^2} \exp\left[-\left((2n-1)^2 \frac{\pi^2 D t}{4\delta^2} \right) \right] \qquad (30)$$

where n is any integer.

Siver [15] showed that for small values of t and large values of δ i.e. $Dt/\delta^2 < 0.1$,

$$k = \frac{2}{\sqrt{\pi}} \sqrt{\left(\frac{Dt}{\delta^2} \right)} \qquad (31)$$

while for larger values of t and small values of δ, i.e. $Dt/\delta^2 > 0.1$,

$$k = 1 - \frac{8}{\pi^2} \exp\left(-\frac{\pi^2 Dt}{4\delta^2}\right) \qquad (32)$$

Hale [16] used a numerical method and found that Siver's solution was accurate at low values of Dt/δ^2, and is no more than 4% too high over most of the range of Dt/δ^2. In convective systems, a transition time is only reached if the current applied is greater than the limiting current density. This is defined as follows :-

$$j_l = zFD\frac{C_b}{\delta} \qquad (33)$$

Combining equations 33 and 29, it follows that the condition $C_s = 0$ is reached When :-

$$j.k = j_l \qquad (34)$$

For $Dt/\delta^2 < 0.1$ and using equation 31, an expression can be obtained for a dimensionless variable, T^* which varies as a function of the transition time and is defined as follows :-

$$T^* = \frac{DT}{\delta^2} \qquad (35)$$

Using equation 31 and 35, the following expression is obtained :-

$$T^* = \frac{\pi}{4}\left(\frac{1}{j^*}\right)^2 \qquad (36)$$

where j^* is a dimensionless variable which is a function of current density; defined as follows :-

$$j^* = \frac{j}{j_l} \qquad (37)$$

Where $Dt/\delta^2 > 0.1$, a similar calculation can be performed to calculate T^* using equation 32 instead of 31. This yields the following expression :-

$$T^* = \frac{4}{\pi^2} \ln\left[\frac{\pi^2}{8}\left(1 - \frac{1}{j^*}\right)\right] \qquad (38)$$

Equations 36 and 38 which are based on Siver's approximation give the transition time in a convective system for a single pulse. In order to solve Fick's equation (equation 22) for repetitive pulses, the boundary condition 25 has to be replaced by the following equations :-

$$\frac{dC}{dx} = \frac{j_p}{zFD} \quad \text{at} \quad x = 0 \quad \text{and} \quad nt_{on} > t > (n-1)(t_{on} + t_{off}) \qquad (39)$$

$$\frac{dC}{dx} = 0 \quad \text{at} \quad x = 0 \quad \text{and} \quad n(t_{on} + t_{off}) > t > n(t_{on}) \qquad (40)$$

Where n is the number of pulses.

Equation 22 subject to the boundary conditions 23, 24, 39 and 40 has been solved by Rosebrugh and Miller [14]. Their solution was applied to pulse plating by Cheh [10] who showed that under the same hydrodynamic conditions that the overall rat of mass transport in pulse plating cannot exceed that observed in plating with direct current.

Chin [17] treated mass transport in pulse plating as a superimposition of a concentration fluctuation (caused by the pulsed current) over a time averaged steady state concentration.

Ibl [6] adopted a different approach to mass transport and proposed a simple duplex diffusion model according to which a pulsating diffusion layer of thickness δ_p exists near the cathode where the concentration fluctuates with the frequency of the applied pulses. Outside this pulsating layer is considered to be a stationary diffusion gradient. The concentration of cations in this outer stationary diffusion layer is not considered to vary with time. The model is further simplified by the assumption of linear concentration profiles. Using this model, the pulse current density is given by the following expression :-

$$j_p = zFD\frac{C_n - C_s}{\delta_p} \qquad (41)$$

and the average current density is given by :-

$$j_m = j_p\frac{t_{on}}{(t_{on} + t_{off})} = j_p\omega \qquad (42)$$

Where C_n is the concentration of cations at $x=\delta_p$ and where ω is the duty cycle.

The thickness of the pulsating diffusion layer is given by making a mass balance over the pulsating diffusion layer :-

$$\delta_p = \sqrt{(2Dt_{on}(1 - \omega))} \qquad (43)$$

At the limiting pulse current density, the surface concentration becomes zero so from equation 41, the following expression is obtained :-

$$j_{pl} = zFD\frac{C_n}{\delta_p} \tag{44}$$

When a mass balance is performed over the outer diffusion layer $\delta - \delta_p$ is used for eliminating C_n and the steady state limiting current density is introduced, the expression

$$j_{pl} = j_l\left(\frac{\delta_p}{\delta}(1 - \omega) + \omega\right)^{-1} \tag{45}$$

is obtained.

On introducing a dimensionless variable which is a function of the pulse period, defined as follows :-

$$(t_{on} + t_{off})^* = \frac{D(t_{on} + t_{off})}{\delta^2} \tag{46}$$

and a dimensionless variable which is a function of limiting pulse current density, defined as :-

$$j_{pl}^* = \frac{j_{pl}}{j_l} \tag{47}$$

The following expression for j_{pl}^* is obtained :-

$$j_{pl}^* = \left[\left(2\omega(t_{on} + t_{off})^*\right)^{0.5}(1 - \omega)^{1.5} + \omega\right]^{-1} \tag{48}$$

This expression is based on the assumption of linear concentration profiles and has the disadvantage that pulse limiting current densities determined at short pulse times and low duty cycles differ from those obtained by Siver's (15) approximation for single pulses. On the basis of an experimental investigation into mass transport in pulse plating, Datta and Landolt (11) suggested that equation 43 be replaced by the equation :-

$$\delta_p' = \sqrt{\left(\frac{4}{\pi} D t_{on} (1 - \omega)\right)} \tag{49}$$

This then yields the following expression for j_{pl}^* :-

$$j_{pl}^* = \left[\left(\frac{4}{\pi} \omega \left(t_{on} + t_{off} \right)^* \right)^{0.5} (1 - \omega)^{1.5} + \omega \right]^{-1} \tag{50}$$

All of the proposed models for mass transport in pulse plating apply to the use of unipolar pulses only since for bipolar pulses, the mathematics becomes very complicated. However, it is reasonable to assume that with bipolar pulses, a similar situation would exist with the formation of a duplex diffusion layer. Calculations based on the diffusion models described can be useful but in practice, the situation may be much more complex than the simple models described.

2.3.2. Practical Aspects of Mass Transport in Pulse Plating.

i) The Effect of Pulsed Current on the Maximum Practical Current Density.

As has been mentioned in earlier parts of this chapter, plating with direct current usually only allows maximum current densities of 10 to 20% of the theoretical limiting current density. This is due to asperities on the cathode surface being privileged from a

viewpoint of diffusion. This causes rough and dendritic deposits.

By the use of pulsed current, the thickness of the pulsating diffusion layer can be controlled by the pulse parameters which are applied. It is possible to produce pulsating diffusion layers which are very thin indeed. The net result of this is that the pulsating diffusion layer is able to follow very small surface asperities which are then no longer favoured from a diffusional aspect. Thus it is possible to plate at the pulse limiting current density provided that the thickness of the pulsating diffusion layer is small enough to follow the surface profile (18). However, it must be remembered that outside the pulsating diffusion layer is a stationary diffusion layer. As the average current density is raised, so the cation concentration at the boundary between the stationary and the pulsating diffusion layers falls so the pulse limiting current density will also fall. The net effect of these processes is that it is not usually possible to plate at a higher average current density by using pulsed current but provided that sufficient relaxation time is allowed after the pulse (so that the average current density does not produce much concentration polarisation), sound deposits can be obtained at the pulse limiting current density.

Puippe (19) confirmed that this could be done for copper, silver and cadmium. Despic, Popov et al.(20,21) used the same reasoning to explain the observed effect of pulse frequency on deposit smoothness.

ii) The Effect of Pulsed Current on Current Efficiency.

As the limiting current density is approached, the concentration of cations at the cathode surface becomes less. This tends to cause a fall in cathodic efficiency. However, most plating solutions are operated well below the limiting current density. An exception to

this can occur in the deposition of some alloys where one or more of the metals being deposited can be under limiting current density conditions. Landolt [22] has shown that for a binary alloy where one metal is deposited under diffusion control and the other metal is deposited under activation control, that the concentration of the metal deposited under diffusion control is always smaller when pulsed current is used than for D.C. and depends on the applied pulse parameters. Many electroplating solutions contain organic additives which may co-deposit under diffusion control. It is quite possible that the use of pulsed current changes the rate of incorporation of these additives and so may be expected to exert an influence on the brightening and levelling capabilities of these organic additives. However, little work has been carried out in this area.

Co-deposition of two species under diffusion control was investigated by Viswanthan et al. [23] for the case where both species were present at the same concentration. It was found that the species depositing at the least negative potentials is expected to be present in the alloy at lower concentrations than with direct current. A mathematical model for pulsed deposition of alloys has been published by Verbrugge and Tobias [24].

iii) The Effect of Pulsed Current on the Throwing Power of Electrolytes.

The effect of pulsed current on throwing power will be fully described in the next section on current distribution. Since current efficiency is reduced as the limiting current density is approached, it may be expected that plating at or near the limiting current density should lead to a better macrothrowing power [2]. This situation is not achievable in practice since the formation of dendritic deposits occurs at current densities much below this. With the use of pulsed current, it is possible to plate at the pulse limiting current density provided that the average current density does not

produce appreciable concentration polarisation and that the thickness of the pulsating diffusion layer is small enough to follow the asperities on the cathode surface. Theoretically, it should be possible to improve macrothrowing power by using this technique. However, this is not a practical method of improving throwing power because at the high frequencies required to produce a thin pulsating diffusion layer, pulse limiting current densities are very high and enormously high pulse current densities with long relaxation times would be necessary. The mass transport situation in pulse plating can also influence the microthowing power of electrolytes. This will be discussed in the next section.

2.4. Current Distribution in Pulse Plating.

When an electrical current is passed through an electrolyte to an irregularly shaped cathode, it is well known that the parts of the cathode which are closest to the anode experience a higher current density than the parts that are further away. This fact is used in the Hull cell to examine the appearance and thickness distributions of plated deposits over a wide range of current densities.

Potential and current distribution are governed by effects of charge and mass transport. A general theoretical treatment would be very complicated mathematically so solutions have been obtained for special cases where current distribution can be described as follows [9] :-

i) Primary Current Distribution.

In this case, the effects of overpotential are neglected and the non uniformity of the current distribution is attributed solely to the geometry of the cell.

ii) Secondary Current Distribution.

In this case, the effect of activation overpotential is considered but concentration overpotential (i.e. mass transfer effects) is considered to be negligible.

iii) Tertiary Current Distribution.

Here, the effects of both activation and concentration overpotentials are considered.

In practical plating applications, other factors such as adsorbed species on the cathode may also influence the current distribution. The addition of organic additives in particular can have a large influence on current distribution. In the following section the effects of pulsed current on the current distribution and deposit uniformity are discussed.

2.4.1. The Effect of Pulsed Current on the Primary Current Distribution.

The primary distribution is independent of the influence of overpotential and the non-uniformity of the current density distribution is considered to be solely due to geometric irregularities or more precisely to differences in resistance of the electrolyte between the anode and various parts of the cathode.

It may be expected that since the primary current distribution depends on differences in the electrolyte resistance that the conductivity of the electrolyte would have an influence on the primary distribution. However, this is not the case since if the electrolyte conductivity is high, the overall resistance is very low so small changes in resistance have a large influence on the current distribution. If the electrolyte conductivity is low,

there is a greater difference in absolute values of resistance at various points on the cathode but when the overall resistance is higher, the net effect on the current distribution is exactly the same as for a high conductivity electrolyte. Thus the primary distribution is independent of solution conductivity and of the level of current density but depends only on the cell geometry.

Because the primary distribution is only dependent upon cell geometry and is independent of current density, the primary distribution is expected to be the same for both direct and pulsed current [25]. In general, in a plating electrolyte, the current density distribution tends towards a primary distribution if the specific conductivity of the electrolyte is low and the "electrode resistance" is low.

2.4.2. The Effect of Pulsed Current on the Secondary Distribution.

When considering the effect of secondary current density distribution, the activation overpotential of the system is taken into account. Concentration polarisation caused by mass transport limitations is assumed to be negligible.

Because the resistance of the metal cathode is much less than that of the electrolyte, the cathode is considered to be an equipotential surface so the level of activation overpotential is in principle the same over the entire cathode surface. This tends to counteract the effect of irregular geometry and equalise the current density distribution. The extent of this effect is dependent on the slope of the current/potential curve. This effect has been quantified for a rotating disc electrode where the extent of the non-uniformity of the current density distribution can be expressed as a dimensionless number called the Wagner number [25].

This is defined as follows :-

$$Wa = \kappa \left(\frac{\left(\frac{d\eta_a}{di} \right)}{L} \right) \qquad (51)$$

Where κ is the specific electrical conductivity of the electrolyte, $d\eta_a / di$ is the slope of the potential/current curve and L is the characteristic length of the cathode (for a rotating disc electrode this is the radius of the electrode).

If the overpotential for metal deposition obeys Tafel's law (26,27), then the slope of the current / potential curve is inversely proportional to the applied current density. This is because as current density is increased, the charge transfer resistance for the metal deposition electrode reaction becomes less. This explains the observed effect with direct current plating that a more uniform metal distribution is usually obtained at lower average current densities and as the current density is raised, so the deposit uniformity becomes less since it tends towards a primary distribution.

When any form of pulsed waveform is applied, whether the pulses are unipolar or bipolar, in order to plate at the same rate as the equivalent direct current density the cathodic cycle has to be at a higher current density than the equivalent direct current density. It may thus be expected that with pulsed current, the current density distribution is less uniform than with direct current. This would usually mean that the uniformity of metal distribution is also adversely affected. This has been confirmed by Ibl (25) for nickel plating and may be expected for any electroplating electrolyte where the cathodic efficiency for metal deposition is close to 100%.

It has been reported in the literature that the use of pulsed current can in some instances improve deposit distributions. However, this is most usually encountered in solutions where the cathodic efficiency for metal distribution is significantly less than 100% and hydrogen is also discharges as an electrode reaction. Here, pulsed current can change the relative efficiencies of metal deposition and hydrogen discharge and may under suitable conditions produce an increase in throwing power. Electrolytes containing organic additives may also have the deposition mechanism changed by pulsed current which may produce changes in the uniformity of metal distribution. Some of these effects are studied in this thesis.

2.4.3. The Effect of Pulsed Current on the Tertiary Current Distribution.

When considering tertiary distribution, the effects of mass transport limitations are taken into account. The influence of concentration overpotential on the metal distribution depends primarily on the relationship between the thickness of the diffusion layer and the characteristic height of asperities on the cathode surface.

As an example, a sawtooth profile is considered with a characteristic height h (see fig 6a). If h is greater than the thickness of the diffusion layer, the diffusion layer will follow the shape of the cathode so that peaks are not privileged from the viewpoint of diffusion. This is termed a macroprofile. In this case, the concentration overpotential acts in the same way as activation overpotential in that it tends to equalise the current density distribution.

Figure 6. Mass Transport to a Sawtooth Profile.

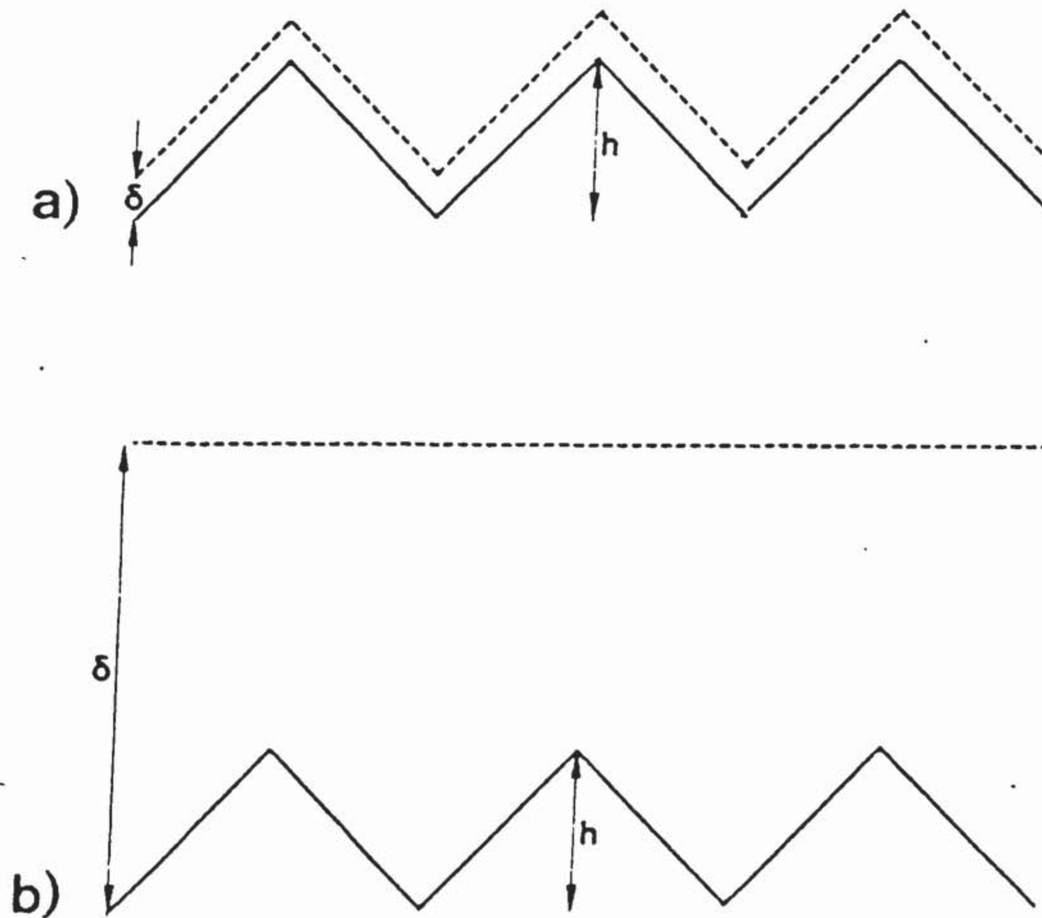

Mass transport to a sawtooth profile; the broken line shows the boundary of the diffusion layer a: macroprofile ($\delta \ll h$) b: microprofile ($\delta \gg h$).

If h is smaller than the thickness of the diffusion layer (fig 6b) diffusion towards the peaks of the asperities is much greater than towards the recesses. This is termed a microprofile. Here, the concentration overpotential acts in opposition to the activation overpotential and makes deposition less uniform over the microprofile.

To consider the effect of pulsed current on the tertiary current distribution, it is necessary to reconsider the mass transport situation. With pulsed current, it is considered that two diffusion layers are present. A pulsating diffusion layer is present close to the cathode where the concentration of cations pulsates with the frequency of the applied pulses and a stationary diffusion layer outside this which extends approximately to the border of convective diffusion which would be obtained by the use of direct current under the same hydrodynamic conditions. The thickness of the pulsating diffusion layer is given by the equation : -

$$\delta_p = \sqrt{2Dt_{on}\left(1 - \frac{t_{on}}{(t_{on} + t_{off})}\right)} \qquad (52)$$

and the metal concentration at the outside of the pulsating diffusion layer is given by using Nernst's approximation of linear concentration profiles and making a mass balance over the diffusion layer as a whole and results in the expression :-

$$C_n = C_b - \frac{j_p}{zFD}\frac{t_{on}}{(t_{on} + t_{off})}\left[\delta_n - \sqrt{2Dt_{on}\left(1 - \frac{t_{on}}{(t_{on} + t_{off})}\right)}\right] \qquad (53)$$

In pulse plating, the thickness of the pulsating diffusion layer is dependent on the length of the pulses. Short pulses produce very thin pulsating diffusion layers and it has been reported that it is possible to obtain pulsating diffusion layer thicknesses of

down to 0.01 μm. If pulse parameters are selected so that the average current density is such that the cation concentration at the interface between the stationary and pulsating diffusion layers (C_n) is close to the bulk concentration (C_b) (i.e. a low average current density producing little overall concentration polarisation) but the on time for the pulse exceeds the transition time (i.e. the cation concentration falls to zero at the cathode surface before the end of each pulse), then the microthrowing power of the electrolyte should be good for asperities down to the characteristic length of the thickness of the pulsating diffusion layer. This has been confirmed by Ibl (25) for the deposition of nickel and copper. In the case of copper, geometric levelling was noted. However, this is not a very practical way of increasing the microthrowing power of electrolytes because using the short pulses necessary to produce thin diffusion layers means that the pulse limiting current densities are very high. To keep the average current density low, long relaxation times must be used. Thus only by using very low duty cycles and enormous pulse current densities is it possible to improve microthrowing power by a large extent except in electrolytes where the free metal content is very low (which gives lower pulse limiting current densities and shorter transition times). Some improvement in the microthrowing power of gold electrolytes has been noted (28).

To sum up, pulsed current may be expected to make macrothrowing power worse but can give good microthrowing power (29) provided that deposition is under mass transport control and the thickness of the pulsating diffusion layer is less than the characteristic height of asperities on the cathode surface.

2.4.4. Current Distribution Using Pulse Reverse Current.

With pulse reverse current, the cathodic pulse is followed by an anodic pulse instead of an off time. As with unipolar pulses, in order to plate at the same rate as with direct current, the current density of the cathodic pulse has to be higher than the average current density. This means that the actual secondary current distribution will be less uniform than for direct current. However, the effects of pulse reverse current on metal distribution are somewhat unpredictable due to changes in the anodic efficiency of the metal at different current densities and passivation effects may also occur. Etching of the deposit during the anodic cycle may increase surface roughness. Some work has been undertaken by Popov et al.(30) to investigate these effects.

2.5. The Effect of Pulsed Current on Electrocrystallisation.

The final stage in the electrodeposition process is the crystallisation of the deposit. In this process, after the charge transfer reaction has taken place, the cations become zero-valent and are deposited as adatoms on the cathode surface. These adatoms move across the cathode surface until they either start new nucleation sites or become incorporated into existing growth sites. If a new growth site is started, the process is termed nucleation. If the adatom is incorporated into an existing growth site, the process is termed growth. The relative rates of growth and nucleation are dependent on chemical and electrochemical parameters and so may be influenced by pulse plating. It is the electrocrystallisation of the deposit which determines the grain size, morphology and physical properties of electrodeposits so because pulse plating can influence electrocrystallisation, it may be expected that physical properties of deposits may be influenced.

With pulsed current, if metal is being deposited at the same rate as for direct current, the overpotential and current density of deposition during the pulses is higher than the average current density. An increase in current density tends to favour fresh nucleation rather than growth so this factor will tend to produce deposits with a finer grain size. However, the off time is certainly not a "dead" time from the viewpoint of electrocrystallisation and during this time, adsorption or desorption of anions, cations or neutral molecules may occur at the cathode surface. These adsorption or desorption processes can block or activate growth sites and so can have a large influence on grain size. Because of this factor, it is not possible to make generalisations about the effect of pulsed current on the grain size and physical properties of deposits.

2.5.1. Effect of Pulse Current Density on Deposit Grain Size.

When investigating the effect of a single parameter when using pulsed current, it is important to realise that it is not possible to change one parameter without affecting another. For example, if duty cycle and frequency are held constant and the pulse current density is increased, then the average current density also increases. If duty cycle and frequency are adjusted so that as the pulse current density increases, the average current density and on time remain the same, then the off time will change and this can influence grain size.

Puippe and Ibl (31) devised a method to investigate the effect of pulse current density by using an off time which was very much longer than the on time. The on time was varied to make the average current density the same as pulse current density was varied. Because the off time was much longer than the on time, varying the on time was considered not to have much influence since this constituted only a small part of the overall cycle time. Thus eliminating any ambiguities of interpretation of results caused

by the influence of the off time.

Using this method of investigation, Puippe discovered that for the systems he investigated, an increase in pulse current density always produced a reduction in grain size when other factors were held constant.

2.5.2 The Effect of Off Time on Deposit Grain Size.

The effect of the off time in pulse plating has also been studied by Puippe (31). It was found that an increase in off time lead to a grain refinement in cadmium plating but in grain growth for gold and copper. It was proposed that the most likely explanation for this observed effect was that for the gold and copper deposits, the off time allowed a recrystallisation of the deposit causing grain growth. For cadmium, it was proposed that the adsorption of sulphate ions could occur during the off time which could cause a reduction in grain size.

Unfortunately, Puippe's conclusions were based on the observed surface morphologies of deposits as revealed by scanning electron microscopy. This can be deceptive since the observed surface features are polycrystalline so an apparent increase in grain size may not necessarily be a true grain size increase. The only way to examine grain size effectively is by the use of the Transmission Electron Microscope.

It can be seen from the above that the effect of pulsed current on the properties of electrochemical systems in practical use is not usually predictable since each system will behave in a different way from a viewpoint of electrocrystallisation.

Chapter 3.

The Effect of Pulsed Current on The Properties of Electrodeposited Metals.

3.1. Electrochemical Properties.

Although the major uses of pulsed current in electrodeposition are concerned with modifying the physical and mechanical properties of metals such as hardness, ductility, porosity, grain size, purity, brightness or internal stress, the advantages which were claimed by earlier workers in the field were centred around modifying the electrochemical properties of the electrolytes. In particular, many workers claimed that higher plating rates could be obtained by the use of pulsed current. Ozerov et al. (32) claimed that the deposition rate could be increased indefinitely by decreasing the duration of the pulses. While it may be true that pulse current density may be increased as the pulse duration becomes shorter (provided that sufficient relaxation time is allowed), it has been shown by Cheh (10,33) that the limiting current density for both pulsed and periodic reverse current is less than for direct current plating. However, as discussed in the section on mass transport, it may be possible in some systems to increase the maximum practical rate of deposition because under suitable conditions, the formation of dendrites can be inhibited by the use of pulsed current (21).

3.1.1. Effect of Pulsed Current on Power Consumption.

Popov et al. (34) claimed that because the average overpotential of deposition was reduced, the power consumption for electrodeposition could also be reduced by the use of pulsed current. However, although the average overpotential is reduced by pulse

plating, the peak overpotential is increased and the plating cell has to be driven to this higher potential in order to maintain the same average plating rate. Thus as duty cycle is reduced, so the overall cell voltage increases. For the same plated area and current density, the current is the same for pulsed and direct current but the cell voltage is higher in the case of pulsed current. Since the power consumed is measured in Watts and the number of Watts is given by the product of the voltage and current, it is clear that more power is used in pulse plating than by plating with direct current. Popov later realised his mistake and published another paper (35) stating that pulsed current increased power consumption.

3.1.2. Effect of Pulsed Current on Deposit Metal Distribution.

The application of pulsed reverse current to cyanide copper electrolytes was found to give improved metal distribution. Most of the early work on cyanide copper electrolytes was carried out by Jernstedt who filed several patents on this (36,37,38,39). Because of the improvements in throwing power obtained with this electrolyte, it became widely believed that the use of modulated current would generally improve the throwing power of electrolytes. However, as the section on current distribution proves, the actual current distribution obtained with modulated current is less uniform from a point of view of macrothrowing power than direct current. The cyanide copper system appears to be fairly unique in its response to periodic reverse current and this was noted by Dini (40) in his review of periodic reverse plating up to 1963. The use of periodic reverse current also gives brighter deposits from a cyanide copper electrolyte and the deposit has a banded structure (40).

Aston University Library & Information Services
Aston Triangle Birmingham B4 7ET England

An earlier review by Bayerns (41) which covers the literature on plating with modulated current up to 1954 notes the effect of increasing frequency on the magnitude of the effects produced by the application of pulsed current. It was stated by Bayerns that the magnitude of the effect produced decreases as frequency is increased and the optimum frequency range was stated to be 0.1 to 100 Hz. This may have been the first observations of the effects of Faradaic flattening due to the capacitance of the double layer.

3.2. Physical Properties of Metals Deposited by Pulsed Current.

By the use of pulsed current, it is possible to plate at current densities and potentials during the pulse which would not be possible by the use of direct current. As the magnitude of the potential and current density affect the rate of nucleation, the physical properties of deposits produced by the use of pulsed current may differ from deposits obtained by direct current. Early evidence of this was provided by Hickling and Rothbaum (42) who claimed finer grained deposits in copper deposits obtained by the use of periodic reverse current. In this section, a brief review of some of the effects of pulsed current on the physical properties of deposits will be presented.

3.2.1. The Effect of Pulsed Current on the Porosity of Deposits.

Porosity may be defined in different ways :-

i) Bulk Porosity - This is defined as the volume fraction of the deposit occupied by voids and discontinuities and will be described more fully in the next section.

ii) Transverse Porosity - This is defined as the fraction of the total surface area at which the basis metal is exposed. It is transverse porosity which is normally referred to when porosity is discussed. It is usually quantified in terms of pores / cm^2.

Factors affecting porosity include surface roughness [43,44], surface defects in the substrate [45], bath parameters [46] and thickness of deposit [47].

Because pulse plating enhances the nucleation rate for a given rate of deposition as compared to direct current, improved surface coverage and a denser build-up of grains may occur. Thus pulse plating may produce deposits of lower porosity as compared to direct current provided that other factors such as thickness and surface roughness are not changed. This has been reported in the literature for gold [48,49,50,51], copper [52], nickel [53] and cobalt [54].

3.2.2. The Effect of Pulsed Current on the Incorporation of Impurities.

i. Inclusion of Hydrogen.

Most electroplating electrolytes have cathodic efficiencies which are less than 100%. This means that an alternative electrode reaction occurs simultaneously with metal deposition. The most common alternative electrode reaction is the discharge of hydrogen by the following process :-

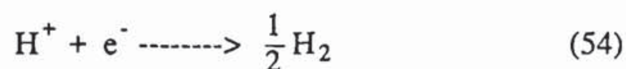

$$H^+ + e^- \text{--------}> \frac{1}{2}H_2 \qquad (54)$$

Some of the hydrogen which is discharged at the cathode is released as hydrogen gas

but some is usually retained in the deposit either as absorbed hydrogen gas, or in some cases chemically combined as a hydride. This hydrogen inclusion can affect the properties of the deposit. For example, it is well known that in zinc plating absorbtion of hydrogen into the substrate can cause embrittlement problems. Metals such as nickel which have a high affinity for hydrogen also absorb hydrogen even though the cathodic efficiency may be high. It should be noted here that the use of pulsed current means that metal is deposited at a higher peak overpotential and this can change the electrode kinetics. Thus the cathode efficiency for metal deposition can be affected by the use of pulsed current. This effect has been noted in the deposition of gold (55)

Pulse plating with unipolar pulses allows a relaxation time which allows desorption of hydrogen from the cathode surface. Thus it may be expected that the use of pulsed current would reduce the hydrogen content of electrodeposits.

Paatsch (56) performed electrochemical hydrogen permeation measurements on high tensile steel specimens after the application of a zinc coating and found that the time period for the first zinc nucleation was most important with respect to the penetration of the co-deposited hydrogen into the basis metal. Once a thin layer of zinc is formed, this acts as a barrier towards further hydrogen permeation. It was found that the use of pulsed current with duty cycles of 10% or less with a short pulse time of 0.1 ms or less gave much lower values for the coefficient of hydrogen diffusion than direct current. This was thought to occur because of the reduced porosity of the zinc due to the higher nucleation rate and also because of a change in electrode kinetics (56).

Tensile testing of plated parts was also carried out and it was discovered that the ocurrence of hydrogen embrittlement could be reduced by the use of pulsed current (57).

Kleinekathofer and Raub (58,59) measured the hydrogen contents of nickel deposits from a Watts and sulphamate electrolyte using a hot extraction technique. They found significantly lower hydrogen contents in deposits produced by pulsed current as compared to direct current with the same electrolyte parameters. This reduction in hydrogen content was thought to occur due to desorption of hydrogen during the off time.

A similar theory was proposed by Faust et al. (60) to explain the observed reduction of internal stress in chromium deposits. It was proposed that during the off time, hydrides of chromium could decompose which would prevent later decomposition when chromium had been deposited on top of the hydride. Knodler (61) measured the hydrogen contents of chromium deposits and found that pulse plated deposits had very high hydrogen contents under certain conditions. This appears to contradict what would be expected. This observation will be fully discussed in later chapters.

Palladium is a metal which has a very high affinity for hydrogen. Since palladium plating electrolytes usually deposit at low efficiency, palladium deposits can have very high hydrogen contents. The effect of pulsed current on the hydrogen contents of palladium deposits has been studied by Locarnini and Ibl (62), it was found that the hydrogen contents of deposits produced by pulsed current were much lower than those produced by direct current.

ii. Inclusion of Organic Impurities.

The inclusion of organic impurities in electrodeposits may arise either from the inclusion of organic material which has been added to modify the properties of the

deposit (i.e. brighteners, levellers or their breakdown products), or from the inclusion of complexing anions or their breakdown products.

The rate of incorporation of organic material into an electrodeposited coating is controlled by adsorption and diffusion. At the same time, the material may undergo electrochemical reaction and breakdown. Little work has been done on the effects of pulsed current on the incorporation of brighteners. Kleinekathofer et al.[58] investigated the effect of pulse plating on the microthrowing power of Watt's nickel electrolytes containing various organic additives. With the addition of 2-butene-1,4 - diol, the microthrowing power was found to be worse with pulsed current than with direct current.

Addition of either saccharin or N- ethylpyridinium bromide was also found to reduce microthrowing power. However, a combination of 0.5 g/l of N- ethypyridinium bromide and 0.25 g/l of saccharin produced better levelling with pulsed current than with direct current using a duty cycle of 50% and a frequency of 170 Hz. No attempt was made to explain these observed effects but it appeared that pulsed current could influence the incorporation mechanism of brighteners. This topic constitutes a major part of the work undertaken in the present research programme on the electrodeposition of copper.

The first major use of pulse plating was in the deposition of precious metals, in particular, the deposition of gold has received much attention. In the connector industry, the use of alloy gold deposits is widely used. These deposits are almost invariably produced from an acidic electrolyte containing gold potassium cyanide and an organic buffer (citrate / citric acid is popular) in the presence of small amounts of cobalt or nickel as a brightener. These deposits usually have a purity of > 98% gold and

have high hardness and wear resistance. By dissolving deposits from these electrolytes in Aqua-Regia, Munier (63) found large amounts of carbonaceous material. He suggested that these inclusions consisted of polymeric hydrocyanic acid. It is now established that in the cobalt containing electrolytes, the included "polymer" consists largely of a cobalt complex, $KCo[Au(CN)_2]_3$, which is precipitated at the cathode during deposition [64,65,66]. The application of pulsed current to these alloy gold systems has been studied by several workers and it is firmly established that the use of pulsed current produces a large reduction in the amount of this complex which is included in the deposits [67,68]. This production of purer gold deposits is not necessarily an advantage because these deposits are usually used on connectors where wear resistance is important. In these cases, an increase in wear rate has been noted by several workers. Branik and Schnabl [69] showed that insertion and withdrawal forces were higher with connectors produced by pulse plating techniques and that wear rates were higher. Other workers [70,71,72] have found similar results. However, these findings have been contradicted by Antler [73] who claimed that organic contaminants from the air could provide sufficient lubrication.

Overall, the weight of evidence suggests that the "polymer" inclusions in gold deposits provide a lubricant film which is an important part of the wear mechanism. For this reason, pulse plating should be used with caution when connectors are being plated.

3.2.3. Effect of Pulsed Current on Grain Size and Deposit Morphology.

i. Grain Size.

This topic has been dealt with to some degree in the section on electrocrystallisation in chapter 2. As already mentioned, Puippe [31] carried out a scientific study of the effect

of pulse current density and off time. He concluded that grain size was reduced by increasing current density and that the effect of the off time depended on the specific electrochemical system. A study of the surface by optical methods or the use of an S.E.M. reveals surface topographical features and not true grain size. Grain size can only be measured by the use of the Transmission Electron Microscope for most electrodeposits because of their small grain size (optical methods can be used after etching if the grain size is large enough). Because of the difficulties in specimen preparation for this technique, there is little literature available on the effect of pulsed current on grain size.

T.E.M. studies have been carried out by Fluhmann et al. (74) on gold / cobalt alloys. The conditions used were :-

a) Direct Current, 1 A/dm^2.
b) Pulsed Current, 10 ms on, 20 ms off, Average current density 1 A/dm^2.
c) Pulsed Current, 10 ms on, 100 ms off, Average current density 1 A/dm^2.

In the case of the coating produced by direct current, many inclusions were noted in the deposit with diameters of approximately 250 A, and with a density of approximately $10^{19}/ cm^3$. Some twinning was noted but dislocations were absent.

In the case of pulsed current 10/20, the grain size was observed to be greater than that produced by direct current and was measured to be about 500 A. Twinning was more pronounced. Some inclusions were noted in the deposit and their density was estimated to be around half of that observed for direct current.

In the case of pulsed current 10/100, the grain size showed a further increase to around 1000 A. There was a complete absence of inclusions in the deposit. Twinning was increased further and dislocations within the crystallites were also visible. It was proposed by Puippe [31] that this increase in grain size was due to recrystallisation during the off time.

T.E.M. studies were carried out by Holmbom and Jacobson [75] on deposition of pure gold by direct current and pulsed current using an average current density of 5 A/dm^2, a 20% duty cycle and frequencies of 20, 200 and 2000 Hz. It was found in this study that plating with D.C. and the lowest pulse plating frequency of 20 Hz, the grain size obtained was around 350 nm. At the higher frequencies of 200 and 2000 Hz, the grain size was reduced to around 200 nm. This is completely different from the observations of Fluhmann [74]. A possible explanation for this apparent contradiction is that in the case of the alloy gold, a large amount of inclusions are co-deposited when plating with direct current. These inclusions will tend to limit grain size by blocking growth sites and encouraging fresh nucleation. With pure gold electrolytes, the inclusion density is much lower. Pulse plating has been shown to produce deposits from alloy gold solutions which have a much lower inclusion density. Thus growth sites are no longer blocked and the deposit grain size increases. With the pure gold electrolytes, since the inclusion density is low, pulsed current has little effect though the increased nucleation rate caused by the increased pulsed current density (as compared to D.C.) may be expected to give some grain refinement.

It appears therefore that Puippe's [31] theory that the observed increase in grain size is due to recrystallisation during the off time may be incorrect in this case since this recrystallisation would presumably occur for both pure and alloy golds. It is more likely that the observed increase in grain size for alloy golds is due to the reduction in

inclusion density.

ii. Deposit Morphology.

Because of its influence on nucleation and growth during the electrocrystallisation process, Pulse plating can influence the surface topography of the growing deposit. Since S.E.M. of surface topographies is a straightforward technique, this has been extensively studied. Numerous examples of the effect of pulsed current on the surface topography of deposits are presented in the book "Theory and Practice of Pulse Plating." Published by the A.E.S.F. [2]. However, due to the diversity of electrolytes, the effects are not predictable. Puippe [31] has shown that for cadmium deposition, a finer surface texture is obtained as compared to deposition with direct current whereas for copper a coarser texture is obtained.

Electrodeposited metals often have a preferred orientation as revealed by X-ray diffraction analysis due to the way the deposit crystallises. Because pulsed current can affect electrocrystallisation, it can influence the preferred orientation of deposits. Some of the results which have been obtained are as follows :-

a) Gold.

Holmbom and Jacobson [75] found a preferred orientation of (111) for gold deposits from a pure gold citrate buffered bath. This preferred orientation was not changed by the application of pulsed current.

b) Silver.

Hayashi et al. (76) studied the influence of pulsed and direct current on silver deposition from both ammoniacal and cyanide based electrolytes. With the cyanide based electrolyte, it was found that with direct current plating, an increase in current density led to a reduction in the preferred orientation in the (111) plane whereas pulsed current produced an increase in the (111) orientation with increasing pulse current density.

c) Palladium - Nickel alloys.

Fukumoto et al. (77) made an investigation of the effect of increasing current density on the orientation of palladium nickel deposits as deposited from an ammoniacal electrolyte. At low current densities, a (111) preferred orientation was obtained. At higher current densities, the (111) orientation decreased and the (110) orientation increased. The same trend was observed in pulse plating with increasing current density.

3.2.4. The Effect of Pulsed Current on the Hardness of Electrodeposits.

Since the application of pulsed current influences the electrocrystallisation of deposits it may be expected that in certain circumstances the hardness of deposits may be affected. Deposition parameters which cause a decrease in grain size and an increase in brightness usually increase hardness. Sutter et al (78) measured hardness of deposits from Watt's and sulphamate nickel electrolytes using an average current density of 5 A/dm^2, a frequency of 50Hz and a variable pulse current density. He found that hardness increased in a linear manner with increased current density. These results are shown in figures 7 and 8.

Figure 7. Hardness vs. Pulse Current Density of Nickel Deposited from a Watt's Electrolyte. (After Sutter et al. (78)).

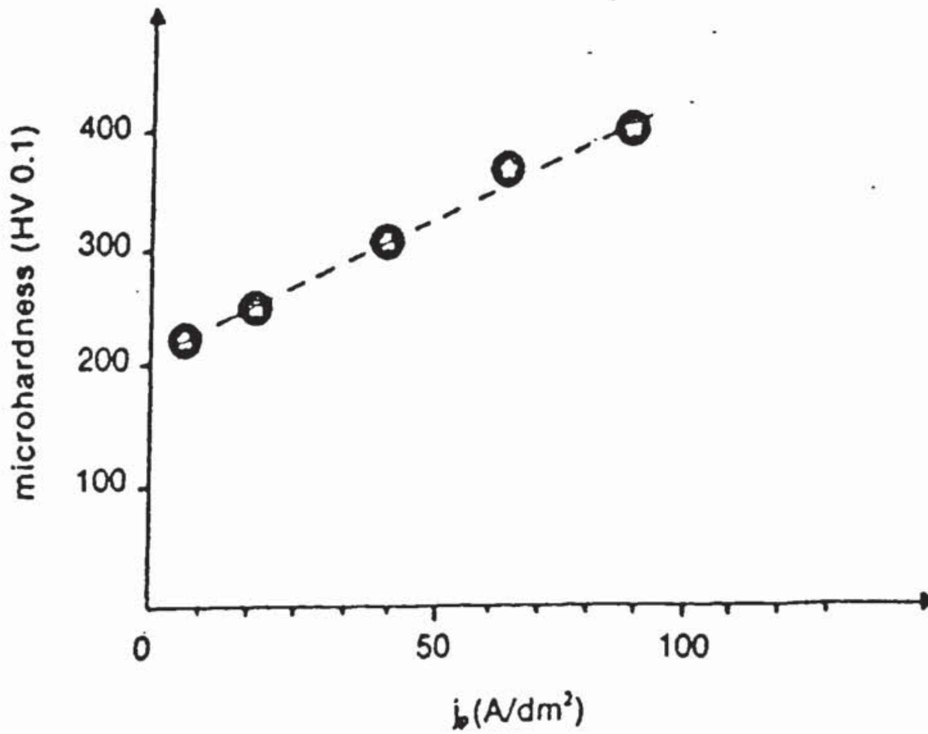

Figure 8. Hardness vs. Pulse Current Density of Nickel Deposited from a Sulphamate Electrolyte. (After Sutter et al. (78)).

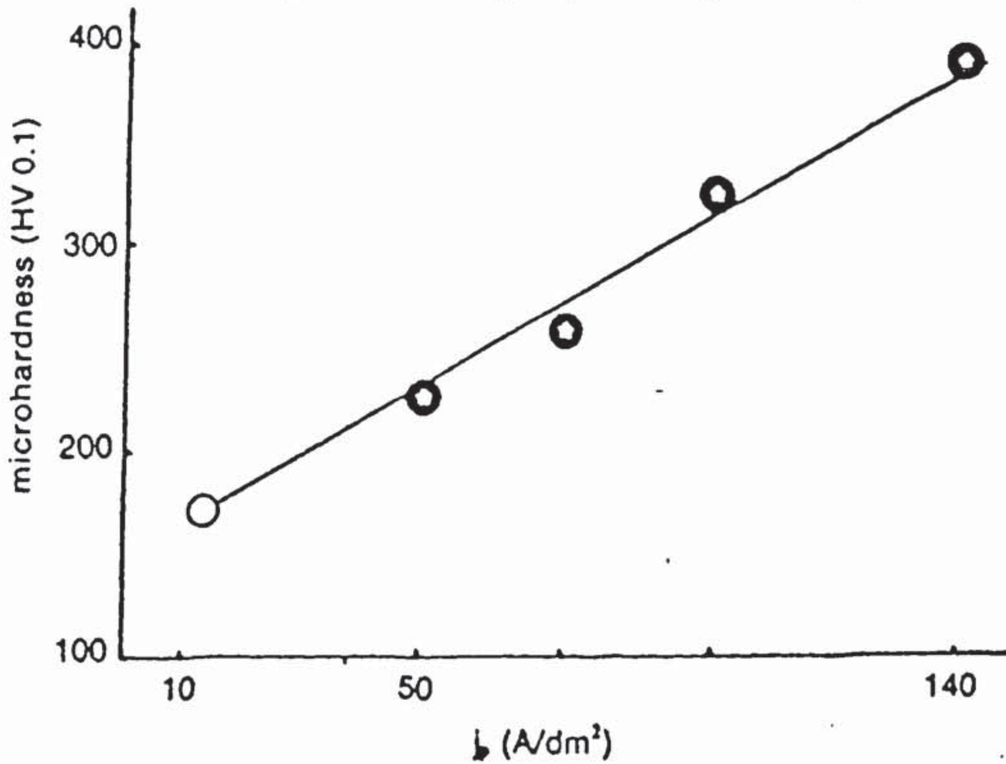

Kendrick et al. (79,80) used pulsed reverse current on chloride based nickel plating electrolytes and produced deposits which were either harder or softer than those produced by direct current depending on the conditions which were used.Some of these results are reproduced in table 1.It was found that short periods of de-plating at low frequencies favoured nucleation rather than growth and so produced fine grained, lustrous deposits.

Table 1. Effect of Pulsed Reverse Current on the Microhardness of Nickel Deposits from an all Chloride Electrolyte.(79)

Frequency (Hz)	Cathode Current Density (A/dm^2)	Anode Current Density (A/dm^2)	% Deplating (%)	Hardness (Hv 50)
D.C.	20	---	---	290
10	20	10	25	368
50	20	5	25	345
100	20	30	25	249
400	20	15	25	171
500	20	20	25	145

Several workers have demonstrated that the deposition of chromium from hexavalent electrolytes by the use of pulsed reverse current causes a reduction in hardness of deposits as compared to deposition with direct current.(81,82). Also it has been shown that the use of unipolar pulses in the deposition of chromium causes significant softening of the deposit (60).

Dini and Johnson (83) studied the use of pulsed current and asymmetric alternating current for the electrodeposition of pure gold from a citrate buffered electrolyte. It was found that the hardness of deposits produced by D.C. and pulsed current were the same but that a significant increase in hardness was obtained by the use of asymmetric alternating current. Knodler (67) measured the hardness of deposits obtained from a

gold-cobalt alloy plating solution at various cobalt contents using both pulsed and direct current using an average current density of $1A/dm^2$,a duty cycle of 10% and a frequency of 44 Hz. These results are reproduced in table 2. Perhaps the surprising feature about these results is that the pulse plated hardnesses are higher than direct current hardnesses although, according to Fluhmann et al. (74), the grain size of the pulse plated deposits is larger than the direct current plated deposits. This shows that hardness is not necessarily related solely to grain size. Pulse plated deposits have a higher density than direct current plated deposits because the amount of 'polymer' inclusion is less and this factor may account for the slight difference in hardness.

Table 2. Effect of Pulsed Current on the Hardness of Deposits from a Gold-Cobalt Alloy Electrolyte.

Cobalt Content (g/l)	Hardness (Hv 100g) (D.C.)	Hardness (Hv 100g) (P.C.)
0.05	198	205
0.10	198	205
0.20	192	228
0.30	198	220
0.40	198	212
0.50	191	220

It is also interesting to note that from these results, it can be seen that hardness values remain remarkably constant over a wide range of cobalt contents.

3.2.5. The Effect of Pulsed Current on the Ductility and Internal Stress of Deposits.

i. Ductility.

Improvements in the ductility of nickel deposited from an all chloride electrolyte by the use of pulsed reverse current has been noted by Kendrick et al.(79,80). They found

that pulse parameters which produced a soft nickel deposit also produced a ductile deposit.

Because the amount of impurities incorporated from alloy gold electrolytes is less with pulse plating techniques than with direct current, a larger grain size results and this also causes an increase in the ductility of the deposit (although it must be remembered that grain size and ductility are not necessarily linked). This effect has been noted by Knodler (67) and Dini and Johnson (83).

In general, little data have been published in the literature on the effects of pulsed current on the ductility of electrodeposits and this represents an area where there are gaps in the knowledge.

ii. Internal Stress.

Many electrodeposits are deposited in a stressed condition. This was even reported by Gore in 1858 (84). The first measurement of stress in an electrodeposits was made by Mills in 1877 (85). This was done by observing the rise or fall of mercury in a thermometer bulb which was chemically silvered and plated with nickel.

Although the occurrence of stress has been known for a long time, no overall theory of the cause of macrostress in electrodeposits has been established. Macrostresses can be tensile or compressive and theories have been developed to explain these conditions. A comprehensive review of the literature dealing with measurement of stress (86), effect of plating parameters on stress (87) and theories of the origins of stress in electrodeposits (88) has been published by Weil. It is not proposed to give a detailed discussion on the theory of the origins of stress here but to mention some of the work

which has been carried out to determine the effect of pulsed current on the internal stress of various electrodeposits.

Crossley, Kendrick and Mitchell (80) found that the use of pulsed reverse current to deposit nickel from an all chloride nickel electrolyte could produce deposits of a considerably lower internal stress than deposits produced by direct current. Kleinekathofer and Raub (58,59) noted that the use of unipolar pulses for the deposition of nickel from Watt's and chloride based electrolytes produced an increase in the level of tensile stress in the deposits. Some of the early research on this present project was to investigate the effect of pulsed current on the internal stress of deposits from a Watt's electrolyte. Some of the results obtained are shown in figure 9. This figure indicates the mean stress obtained after 20 minutes plating (measured with a spiral contractometer) at two different frequencies and varying duty cycle. It can be seen that the tensile stress increases as the duty cycle is reduced and that the effect is greater at the lower frequency. At the high frequency (4999 Hz), Faradaic flattening probably occurs which accounts for this observation. These results confirm the findings of Kleinekathofer and Raub (58,59).

It was also claimed by Kleinekathofer and Raub that stress in sulphamate based electrolytes for the deposition of nickel could be controlled by the application of pulsed current since the level of internal stress tended towards zero as the duty cycle was decreased. However, the stress in the deposits in the experiments was compressive and so tended towards zero because it became more tensile. This situation is unlikely to be found in commercial practice because the current densities used in commercial practice are higher than those used by Kleinekathofer and Raub and the stress in most commercially applied deposits tends to be slightly tensile. On small scale experiments, anodic oxidation of the sulphamate ion can occur which produces a compound which

Figure 9. Mean Internal Stress vs. Duty Cycle at Two Different Frequencies of Nickel Deposited from Watt's Electrolyte.

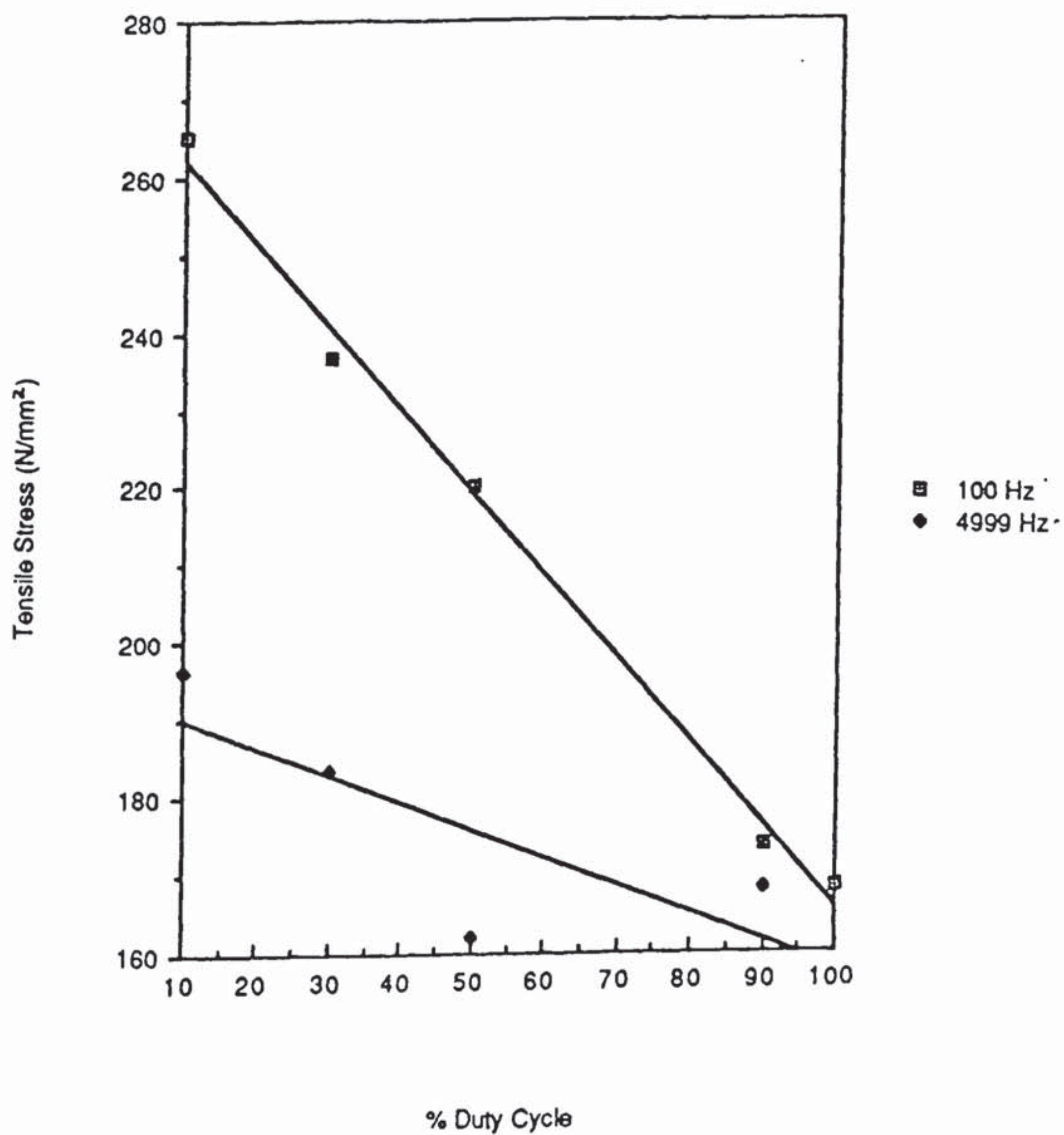

causes deposits to become highly compressively stressed (89,90). Thus it is difficult to design experiments which accurately reflect commercial practice. It is most likely that the use of unipolar pulses in nickel electrolytes tends to make internal stresses more tensile regardless of the system. The use of pulsed reverse current has been shown to reduce the level of tensile stress in chloride based solutions [80].

The use of unipolar pulses in the deposition of chromium has been shown by Faust et al. [60] to give crack free deposits of chromium. This was thought to be due to a decrease in the internal stress of the deposits. The use of pulsed reverse current also produces a reduction in crack density of deposits of chromium [81,82] so it is probable that this also causes a reduction in tensile stress. The effect of pulsed current on the internal stress of chromium deposits has been investigated in this research and will be more fully discussed in later chapters. Bidmead et al.[91] used current surging (the application of current pulses to a continuous "base" current) to increase the level of internal stress of deposits and promote microcracking of decorative deposits at lower thicknesses than would otherwise have been possible. Thus, current interruptions or reversals when chromium plating tend to prevent the deposit from cracking whereas current surging tends to promote cracking.

Knodler [67] found that failure of alloy gold plated contacts plated by direct current could often be attributed to cracking due to high tensile stresses being developed. He found that the use of pulsed current could significantly reduce the level of internal stress in gold deposits. Some of these results are reproduced in figure 10. This reduction in stress could be attributed to the increase in the purity of deposits obtained from these electrolytes.

Figure 10. Internal Stress of D.C. and P.C. Plated Gold/Cobalt and Gold/Nickel Alloy Deposits vs. Temperature. (After Knodler. (67)).

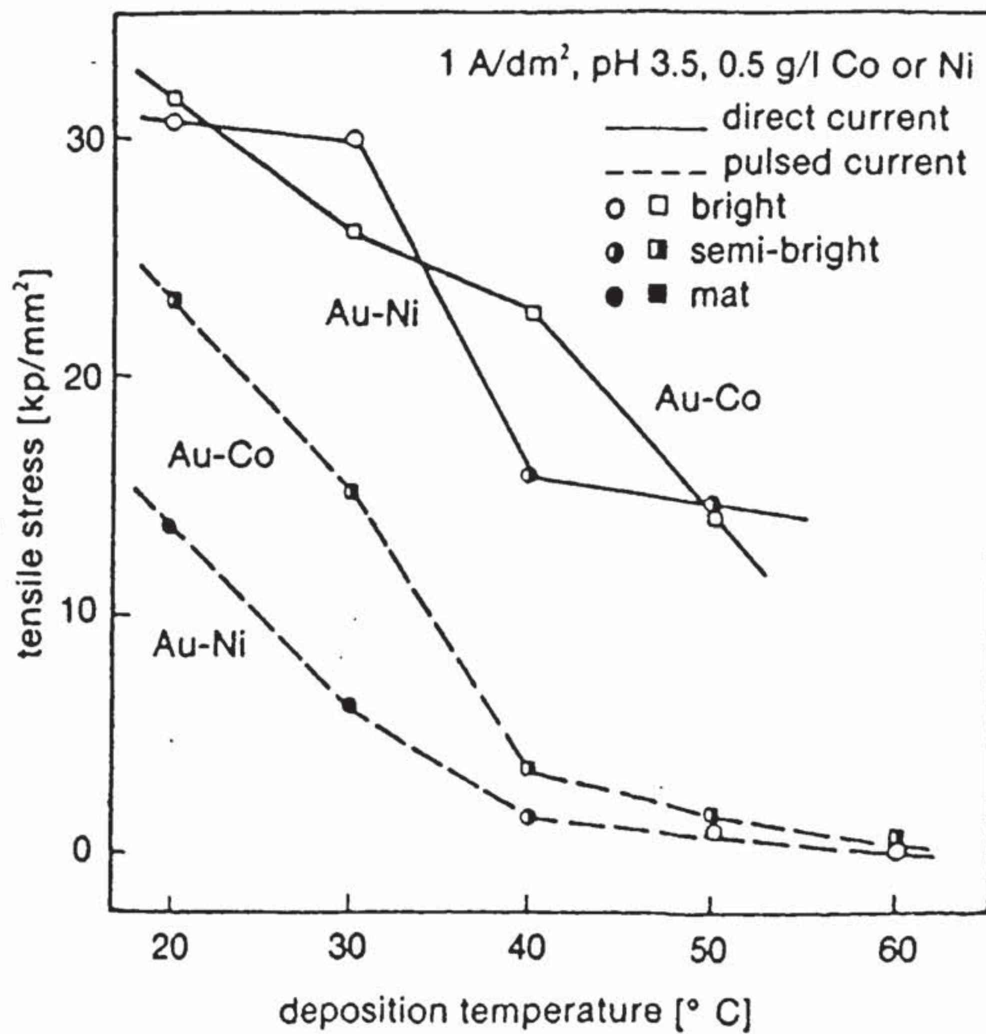

3.2.6. The Effect of Pulsed Current on the Properties of Electrodeposited Alloys.

With the use of pulsed current, it is possible to plate at deposition potentials which would not be practical using direct current due to mass transport limitations. Thus, pulse plating has potential applications in the area of difficult to deposit alloys. By programming trains of pulses with different deposition potentials, it is also possible to produce compositionaly modulated alloys from one single electrolyte. This has been achieved for deposits of copper/nickel and copper/cobalt (92,93).

Lashmore et al. (94) electrodeposited alloys of nickel/phosphorus by the use of pulsed current. The structures of the deposits produced were found to be amorphous glasses and alloys with a phosphorus content of up to 40 atomic percent were achieved. With direct current, a much lower phosphorus content was obtained. The pulse plated deposits were found to have a higher hardness and a more uniform microstructure.

Lashmore et al. (95) also deposited alloys of nickel/chromium by the use of pulsed current. the amount of chromium could be controlled in the deposit by changing the duty cycle for a given average rate of deposition. It was found that the amount of chromium in the deposit was decreased as the duty cycle was reduced. Pulse plated deposits were also found to have a finer surface texture than deposits produced by direct current.

Pulse plating has also been used to control the alloy composition in palladium/nickel deposition (96,97) and for deposition of palladium /silver (98) and nickel/molybdenum (99). The possible applications of pulsed current in the deposition of alloys are numerous and much work remains to be done to establish the theory and practice of

plating alloys with pulsed current. A review of the applications of pulsed current to the deposition of alloys is given in the A.E.S.F. publication "Theory and Practice of Pulse Plating." [2].

Chapter 4.

The Electrodeposition of Chromium.

4.1. Introduction.

Chromium is a metal which is widely used as an electrodeposited coating. It is applied as a decorative coating over a bright nickel underlay and this combination gives good appearance with high corrosion resistance. Chromium also has several useful engineering properties. The hardness and wear resistance of the coating is very good and chromium plated surfaces have a low coefficient of friction when run against other metals [(100)].

The deposition of chromium from aqueous solutions is not as straightforward as for many other metals due to the chemical properties of chromium. Chromium forms salts with a stable oxidation state of III. Thus, the trivalent oxidation state is the stable state. Trivalent metal cations have a high charge density and so have a strong tendency to form tightly bound complexes with ligands which makes them difficult to reduce. Also, trivalent chromium can easily be oxidised to hexavalent chromium by anodic oxidation in the plating cell. A buildup of hexavalent chromium will reduce coverage and plating efficiency. For these reasons, the application of trivalent electrolytes in commercial electroplating practice has been limited to electrowinning applications[(101)] until recently, when decorative trivalent chromium electroplating processes have been developed commercially [(102)].

Divalent chromium is strongly reducing and is unstable in aqueous solution so it is not possible to formulate aqueous electrolytes based on these salts. Thus chromium is

deposited commercially largely from electrolytes based on chromic oxide (CrO_3). In aqueous solution, this reacts with water to form the dichromate ion ($Cr_2O_7^{2-}$). On first consideration, the electrochemical reduction of chromium from this species seems to be unlikely since six electrons have to be transferred to reduce the chromium from the hexavalent to the metallic state. Also, oxygen is chemically bonded to the chromium and these bonds have to be broken before the chromium can deposit. As a solution of chromic oxide (also called chromic acid) is highly acidic, it would be expected that reduction of hydrogen would be the only reaction. However, it was discovered by Fink et al.(103) and Liebreich (104) in 1924 that chromium could be deposited from electrolytes containing chromic oxide and a small quantity of sulphate ion. This was the foundation of modern chromium electroplating and electrolytes using only sulphate as a catalyst are still widely used today. An early history of chromium plating is given by Dennis and Such (101) in their book " Nickel and Chromium Plating." An improvement in the cathodic efficiency of chromium plating electrolytes came about with the introduction of silicofluoride ions as a catalyst in combination with sulphate ions (105). These electrolytes give higher efficiencies but the presence of fluoride ions leads to the cathodic etching of the substrate in low current density areas where chromium does not plate. Recently, high efficiency electrolytes have been developed which are fluoride free and consequently have a low etch rate on steel (106).

It is proposed in this chapter to give an outline of the types of electrolytes, mechanism and properties of chromium plate and to review the work which has been carried out on the deposition of chromium by the use of pulsed current.

4.2. The Mechanism of Chromium Plating.

As has been mentioned in the introduction, it is not possible to produce chromium by electrolysis of a solution of chromic acid in water if the chromic acid is of very high purity (100). There must also be present one or more species which act as catalysts. the commonest of these are the sulphate and silicofluoride ions. For successful operation, the ratio of chromic acid to catalyst must be maintained within definite limits. In the case of sulphate ion, this ratio is about 100:1. At present, there is no completely satisfactory theory to explain the mechanism of chromium deposition. Early theories were based on the assumption that the reduction of chromium was from the trivalent state which is formed in hexavalent electrolytes after a period of electrolysis. Kasper (107) suggested that the deposition of chromium took place via the direct reduction of Cr(VI). This theory was supported by work by Ogburn and Brenner (108) who showed, using radioactive isotopes of hexavalent and trivalent chromium, that electrodeposition of chromium was from the hexavalent chromium. Many of the theories proposed for the deposition of chromium do not adequately explain the role of the catalyst. Silverman (109) suggested that the addition of sulphate to a solution of chromic acid produced complexes with deposition taking place from a complex cation. This theory does not explain the fact that the optimum ratio for sulphate ions is 100:1. With this ratio, bulk complexing of the chromium in solution is unlikely to occur to a great extent. It is more likely that the sulphate ion is adsorbed at the cathode surface and acts as an exchange ion in the formation of a cation complex which can ultimately be reduced to metallic chromium.

It has been established by Kasper (107) that a film of partially reduced chromium compounds is formed at the cathode surface during deposition. Rogers (110) stressed

the importance of the cathode film and its pH on the properties of the chromium deposited. This cathode film is necessary for the deposition of chromium and the catalyst system used in the electrolyte can affect its composition and formation. Chromium is deposited from complexes formed in this film rather than from the bulk electrolyte. Snavely (111) has shown that hexavalent chromium is capable of being reduced to trivalent chromium by atomic hydrogen so it is probable that the first stages of reduction may be by chemical as well as electrochemical mechanisms.

Formation of the cathode film depends upon a number of variables. Variation of temperature, electrolyte composition or current density can change the characteristics of the film. Current interruptions may also dramatically change the film composition. For this reason, chromium plating electrolytes are very sensitive to current interruptions. Changes in the characteristics of the cathode film can cause changes in deposit characteristics and current efficiency.

4.3. Operating Parameters for the Deposition of Chromium.

4.3.1. Electrolyte Constituents.

Chromium plating baths are essentially very simple in bath chemistry and generally contain only chromic acid as the source of chromium for deposition and one or more catalyst anions. Where complicated shapes are to be plated, an electrolyte catalysed only by sulphate is usually employed because the etch rate of the electrolyte on areas which remain unplated is much lower than that of mixed catalyst electrolytes.

Higher efficiency electrolytes usually contain a mixture of sulphate and silicofluoride ions as catalysts. Maintaining the correct concentration of silicofluoride ions in solution

is difficult due to the low solubility of many silicofluoride salts. Self regulating baths use a combination of sparingly soluble silicofluoride and sulphate salts which give the correct concentration of sulphate and silicofluoride at the operating temperature. These baths have the disadvantage that following a change in bath temperature, it takes time for the catalyst system to re-equilibriate. A more modern development is the development of totally soluble silicofluoride catalysts which can be added on an ampere hour basis. These catalyst systems are usually based on more soluble salts such as magnesium silicofluoride.

The most recent development has been the introduction of fluoride free catalyst systems which have a relatively high efficiency, the first of these systems was developed by M&T Chemicals Ltd [106]. These systems have the advantage of a low etch rate on exposed areas of steel and high cathodic efficiency, however, they can be aggressive to the insoluble lead anodes which are used in chromium plating installations. Lead anodes are always used in chromium plating because anodes of chromium dissolve with an efficiency of 100% or higher whereas the chromium only deposits with an efficiency of 12 - 26%. This would lead to a buildup of chromium in the solution. Also, the chromium, as dissolved from this type of anode, would be trivalent chromium which would not deposit from these electrolytes. Lead anodes when operated at the correct current density form a film of lead dioxide on their surface which is capable of oxidising trivalent chromium to hexavalent. Buildup of trivalent chromium is thus prevented since it is oxidised at the anode. Pure lead is rarely used as an anode material since this is attacked by the electrolyte to an unacceptable degree (forming lead chromate). Alloy anodes of antimonial lead are more commonly used as these are harder and have longer life.

4.3.2. Operating Conditions.

i. Chromic Acid Concentration and Catalyst Ratio.

Chromium can be deposited from baths containing from around 50 to 1000 g/l of chromic acid. Most commercial electrolytes are based on chromic acid concentrations of 150 to 400 g/l. Baths containing lower concentrations of chromic acid tend to have higher cathodic efficiency for a given catalyst system but are lower in conductivity and thus require a higher voltage for a given current density. Dilute baths are also much more sensitive than the more concentrated baths to changes in catalyst concentration from dragin or dragout and so require more careful analysis and maintenance. Usually, the more concentrated solutions are used for decorative applications and the more dilute formulations are employed for hard chromium applications.

From a commercial point of view, there is much to be gained from using the more dilute formulations where possible. Chromium is an expensive metal and dragout is difficult to treat due to the amphoteric nature of hexavalent and trivalent chromium ions. Dilute solutions are less viscous than concentrated solutions and contain less chromium. Thus dragout is minimised by using these formulations and effluent treatment costs are reduced.

ii. Temperature and Current Density.

The thickness and composition of the cathode film depends on the temperature of the electrolyte and the current density at which the deposition is carried out. At low current densities, the cathode film is not formed so no deposition of chromium can occur.

Because of this, the covering power of chromium solutions is very poor and high current densities have to be used to deposit chromium. Normally, the optimum temperature for the maximum bright plating range goes up as the average current density is increased, thus, hard chromium electrolytes are usually operated at somewhat higher temperatures than decorative solutions. Table 3 shows some typical values for temperature, current density and cathode current efficiency for various electrolytes (101).

Table 3. Operating Conditions for Various Chromium Plating Processes.

Type of Deposit	Temperature of Solution (°C)	Current Density (A/dm^2)	Cathode Efficiency (%)
DECORATIVE.			
i) Sulphate Catalysed	38	10	8
ii) Sulphate/silicofluoride	45	15	15
HARD.			
i) Sulphate Catalysed	55	50	12
ii) Sulphate/silicofluoride	55	50	22

It should be noted in this section that the cathode current efficiency for deposition is also a variable which is current density dependent. Cathode efficiency falls in chromium plating processes as the current density is reduced. This means that the throwing power of the solutions is very poor. For hard chromium applications, special anode arrangements have to be made to obtain an even deposit on awkwardly shaped parts.

4.4. Physical Properties of Electrodeposited Chromium.

Chromium is electrodeposited from hexavalent electrolytes in the form of body centred cubic chromium and deposits with an almost perfect (111) orientation (112). It is a relatively active metal and so forms a thin oxide film on its surface. This tenacious oxide film serves to protect the underlying metal from further oxidation so that chromium deposits stay bright for extended periods of time. As deposited from conventional electrolytes, chromium has a hardness of 800 - 1000 Hv and good wear resistance (Although the hardness is greatly reduced by heat treatment which presumably causes some recrystallisation). Electrodeposited chromium is extremely brittle and it is not possible to measure the ductility by conventional means.

Chromium deposits with a high tensile stress which usually exceeds the ultimate tensile strength of the coating. This causes the deposit to crack spontaneously as plating proceeds. Cracking causes stress relief in the coating and means that the mean internal stresses within the coating tend to decrease with increasing thickness. Cracking of chromium deposits is a cyclic process with time. Compressive stresses have been noted in very thick chromium deposits (113). This was postulated to occur due to the wedge effect of chromium deposited into already existing cracks.

During the early stages of deposition, the substrate has a large influence on the sign and magnitude of the internal stresses. When chromium is deposited onto bright nickel, hydrogen is adsorbed by the nickel coating which produces very large compressive stresses. This effect has been noted by Dennis (114). On steel, this effect is not obtained and stresses are tensile even during the first stages of deposition. Thus the true stress of the chromium coating is not measured. Caution must therefore be used in

choosing experimental technique for stress determination.

Snavely [111] deposited hexagonal close packed and face centered cubic hydrides of chromium instead of the more usual body centred cubic chromium metal by modifying the deposition parameters. He proposed that the structure of the chromium deposited from the hexavalent electrolyte was dependent on the pH of the cathode film and that conditions producing a high pH in the cathode film would produce hydride containing deposits whereas a low pH would give body centred cubic chromium metal. Snavely believed that chromium was initially deposited as a hydride in all cases and that the stability of these chromium hydrides was increased with an increase in pH. Thus at low cathode film pH's, the hydride would decompose very quickly to b.c.c. chromium with a resultant shrinkage of some 15%. Because the coating is restrained in the plane of the substrate, this shrinkage was proposed as the cause of the high tensile stress and subsequent cracking of the chromium deposit.

4.5. The Effect of Pulsed Current on Electrodeposited Chromium.

As has already been noted, hexavalent chromium plating electrolytes are very sensitive to current interruptions, so much so that single phase rectification is not usually adequate for commercial operation because the ripple of the current is sufficient to cause "whitewashing" and to cause the deposit to become soft. The reason for this sensitivity to current interruptions is probably the effect of these on the formation and composition of the cathode film.

Probably the first use of pulsed current to electrodeposit chromium was by Faust et al.[60] who used pulsed current to deposit chromium directly onto aluminium in 1961 using low frequency (100 Hz, 50% duty cyle). It was noted by Faust that the use of

pulsed current reduced the tensile stress of the chromium deposit and gave good adhesion. By this method, crack free deposits of chromium were obtained which were softer than conventionally deposited chromium. The deposits were also dull and required subsequent polishing. The noted reduction in stress was postulated to occur because deposited chromium hydrides could decompose on the surface during the off time followed by subsequent incorporation of the deposited atom of chromium into the lattice thus avoiding the shrinkage which would be encountered if the hydride decomposed when already covered by another layer of chromium.

4.5.1. The Effect of Pulsed Current on the Hydrogen Content of Chromium Deposits.

In 1971, Knodler (61) measured the hydrogen contents of various chromium deposits plated with pulsed and direct current using a hot extraction technique. He found that using a sulphate catalysed electrolyte (100:1 chromic acid: sulphate ratio), much higher hydrogen contents were found in the deposits produced by pulsed current than those plated with direct current. Results were also obtained for electrolytes with a self regulating sulphate/silicofluoride catalyst system. Some of the results obtained are shown in table 4.

Table 4. Hydrogen Contents of Chromium Deposits.

Plating Conditions	(H:Cr). At. Ratio
Direct Current. Sulphate Catalysed. (250g/l chromic acid)	0.02
Direct Current. Mixed Catalyst. (250 g/l chromic acid)	0.02
Pulsed Current 1: 2, Sulphate Catalysed. (250g/l chromic acid)	0.75
Pulsed Current 1: 2, Mixed Catalyst. (250g/l chromic acid)	0.70
Pulsed Current 1: 2, Sulphate Catalysed. (100g/l chromic acid)	0.56
Pulsed Current 1: 2, Mixed Catalyst. (100g/l chromic acid)	0.12

(50°C, 40 A/dm^{2}) Pulse plating conditions 1 msec on, 2 msec off.

It was further noted by Knodler that hydrogen contents of deposits were increased by :-

i) Increasing the chromic acid concentration.

ii) Increasing the current density.

iii) Reducing the plating temperature.

iv) Using a sulphate catalysed rather than a mixed catalyst system.

v) Using low duty cycles with pulsed current.

vi) Using low pulse frequencies.

The lowest hydrogen contents were given by using mixed catalyst electrolytes with low chromic acid concentrations at high temperatures using high frequencies and duty cycles of 50% or greater. Deposits with high hydrogen contents were examined using X-ray diffraction techniques and found to consist largely of hexagonal close packed chromium hydride rather than the normal body centred cubic structure. It has also been reported (115) that deposits produced by single phase rectification (50% ripple) give deposits containing h.c.p. chromium hydride. No explanation was suggested by Knodler as to the cause of these observed phenomena.

It appears therfore that Faust's hypothesis that decomposition of hydrides during the off time was responsible for the observed reduction in tensile stress of deposits was not supported by experimental evidence since decomposition of hydrides during the off time would give rise to deposits with low rather than high hydride contents.

Because of this apparent anomaly, an investigation of the effect of pulsed current on the crystallographic structure of chromium deposits produced by pulsed and direct current has been carried out in the present study and a hypothesis has been proposed to explain the co-deposition of hydrides under certain conditions of pulsing.

4.5.2. The Effect of Pulsed Current on Crack Formation and Visual Appearance of Chromium Deposits.

It has been noted by several authors that pulsed or pulse reverse current can produce crack free chromium deposits. Early work was carried out by Saiddington and Hoey [116] who observed that the formation of cracks was associated with increases in deposit thickness, cracks tended to occur cyclically. From their study, it was concluded that crack formation was reduced considerably when the current was interrupted such that no more than 0.5 μm of chromium was deposited between interruptions. Current interruptions were found to be effective only when long enough to produce a discontinuity in the deposit. A short period of current reversal could be used to achieve the same effect. Systems for depositing crack free chromium commercially using pulsed reverse current have been developed by Reby and Sutter [81] and Colombini [82] based on Saiddingtons observations.

It was further noted by Saiddington [117] that deposits produced by pulsed reverse current were duller than deposits obtained by direct current. Surface examination revealed that there was a considerable increase in the nodularity of the deposits when pulsed reverse current was used. This was considered to be caused by the formation of fresh nucleation sites each time the current was interrupted or reversed which could cause three dimensional nucleation. This provides a possible explanation for the observed reduction in stress.

Crack free deposits can also be produced by pulsed current using unipolar pulses. As has been mentioned, Faust et al [60] produced crack free deposits using this method. Higher frequencies were used by Nesnidal [118] to achieve the same effect. The latter

noted that the higher frequencies gave brighter deposits than lower frequencies and suggested an optimum duty cycle of 75%. The use of pulsed or pulsed reverse current to deposit chromium produces duller deposits than are produced by direct current. Depending on the conditions used (with regard to current density, temperature and pulse conditions), deposits range from a dull matt finish to a semi-bright finish. The duller deposits also are softer than deposits produced by direct current.

4.5.3. The Effect of Pulsed Current on the Cathodic Efficiency of Chromium Plating Electrolytes.

Surprisingly, there is little published information on the effect of pulsed current on the cathodic efficiencies of chromium plating electrolytes. Nesnidal [118] plated mandrels with hard chromium from a conventional sulphate catalysed electrolyte under various conditions of pulsing. The results were published in terms of time, current density and deposit thickness. Some of these results have been converted into efficiencies by the present author and the results are shown in table 5.

Table 5. Efficiency of Sulphate Catalysed Electrolyte With Pulsed Current.

Plating Conditions.		Current Density j_m (A/dm^2)	Cathodic Efficiency (%)
Direct Current		31	12.1
Pulsed Current	2500 Hz, 75% Duty Cycle	31	12.7
Pulsed Current	2500 Hz, 50% Duty Cycle	31	11.8
Pulsed Current	2500 Hz, 25% Duty Cycle	62	15.0
Pulsed Current	2500 Hz, 15% Duty Cycle	31	18.3

Electrolyte containing 250 g/l chromic acid, 2.5 g/l sulphate used at 50 ^oC.

It can be seen from the results shown in this table that an increase in efficiency is apparent at a duty cycle of 15%. An increase in efficiency has also been noted when pulsed reverse current is used for the deposition of hard chromium [82]. An investigation of the effect of pulsed current on the efficiency of hard chromium deposits is given later in this thesis and a hypothesis is proposed to explain these effects.

4.5.4. The Effect of Pulsed Current on the Corrosion Resistance, Wear Resistance and Fatigue Properties of Hard Chromium Deposits.

The fact that pulsed current can produce crack free chromium deposits could improve the corrosion resistance of the coating for applications where the plated component is not subject to deformation in use. Because of the thin protective oxide layer on the surface of the chromium, the corrosion resistance of the coating is potentially good but because conventionally deposited coating are cracked, corrosion of the substrate can occur through these cracks. Crack free chromium coatings are very brittle however and any deformation of the coating will cause macro cracks exposing the substate. Because of the small surface area exposed, the corrosion current density at these cracks would be very high and corrosion of the damaged area would be rapid. No data have been published comparing the wear resistance of pulse plated chromium deposits to that of conventionally deposited chromium. This represents an area where more research is needed.

Knodler [61] compared the corrosion resistance of pulse plated chromium coatings with that of direct current coatings under conditions of corrosion/abrasive wear in mining brine. Chromium deposits of 40 μm thickness were deposited on cylindrical samples of steel and subjected to abrasive wear by loading the rotating sample with an alumina rod. Pulse plated deposits were found to be much more corrosion resistant than those

produced using direct current. Potentiodynamic scans carried out in the same brine solution revealed that the pulse plated deposits gave a different anodic behaviour and produced a passive region in the polarisation curve.

The effect of chromium plating on the fatigue strength of steel has been investigated by Hammond and Williams (113). Knodler (61) also studied the effect of chromium plating on the fatigue strength of steel (0.45% C). Standard Wohler (rotating beam) test pieces were used in the annealed state and plated to a thickness of 40 μm with direct and pulsed current. It was found that microcracked deposits produced a small reduction in the fatigue strength of the steel but that crack free deposits gave a substantial reduction in the fatigue strength. An explanation for this was as follows :- In a coating which is already cracked, further cracks induced by the fatigue test tend to propagate only through the coating. In a crack free deposit, the fatigue test can induce large macro cracks which are more likely to propagate into the substrate thus lowering the fatigue strength of the underlying steel.

Chapter 5.

The Electrodeposition of Copper From Acidic Electrolytes.

5.1. Introduction.

The electrodeposition of copper from acidic electrolytes has wide commercial applications in the electroforming and electroplating industries and also has applications in the production of copper powders and in the electrorefining industry.

Examples of copper electroforms include electrotypes, gramophone records, heat exchangers and, more recently, the production of waveguides for microwave applications. A major application for electroplated copper was that it was often used as an undercoat underneath nickel/chromium layers on car bumpers. Acid copper solutions containing organic brightening and levelling agents have very good levelling properties and acid copper deposits are frequently used as an undercoat in order to eliminate polishing or buffing (although the development of very high levelling nickel electrolytes has reduced the use of acid copper in this area).

A major use for the acid copper electrolyte came about with the microelectronics revolution and the developing need for more complicated printed circuit boards as component packing densities increased. It was no longer possible to produce printed circuit boards with all of the interconnects printed on one side of the board so double sided boards were developed where the patterns on both sides of the board were connected by plating copper through the holes. This was achieved by activating the laminate in the holes using a palladium colloid catalyst, plating a thin layer of electroless copper on the activated surface and building up the thickness of copper in the hole

using electrodeposited copper. In order to deposit an even thickness of copper in the holes, a solution with high throwing power was required. the cyanide copper electrolyte has a good throwing power but is not suitable for printed circuit production because the highly alkaline solution causes degradation of the epoxy laminate. The pyrophosphate electrolyte rapidly became established as the electrolyte to use for these purposes because the sulphate based copper electrolytes had very poor throwing power.

As the demands of the electronics technology became greater and multilayer boards were produced, the limitations of the pyrophosphate electrolyte became evident. The electrolyte was sensitive to very small amounts of organic impurities which caused "skip" plating and brittle deposits which subsequently cracked when components were soldered to the board. To overcome these problems, supply houses developed high throwing power sulphate based acid copper electrolytes with a high acid/low metal formulation. Stable organic additives were developed which could withstand the high acidity levels of the electrolytes and gave the required deposit structure and ductility to withstand the thermal shock imposed on the deposits when the boards were soldered. These sulphate based electrolytes rapidly replaced the pyrophosphate electrolytes and became standard in the industry.

The latest trend in the electronics industry is to use surface mounted components in order to further increase component packing density. With this technology, the holes in the boards are only to connect the circuit and are no longer required for component leads. Thus holes are produced which are very small and this causes problems when trying to plate an even thickness of copper. The throwing power of the acid copper electrolytes available at present is not sufficient to plate these holes satisfactorily. One solution to this problem is to use electroless copper to deposits the entire thickness of

copper required (25 μm). Electroless copper solutions which are capable of achieving this have to be very stable and produce a copper deposit which is can meet the stringent thermal shock requirements. In order to achieve this, the plating rate of these solutions is very slow which causes large scale production difficulties. Because of the impracticality of building the entire thickness of copper with an electroless solution, ways are being sought to improve the throwing power of acid copper electroplating solutions. This constitutes one of the major aims of this thesis.

5.2. The Mechanism of Deposition from the Acid Copper Electrolyte.

In this consideration of the mechanism of copper deposition, the sulphate based electrolyte will be considered. Unlike the mechanism for chromium which has not been fully established, the mechanism for the deposition of copper from an acidic electrolyte is relatively straightforward.

5.2.1. Electrochemical Reduction of the Cupric Ion.

In acidic solutions, the copper II ion is usually present as the aquo ion. Solutions of copper sulphate are slightly acidic due to the polarising nature of the copper II, this is due to the following reaction :-

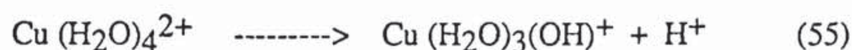

$$Cu(H_2O)_4^{2+} \text{ ---------> } Cu(H_2O)_3(OH)^+ + H^+ \qquad (55)$$

Copper is more noble than hydrogen in the standard electrochemical series and so would be expected to deposit with a cathodic efficiency of 100% provided that mass transport does not impose limitations.

Reduction occurs via the transfer of two electrons to the copper ion at the cathode surface :-

$$Cu^{2+} + e^- \text{-------->} Cu^+ \quad (56)$$

$$Cu^+ + e^- \text{---------->} Cu \quad (57)$$

Copper can be deposited from solutions containing only copper sulphate at low current densities. At higher current densities, reaction 55 causes co-deposition of basic salts and gives rise to a spongy deposit. The addition of sulphuric acid to the electrolyte prevents this and allows the deposition of smooth deposits at higher current densities than for and electrolyte based entirely on copper sulphate.

Because the copper II ion is so easily reduced, problems are encountered when plating active metals (such as steel) because an immersion deposit of copper is easily formed :-

$$Fe + Cu^{2+} \text{---------->} Fe^{2+} + Cu \quad (58)$$

This immersion deposit tends to have poor adhesion and causes the deposit to lift after plating. A "strike" deposit from a cyanide based electrolyte is required in these cases.

5.2.2. Anodic Reactions.

At the anode, copper is oxidised from copper metal to the cupric ion. At high current densities, an oxide film can develop on the anode surface which forms a passive layer and so a large increase in the cell voltage is required in order to maintain the correct current density. Anodes can also dissolve very unevenly in acidic electrolytes due to this effect. In order to overcome this problem, phosphorised anodes were developed which dissolve more evenly and have less tendency to passivation problems.

A small amount of chloride in the electrolyte can promote even dissolution of anodes and is required in electrolytes containing addition agents for these to function correctly. However, an excess of chloride ion can give rise to a film of sparingly soluble copper (I) chloride on the anode which can again cause passivation.

5.2.3. Conductivity, Cathodic Polarisation and Throwing Power.

Because of the high acid content, acid copper electrolytes tend to have high conductivities. The copper ion is easily reduced. This means that the activation energy which needs to be supplied in order to reduce the ion is low, thus cathodic polarisation tends to be very low in these electrolytes. This in turn means that the throwing power of these electrolytes is very poor and generally closely approximates to a primary current density distribution (119). As acid copper electrolytes were adapted for plating "through holes" on printed circuit boards, ways had to be found to increase the throwing power of these electrolytes. This was achieved by using a high acid content to maximise the electrolyte conductivity and a low metal content in order to maximise cathodic polarisation potentials. This procedure maximises the Wagner number and so gives optimum throwing power. Although these electrolytes gave good throwing power, the low metal content meant that agitation and current density and temperature control became critical and reduced the overall plating rate which could be used. The high acid content also presented problems for the supply houses because it was difficult to formulate brighteners which were stable in these electrolytes. In spite of these problems, these electrolytes have become standard for the production of printed circuit boards.

Modern acid copper electrolytes can be split into two types. The standard electrolyte is used for decorative and electroforming applications and the high throwing power

electrolyte is most usually employed for the production of printed circuit boards, typical formulations are shown in table 6.

Table 6. Typical Formulations for Acid Copper Electrolytes.

Type of Solution	Copper Sulphate (g/l)	Sulphuric acid (g/l)	Chloride Ion (mg/l)
Standard (Decorative & Electroforming).	200 - 250	50 -100	80 - 200
High Throwing Power (for printed circuits).	50 - 100	180 -220	40 - 80

5.2.4. Current Density and Temperature.

Operating temperatures for acid copper baths may vary from 18 to 60°C but usually, a temperature of between 20 and 35°C is used since in this range, little or no heating and cooling is required. Higher temperatures allow higher current densities to be used but tend to reduce throwing power and cause a higher rate of breakdown of addition agents.

Current densities which can be used in acid copper deposition depend upon the electrolyte formulation, the rate and type of agitation used, the temperature of the electrolyte and the application. Decorative applications commonly use an average current density of 4-5 A/dm^2 wheras electroforming applications frequently use current densities of 15-20 A/dm^2. The throwing power of the electrolyte is adversely affected by increasing the current density and high throwing power electrolytes are usually operated at relatively low current densities (2-3 A/dm^2). For applications where maximum throwing power is required, current densities of 1 A/dm^2 may be required.

5.2.5. Addition Agents.

In the majority of electroplating applications for acid copper plating, addition agents are added to the electrolyte in order to modify the deposit properties. Addition agents may be used as grain refiners or brighteners, as levellers or to harden the deposit. Many commercial brightener systems are available for acid copper systems.

Early examples of addition agents used in acid copper electrolytes include gelatin and glycine. These agents were used as grain refiners. These molecules are adsorbed at the cathode surface and tend to increase cathode polarisation because of this (120). One of the first brightening agents used in acid copper electrolytes was thiourea (121). However, this compound gives a limited bright range and its concentration is critical. Because of these problems, thiourea has been superseded by brighteners which are easier to control and which do not cause a deterioration in the properties of the electrodeposited copper.

An early example of an acid copper brightener was the use of the sulphonation products of aromatic compounds prepared by the reaction of toluene with thionyl chloride in the presence of anhydrous aluminium chloride and sulphuric acid (122,123) a version of this process was used commercially by W.Canning Ltd. (124). Many compounds have been patented as brighteners and it is not possible to give a comprehensive list here. The most modern brightener systems usually consist of a polyether which acts as a grain refiner in synergistic combination with a sulphopropyl sulphide (125,126,127,128,129). This combination of addition agents gives a stable brightener system with few harmful breakdown products. In addition to these compounds, brightener systems may also contain levelling agents which act as diffusion controlled inhibitors. Typical examples of these levellers would be substituted thioureas or

phenosafranine dyes.

The actual mechanism of brightening is little understood but levelling occurs because diffusion of the levelling agent to peaks on a microprofile is much faster than diffusion to the troughs. These organic molecules act as deposition inhibitors and so increase the activation energy (polarisation overpotential) required to deposit metal at a given rate (current density). Thus, since the cathode is considered to be an equipotential surface, deposition rates are reduced on peaks because of the adsorption of the levelling agent which causes an enhanced deposition rate in troughs [130].

Possible mechanisms of addition agent incorporation have been discussed by Edwards [131,132,133,134,135,136] but the experimental work carried out by Edwards was concentrated on the addition agents which are commonly used in nickel solutions. Some studies have been made of the incorporation of brighteners in copper deposits [137,138,139], but no systematic study has been undertaken. Thus the mechanism of incorporation for modern copper brighteners has not been established.

5.3. The Structure and Properties of Electrodeposited Copper.

The physical properties of electrodeposited copper from acidic electrolytes have been reviewed by Safranek [140]. By varying addition agent concentrations and formulations, copper deposits with various properties can be produced. Copper deposits usually have good ductility and elongation values of between 5 and 25% can be obtained. The tensile strength of the deposits usually varies between 200 - 400 N/mm^2 and hardness values of 50-200 Hv can be obtained.

5.3.1. Grain Structure of Electrodeposited Copper from Acidic Electrolytes.

Electrodeposits from sulphate based electrolytes containing no additives are columnar in structure. Copper is deposited from these electrolytes as randomly oriented f.c.c. crystals (141) unless deposited at current densities of less than 1.5 A/dm^2 when the basis metal can affect the orientation of the crystal structure (142).

Additions of gelatin or phenolsulphonic acid tend to produce a fibrous structure (this is caused by grain refinement in x and y directions but not in the z direction. It is essentially a modified columnar structure.). This is up to 20% harder than columnar copper produced from an additive free electrolyte. Modern additives produce a fine grained equiaxed structure. The production of copper deposits having this structure is particularly important for the production of printed circuit boards. This is because the deposit turns through 90° at the top of the hole in the board, and a columnar structure causes weakness at this point which can result in cracking of the deposit when components are soldered to the board (i.e. when the board is subjected to thermal shock). Ductility is also of prime importance in printed circuit board production since the coefficient of thermal expansion for epoxy/glass laminate is higher than that of copper. A ductile deposit of copper can elongate to accommodate this whereas a brittle deposit will crack. Thus, modern brightener systems developed for printed circuit board production are aimed at providing maximum ductility and an eqiaxed grain structure.

5.4. The Effect of Pulsed Current on Electrodeposited Copper from Acidic Electrolytes.

Because of the simplicity of the acid copper electrolyte, this system has been widely studied. The reduction of copper involves the transfer of two electrons and the kinetics of reduction have been studied by the use of pulsed current. However, few practical applications of the pulse plating process have been discovered. This section gives a brief review of some of the work which has been undertaken with pulsed current on the acid copper system.

5.4.1. The Effect of Pulsed Current on the Efficiency of Copper Deposition from the Acid Copper Electrolyte.

The efficiency of deposition of copper from the acidic sulphate based electrolyte is usually 100% provided that the electrolyte is not used under conditions of mass transfer limited deposition. The application of pulsed current to this system can cause a measurable decrease in efficiency. This was first noted by Kushner [143] in 1965 and by Lamb [144] in 1969, who observed that current efficiency decreased as pulse duration decreased. This phenomenon was investigated in more detail in 1977 by Cheh, Linford and Wan.[145]. Here, a systematic investigation was carried out and some of the results are shown in figure 11 . It can be seen from the results shown in this figure that the pulse time had a greater influence on the cathodic efficiency than the relaxation time. Kushner [143] had attributed this to chemical dissolution during the relaxation time but a loss of 20% copper due to chemical attack seems unlikely. Cheh et al. [145] stated that this reduction in efficiency was due to a change in the kinetics of reduction.

It has been proposed by Mattson and Bockris [146] that the mechanism for copper

Figure 11. Current Efficiency vs. Various Pulse Parameters for an Acid Copper Electrolyte. (After Cheh et al. (145)).

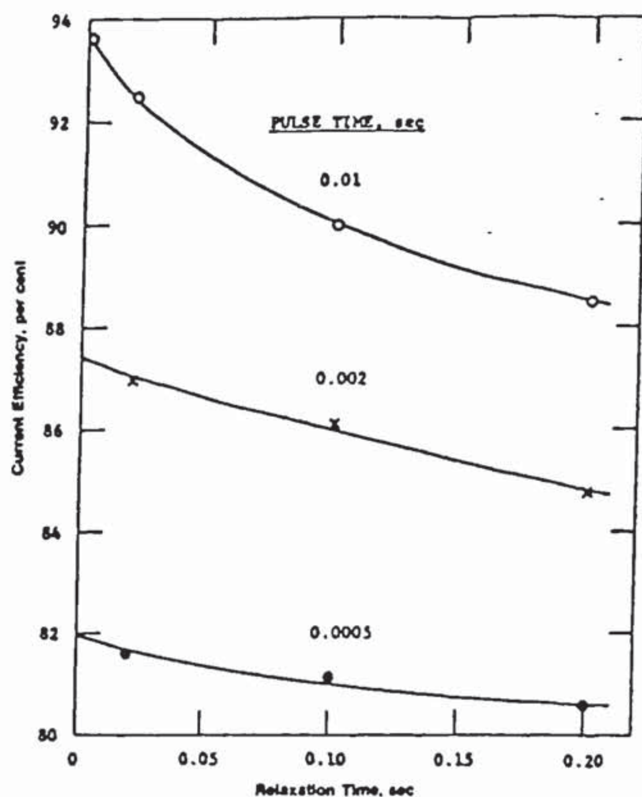

Average Current Density

40 mA/cm^2.

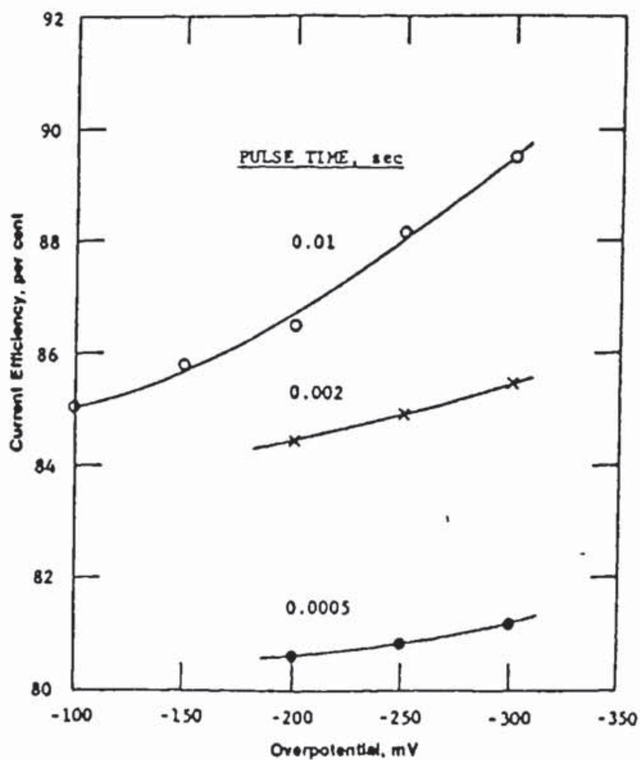

Relaxation Time

0.2 sec.

reduction was as described in equations 56 and 57. The observed reduction in efficiency was explained by Cheh et al.[145] by the fact that cuprous ions would be formed during the pulse which could disproportionate during the relaxation time according to the reaction :-

$$2Cu^{+} \text{ --------> } Cu^{2+} + Cu \qquad (59).$$

Evidence in support of this theory was produced when light scattering techniques were used to detect the presence of colloidal copper at the cathode surface [145].

5.4.2. The Effect of Pulsed Current on the Throwing Power of Acid Copper Electrolytes.

The throwing power of the acid copper electrolyte is particularly important in the production of printed circuit boards. A number of investigations has been carried out on the effect of pulsed current on the throwing power of the acid copper electrolyte. As mentioned in chapter 2, the fact that a higher current density is applied during pulses than with direct current (for the same average rate of deposition) means that the current density distribution would be expected to tend towards a primary distribution which would make the throwing power worse. This was confirmed by Cheh et al.[55]. The fact that pulsed current tends to reduce throwing power was exploited by Vilambi and Chin [147] who used pulsed current to selectively deposit copper from an acid sulphate bath on a localised area of an unmasked cathode.

The use of pulsed reverse current can improve deposit distribution from a cyanide copper electrolyte[36,37,38,39]. However,when an acid system is considered, if anodic and cathodic efficiencies are assumed to be 100%, the same argument applies as

for unipolar pulses: The cathodic current density has to be higher than the equivalent current density for direct current (for the same deposition rate) so the distribution would be expected to be worse if anodic and cathodic current densities are the same. If short anodic pulses of high current density are used, the current distribution during the anodic phase would tend towards a primary distribution which would tend to dissolve metal more from high current density areas and so improve the deposit distribution. This reasoning was used by White and Galasco (148) who attempted to use pulsed reverse current to improve the deposit distribution on printed circuit boards. It was found that at high current densities, passivity of the deposit occurred which prevented dissolution of the copper and made the distribution worse. White and Galasco (148) also investigated the use of pulsed reverse current using lower anodic current densities and it was found that using an electrolyte containing proprietary additives, an improved deposit distribution could be obtained as compared to deposition with direct current at an equivalent deposition rate. This implied that the use of pulsed reverse current in combination with certain additives may give rise to an improved deposit distribution. The investigation of the effects of pulsed reverse current on the distribution of copper plated from electrolytes containing organic additives constitutes a major part of the research in this thesis.

The effect of pulsed reverse current on acid copper electrolytes has also been studied by Mann (149) but very high frequencies and short anodic pulses were used in this study. It is doubtful whether an anodic pulse actually occurred in this study. Nevertheless, he concluded that pulsed reverse current could improve throwing power.

5.4.3. The Effect of Pulsed Current on the Structure and Properties of Copper Deposits.

The effect of pulsed current on the microstructure of copper deposits was studied by Lamb (144). At 2000Hz, 10% duty cycle and an average current density of 10 A/dm^2, a columnar structure similar to that obtained by direct current was obtained, but with a grain size which was estimated to be 3-4 times smaller. At 1000Hz, 0.5% duty cycle and an average current density of 5 A/dm^2, an equiaxed structure was obtained. Cavallotti et al.(150) also reported a reduction in grain size for an increase in pulse current density using a tartrate based electrolyte. Ductility of pulse plated deposits was measured by White and Galasco (148). It was found that both pulsed and reverse pulsed current caused a reduction in ductility when used with an electrolyte containing proprietary additives, but that ductility could be improved in an additive free solution by the use of pulsed reverse current.

Chapter 6.

Selection of Pulse Parameters for Experimental Work.

6.1. Introduction.

As described in the literature review, the capacitance of the double layer at the electrode/electrolyte interface limits the maximum frequency of pulses which can be applied without significant "smoothing" of the waveform [4]. It is important when using unipolar pulses that the pulse length is longer than the time necessary to obtain a Faradaic current of 99% of the total current. It is also important that the interval between the pulses is long enough for the double layer to discharge before the next pulse. Because of the importance of defining the maximum useful frequency in pulse plating, a computer model was developed to compare definitions of the degree of smoothing of the waveform.

Selection of duty cycle and the pulse parameters used in pulsed reverse current were chosen with practical considerations of rectifier capacity in mind and sections are included in this chapter describing the reasons for the choice of these parameters.

6.2. A Computer Model of Degree of Flattening.

Puippe and Ibl [5] provide a method for calculating the charge time of the double layer as described in the literature review. Using this method, a computer program was developed for the B.B.C. microcomputer. A copy of this program is shown in table 7. This program cannot be used directly to calculate charge times since it is necessary to know the transfer coefficient, the double layer capacitance and the exchange current

Table 7. Program To Calculate Charge Parameters.

```
10 REM  Program to Calculate Charge
20 REM  and Discharge Times for the
30 REM  Double Layer.  By T. Pearson.
40 REM  V3.0  August 1989. For B.B.C. Model B.

50 REM  Main Program Loop

60 MODE 7
70 CLS
80 REPEAT
90 PROCinit
100 PROCgetdata
110 PROCcalctc
120 PROCprintres1
130 PROCcalctd
140 PROCprintres2
150 UNTIL  FALSE

160 REM  Initialisation Procedure

170 DEF PROCinit
180  R=8.314: F=96500: Int=0.001: If=0: If1=0: P=0.01: P1=0: Chargetime=0:
Discharge=0: Current=0: CPotential=0: DPotential=0
190 ENDPROC

200 REM  Data Collection Routine

210 DEF  PROCgetdata
220 PRINT""  Capacitance in Microfarads? "
230 INPUT C
240 PRINT"  Ionic Charge? "
250 INPUT Z%
260 PRINT"  Transfer Coefficient? "
270 INPUT A
280 PRINT"  Pulse Current Density  (A/sq cm)? "
290 INPUT IP: IC1=IP
300 PRINT"  Temperature  (C)? "
310 INPUT T
320 PRINT"  Exchange Current Density  (A/sq cm)? "
330 INPUT ECD
340 CLS
350 PRINT""CALCULATING PARAMETERS - PLEASE WAIT."
360 ENDPROC

370 REM  Calculation of charge time and
380 REM  other parameters.

390 DEF  PROCcalctc
400 REPEAT
410 TC=R*(T+273)
420 REM  Calculation of If for interval
430 REM  using Volmer - Butler Equation.
```

```
440 AC1=(A*Z%*F*P)/TC
450 AC2=(-(1-A)*Z%*F*P)/TC
460 If=ECD*(EXP(AC1)-EXP(AC2))
470 IC=IP-If
480 REM  Calculation of time required.
490 REM  to change potential by Int.
500 TN=C*((P-P1)/(If-If1))*LN(IC1/IC)
510 REM  Calculation of Chargetime.
520 Chargetime=Chargetime + TN
530 REM Calculation of Integrated Current during charge time.
540 Current=Current + (If*TN)
550 REM  Calculation of Integrated Potential during charge time.
560 CPotential=Cpotential + (P*TN)
570 IF If>=0.8*IP THEN Int=0.0001
580 P1=P: P=P+Int: If1=If: IC1=IC
590 UNTIL If>=0.99*IP
600 ENDPROC

610 REM  Calculation of Discharge time
620 REM  and other parameters.

630 DEF PROCcalctd
640 PRINT'"CALCULATING PARAMETERS - PLEASE WAIT."
650 Int=0.001: P1=P
660 REPEAT
670 TC=R*(T+273)
680 AC1=(A*Z%*F*P)/TC
690 AC2=(-(1-A)*Z%*F*P)/TC
700 If=ECD*(EXP(AC1)-EXP(AC2))
710 IC=If
720 TN=C*((P-P1)/(If-If1))*LN(IC1/IC)
730 Discharge=Discharge + TN
740 DPotential =DPotential + (P*TN)
750 IF If<=0.2*IP THEN Int=0.0001
760 P1=P: P=P-Int: If1=If: IC1=IC
770 UNTIL If<=0.01*IP
780 ENDPROC

790 REM  Interim Results.

800 DEF PROCprintres1
810 CLS
820 PRINT''"Charge time = ";Chargetime;" Microseconds"
830 PRINT'"Integrated Faradaic Current = ";Current;" Microcoulombs /sq cm"
840 PRINT'"Integrated Potential (charge) = ";CPotential;" Volt microseconds"
850 PRINT'"Peak Overpotential = ";P;" Volts"
860 ENDPROC

870 REM  Final Results.

880 DEF PROCprintres2
890 CLS
900 PRINT''"Discharge time = ";Discharge;" Microseconds"
910 PRINT'"Integrated Potential (Discharge) = ";DPotential;" Volt microseconds"
920 ENDPROC
```

Program Variables.

R	=	Gas Constant.
F	=	Faraday Constant
Int	=	Interval of change of potential
If, If1	=	Faradaic current at intervals n and n+1
P,P1	=	Potential at intervals n and n+1
Chargetime	=	Integrated Charge time for Double Layer
Discharge	=	Integrated Discharge time for Double Layer
C	=	Double Layer capacitance
Z%	=	Ionic charge of reducing species
A	=	Transfer Coefficient
IC,IC1	=	Capacitative current at intervals n and n+1
IP	=	Pulse current density
T	=	Temperature
ECD	=	Exchange current density
TC	=	Temperature coefficient
TN	=	Time taken to increase potential by Int

density and these quantities are not usually available. Maksimovic et al [7] suggested that degree of flattening could be determined by measuring the change in the average cathodic overpotential as frequency is increased. Puippe and Ibl defined degree of flattening in terms of current rather than potential. Using data obtained by Farr and Ashiru [151] for values of double layer capacitance and exchange current density for a silver cyanide electrolyte, the program in table 7 was used to compare the degree of flattening as defined by Maksimovic et al [7] with the degree of flattening as defined by Puippe and Ibl [5]. The parameters used for the calculation were as follows :-

Double Layer Capacitance	= 53 $\mu F/cm^2$.
Exchange Current Density	= 1.3×10^{-3} A/cm^2.
Transfer Coefficient	= 0.5 (estimated)
Ionic Charge	= 1
Temperature	= 18°C
Average Current Density	= 0.02 A/cm^2.
Pulse Current Density	= Varied according to duty cycle.

Using these parameters, the computer program was used to calculate charge and discharge parameters for various duty cycles as shown in table 8.

Table 8. Computer Calculated Charge and Discharge Parameters for Various Duty Cycles.

Duty Cycle	j_p	t_c	t_d	η_a	Σj_f	$\Sigma \eta_c$	$\Sigma \eta_d$
33%	0.06	374	2182	191	12.35	52.5	103.9
10%	0.20	130	1089	252	12.75	23.5	87.0
5%	0.40	68.9	619	287	12.45	13.8	66.5

Where,

j_p = Pulse Current Density (A/cm^2).

t_c = Charge time for double layer (μs)

t_d = Discharge time for double layer (μs)

η_a = Peak overpotential of pulse (mV)

Σj_f = Integrated Faradaic Current during charge (μCoulombs/cm^2)

$\Sigma\eta_c$ = Integrated Overpotential during charge (Vμs)

$\Sigma\eta_d$ = Integrated Overpotential during discharge (Vμs)

Using these parameters, the methods of calculation of degree of flattening proposed by Puippe and Ibl (5) and Maksimovic et al (7) were compared under various pulse conditions. The method of calculation used was as follows :-

Puippe and Ibl defined degree of flattening as :-

$$\Delta = \frac{j_p t_{on} - \int_0^{t(on)} j_f \, dt}{j_m t_{off}} \qquad (60)$$

For a given set of pulse conditions, j_p, j_m, t_{on} and t_{off} are known quantities and the integrated coulombic charge during the charge time can be determined by the computer program shown in table 7. From this, the integrated Faradaic current during the pulse can be calculated from the following equation :-

$$\int_0^{t(on)} j_f \, dt = \int_0^{tc} j_f \, dt + j_p \left(t_{on} - t_c\right) \qquad (61)$$

Where t_c is the charge time for the double layer.

Thus, equation 60 can be solved and values for delta can be calculated from pulse parameters provided that the pulse length is greater than the charge time and the interval between the pulses is greater than the off time. It should be noted here that in this mathematical model, the effects of concentration overpotential are assumed to be negligible.

Maksimovic et al argued that potential flattening should be linked to current flattening and so degree of flattening could be defined as follows :-

$$\Delta^* = 1 - \frac{\Delta\eta_{(\lambda)}}{\Delta\eta_{(0)}} \qquad (62)$$

The denominator of this expression represents the change in average overpotential between direct current and the pulse conditions used assuming no flattening and is defined as follows :-

$$\Delta\eta_{(0)} = \eta_{(d.c.)} - \frac{\eta_p t_{on}}{(t_{on} + t_{off})} \qquad (63)$$

where η_{dc} is the overpotential which would be obtained using an equivalent direct current and η_p is the peak overpotential reached during the pulse.

The numerator of the expression represents the change in average overpotential between direct current and the pulse conditions used where flattening occurs and for unipolar pulses is defined by equation 64.

$$\Delta\eta_{(\lambda)} = \frac{\int_0^{tc} \eta\, dt + \eta_p (t_{on} - t_d) + \int_0^{td} \eta\, dt}{(t_{on} + t_{off})} \tag{64}$$

These parameters can be determined by the computer program so values of delta by Maksimovic's method can be compared with values obtained using Puippe and Ibl's method.

Values were calculated for several sets of pulse parameters and the results are tabulated in table 9. It can be seen from the results displayed in this table that the calculated values for degree of flattening as proposed by Puippe and Ibl do not correspond to the values obtained using the method proposed by Maksimovic. The differences are clearly shown if a plot of frequency or the ratio of t_{on}/t_c is plotted against degree of flattening.

Table 9. Comparison of Methods of Calculation of Degree of Flattening.

Frequency (Hz)	Duty Cycle	t_{on}/t_c	Δ (Ibl)	Δ^* (Maksimovic)
100	33%	8.9	0.07755	0.1335
200	33%	4.45	0.1518	0.266
300	33%	2.94	0.2318	0.400
100	10%	7.7	0.0744	0.0768
300	10%	2.54	0.2233	0.233
400	10%	1.92	0.296	0.307
500	10%	1.54	0.368	0.385
100	5%	7.255	0.07973	0.0543
300	5%	2.42	0.2396	0.1631
500	5%	1.45	0.400	0.2718
700	5%	1.036	0.557	0.3807

Figures 12 and 13 show plots of frequency vs degree of flattening as produced by equations (60) and (62).

Figure 12. Frequency vs Δ (after Ibl (5)) for Various Duty Cycles.

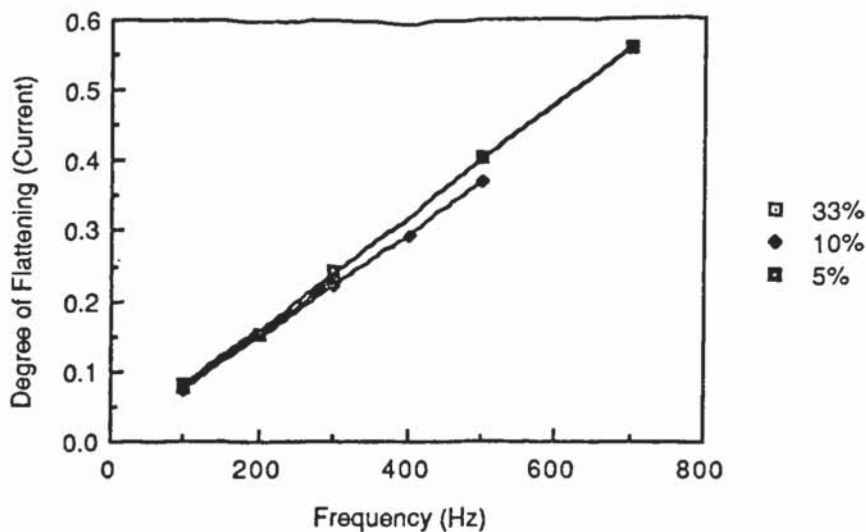

It can be seen from figure 12 that a linear relationship exists between frequency and degree of flattening (based on Faradaic current) for the range studied where on time is longer than charge time. The slope of the lines is relatively independent of duty cycle. Figure 13 shows the relationship between flattening of overpotential as defined by Maksimovic's equation and frequency. It can be seen from this figure that again, degree of flattening of potential has a linear relationship with frequency over the range studied but in this case, the slopes of the lines are dependent on the duty cycle of the applied pulses. A similar difference can be observed if the ratio of pulse time/charge time is plotted against degree of flattening. This is shown in figures 14 and 15.

Figure 14 shows the curve for delta vs t_{on}/t_c ratio. This is the same as the curve produced by Puippe and Ibl (5) as illustrated in the literature review in this thesis. The degree of flattening is virtually independent of duty cycle. Figure 15 however shows that Maksimovic's definition of degree of flattening is strongly dependent on duty cycle.

Figure 13. Frequency vs Δ^* (After Maksimovic (7)) for Various Duty Cycles.

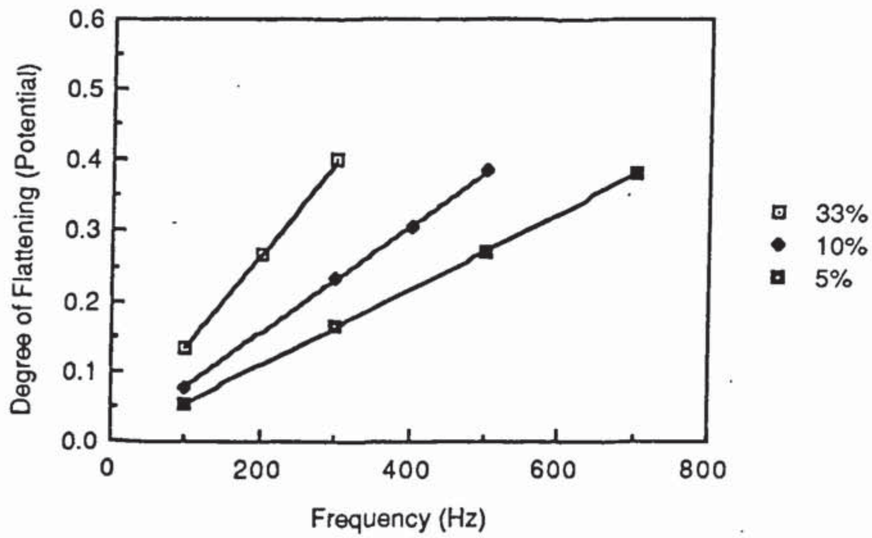

Figure 14. T_{on}/t_c vs Δ (After Ibl (5)) for Various Duty Cycles.

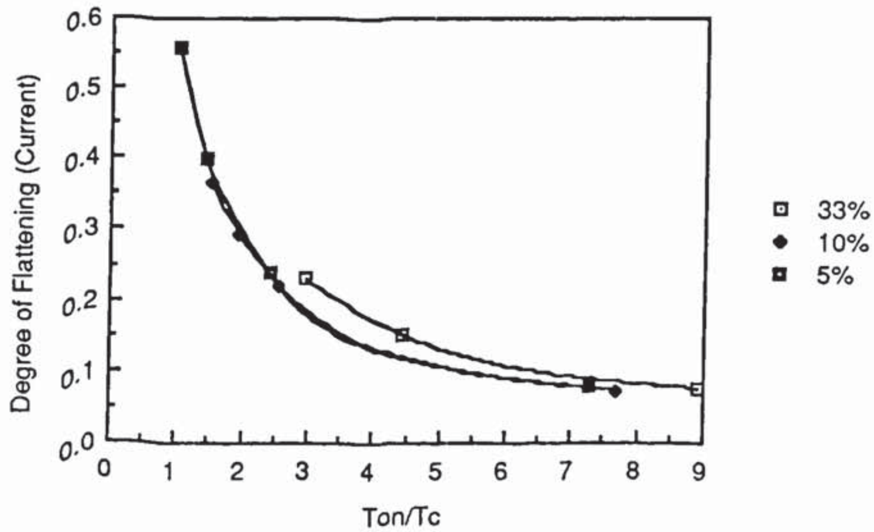

Figure 15. T_{on}/t_c vs Δ^* (After Maksimovic (7)) for Various Duty Cycles.

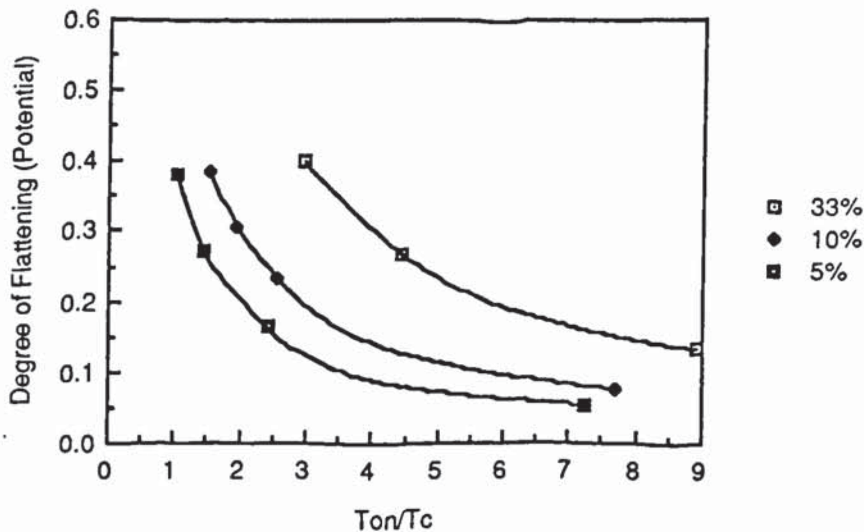

It is clear from the results obtained from the computer simulation that measurement of potential flattening as suggested by Maksimovic et al (7) does not give a good indication of the degree of flattening of the Faradaic current. Puippe and Ibl's method of defining degree of flattening relies on the measurement of charge quantities and it can be seen from table 8 that the coulombic charge accumulated during charging of the double layer is virtually the same for all duty cycles. By comparison, it can be seen from the same table that the integrated change in potential during both charge and discharge is dependent on the duty cycle and is larger for higher duty cycles. This explains the dependence of the values of degree of flattening on duty cycle when Maksimovic's method is employed.

The outcome of the computer simulation was the conclusion that potential measurements could not be used to accurately calculate degree of flattening. Since

charge quantities could not be measured easily, this lead to a problem in the selection of maximum pulse frequency for experimental use. For the work carried out on the deposition of copper by pulsed reverse current, the maximum frequency used was 100 Hz. Work on chromium involved the use of unipolar pulses. In this case, the charge time was roughly estimated from an oscilloscope trace of the potential waveform using a S.C.E. reference electrode. The charge time, defined as the time taken for the potential to reach a value of 90% of the steady state value for the operating pulse current density of 80 A/dm^2, was estimated to be 50 microseconds. Conditions were chosen so that at the highest frequency used, the pulse length would be at least three times the length of the charge time. This lead to the choice of a maximum frequency of 3000 Hz for these experiments.

6.3. Selection of Duty Cycle.

Duty cycle is usually defined as the percentage time during one cycle of a unipolar pulse when the current is on. As the duty cycle is reduced, so the pulse current density required to maintain a particular average current density increases exponentially. An example of this is shown in figure 16 where the pulse current density required to maintain a current density of 40 A/dm^2 is plotted against duty cycle.

It can be seen from this figure that at duty cycles below around 50%, the current density needed to be applied during the pulses becomes too high for practical application. Thus, in the experimental work carried out on the deposition of chromium, a duty cycle of 50% was selected.

Figure 16. Pulse Current Density vs Duty Cycle at Fixed Average Current Density. (40 A/dm^2).

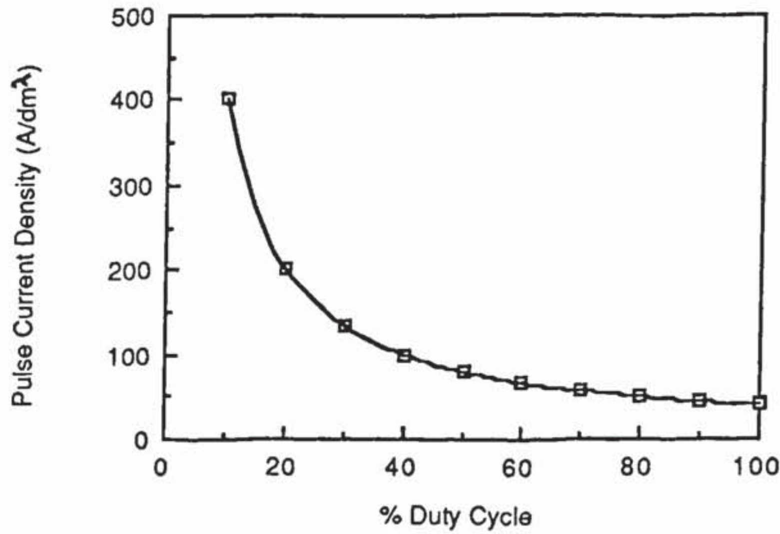

6.4. Selection of Pulse Parameters for Pulsed Reverse Current.

The average current density of a pulsed reverse current waveform is given by the following equation :-

$$j_m = \frac{(j_c \cdot t_{on\ (c)}) + (j_a \cdot t_{on\ (a)})}{(t_{on\ (c)} + t_{on\ (a)})} \quad (65)$$

Where :-

j_m = Average Current Density (A/dm^2)

j_c = Peak Cathodic Current Density (A/dm^2)

j_a = Peak Anodic Current Density (A/dm^2)

$t_{on(c)}$ = Cathodic Pulse Time (seconds)

$t_{on(a)}$ = Anodic Pulse Time (seconds)

As can be seen from the above, there are a large number of variables in this equation so from a point of view of experimental design, it is important to minimise the number of variables studied in a series of experiments to avoid confusion.

In an electroplating electrolyte, the throwing power is usually dependent on the applied average current density. In order to prevent this confusing the experimental results, all laboratory experiments were performed at the same average rate of metal deposition. This was confirmed by weighing test panels before and after plating. The average current density was fixed at 3 A/dm^2 because this is commonly used in commercial practice. Having fixed j_m, the effect of varying the cathodic : anodic time ratio and the anodic : cathodic current density ratio was studied, the resultant peak anodic and cathodic current densities being calculated by the use of simultaneous equations. For the majority of the experiments, a fixed cathodic pulse time of 10 ms was selected and anodic pulse times of 0.5, 1 and 2 ms studied using anodic : cathodic peak current density ratios of 1:1, 2:1, 3:1 and 4:1.

After the optimum ratio of anodic/cathodic time and the anodic/cathodic peak current density was determined experimentally from this series, further tests were performed using the same ratios but longer times to determine the effect of pulse length.

Chapter 7.

Experimental Procedure.

7.1. Introduction.

From the literature review, it was concluded that in the case of deposition of chromium, the most significant effect of using pulsed current was the ability to produce crack free deposits from chromium plating electrolytes which would usually produce cracked deposits (60,61). Also, the use of pulsed current for the deposition of chromium has been reported to produce deposits with high hydrogen contents. The purpose of the experimental work carried out on the deposition of chromium was to attempt to determine the reasons for these observed effects and to produce a hypothesis to explain the incorporation of hydrides in the chromium deposits and the reduction in tensile stress obtained by the use of pulsed current.

In the case of copper deposition, a commercial need was identified in the literature review for an improved throwing power of copper as deposited from acid copper electrolytes used in the printed circuit industry. Here, the available literature shows little evidence that the use of pulsed current can improve the throwing power of acid copper electrolytes (147). In fact, theory would predict that the use of pulsed current should produce a deterioration in throwing power (25). However, commercially applied copper deposits on printed circuit boards are never produced from additive free electrolytes because the resultant columnar structure of the deposits is unsuitable for through-hole deposition. The addition of organic compounds to the electrolyte can change the deposit structure to equiaxed and so produces a deposit with better thermal shock properties when applied to printed circuit boards. The organic additives used in

these electrolytes are highly surface active and so can influence the polarisation characteristics of the electrolyte. Thus, if pulsed current can influence the adsorption characteristics of these compounds, it may influence the throwing power of these electrolytes. The aim of the experimental work on the deposition of copper was to investigate the effect of pulsed current on the adsorption characteristics of the organic compounds frequently used as additives in these systems. This represents a new area of research where there are no published data by other workers.

7.2. Pulse Plating Equipment.

The pulse plating equipment used in the experimental work was a P.D.M. pulse plating unit supplied by J.C.T. Controls. This unit is a microprocessor controlled switch which enables up to 9 channels to be programmed individually with a pulse frequency of between 16 and 4999 Hz and a duty cycle of 5 to 99%, in either forward or reverse direction. The channels are switched sequentially and can have a time duration of between 0.0001 and 90 seconds. This combination gives great flexibility over the applied waveform. Early production versions of the unit left the output terminals of the unit in a short circuited condition at the end of a pulse to avoid damage to the switching Field Effect Transistors. Unfortunately, this condition allowed the double layer to discharge through the unit at the end of a pulse leading to power wastage and serious loss of cathodic efficiency at high frequencies and low duty cycles. The cause of this problem was realised quickly during the initial trials at Aston and the circuitry was modified to eliminate the problem by altering the switching mechanism so that at the end of a pulse, the output terminals were left in an open circuit condition.

For the work on pulsed reverse current for copper, the unit was further modified so that separate rectifiers could be used for the forward and reverse pulses. this enabled

independent control of the forward and reverse current densities. This modification was subsequently included in the production models of the P.D.M.

7.3. Selection of Plating Electrolytes.

7.3.1. Electrolytes for Deposition of Chromium.

The main aim of the experimental work concerned with the deposition of chromium was to investigate the use of pulsed current to produce crack free deposits of chromium. The work was confined to the production of hard chromium electrodeposits which are usually produced to much greater thicknesses than decorative deposits and deposited directly onto steel. Because of this factor, electrolyte formulations were chosen which are usually used for the production of hard chromium deposits. The formulations chosen were a sulphate catalysed electrolyte, a mixed sulphate/silicofluoride catalysed electrolyte and a high efficiency, fluoride free electrolyte. the sulphate catalysed electrolyte was prepared to the following formulation :-

Chromic acid	250 g/l
Sulphate ion (added as Na_2SO_4)	2.5 g/l

After preparation, the electrolyte was electrolysed for 10 Ahr/l at the normal working current density in order to generate some trivalent chromium (necessary for maximising covering power and efficiency). The other electrolytes were commercial formulations supplied by W.Canning Ltd. ready for use. Chromefast C was used as the sulphate/silicofluoride electrolyte and Mach 1 was chosen as the high efficiency fluoride free electrolyte.

7.3.2. Electrolytes for the Deposition of Copper.

The main aim of the work on the deposition of copper was to use pulsed current to maximise the "throwing power" of acid copper electrolytes as used in the printed circuit industry for the production of plated through holes. It was thought that it was important to maintain a similar rate of deposition as is currently employed in the production of printed circuit boards so a fairly typical "High throw" formulation was used for the work as follows :-

Copper Sulphate (Hydrated)	75 g/l
Sulphuric acid (98%)	114 ml/l
Chloride ion (added as NaCl)	80-200 p.p.m.

In addition to studying the effects of pulsed reverse current on an additive free electrolyte, the major part of the work was to investigate the effect of pulsed reverse current on electrolytes containing organic additives as is the case in commercial practice. A large amount of patent literature exists covering a very wide range of organic additives (125,126,127,128,129), however, these patents usually include a combination of a polyether and a sulphopropyl sulphide. This combination of additives gives a bright deposit but little or no levelling. Commercial formulations often additionally contain a compound which acts as a diffusion controlled inhibitor and gives levelling. In order to simplify the initial experimental investigation, a simple brightener system was investigated using the following compounds :-

1. A random co-polymer of ethylene and propylene oxide containing 25% by weight of propylene oxide. This is availible from Shell chemicals ltd. under the name

"Oxilube". The product is available in several molecular weight ranges and molecular weights of 18,000, 50,000 and 92,000 were used in the tests.

2. A sulphopropyl sulphide. There are many compounds of this class patented as brighteners, they are formed by reacting a sulphur containing compound with propane sultone (the gamma lactone of 3-hydroxypropanesulphonic acid). This readily undergoes ring opening and attaches a sulphopropyl group to the other reactant to form organo-sulphur compounds which are readily soluble in strongly acid media. The simplest sulphopropyl sulphide is mercaptopropane sulphonic acid (MPS) which is produced by reacting propane sultone with sodium hydrogen sulphide. This is rarely used commercially because of its lack of acid stability due to the active mercapto group. Sulphides are readily oxidised to disulphides by reaction with hydrogen peroxide and this process increases the acid stability of the compound. Thus in commercial practice, it is the disulphide of MPS which is most commonly used in brightener formulations. In the experimental work, the effects of both of these compounds were studied. The formulae of the compounds are as follows :-

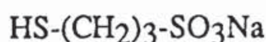

$HS\text{-}(CH_2)_3\text{-}SO_3Na$

Sodium 3-Mercaptopropanesulphonate (MPS)

$NaO_3S\text{-}(CH_2)_3\text{-}S\text{-}S\text{-}(CH_2)_3\text{-}SO_3Na$

Bis(3-sulphopropyl)disulphide disodium salt (SSP)

In order to simplify the interpretation of data, the effects of levelling agents were not studied.

7.4. Pretreatment.

To give good adhesion, the pretreatment of the parts to be plated is very important. The surface of the metal to be plated must be free of oils, greases or other form of organic contamination and any oxide film which may be present on the surface must also be removed. To achieve this, metal parts are usually degreased using a suitable solvent followed by an electroclean in an alkaline cleaner. These cleaners contain surfactant blends which remove all traces of organic film and produce a surface which will support a continuous film of water free of "breaks". The cleaning action is speeded up by the scrubbing action of the gasses released during electrocleaning. Non ferrous metals are usually cleaned using a cathodic clean because anodic cleaning tends to oxidise the surface. Ferrous metals have to be cleaned anodically because in this case, hydrogen is adsorbed rapidly by the metal surface and this leads to embrittlement problems.

After the alkaline cleaning stage, the parts are rinsed thoroughly and given an acid dip to remove any remaining oxide and thus activate the surface. After a final rinse, the parts are ready for plating. For the work on chromium, the chromium metal was deposited directly onto steel. The process sequence for the pretreatment of this material was as shown below.

1.	Degrease with acetone.	1 minute
2.	Anodic electroclean in Activax*	3 minutes, 50 ^{o}C
3.	Rinse in cold water	1 minute
4.	Dip in 10% Sulphuric acid	1 minute
5.	Rinse in cold water	1 minute
6.	Plate.	

(* Activax is a trademark of W. Canning Ltd.)

For the work on copper deposition, the specific application which was studied was the application of copper to printed circuit boards. The substrate material chosen for this work was therefore FR4 printed circuit boards 3.2 mm in thickness with holes of various sizes drilled and coated with 2.5 µm of electroless copper. The pretreatment sequence used for this material was as for chromium except a cathodic clean was used in stage 2 instead of an anodic clean.

7.5 Measurement of Internal Stress.

As has been mentioned in the literature review, one of the major effects of pulsed current on the properties of electrodeposited chromium is the ability to produce crack free deposits of chromium. It was therefore necessary to investigate the effects of pulsed current on the internal stresses developed during the deposition of chromium.

Macrostresses in electrodeposits can be determined either by mechanical means or by the application of X-ray techniques. The application of X-ray techniques to the determination of stress in electrodeposits has not been widely applied for the following reasons :-

1. Due to the very fine grain size encountered in many electrodeposits (particularly chromium electrodeposits), the diffraction lines are broadened. Microstresses within the deposit may also cause line broadening.

2. Many electrodeposits have a preferred orientation (including chromium) which can reduce the intensity of the diffraction line to such an extent that the determination of stress becomes impossible.

3. Lattice faults can shift a diffraction line or change its symmetry. As these faults are not uniformly distributed throughout the deposit, particularly where there is preferred orientation, errors can be introduced into the calculations.

Because of the problems with using the X-ray technique, mechanical methods of internal stress determination were used. The most common mechanical method of measuring stress is to plate a flexible cathode on one side only. Stresses within the deposit then cause the cathode to bend one way or the other (depending on whether the stresses are compressive or tensile). There are a number of different versions of this stress measuring technique which vary mainly in the way the deflection of the cathode is measured. A popular instrument for the measurement of internal stress is the spiral contractometer. This instrument was designed by Brenner and Senderoff for the U.S. National Bureau of Standards in 1949 (152). In this case, a flat strip of copper or stainless steel is wound to form a helix and is plated on the outside only. Under compressive stress, the spiral tends to unwind and under tensile stress, it becomes more tightly wound. The change in the radius of curvature of the helix is thus a measure of the deposit stresses. This is determined by the angular displacement of one end of the helix while the other end is held rigid. The angular displacement is magnified by the use of gears and is read from a dial. This instrument provides a simple method of measuring stress but the helices required had a relatively large surface area and it was not possible to apply the necessary current density due to limitations of rectifier capacity and the heating effect of the high current on a small solution volume. Thus an alternative method of stress determination was chosen which was the Hoar and Arrowsmith method (153). This technique was devised by Arrowsmith and Hoar in 1957. It involves plating a thin strip of steel on one side only. The strip is anchored at the bottom and any tendency for it to bend is opposed by a magnetic force provided by coils placed on either side of this strip. An armature of iron wire is passed through the

strip and the force exerted by this armature is proportional to the coil current. Movement of the strip is detected by an optical lever system and the coil current is continuously adjusted so that no deflection of the strip occurs. A diagram of the apparatus used in the experimental work is shown in figure 17. Stress in the deposit is calculated from the following equation :-

$$S = \frac{4\,m^3\,G}{b\,t\,l\,(3\,m - 1)\,x} \qquad (66)$$

Where :-

S = Stress (N/mm^2)

G = Restoring force (N).

m = Support / Armature length (mm)

b = Width of test strip (mm)

t = Thickness of test strip (mm)

l = Plated length (mm)

x = Plating thickness (mm)

The restoring force G is calculated from a calibration graph plotting coil current vs applied force (applied by weights).

This technique of stress measurement is a null deflection technique and so eliminates the stress relief encountered by other methods which allow bending of the strip. The method is also very sensitive.

Disadvantages of the technique are that the armature is prone to sticking in the coils and the mirror on the optical lever system tends to become covered in plating solution (particularly in chromium plating solutions). Also, the technique cannot be used where air agitation is required in the electrolyte.

Figure 17. Schematic Diagram of Hoar and Arrowsmith Apparatus.

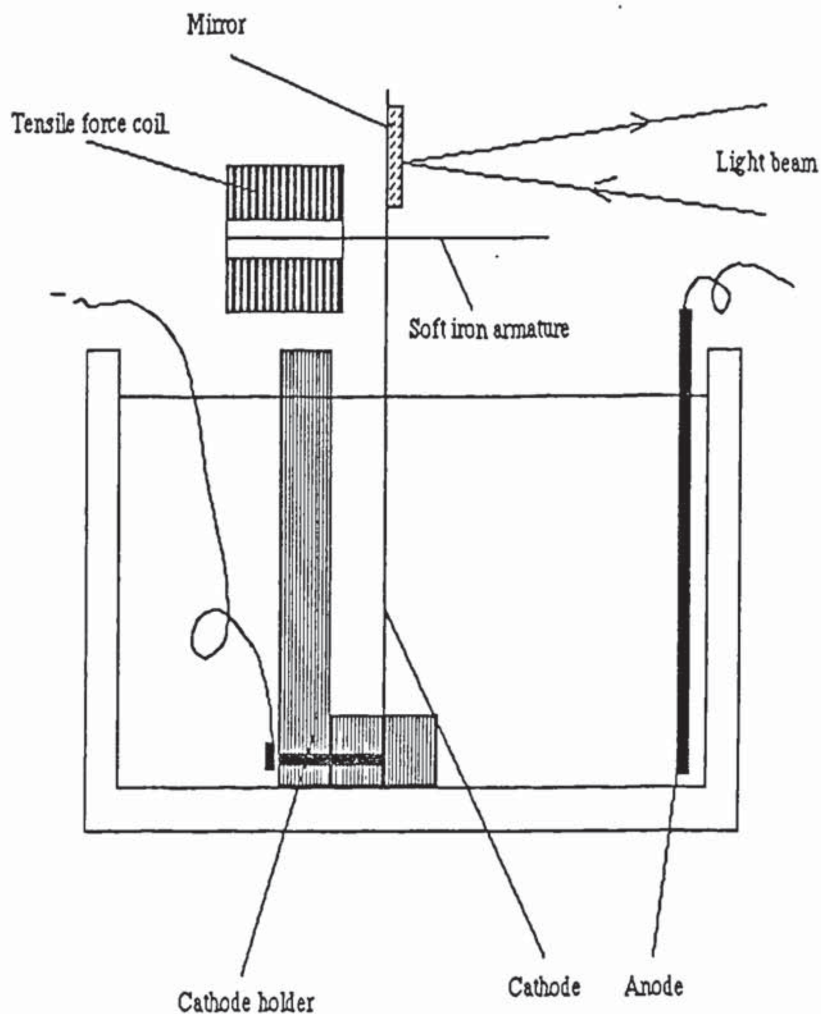

N.B. The compressive force coil is not shown for the sake of clarity.

In operation, "robbers" are used on either side of the cathode strip to give an even current density on the cathode surface.

The main source of error in the method is caused by the tendency of the thin strip to bend into an "S" shape thus causing measurement errors(101). This is minimised by keeping the armature as close to the electrolyte level as possible. The evolution of hydrogen on one side only of the strip can also cause bending.

This technique was used to determine the variation of internal stress with plating thickness of chromium deposited from a sulphate catalysed electrolyte using both direct and pulsed current.

7.6. Determination of Electrolyte Covering Power.

In the case of copper deposition, the covering power (ability to produce a deposit in low current density areas) is good and it was not felt necessary to attempt to measure this. However, in the case of chromium deposition, cathodic efficiency rises as current density increases. This results in a very poor throwing power and also poor covering power. The covering power of the chromium electrolytes was assessed by plating Hull cell panels in a standard Hull cell at a cell current of 10A for 5 minutes using both direct and pulsed current. Tests were carried out using both polished brass and steel as the substrate material in order to assess the effect of substrate on the covering power.

Covering power was determined by measuring the length of the Hull cell panel which was covered in chromium and then converting this into a current density value for minimum coverage using the equation (154):-

$$j = I\left(5.1 - 5.24 \log_{10} X\right) \qquad (67)$$

Where :-

j = Current density at distance X (A/dm^2)

I = Plating current applied to test panel (A)

X = Distance from high current density end of Hull cell panel (cm)

7.7. Determination of Deposit Thickness.

7.7.1. Determination of Thickness by Microsection.

Cross sections of the test panels to be measured were cut, supported using sample clips and mounted in Bakelite using a Metaserv automatic mounting press. The samples were then ground, polished and etched using 10% ammonium persulphate solution for the copper samples and 1% Nital for the chromium samples on steel. The etching treatment was simply to differentiate clearly between the coating and the substrate. The thickness of the coating was then measured using a Leitz microhardness tester equipped with a measuring scale calibrated in µm.

7.7.2. Determination of Thickness by Coulometric Methods.

This method of coating thickness determination relies on the anodic dissolution of the coating under galvanostatic conditions. The electrolyte is chosen so that the anodic efficiency of dissolution of the coating is 100%. The coating thickness can then be calculated from the number of coulombs required to completely remove the coating. The end point for the process is detected by the change in electrode potential which occurs when the coating is penetrated and the substrate begins to be dissolved.

A Twin City Instruments coating thickness computer was used for coulometric thickness determinations using electrolytes supplied by the manufacturers. The instrument was calibrated by measurement of the thickness of samples where the coating thickness has been determined by microsection.

7.8. Determination of Throwing Power.

7.8.1. Determination of Macro Throwing Power.

Macro throwing power was assessed by plating Hull cell panels and measuring the coating thickness at various current densities. In the case of the acid copper electrolytes, a polished brass Hull cell panel was plated in an air agitated Hull cell at 2A for 1 hour. The panel was then nickel plated to protect the copper and microsectioned at distances along the test panel corresponding to primary current densities of 6,4,3,2 and 1A/dm^2. From the thicknesses obtained at these current densities, the throwing power was calculated using the Field formula :-

$$T\% = \frac{P - M}{P + M - 2} \cdot 100 \qquad (68)$$

Where :-

T% = Percentage throwing power

P = Ratio of the primary current densities

M = Ratio of the metal thicknesses

In these determinations, the primary current density ratios were calculated from the high current density end downwards.

7.8.2. Determination of "Hole Throwing Power."

In the production of printed circuit bords, the ratio of the thickness of copper deposited on the surface of the boards compared to the thickness of copper deposited in the holes is of primary importance. Ideally, the thickness of copper in the holes should be at least as thick as the copper deposited on the surface of the board. Since the centre of the hole represents a low current density area, this presents a considerable problem.

In order to assess hole throwing power, a test cell was designed to try to match as closely as possible (on a small scale) conditions met in practice. A test panel was used consisting of a piece of FR4 printed circuit board 3.2 mm in thickness with rows of holes of various diameters drilled in it. The hole diameters used were 0.6, 0.8, 1.0, 1.2 and 1.4 mm giving corresponding hole aspect ratios of 5.3:1, 4:1, 3.2:1, 2.6:1 and 2.3:1. The board was coated with 2.5 μm of electroless copper to metallise the holes and plated in the test cell. After plating, the board was sectioned and mounted. Grinding and polishing was then carefully carried out so that the holes were cross sectioned at their centres. To check this, the hole diameters were measured. The average thickness of copper on the surface of the boards was determined from 10 measurements and the average thickness of copper in the centre of the hole determined from 4 measurements taken from the centres of 4 separate holes of the same diameter i.e. 16 readings for each hole diameter. Sections were taken from holes at the centre of the board to minimise edge effects. The results were expressed as a percentage value of the ratio of copper in the hole / copper on the surface.

Figure 18 shows a schematic diagram of the test cell used for the throwing power determinations. In all of the tests, the stroke rate, stroke length and rate of airflow were held constant. The parameters used were as follows :-

Cell Dimensions (internal)	20cm (L) x 10cm (W) x 12cm (D)
	(working depth 10cm)
Working volume -	2 Litres
Stroke rate -	0.5 / sec
Stroke length -	3 cm
Rate of airflow -	2.4 l/min for each agitation tube.

The test cell was designed with both mechanical cathode agitation and air agitation because this is what happens in practice. The high throwing power electrolyte is low in metal content so good agitation is essential. Air agitation provides bulk solution movement and the cathode movement ensures that electrolyte is forced through the holes to replenish the depletion in metal ions. The above factors were maintained constant to ensure that the hydrodynamic conditions prevailing at the cathode surface were as consistent as possible.

In addition to the tests carried out in the laboratory plating cell, tests were performed on boards plated under commercial conditions, trials were carried out on 3.2 mm thick boards with a British Standard test pattern applied with added large ground planes on one side of the board only. This also enabled a comparison of the surface copper distributions by obtaining the ratios of the copper metal thickness deposited on isolated pads on one side of the boards to the thickness of copper on the ground planes on the opposite side of the boards.

Figure 18. Schematic Diagram of Test Cell Used for Throwing Power Determinations.

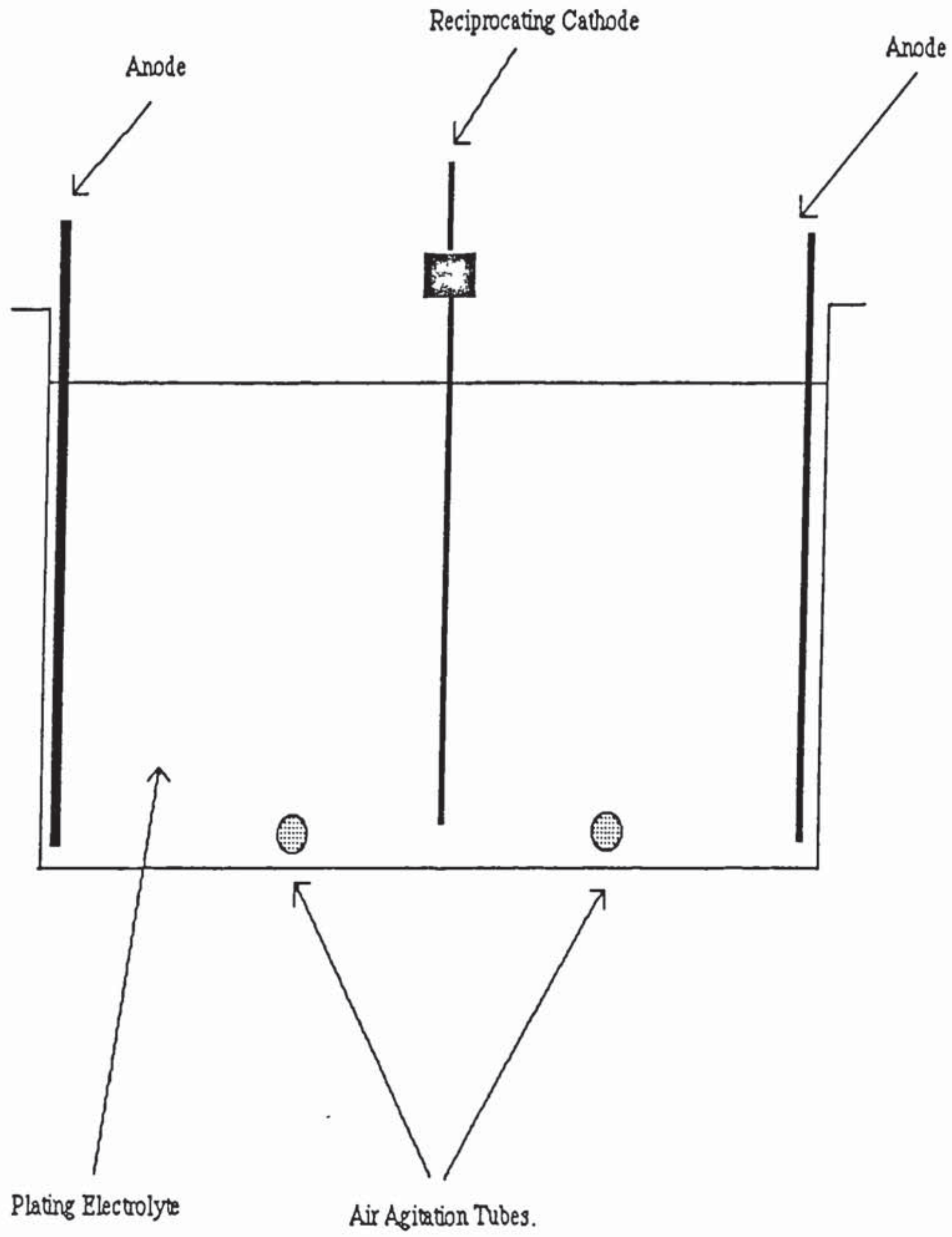

To assess the hole throwing power of the electrolyte, each test board was microsectioned at four specific sites to determine the throwing power obtained with different circuit patterns. The patterns used were as follows:-

Series 1. - Isolated pads with 0.8 mm holes at the centre of the test boards.

Series 2. - Isolated pads with 0.8 mm holes at a corner of the board.

Series 3. - 0.8 mm holes with isolated pads on one side and a ground plane on the other, situated towards the edge of the board.

Series 4. - 0.5 mm holes on isolated pads near the edge of the board.

The pulse conditions used were as shown in table 10. All of the boards were plated using an average current density of 3 A/dm^2 in the case of pulsed reverse current and at a current density of 2 A/dm^2 in the case of direct current. All of the boards in the test were plated for 1 hour. The brightener system used in the tests was Lea-Ronal Coppergleam.

Table 10. Pulse Conditions Used on the Commercial Test Boards. (Average Current Density 3 A/dm^2).

Board Number	Forward Pulse Conditions (10 ms)	Reverse Pulse Conditions	Anodic/Cathodic Current density Ratio.
1	3.3 A/dm^2	0.5 ms 6.0 A/dm^2	1.81:1
2	3.4 A/dm^2	0.5 ms 8.0 A/dm^2	2.35:1
3	3.5 A/dm^2	0.5 ms 10.0 A/dm^2	2.86:1
4	3.6 A/dm^2	0.5 ms 12.0 A/dm^2	3.33:1
5	3.4 A/dm^2	1.0 ms 4.0 A/dm^2	1.18:1
6	3.5 A/dm^2	1.0 ms 5.0 A/dm^2	1.43:1
7	3.6 A/dm^2	1.0 ms 6.0 A/dm^2	1.67:1
8	2.0 A/dm^2	----------------	D.C.

7.9. Determination of Cathodic Efficiency.

Cathodic efficiency can be determined accurately by connecting a copper coulometer in series with the plating bath. Since the efficiency of copper deposition is 100% under normal circumstances, the number of coulombs passed during the experiment can be calculated from the weight of copper which is deposited. However, when pulsed current is used, this method of coulometry is unsuitable because the copper coulometer introduces extra capacitance which may distort the form of the Faradaic waveform and because the reduction of copper involves the transfer of two electrons, pulsed current can affect the kinetics of this process and may reduce the cathodic efficiency[145]. Thus for the efficiency determinations in this thesis, the average current was measured using an analogue meter and multiplied by the time of plating to give the number of coulombs passed. From this, the theoretical weight of deposit could be calculated from the following equation :-

$$W = \frac{i.t}{zF} \cdot \frac{1}{A.W.} \qquad (69)$$

Where :

i = Average current in amps.

t = time in seconds.

z = ionic charge of reducing species

F = Faraday constant (96500 coulombs)

A.W. = Atomic weight of metal.

The cathodic efficiency can then be calculated by comparing the theoretical weight of deposit with the actual weight of deposit as follows :-

$$\% \text{ Efficiency} = \frac{\text{Actual Weight of Deposit}}{\text{Theoretical Weight of Deposit}} \times 100 \qquad (70)$$

Thus the cathodic efficiency was calculated simply by weighing a test panel before and after plating.

7.10. Determination of Cathode Potential.

For the studies on the effect of organic additives on the deposition of copper, it was necessary to measure cathode potential at various current densities. This is because the surface active nature of the organic additives may modify the polarisation characteristics of the plating electrolyte and this may in turn be influenced by the application of pulsed current.

Cathode potential at a given current density is usually determined by the use of a potentiostat driven in galvanostatic mode and determining the cathode potential by the use of a reference electrode. The use of a rotating disc electrode means that the hydrodynamic conditions can be maintained fairly constant.

The above method cannot be used for studying the effects of pulsed reverse current on an electrolyte system because a galvanostat cannot be used with pulsed reverse current and rotating disc electrodes are too small to be able to control current parameters accurately without a galvanostat. Rotating disc electrodes have a further disadvantage in that they do not reproduce the hydrodynamic conditions encountered in practice. In order to assess the effect of pulsed reverse current on the polarisation behaviour of electrolytes, a test cell of fixed geometry was devised consisting of a circular copper cathode 6cm in diameter plated on one side only. An air agitation coil was fixed below the cathode and fed with a constant volume of air during the experiments. A diagram of the apparatus used is shown in figure 19. In order to measure the cathode potential, a

Figure 19. Schematic Diagram of Apparatus used for Cathode Potential Measurement

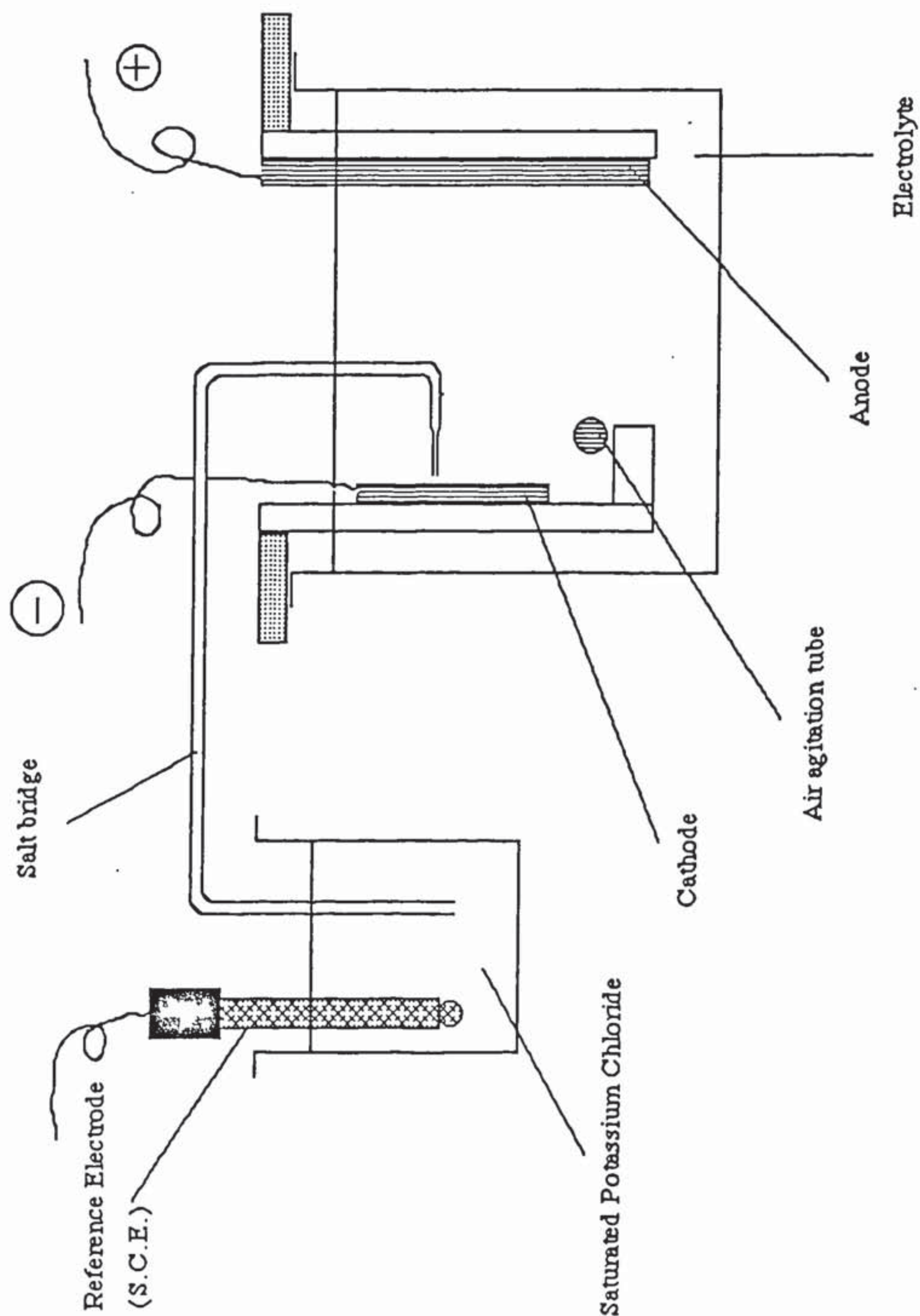

salt bridge capillary was positioned so that it was 1 mm from the surface of the cathode centre and used in conjunction with a Saturated Calomel Electrode to measure the average cathodic overpotential. A solartron digital voltmeter was used for this purpose. For the direct current measurements, a Farnell rectifier was used in constant current mode. An initial deposit of copper was plated on the cathode at 3 A/dm^2 for 10 minutes before readings were taken. Potential readings were taken at current densities of 0.5, 1, 2 and 3 A/dm^2. In all cases, the potentials were allowed to stabilise before a reading was taken. In the case of electrolytes containing organic additives, this could take up to 10 minutes. A note was also made of the unpolarised electrode potentials.

In the case of pulsed reverse current, the circuit shown in figure 20 was used to determine average overpotentials, this was done using a cathodic pulse time of 10 ms, an anodic pulse time of 0.5 ms and a anodic/ cathodic current density ratio of 3:1. These parameters were chosen because they have been shown to work in practical applications (155). Average current densities of 0.5, 1,2 and 3 A/dm^2 were used.

7.11. Potentiodynamic Scans.

In order to assess the effect of pulsed current on the electrochemical behaviour of chromium coatings deposited on to steel, potentiodynamic scans between -0.9V and +1.0V (vs S.C.E.) were performed on the test specimens using a Princeton Research instrument.

Figure 20. Circuit Diagram for Polarisation Studies using Pulsed Reverse Current.

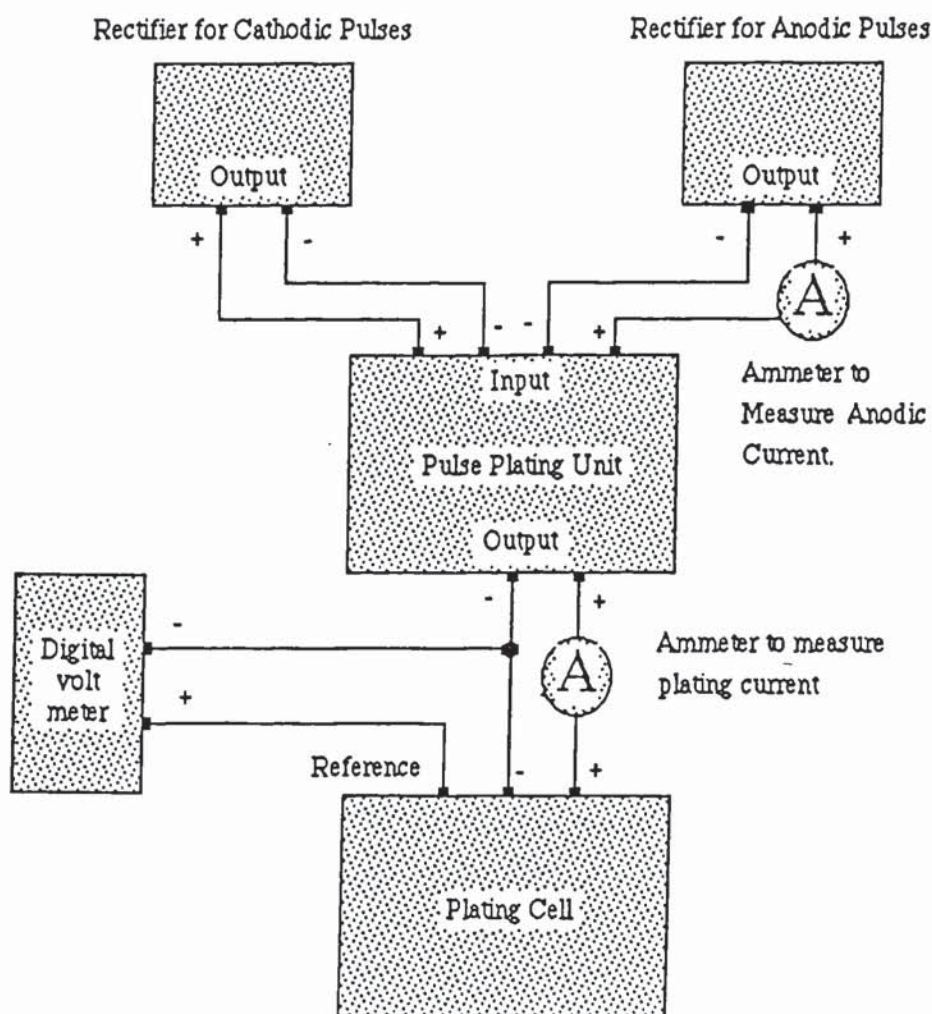

The electrolyte used for all the tests consisted of an acidified saline solution with the following composition :-

Sodium Chloride	50 g/l
Acetic acid	to adjust pH to 3.1-3.2

Samples were prepared for potentiodynamic testiing by plating pins made of E.N. 31 steel with a thickness of 40 µm of chromium plated at an average current density of 40 A/dm^2 at a temperature of 52-54^oC.

7.12. Polarographic Studies.

The oxidation and reduction behaviour of the sulphopropyl sulphides used as addition agents in the experimental work was studied using differential pulse polarography. A Metrohm instrument was used for this work using the following conditions :-

Reference electrode	Ag/AgCl
Counter electrode	Carbon
Working electrode	Dropping mercury *
Support Electrolyte	10% H_2SO_4
Potential scan range	+0.1 to -1.0 V

* N.B. The Metrohm system uses pumped mercury rather than gravity fed which gives a more reproducible drop size.

The half wave potentials for reduction of SSP and the oxidation of MPS were determined under these conditions. The potential of the dropping mercury electrode vs

the reference electrode in the support electrolyte used was measured under open circuit conditions using a digital volmeter to give the "rest potential" of the cell. This enabled the estimation of the applied overpotential.

7.13. Hardness Testing.

The hardness of the coating evaluated in the experimental work was determined using a Leitz micro hardness tester equipped with a Vickers indenter. Hardness values were measured on cross sections of the deposits which were mounted and polished as described in section 7.7.1.. To obtain accurate hardness readings, a coating thickness of three times the size of the indentation is required. This lead to the choice of a 100g load for chromium hardness determinations but a load of 50g for the copper deposits which are considerably softer. In all cases, the hardness value quoted in the results is the mean value of 10 readings.

7.14. Microscopy.

7.14.1 Surface Examination.

Initial observations of deposit surfaces were made using optical microscopy. Crack counts on chromium deposits were determined using an optical microscope equipped with a 200 μm graduated scale. The number of cracks crossing this scale were counted and this value was converted to cracks/cm. Cracks were counted using unetched samples. Surface topography of the deposits was also examined by the use of Scanning Electron Microscopy. In some cases, gold coating of the samples was required before examination.

7.14.2. Examination of Grain Structure.

The grain size and structure of copper deposits obtained by various plating conditions was examined by the use of Transmission Electron Microscopy. Thin foils were prepared by plating the copper to a thickness of 50 μm onto a stainless steel plate which was masked around the edges, dipped in chromic acid solution before plating and rinsed thoroughly. The chromic acid pretreatment ensures that the resultant copper coating is non adherent and can be peeled off after plating. Discs were then cut from the centre of the foil using a 3mm punch and thinned to an electron transparent thickness using a Tenupol jet polisher. This instrument polishes the disc from both sides by jetting electropolishing electrolyte at the disc which is made anodic. Electropolishing of the disc then commences and continues until the disc is perforated. Perforation of the disc is detected by a photodiode on one side of the disc which detects a light beam on the other side of the disc when perforation occurs. Provided that the conditions were suitable, the area around the perforation is electron transparent and can be examined. The conditions used to prepare the discs used in the experimental work were as follows :-

Electrolyte flow rate	3 (on a scale of 1-10)
Cell voltage	10 V
Temperature	20 ^{o}C

The electropolishing electrolyte used gave good results under these conditions and had the following composition (by volume) :-

Phosphoric Acid	500 ml
Industrial Methylated Spirit	300 ml
Water	To 1 litre

After preparation, the foils were stored under vacuum to prevent oxidation and examined using a J.E.O.L. transmission electron microscope using bright field illumination and an accelerating voltage of 100 kV.

It was not possible to study the grain structure of chromium deposits using this technique due to the difficulty of producing thin foils of chromium. Chromium deposits in a very brittle condition and with a high tensile stress. This makes it very difficult to produce self supporting foils thin enough for examination by T.E.M.

7.15. X-Ray Diffraction Studies.

In order to identify any hydride phases present in the chromium deposits produced under various plating conditions, samples consisting of flat steel plates were plated to a thickness of 30 μm and subjected to X-ray diffraction analysis within 1 hour of plating. It was necessary to process the samples quickly because chromium hydrides are thermally unstable and decompose slowly at room temperature to produce body centred cubic chromium metal.

A Philips X-ray diffractometer was used for the tests and the following conditions were employed :-

Radiation	Cu K α
Filter	Nickel
Detector	Proportional counter
Divergent slit	1°
Receiving slit	4°
Scan Range	35 - 90°

The peaks obtained were indexed using published values for the lattice parameters and the structure of the deposits was determined from these peaks.

7.16. Determination of Sulphur Incorporation in Copper Deposits.

When studying the effects of organic additives on the deposition of copper, an understanding of the mechanism of incorporation of the sulphopropyl sulphides could possibly be achieved by measuring the rate of incorporation of sulphur under different conditions. Edwards (131-136) determined the mechanism of incorporation of various organosulphur compounds in nickel deposits by using radioactively labelled sulphur atoms. However, radioactively labelled MPS and SSP was not available so this technique could not be used. Because of this, alternative analytical methods for determining sulphur content were investigated. Energy dispersive X-ray analysis was attempted but the levels of sulphur in the deposit were below the detection limit for this method. Auger electron spectroscopy was considered to have inadequate sensitivity.

Finally, it was decided to try Proton Induced X-ray Emmision analysis (P.I.X.E.). In this technique, the sample is bombarded with a beam of high energy protons produced in a particle accelerator and the characteristic emitted X-ray spectrum is recorded. This method is capable of detecting sulphur at levels of 0.0005 %. To try this method, a foil of copper 100 µm thick was prepared from an electrolyte containing 100 p.p.m. of polyether and 40 p.p.m. of MPS. This was subjected to analysis by P.I.X.E. but no sulphur incorporation was detected. This suggests that the level of sulphur incorporation in copper deposits is extremely small or that sulphur is not incorporated at all.

Chapter 8.

Experimental Results - Chromium.

8.1. Coating Properties.

Since hard chromium deposits are usually applied for engineering purposes, mechanical properties are of primary importance. In the literature review, it was noted that crack free deposits could be obtained by the use of pulsed or pulsed reverse current. The aim of the experimental work was to assess the effect of unipolar pulsed current on the properties of electrodeposited chromium, a duty cycle of 50% was used (except where stated) and the effect of varying pulse frequency between 16-3000 Hz was studied. In all experiments, (except Hull cell tests) a fixed average current density of 40 A/dm^2 and a temperature of 52-54 ^oC was used.

8.1.1. Hardness of Coatings.

Table 11 shows the Vickers hardness values obtained from the three experimental electrolytes. The results are also plotted graphically in figure 21 using a logarithmic scale for frequency. A logarithmic scale was chosen because on a linear scale, a frequency of 0 is meaningless and causes confusion.

It can be seen from the results displayed in figure 21 that the hardest deposits were obtained at the highest frequencies for all the electrolytes. In all cases, the hardness of the deposits was reduced as frequency was lowered. At the highest frequency used in the experiments, the hardness values obtained for the coatings were similar to those obtained by the use of direct current (as shown in table 11).

Table 11. Effect of Frequency on the Hardness of Deposits Obtained from Three Different Chromium Electrolytes.

Frequency (Hz)	Type of Chromium Plating Bath. Sulphate	Chromefast	Mach 1
16	520	580	560
100	680	700	570
500	700	720	570
1000	760	770	730
1750	850	880	980
2500	1010	1060	1110
3000	1050	1080	1150
D.C.	1180	1100	1200

Figure 21. Effect of Frequency on the Hardness of Deposits Obtained from Three Different Chromium Electrolytes.

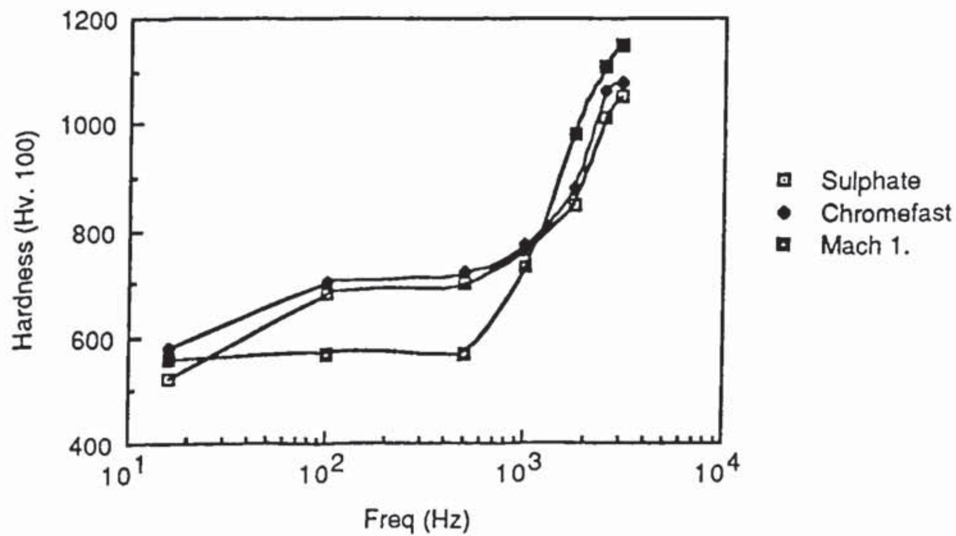

8.1.2. Internal Stress of Deposits.

The mean internal stress of deposits obtained from the sulphate catalysed electrolyte was determined at duty cycles of 50 and 70% at frequencies of 100 and 2500 Hz by the use of the Hoar and Arrowsmith technique, as described in section 7.7 in the experimental procedure. The coil calibration graph is shown in figure 22.

Figure 22. Coil Calibration Graph for Hoar and Arrowsmith Apparatus.

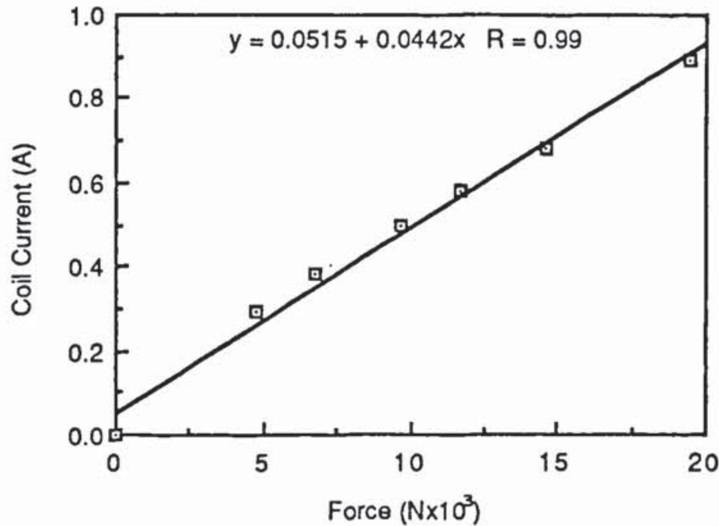

This figure shows good correlation of data (coefficient of correlation of 0.99). Using the calibration data, mean stress measurements were taken at various time intervals by noting the coil current required to maintain null deflection at each measurement point.

After each test was run, the strip was weighed to determine the thickness of chromium. Each time point could then be converted to a corresponding thickness value. Stress values were calculated for each point and mean tensile stress plotted against deposit thickness. These results are shown in figures 23 and 24.

It can be seen from the results shown in these figures that the application of pulsed current to the sulphate catalysed electrolyte caused a net reduction in the measured internal stress as compared to deposition by direct current. the reduction in stress was greater at 50% duty cycle than at 70% duty cycle. Microscopic examination of the test

Figure 23. The Effect of Pulsed Current on the Mean Internal Stress of Deposits Obtained from the Sulphate Catalysed Electrolyte at a Frequency of 100 Hz and Duty Cycles of 50 and 70%.

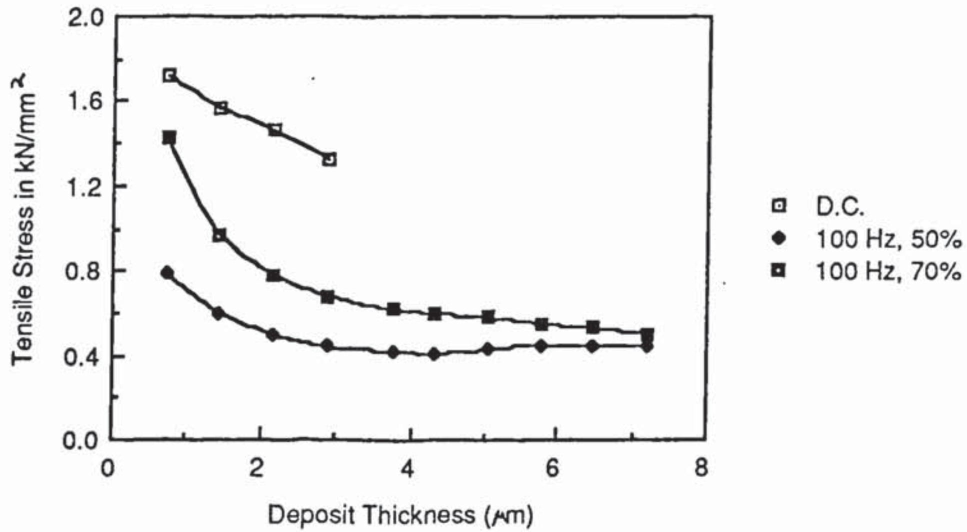

Figure 24. The Effect of Pulsed Current on the Mean Internal Stress of Deposits at a Frequency of 2500 Hz and Duty Cycles of 50 and 70%.

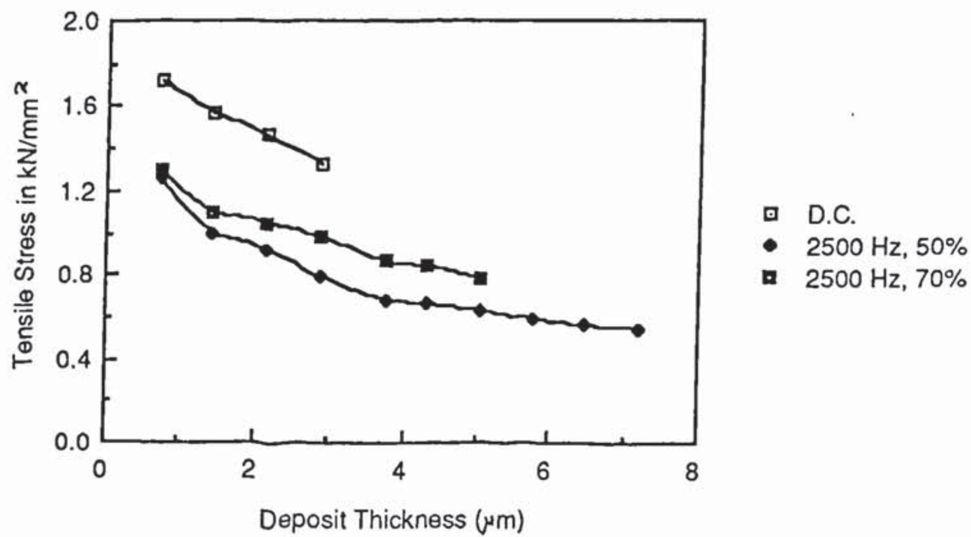

pieces after plating revealed that the deposits obtained at 100 Hz were cracked. This would have resulted in some stress relief. the deposits produced at the higher frequency of 2500 Hz were crack free so the measured reduction in stress in this case was not due to cracking of the deposit and represented a genuine stress reduction.

8.1.3. Visual Appearance, Crack Formation and Surface Topography of Deposits.

All of the experimental observations of visual appearance and surface topography and crack counts were performed on deposits plated onto flat mild steel plates ground to a standard finish and plated with 30 μm of chromium.

8.1.3.1. Visual Appearance.

The visual appearance was assessed by categorising deposits as bright, semi-bright or dull. As the classification of semi-bright covered a fairly wide range of appearances from virtually dull to almost fully bright, this category was further subdivided into categories of dull/semi-bright, semi-bright/bright, semi-bright, semi-bright/bright and bright/semi-bright in order of increasing brightness. Although this system is fairly arbitrary, it gives a good idea of the way in which pulsed current affects the visual appearance of the deposits. The effect of pulsed current on the visual appearance of the deposits is summarised in table 12.

It can be seen from the results shown in table 12 that in general, the appearance of the deposits improved with an increase in frequency but in terms of brightness, it was never better than the D.C. plated deposit. The Mach 1 electrolyte gave the brightest deposits and the sulphate catalysed electrolyte tended to produce the dullest deposits.

Table 12. The Effect of Varying Frequency on the Visual Appearance of Three Different Chromium Deposits.

Frequency (Hz)	Type of Chromium Plating Bath. Sulphate	Chromefast	Mach 1
16	Semi-bright	Semi-bright	Semi-bright
100	Dull	Dull	Dull/Semi-bright
500	Dull	Dull/Semi-bright	Semi-bright
1000	Dull/Semi-bright	Semi-bright	Bright
1750	Semi-bright	Semi-bright/Bright	Bright
2500	Semi-bright	Semi-bright/Bright	Bright
3000	Semi-bright/Bright	Bright/Semi-bright	Bright
D.C.	Bright	Bright	Bright

8.1.3.2. Crack Characteristics of Deposits.

Crack counts were performed on deposits by using an optical microscope with a graduated scale. Crack counts are given as cracks/cm. Each value quoted in table 13 is an average of ten readings.

Table 13. The Effect of varying Frequency on Crack Characteristics of Deposits from Three Different Electrolytes.

Frequency (Hz)	Type of Chromium Plating Bath. Sulphate	Chromefast	Mach 1
16	Crack Free	Crack Free	Crack Free
100	120	Crack Free	Crack Free
500	Crack Free	Crack Free	Crack Free
1000	Crack Free	Crack Free	50
1750	Crack Free	Crack Free	70
2500	Crack Free	Crack Free	80
3000	Crack Free	Crack Free	120
D.C.	240	400	350

All crack counts were performed on unetched samples. Crack free deposits were obtained throughout the frequency range studied with Chromefast C and the sulphate catalysed electrolyte (except at 100 Hz), whereas the Mach 1 electrolyte produced cracked deposits at frequencies above 500 Hz. The cracked deposits obtained from the Mach 1 electrolyte using pulsed current had a much lower crack density than deposits obtained from the same electrolyte using direct current and the crack density increased progressively with increasing frequency.

8.1.3.3. Surface Topography of the Deposits.

Figures 25,26, 27 and 28 show S.E.M. photographs of some typical surface topographies of the deposits obtained. Figure 25 shows deposits obtained at 100 Hz from the three different electrolytes. Figure 25a shows the surface topography obtained from the sulphate catalysed electrolyte. Here it can be seen that a pattern of interwoven platelets of chromium is produced. Figure 25b Illustrates the surface topography from the Chromefast C electrolyte which shows a much finer surface texture than the deposit from the sulphate catalysed electrolyte. The Mach 1 electrolyte (figure 25 c) gives a texture which is similar to that obtained with Chromefast C, but slightly coarser.

Figure 26 shows the surface topographies of deposits from the three different electrolytes at 3000 Hz. The sulphate catalysed electrolyte (26a) produced a deposit which was crack free but quite nodular in appearance which accounts for the fact that the deposit was not fully bright. Figure 26b shows a deposit from the Chromefast C electrolyte. It can be seen that this electrolyte also produces crack free deposits. These are much less nodular than deposits from the sulphate catalysed electrolyte. The mach 1 electrolyte produces a fully bright deposit at these frequencies (26c) which is cracked but with a much reduced crack density as compared to deposits produced from this electrolyte by direct current.

Figure 25. The Effect of Pulsed Current on the Surface Topography of Chromium Deposits at 100 Hz, 50% Duty Cyle at 40 A/dm^2, 54 ^{o}C.

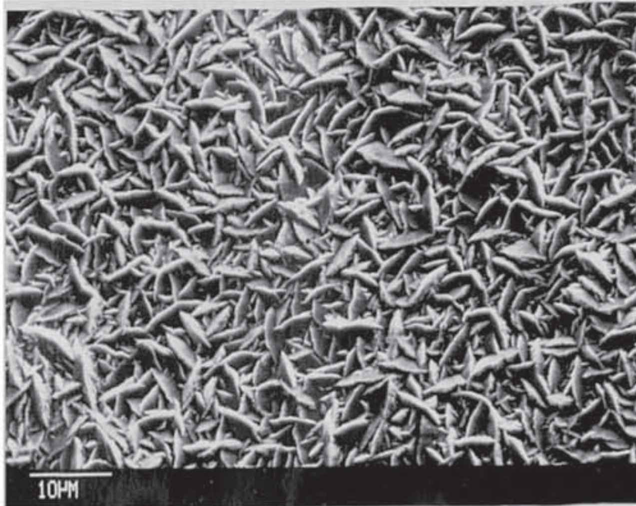

25a) Deposit from Sulphate Catalysed Electrolyte.

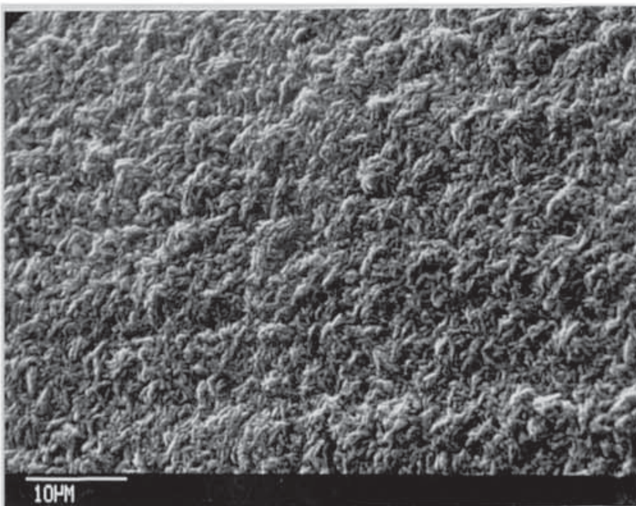

25b) Deposit from Chromefast C Electrolyte.

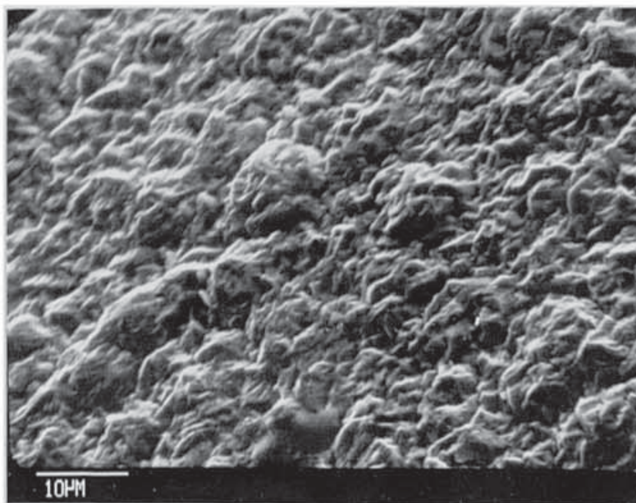

25c) Deposit from Mach 1 Electrolyte.

Figure 26. The Effect of Pulsed Current on the Surface Topography of Chromium Deposits at 3000 Hz, 50% Duty Cycle at 40 A/dm^2, 54 ^oC.

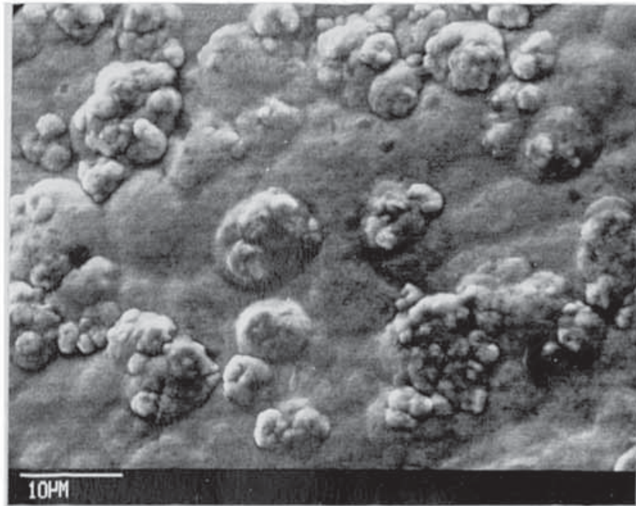

26a) Deposit from the Sulphate Catalysed Electrolyte.

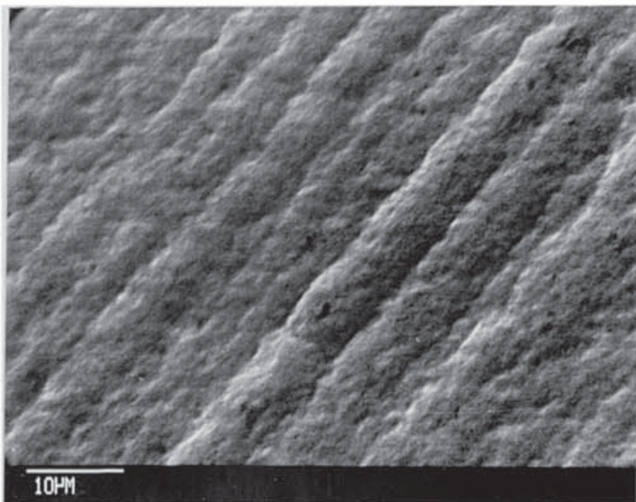

26b) Deposit from Chromefast C Electrolyte.

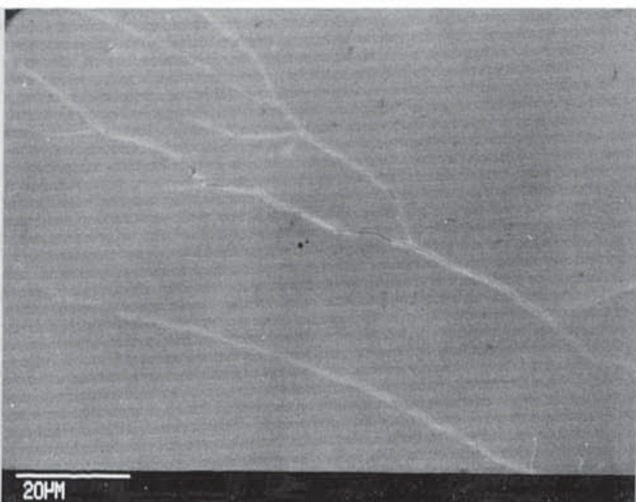

26c) Deposit from Mach 1 Electrolyte.

Figure 27. Surface Topographies of Three Different Chromium Deposits Plated with Direct Current at 40 A/dm^2, 54 ^oC.

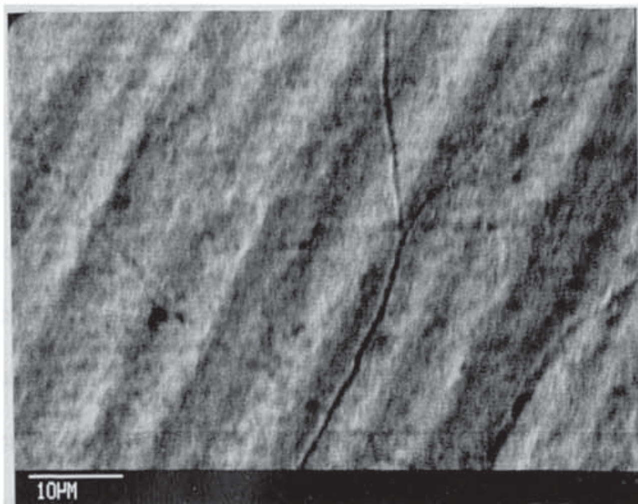

27a) Deposit from Sulphate Catalysed Electrolyte.

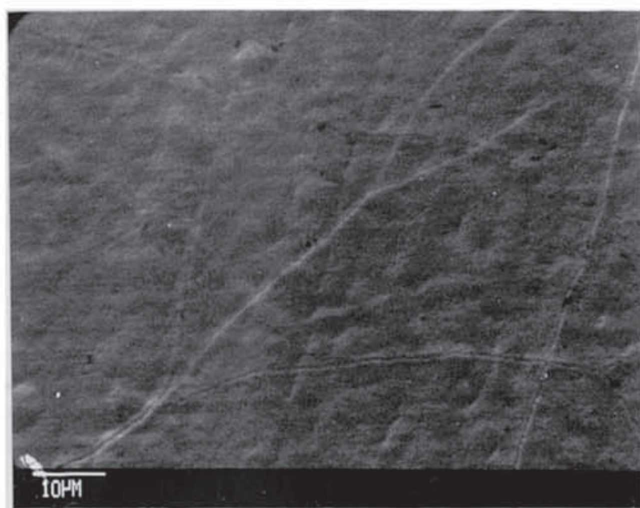

27b) Deposit from Chromefast C Electrolyte.

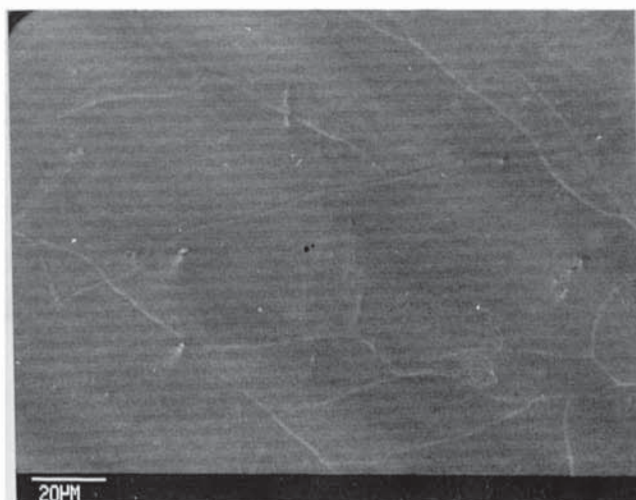

27c) Deposit from Mach 1 Electrolyte.

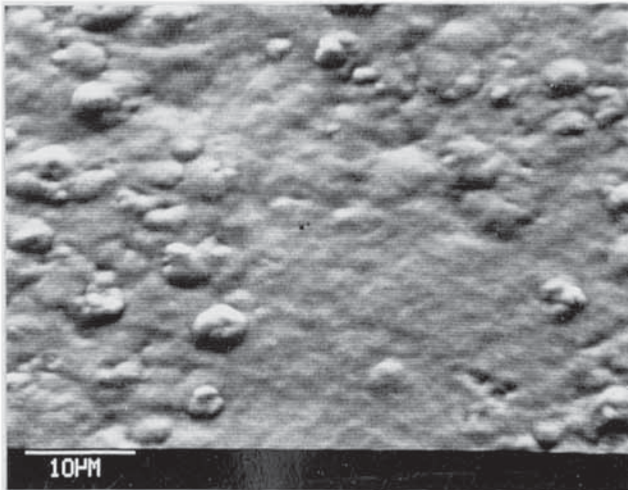

28b) Deposit Produced by Pulsed Current at 3000 Hz, 50% Duty Cycle.

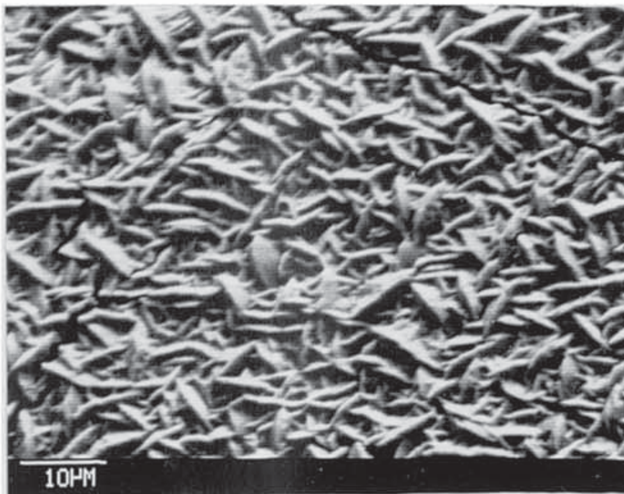

28c) Deposit Produced By Pulsed Current at 100 Hz, 50% Duty Cycle.

8.1.4. Anodic Behaviour of Coatings.

The results shown in figure 28 suggest that the behaviour of the coatings under anodic (corrosive) conditions may vary considerably depending upon whether they are deposited in a cracked or a crack free condition. To test this hypothesis, steel pins coated with chromium deposited from a sulphate catalysed electrolyte were subjected to potentiodynamic scans as described in the experimental procedure section.The results of these tests are shown in figures 29, 30 and 31.

Figure 29 illustrates the results obtained with the deposit produced by direct current. In this case, the anodic current rose steadily as potential was increased and reached a value in excess of 10^7 nA/cm^2 at a potential (vs S.C.E.) of 0.5 V. Estimation of the value of the corrosion current density (I_{corr}) yields a value of around $5x10^3$ nA/cm^2.

Figure 30 shows the results obtained from the deposit produced at 3000 Hz, 50% duty cycle with pulsed current. It can be observed that the behaviour of the coating in the electrolyte used for the test was completely different to that of the coating applied by direct current. In this case, a very large passive region is apparent in the anodic current/voltage curve and a current of $<10^4$ nA/cm^2 was obtained over this passive region at potentials up to 0.8V vs S.C.E. above which the current increased rapidly and the coating was observed to dissolve as hexavalent chromium (orange). The value of I_{corr} obtained from this scan was $6.5x10^1$ nA/cm^2 which is at least an order of magnitude lower than the value obtained in the case of the D.C. deposit.

Figure 31 shows the results obtained for the deposit produced at 100 Hz, 50% duty cycle by the use of pulsed current. In this case, a passive region is not formed and the current increased rapidly with increasing potential giving a value in excess of 10^7 nA/cm^2 at a potential of only 0.1V vs S.C.E. The I_{corr} value obtained was similar to that obtained with the deposit produced by direct current but the rate of dissolution of the coating under anodic conditions was much more rapid. Chromium was observed to dissolve at the surface during the test giving a green colour. This suggested that the coating was dissolving as trivalent chromium.

Figure 29. Potentiodynamic Scan of Deposit Produced by Direct Current from Sulphate Catalysed Electrolyte.

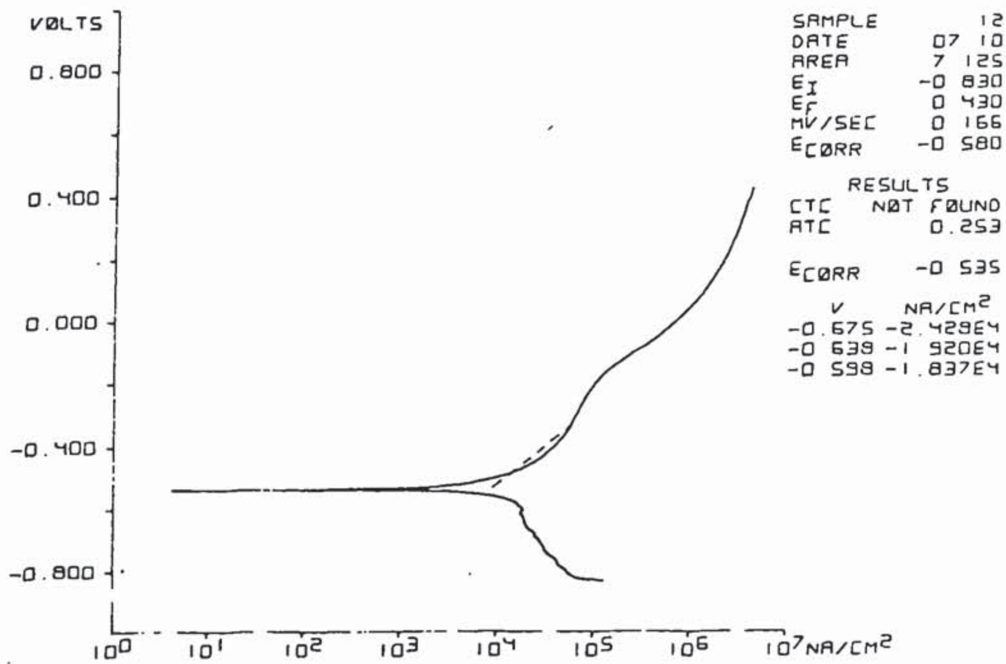

Figure 30. Potentiodynamic Scan of Deposit Produced at 3000 Hz, 50% Duty Cycle from Sulphate Catalysed Electrolyte.

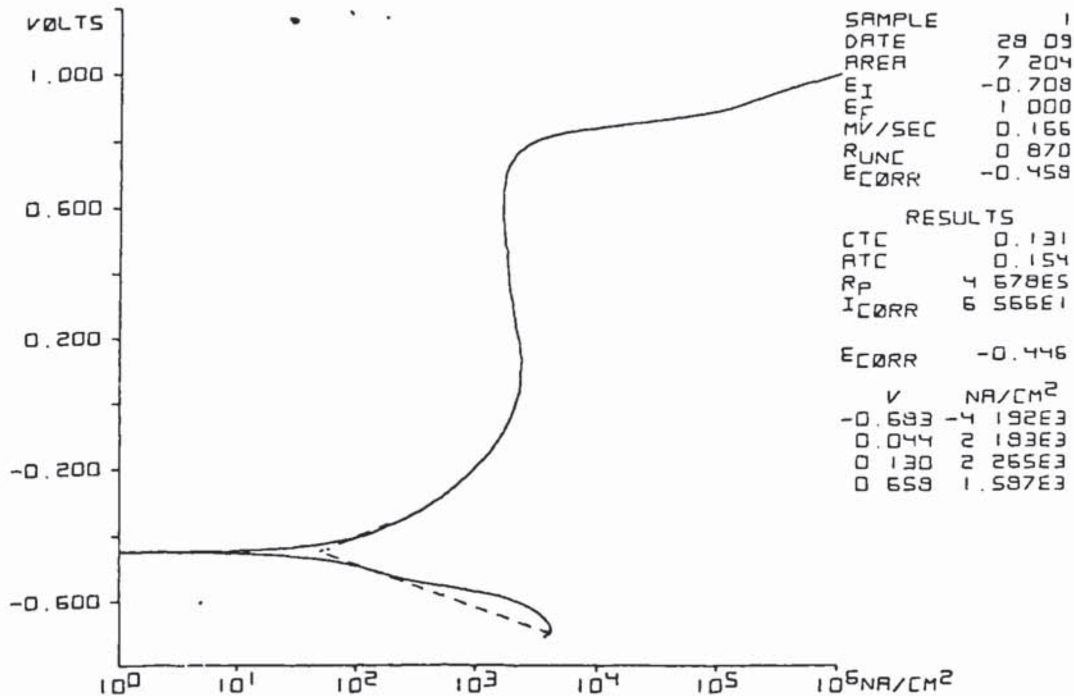

Figure 31. Potentiodynamic Scan of Deposit Produced at 100 Hz, 50% Duty Cycle Using Pulsed Current.

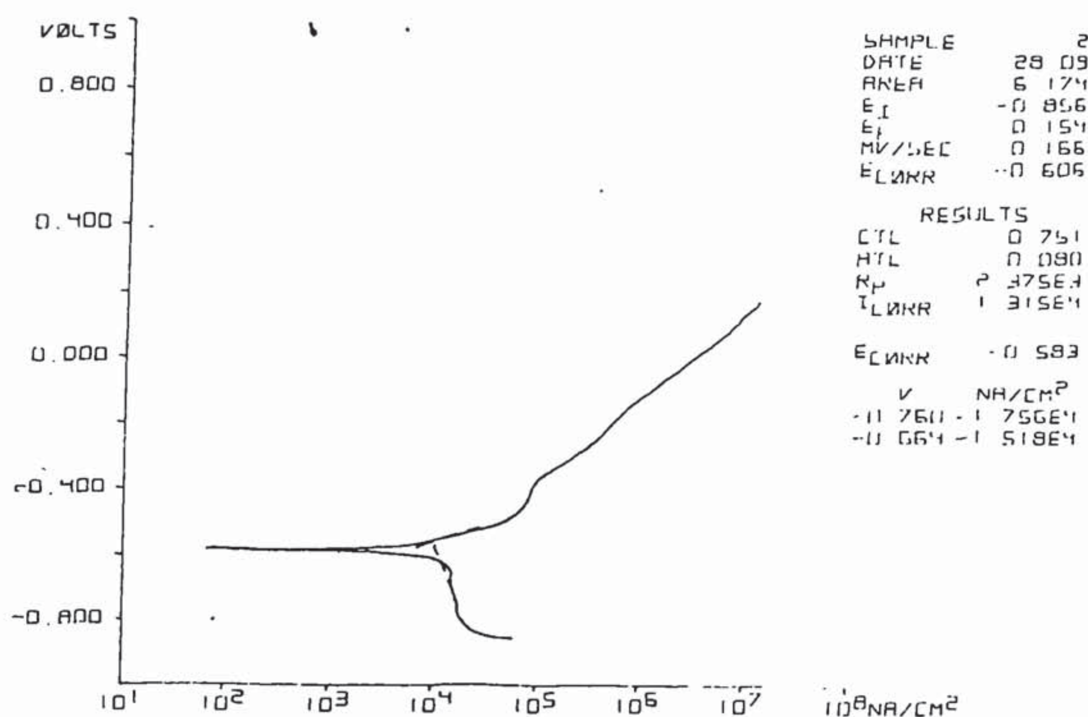

8.1.5. Composition and Orientation of Deposits.

The composition and orientation of the deposits obtained from the three electrolytes was assessed by phase analysis by X-ray diffraction as detailed in the experimental procedure section. Snavely (111) reported that in addition to body centred cubic chromium, hexagonal close packed and face centred cubic hydrides could also be formed under certain plating conditions. Lattice parameters were found from literature values (156,111) and the expected reflections were calculated from standard equations derived from the Bragg equation as described by Cullity (157). For cubic cell structures (i.e. body centred cubic and face centred cubic), the equation is as follows :-

$$\mathrm{Sin}\,\theta = \frac{\lambda}{2a}\sqrt{\left(h^2 + k^2 + l^2\right)} \qquad (71)$$

and for hexagonal close packed arrangements;

$$\text{Sin}\,\theta = \frac{\lambda}{2}\sqrt{\left(\frac{4}{3}\frac{h^2 + kh + k^2}{a^2} + \left(\frac{1}{c^2}\right)\right)} \qquad (72)$$

Where :-

θ	= Diffraction angle
λ	= Wavelength of radiation
h,k,l	= Miller Indices
a,c	= Lattice Parameters.

Literature values of lattice parameters are as follows :-

Body Centred Cubic Chromium (156). $a = 2.8839$ Angstom units

Face Centred Cubic Chromium Hydride(156) $a = 3.8605$ Angstrom units

Hexagonal Close Packed Chromium Hydride (111) .

$a = 2.717$ Angstrom units

$c = 4.418$ Angstrom units

From these values and equations 71 and 72, the expected reflections using copper $K\alpha$ radiation (wavelength 1.5406 Angstrom units) are as shown in table 14. The data from this table were used to assess the phases present in the deposits examined from the three different electrolytes under different plating conditions. The results of these investigations are shown in table 15. It can be seen from the results shown in this table that throughout the frequency range studied, the Mach 1 electrolyte produced deposits consisting only of b.c.c. chromium metal and showed no tendency to co-deposit

hydrides. The Cromefast C electrolyte produced deposits containing h.c.p. hydride at frequencies of 100-500 Hz whereas the sulphate catalysed electrolyte produced deposits containing h.c.p. and f.c.c. hydrides at frequencies of 100-1000 Hz.

Table 14. Expected Diffraction Angles for Chromium Phases using Copper Kα Radiation.

Phase Structure	Miller Indices (h,k,l)	Diffraction angle 2θ (Degrees)
b.c.c. Chromium	110	44.44
b.c.c. Chromium	200	64.6
b.c.c. Chromium	211	81.8
h.c.p. Hydride	100	38.2
h.c.p. Hydride	101	43.5
h.c.p. Hydride	102	57.4
h.c.p. Hydride	103	76.1
f.c.c. Hydride	111	40.7
f.c.c. Hydride	200	47.3
f.c.c. Hydride	220	68.8
f.c.c. Hydride	311	83.1

Table 15. The Effect of Varying Frequency on the Phases Present in Deposits from Three Different Chromium Electrolytes.

	Type of Chromium Plating Bath.		
Frequency (Hz)	**Sulphate**	**Chromefast**	**Mach 1**
16	b.c.c.	b.c.c.	b.c.c.
100	h.c.p./b.c.c.	h.c.p./b.c.c.	b.c.c.
500	f.c.c./b.c.c./h.c.p	b.c.c./h.c.p.	b.c.c.
1000	b.c.c./f.c.c.	b.c.c.	b.c.c.
1750	b.c.c.	b.c.c.	b.c.c.
2500	b.c.c.	b.c.c.	b.c.c.
3000	b.c.c.	b.c.c.	b.c.c.

Examples of typical X-ray Diffraction spectra of deposits from the sulphate catalysed electrolyte are shown in figure 32a-f. In this figure, all of the relevant peaks have been indexed and identified.

Figure 32a shows the X-ray diffraction spectrum of a deposit produced by direct current. It can be seen from this figure that no peaks are present. This can be explained by the fact that bright chromium deposits with an almost perfect (111) orientation[112]. Since only those crystal planes which are parallel to the surface give a reflection during X-ray diffraction analysis, no peaks are visible because (111) planes do not give a reflection with body centred cubic structures.

Figure 32b shows that with the application of pulsed current at 2500 Hz, peaks for the (110), (200) and (211) planes are now clearly visible which shows that the use of pulsed current at this frequency has induced some randomisation of orientation. This was also observed to occur in deposits from Chromefast C and Mach 1 though the frequency at which this was observed varied according to the electrolyte. In all cases, increasing the frequency tended to increase the amount of (111) orientation (i.e. decrease the size of the observed peaks). Mach 1 produced deposits with a perfect (111) orientation at frequencies above 500 Hz whereas Chromefast C showed some disorientation at the highest frequency used (3000 Hz).

Figure 32c shows the X-ray diffraction spectrum of the deposit produced from the sulphate catalysed deposit at 1000 Hz, Here, the peak for the (111) plane of f.c.c. hydride can be seen. Figure 32d shows that at 500 Hz, the (111) f.c.c. peak is now larger than the (110) b.c.c. peak and peaks for h.c.p. hydride are also evident. At 100 Hz (Fig. 32e), the (111) f.c.c. peak is no longer produced and the h.c.p. peaks are more pronounced. At still lower frequencies (16 Hz, figure 32f) it can be seen that hydride phases are no longer co- deposited and the deposit has reverted to b.c.c.

Figure 32. X-ray Diffraction Spectra of Deposits Produced from a Sulphate Catalysed Electrolyte.

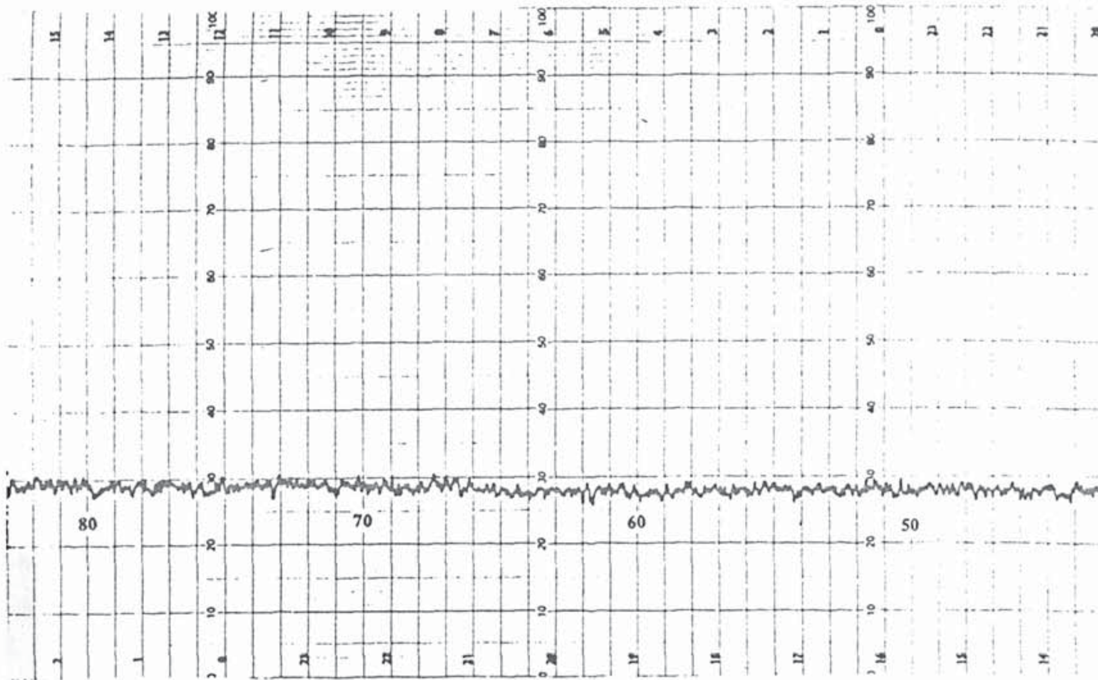

32a) Deposit Produced by Direct Current.

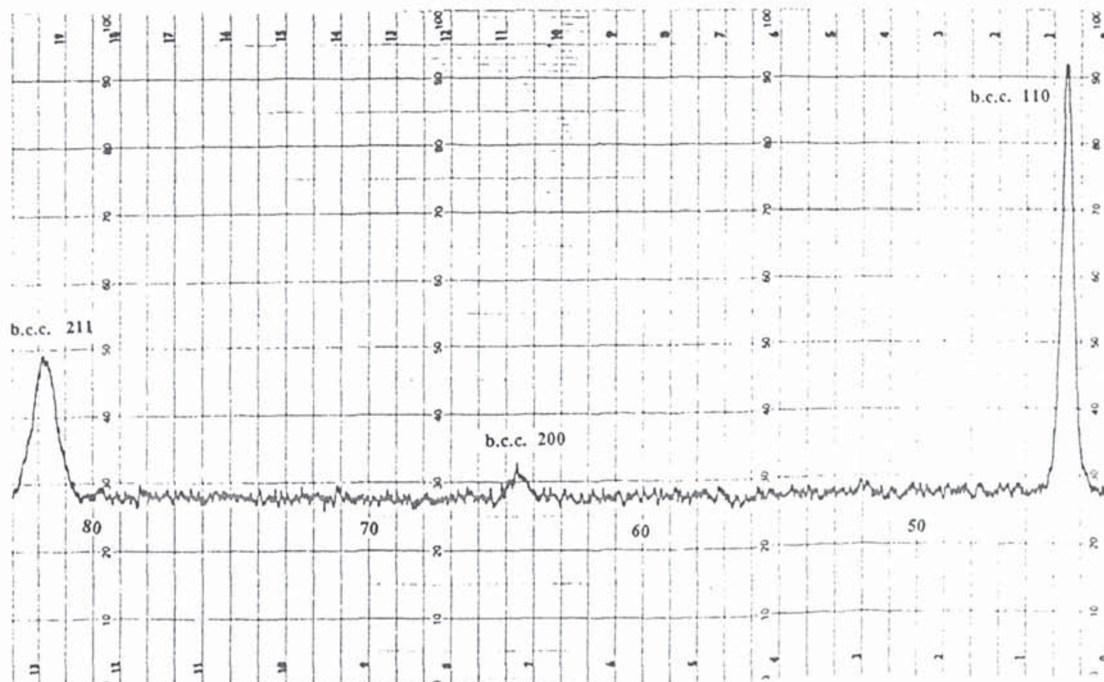

32b) Deposit Produced at 2500 Hz, 50% Duty Cycle

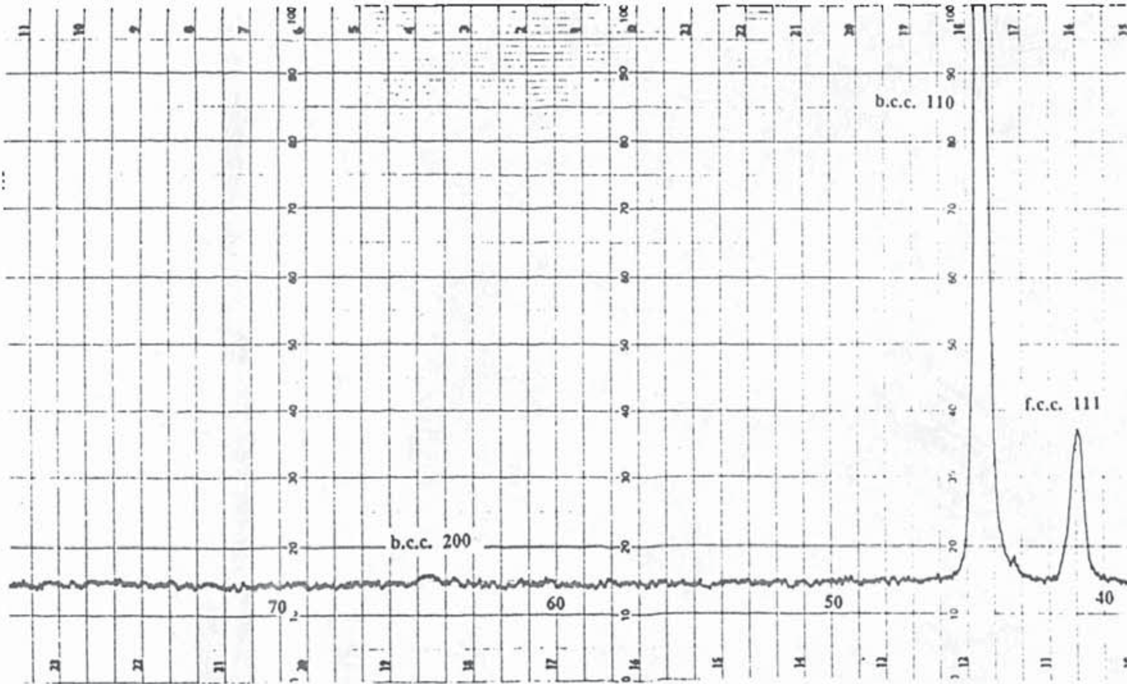

32c) Deposit Produced at 1000 Hz, 50% Duty Cycle.

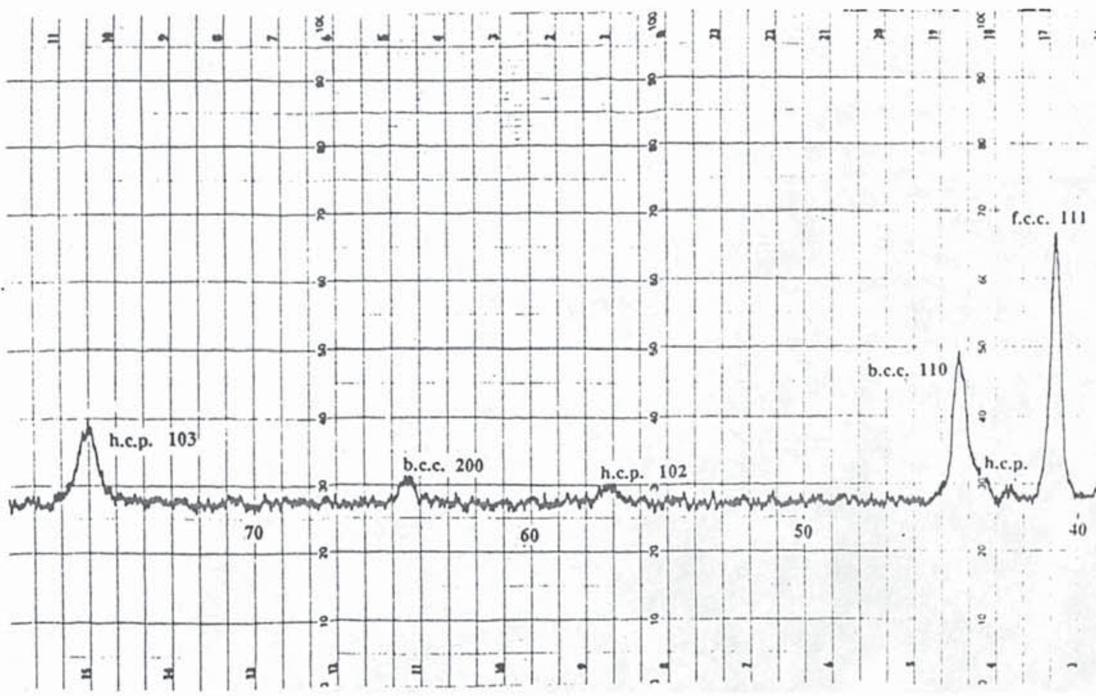

32d) Deposit Produced at 500 Hz, 50% Duty Cycle

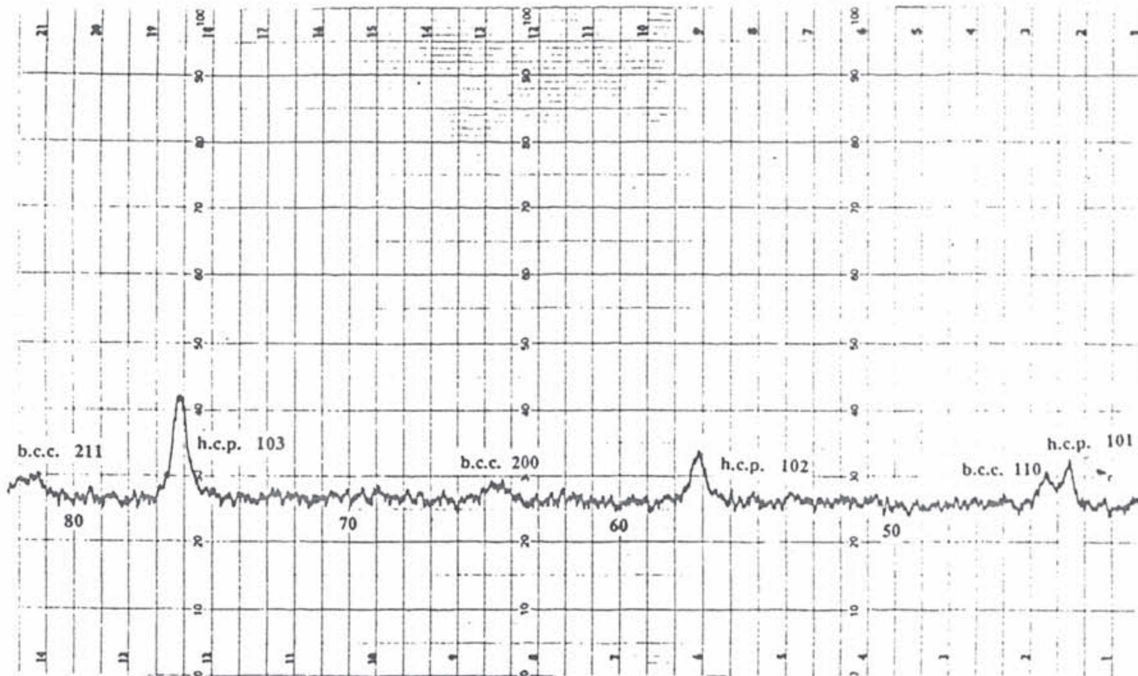

32e) Deposit Produced at 100 Hz, 50% Duty Cycle

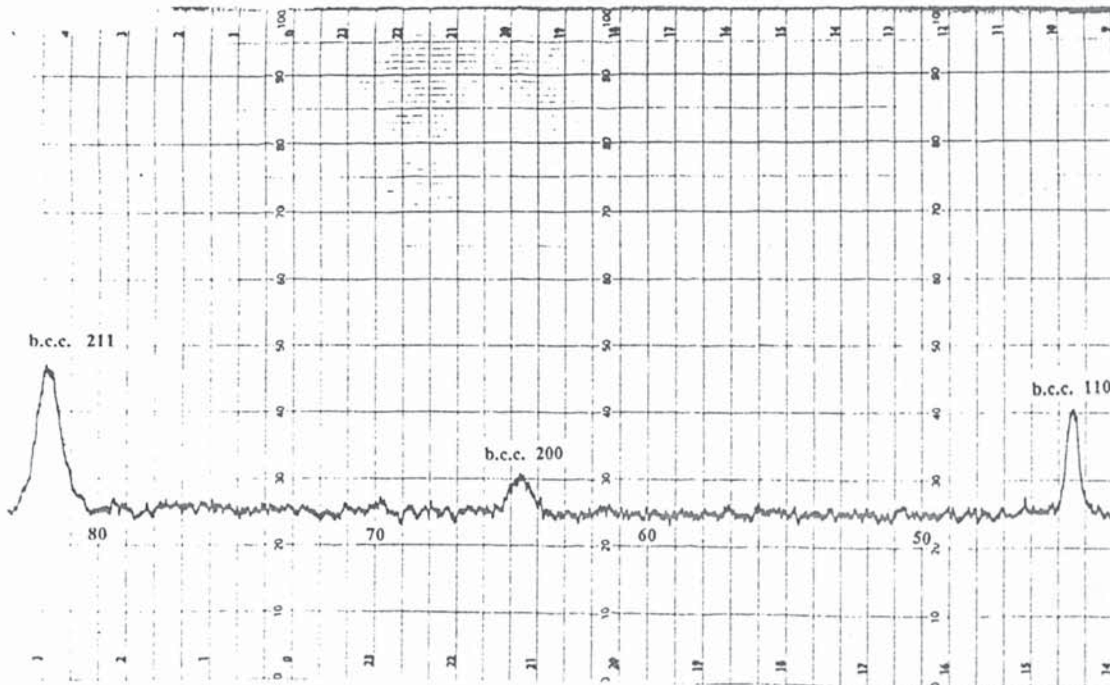

32f) Deposit Produced at 16 Hz, 50% Duty Cycle.

8.2. Electrochemical Properties.

8.2.1. Cathodic Efficiencies.

Cathodic efficiencies of the three electrolytes used for the tests were determined by the method described in the experimental procedure. The efficiencies determined are listed in table 16 and plotted graphically in figure 33.

Table 16. The Effect of Varying Frequency on the Cathodic Efficiencies of Three Different Chromium Plating Electrolytes.

Frequency (Hz)	Type of Chromium Plating Electrolyte. Sulphate	Chromefast	Mach1
16	10.9 %	14.3 %	19.2 %
100	14.0 %	12.2 %	17.2 %
500	16.4 %	21.5 %	16.0 %
1000	16.9 %	22.2 %	15.9 %
2000	14.2 %	22.2 %	18.6 %
3000	14.0 %	22.0 %	19.9 %
D.C.	13.1 %	22.4 %	23.1 %

All of these efficiencies were determined at an average current density of 40 A/dm^2.

It can be seen from these results that over the range of frequency studied in the tests, the two high efficiency electrolytes (Chromefast C and Mach 1) produced lower efficiencies than was obtained by the use of direct current. In both of these electrolytes, the efficiency was observed to fall to a minimum value at a particular frequency, then increase at the lowest frequencies used. The sulphate catalysed electrolyte behaved differently from the high efficiency electrolytes in that an increase in cathodic efficiency was obtained between 100 and 1000 Hz.

Figure 33. The Effect of Varying Frequency on the Cathodic Efficiencies of Three Different Chromium Plating Electrolytes.

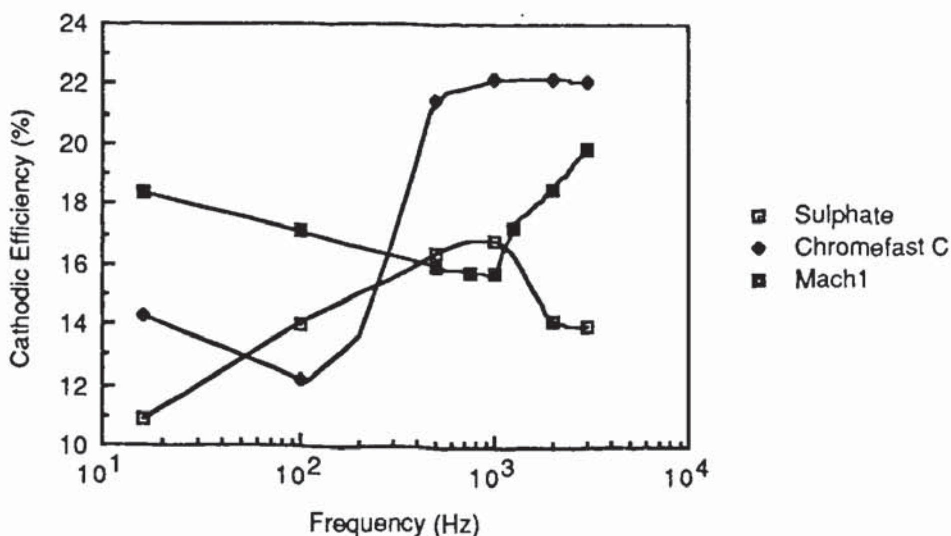

8.2.2. Covering Power.

Covering power of the three different electrolytes was assessed by plating Hull cell panels at a cell current of 10A. The Minimum current density at which chromium was deposited was recorded. On steel Hull cell panels, the use of pulsed current had little effect on the covering power over the frequency range studied. Coverage down to a current density of 6 A/dm^2 was obtained. It was noted however that plating directly onto brass Hull cell panels produced a marked reduction in covering power when pulsed current was used. These results are shown in table 17 and are plotted on fig 34.

It can be seen from these results that both the Mach 1 and sulphate catalysed electrolytes suffered a marked reduction in covering power when chromium was deposited from these electrolytes directly onto brass. The Chromefast C electrolyte appeared to be less affected than the other two electrolytes.

Table 17. The Effect of Varying Frequency on the Covering Power of Three Different Chromium Plating Electrolytes on a Brass Substrate.

Frequency (Hz)	Sulphate	Chromefast	Mach 1
16	6.7	5.7	11.0
100	8.0	7.4	13.5
500	12.2	7.4	11.4
1000	11.4	8.0	9.1
2000	9.1	8.0	9.1
3000	8.1	7.0	8.1
D.C.	4.5	4.8	6.7

Covering powers are expressed as minimum current density where a deposit was obtained (A/dm^2).

Figure 34. Frequency vs Covering Power (A/dm^2) on a Brass Substrate.

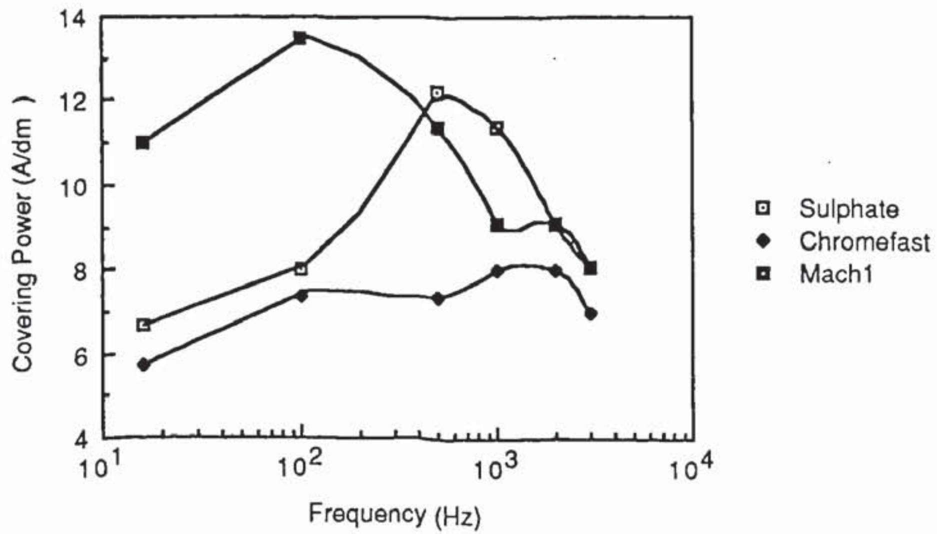

Chapter 9.

Discussion of Results - Chromium.

9.1. Hardness and Internal Stress.

The application of pulsed current to all three of the chromium plating electrolytes studied caused a softening of the deposit. Puippe [31] has noted that for some metals, grain refinement occurs when pulsed current is applied due to either the increased nucleation rate caused by the higher pulse current density (as compared to an equivalent deposition rate with direct current) or by adsorption of ions or organic species onto growth sites during the interval between pulses thus causing blockage of growth sites. In other electrochemical systems, the application of pulsed current can cause grain growth by allowing desorption of molecules or ions from growth sites thus causing the growth sites to be activated. It is possible that the deposition of chromium may fall into this latter category and the softer deposits may be due to an increase in grain size but this could only be confirmed by the use of Transmission Electron Microscope. However, it is extremely difficult to produce specimens of chromium deposits suitable for examination by T.E.M. due to the high tensile stress of the deposits which causes curling of deposits and the extreme brittleness of the deposits. Thus it was not possible to confirm experimentally that an increase in grain size had occurred.

Another factor which may influence the deposit hardness is the level of internal tensile stress and the stress reduction observed may also be a factor in reducing hardness. It was also noted in the results section that an effect of pulsed current was to cause disorientation of the deposit and a change in orientation of the deposit may significantly affect hardness. The appearance of hydride phases at certain frequency ranges could

also have an influence on the hardness of the deposits since chromium hydrides are likely to have very different physical and mechanical properties from those of b.c.c. chromium metal.

The reduction in stress determined in the results has been noted by other authors (60,61,81,82,116,117,118). Faust et al (60) noted that the use of pulsed current in chromium plating solutions produced deposits which were crack free and had a lower tensile stress than deposits produced using direct current. It was proposed that this reduction in stress was due to the decomposition of chromium hydrides during the interval between the pulses. The experimental results reported in the results section 8.1.5. suggest that this hypothesis may be incorrect for the following reasons :-

(i) No evidence was found for the presence of hydrides in deposits produced by direct current which suggests that any hydrides formed at the cathode surface decompose before they are covered with fresh chromium.

(ii) If the reduction in stress were due solely to the decomposition of hydrides, it would be expected that this would occur in all three of the electrolytes tested regardless of the catalyst system. In fact, the Mach 1 electrolyte produced cracked deposits at all frequencies above 500 Hz.

(iii) Deposits obtained at low pulse frequencies from the sulphate and Chromefast C electrolytes had very high hydride contents. This confirms the work of Knodler (61) who determined the hydrogen contents of chromium deposits produced under pulsed conditions and found very high hydride contents. If Faust's hypothesis were correct, the longer "off times" at the lower pulse frequencies should allow more time for hydride decomposition and thus give rise to deposits with very low hydride contents.

It appears therefore that the reduction in tensile stress observed in the results is not caused by decomposition of hydrides at the cathode surface but must occur due to other factors.

The fact that chromium electrodeposits usually have a very strong preferred orientation means that micro stresses within the deposit may align to produce a high level of macrostress. It is possible that the disorientation of the deposit noted in the results causes a redistribution of the micro stresses so that an overall reduction in the macrostress of the deposit occurs. The disorientation effect has also been observed by Saiddington and Hoey (116) who used current interruptions lasting several seconds in their work. This disorientation effect or "Three dimensional nucleation" (as it was termed by Saiddington) also explains the deterioration in the visual appearance of the chromium deposits when pulsed current is used since this effect increases the nodularity of the deposits.

9.2. Crack Formation and Anodic Behaviour.

A major effect of the use of pulsed current to deposit chromium is the production of crack free deposits. This is due to a reduction in the internal tensile stress of the deposits. It is this change in the deposits characteristics which accounts for the observed change in anodic behaviour of the coatings during electrochemical corrosion testing.

Deposits plated using direct current tend to crack in layers (116). This can be observed by examining a cross section of a hard chromium deposit. These layers of cracks form a three dimensional interconnecting network of discontinuities. Under anodic

conditions, these cracks open up and the substrate (steel) dissolves preferentially because it is less passive than the chromium. This explains the results observed in the case of the potentiodynamic scan of the deposit produced by direct current where current increased progressively with potential. In the crack free deposits, the chromium forms a continuous layer and its passive nature is apparent from the shape of the potentiodynamic scan of the deposit produced at 2500 Hz, 50% duty cycle.

The deposit produced at 100 Hz, 50% duty cycle showed a greater increase of current with potential than the deposit plated with direct current . This was probably due to two factors. Firstly, X-ray diffraction analysis of this coating showed that it consisted largely of h.c.p. chromium hydride which is likely to behave differently from b.c.c. chromium under conditions of anodic polarisation. Secondly, h.c.p. chromium hydride is thermally unstable and decomposed spontaneously at room temperature into b.c.c. chromium. *This change is accompanied by a volume reduction of around 15%* (111) and so increases the deposit stress and causes the deposit to crack. Thus, if the use of pulsed current is to be applied to improve the corrosion resistance of coatings, parameters must be selected so that co-deposition of hydrides is avoided.

Although the results of the potentiodynamic scans and work reported by other workers (62,81,82) suggests that the corrosion resistance of chromium coating can be increased substantially by the use of pulsed current, it must be realised that chromium is a very brittle coating. Thus any deformation of the substrate material is likely to propagate macro cracks throughout the deposit which would give extremely high corrosion current densities where the deposit was cracked and could give severe corrosion at these points.

Due to the poor throwing power of chromium electrolytes, when thick deposits are applied it is usually necessary to grind the deposits and this may also cause them to crack. Heat treatment is carried out when the deposit is applied to high tensile steels to eliminate the problem of hydrogen embrittlement by allowing diffusion of hydrogen out of the coating. Occluded hydrogen usually results in compressive stress. Heat treatment which removes this hydrogen increases the level of tensile stress in the coating . Again this may lead to cracking. Thus it is apparent that more work needs to be carried out in this area to clarify the effects of pulsed current on the corrosion resistance of commercially applied deposits.

9.3. Deposit Composition.

The experimental results showed that under certain conditions of pulsing, hydrides were co-deposited. this effect has been noted by other workers (61,115) but no hypothesis has been presented to explain these phenomena.

Snavely (60) proposed that the structure of electrodeposited chromium was primarily dependent upon the cathode film pH. During the process of electrolysis, large amounts of hydrogen gas are produced at the cathode surface by the reduction of hydrogen ions. The net effect of this process is to raise the pH of the electrolyte adjacent to the cathode surface above that of the bulk solution thus forming a "cathode film". It was proposed that under plating conditions producing a low pH in the cathode film, any hydrides formed are unstable and decompose immediately. The resultant deposit would consist entirely of b.c.c. chromium. As the pH of the cathode film is increased progressively, the stability of the hydrides increases and they become incorporated in the deposit in greater amounts. Thus conditions producing a high cathode film pH will also lead to the production of deposits with high hydride contents.

It was also proposed by Snavely [60] that the reduction of chromium proceeded in a stepwise manner. As the reduction of chromium involves the transfer of six electrons and the breaking of several chemical bonds, this would appear to be a reasonable assumption. Thus the final stages of reduction will proceed via the production of divalent chromium at the cathode surface. Divalent chromium is strongly reducing and any of this which escapes into the cathode film will react with hexavalent chromium by the following reaction :-

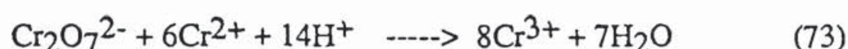

$$Cr_2O_7^{2-} + 6Cr^{2+} + 14H^+ \;\text{----->}\; 8Cr^{3+} + 7H_2O \qquad (73)$$

This reaction consumes hydrogen ions and so would tend to raise the pH of the cathode film.

Since the chromous ions are positively charged and are probably adsorbed on the cathode surface, it is unlikely that much of this divalent chromium can escape when using direct current. However, with pulse plating, if the off time is long enough divalent chromium can escape into the cathode film and increase its pH. This may account for the observations on hydride inclusions noted with pulse plated deposits. These observations may be explained as follows :-

At the end of a pulse, there are two processes which can occur. Firstly, the cathode film begins to disperse which allows the ingress of the bulk electrolyte. This has the effect of lowering the cathode film pH. Secondly, reaction 73 can occur which tends to raise the cathode film pH. These two processes act in opposition and the net result on the cathode film pH depends upon the relative rates of these processes. This is best illustrated by taking the sulphate catalysed electrolyte as an example. At a frequency of 16 Hz, the off time is long enough to allow sufficient dispersion of the cathode film to

produce a net lowering of the pH of the electrolyte adjacent to the cathode and the deposit obtained is purely b.c.c. chromium. As the frequency is raised to 100 Hz, dispersion of the cathode film no longer occurs between current pulses but the "off time" is long enough to allow the escape of divalent chromium from the cathode surface. Over a number of pulses, this has the effect of raising the net equilibrium pH of the cathode film and inducing the co-deposition of hydrides. At frequencies in excess of 2000 Hz, the "off time" becomes too short to allow the escape of divalent chromium from the cathode surface so the net equilibrium cathode film pH will be approximately the same as for deposition with direct current and the deposit becomes b.c.c. chromium again.

The different electrolytes used in the experimental work showed different tendencies for these processes to occur. This is most probably due to differences in the kinetics of the two opposing processes because of the different catalyst systems. The two high efficiency electrolytes showed much less tendency to produce hydrides than the sulphate catalysed electrolyte; the Mach 1 electrolyte produced deposits of b.c.c. chromium throughout the frequency range studied. It is important when producing deposits for commercial use to avoid the co-deposition of hydrides as these have low mechanical strength and decompose at room temperature causing cracking of the deposit.

9.4. Cathodic Efficiency.

In order to provide an explanation of the observed effects of pulsed current on the cathodic efficiency of the electrolytes used in the experimental work, it is necessary to consider the implications of interrupting the current supply. Cathodic efficiency is determined to some extent by the pH of the cathode film. Conditions producing a high

cathode film pH (for example low temperature or high trivalent chromium content) tend to gave higher plating efficiencies for a given catalyst system because the lower hydrogen ion content in the cathode film at these higher pH's causes the efficiency of hydrogen discharge to be reduced thus increasing the efficiency of chromium deposition.

Current interruptions in the power supply during deposition affect the formation of the cathode film and so would be expected to influence the cathodic efficiency. Two of the processes occurring at the cathode surface have already been described in section 9.3. The dispersion of the cathode film during the off time would tend to give a lower pH at the cathode surface so would be expected to reduce cathodic efficiency. Opposing this process is the escape of divalent chromium into the cathode film which would tend to raise the pH of the cathode film thus increasing the cathodic efficiency. Additionally, there are two more factors to consider. The partial reduction of chromium followed by it's escape into the cathode film involves the consumption of power which would tend to reduce efficiency. Finally, for a constant duty cycle, as frequency is reduced, both the pulse time and the interval between the pulses is increased. Increasing the pulse time tends to maintain the formation of the cathode film so as frequency is lowered beyond the point at which the cathode film is fully dispersed, the increasing pulse time would be expected to increase the efficiency towards the value obtained by deposition with direct current.

It is clear from these considerations that the net effect of pulsed current on the cathodic efficiencies is a composite of several factors acting in opposition. In the case of the high efficiency electrolytes (Chromefast C and Mach 1), it is probable that the cathode film disperses relatively quickly and so the factors which tend to reduce efficiency predominate. Because of this rapid dispersion of the cathode film, partially reduced

chromium can escape into the bulk electrolyte at the end of a pulse. This causes a fall in efficiency to a minimum value as frequency is reduced. As frequency is reduced still further, the efficiency begins to increase again due to the influence of the increasing pulse time. The cathode film formed by the sulphate catalysed electrolyte is probably much more viscous than that produced by the high efficiency electrolytes and so is slower to disperse. Thus the effect of the escape of divalent chromium increases the cathode film pH which causes an increase in cathodic efficiency over the frequency range of 100 - 1000 Hz.

9.5. Covering Power.

The experimental results showed that the covering power of the three electrolytes was little influenced by the use of pulsed current when the chromium was deposited onto steel but that the covering power was strongly affected when the chromium was deposited onto brass Hull cell panels. This suggests that the covering power of chromium plating electrolytes is strongly substrate dependent when pulsed current is used.

This observed reduction in the covering power of chromium plating electrolytes is perhaps surprising because a method commonly used in commercial practice to improve covering power is to initially apply a high current density to "strike" the deposit then lowering the current density to the working value to prevent "burning". When pulsed current is applied at a 50% duty cycle, the pulse current density is twice the average current density so it would be expected that this would improve the covering power. The observed results indicate that other factors act in opposition to this expected effect and exert a greater influence on the overall covering power. It is possible that during the interval between the pulses, dispersion of the cathode film occurs most rapidly in the

low current density areas. However, this does not explain the dependence of the covering power on the substrate. The experimental data obtained was not sufficient to obtain a satisfactory hypothesis for the observed effect of pulsed current on covering power and this represents an area where more work is required.

Chapter 10.

Conclusions - Chromium.

1. The application of unipolar pulses for the electrodeposition of chromium caused a reduction in the hardness of the deposits obtained from three different types of chromium plating electrolytes. In all cases, hardness of the deposit increased as frequency was increased and at the highest frequenccies used in the tests (3000 Hz), deposit hardnesses similar to those obtained by the use of direct current were obtained.

2. The application of pulsed current caused a reduction in the tensile stress of chromium deposits and produced crack free coatings under suitable conditions. The tendency of the deposits towards cracking depended upon the catalyst system. The Mach 1 electrolyte showed the greatest tendency to crack and produced cracked deposits above 500 Hz. The sulphate catalysed electrolyte and Chromefast C produced crack free deposits over a frequency range of 200 - 3000 Hz.

3. The anodic behaviour of the crack free coatings deposited onto steel was very different from that of cracked coatings and showed a much lower corrosion rate. Improved corrosion protection should be provided by these coatings provided that they remain crack free in service.

4. The visual appearance of the deposits was affected by the use of pulsed current. Deposits plated using pulsed current tended to be more nodular than those produced using direct current.

5. Pulsed current was found to induce co-deposition of hydride phases over certain frequency ranges. The sulphate catalysed electrolyte was the most prone to the production of hydride containing deposits and at an average current density of 40 A/dm^2 and a duty cycle of 50% produced hydride containing deposits from around 50 -1500 Hz. Chromefast C deposits small amounts of hydride from 100 - 500 Hz and Mach 1 shows no tendency towards hydride co-deposition. It is important when selecting pulse parameters for commercial use to select conditions that do not result in the production of hydrides.

6. The cathodic efficiency of the three electrolytes used in the test was affected by the use of pulsed current. The two high efficiency electrolytes (Chromefast C and Mach 1) showed a reduction in efficiency as compared to deposition with direct current. Efficiency was maximised by the use of high frequencies with these electrolytes. Using the sulphate catalysed electrolyte, an increase in cathodic efficiency to around 17% could be achieved by depositing chromium using pulse parameters which were hydride inducing.

Chapter 11.

Experimental Results - Copper.

11.1. Results of Polarisation Studies.

Results of the polarisation studies are given in the form of Tafel plots i.e **cathodic polarisation potential vs log of the current density in A/dm^2**. If ideal Tafel behaviour is obeyed, these plots would all be straight lines. In all cases, a cathodic pulse time of 10 ms and an anodic pulse time of 0.5 ms was used at a anodic/cathodic current density ratio of 3:1.

11.1.1. The Effect of Direct and Pulsed Reverse Current on Electrodeposition from the Base Electrolyte.

It can be seen from the results shown in figure 35 that with both pulsed and direct current, Tafel behaviour was followed reasonably closely over the current density range studied. The slopes of the lines were also very similar. Thus from a polarisation point of view, the use of pulsed reverse current with an electrolyte without additives would not be expected to improve throwing power.

11.1.2. The Effect of Direct and Pulsed Reverse Current on Electrodeposition from Electrolytes Containing Single Additives.

The effect of single additives on the polarisation characteristics of the electrolytes at a chloride concentration of 60 p.p.m. was studied. The effect of adding :-

i) 75 p.p.m. A polyether (Oxilube 50,000 * - referred to as Ox).

ii) 40 p.p.m. Mercaptopropane sulphonic acid - sodium salt

(Referred to as MPS.)

iii) 40 p.p.m. bis (3-Sulphopropyl) disulphide - disodium salt.

(referred to as SSP.)

was studied using direct and pulsed reverse current; results are shown in figures 36 and 37. The concentrations used were chosen because these are typical of the concentrations used in commercial brightener systems.

* Oxilube is a trade mark of Shell Chemicals Ltd. It is a random co-polymer of ethylene and propylene oxides containing 25% proplyene oxide by weight. The average molecular weight used in the tests was 50,000 except where stated.

Figure 35. The Effect of Pulsed Reverse and Direct Current on Electrolyte Polarisation Characteristics: Base Electrolyte.

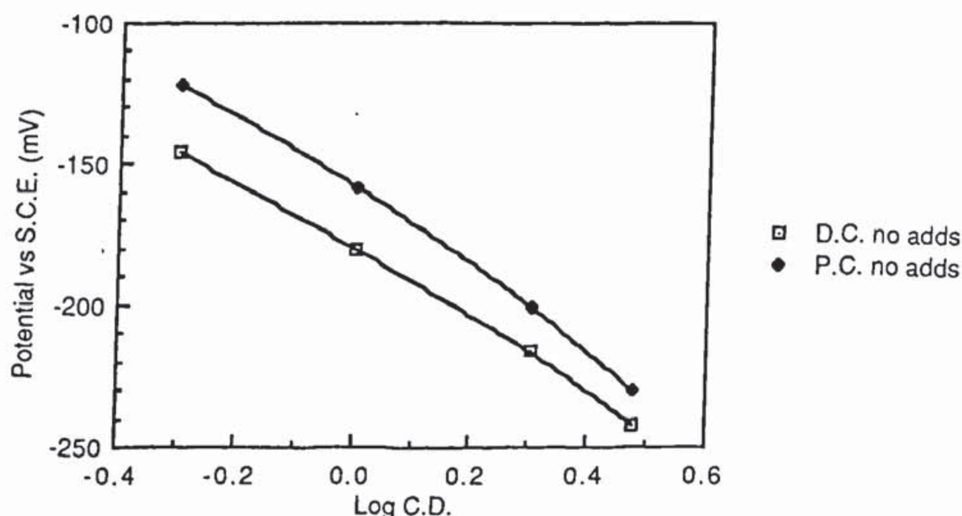

Figure 36. The Effect of Single Additives on Electrolyte Polarisation Characteristics: Direct Current.

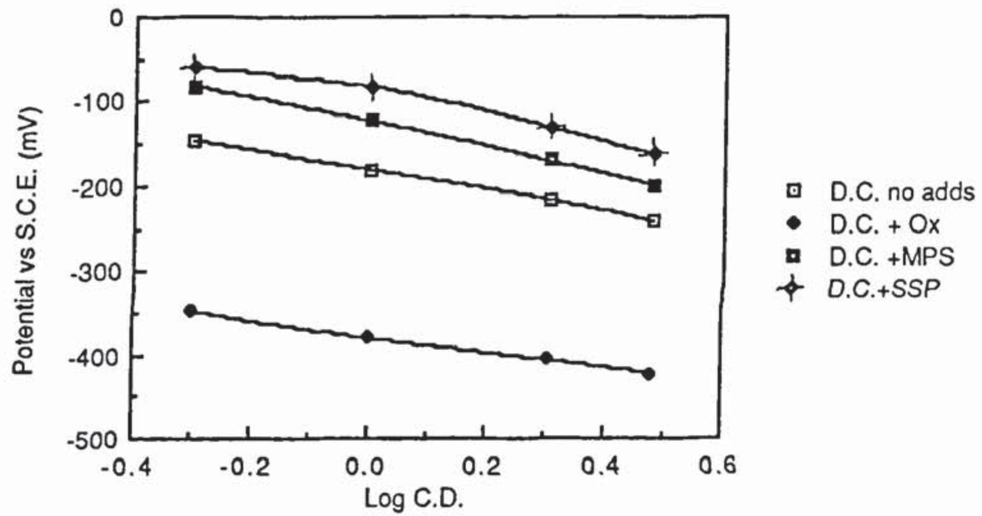

Figure 37. The Effect of Single Additives on Electrolyte Polarisation Characteristics: Pulsed Reverse Current .

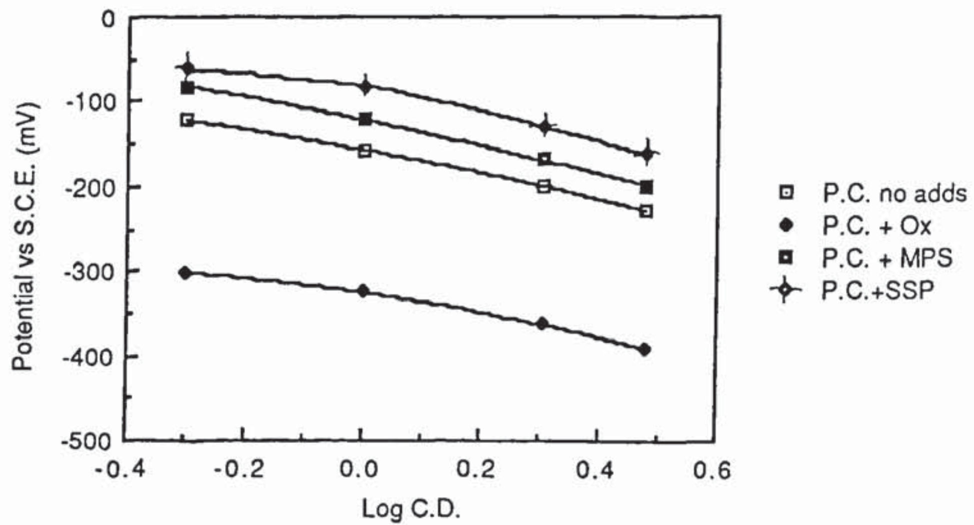

It can be seen from the results shown in figure 36 that Oxilube shifted the potential at which deposition took place to more negative values. This was probably due to a surface blocking effect caused by the long polymer chains. The two sulphopropyl sulphides used in the experiment shifted the deposition potential to less negative values. It is probable therefore that they had some catalytic effect on deposition. As in figure 35, the slopes of all the lines are similar indicating that these additives would have little effect on the throwing power.

It can be seen from the results shown in figure 37 that the trends observed with pulsed current are the same as for direct current in that the polyether still produced a large shift to more negative values in the deposition potential at a given current density while the sulphur compounds produced a shift to less negative potentials due to their catalytic effect. Again the slopes of the lines are not significantly different, thus the addition of single additives would not lead to an increase in throwing power by using pulsed reverse current.

11.1.3. The Effect of Direct and Pulsed Reverse Current on Electrodeposition from Electrolytes Containing Sulphopropyl Sulphides and Polyether in Combination.

The effects of direct and pulsed reverse current were then examined using two additives in combination. These measurements were taken at several different chloride levels. The results of these measurements are shown in figs 38,39,40 and 41.

Figure 38. The Effect Combined Additives on Electrolyte Polarisation Characteristics at Three Different Chloride Concentrations: Direct Current - 40 ppm MPS, 75 ppm Oxilube 50,000

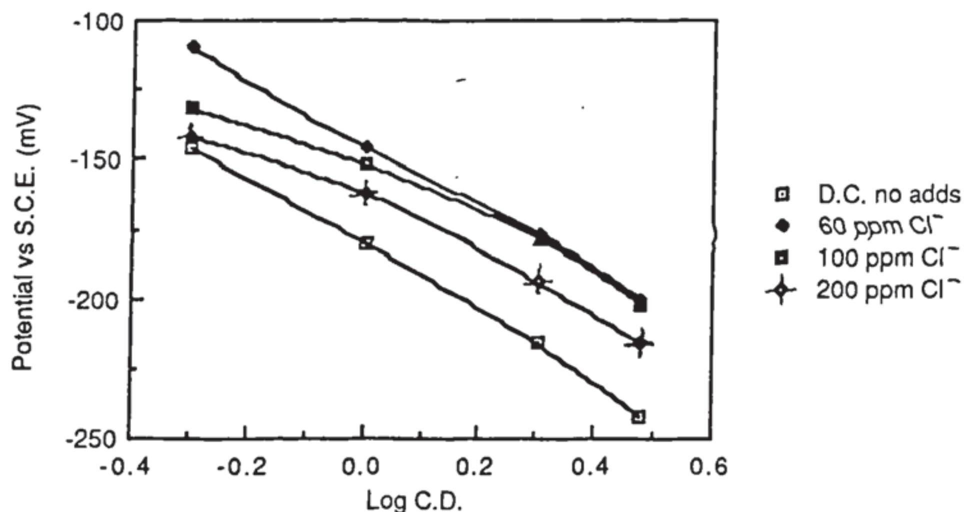

This figure indicates that with direct current, there would be little effect on the throwing power when the additives are combined. Additions of chloride produced a shift in deposition potential to more negative values which suggested that chloride may influence the adsorbability of the polyether. However, deposition potentials with the combined additives were still less negative than when no additives were present which suggested that the sulphopropyl sulphide was preferentially adsorbed.

Figure 39 shows the effect of chloride concentration on the polarisation characteristics of an electrolyte containing 40 ppm of SSP and 75 ppm of Oxilube 50,000 using direct current .

It can be seen from these results that this additive behaved similarly to MPS. Again, raising the chloride level raised the deposition potential but did not change the slope of the polarisation curve.

Figure 39 The Effect of Combined Additives on Electrolyte Polarisation Characteristics at Three Different Chloride Concentrations: Direct Current - 40 ppm SSP, 75 ppm Oxilube 50,000

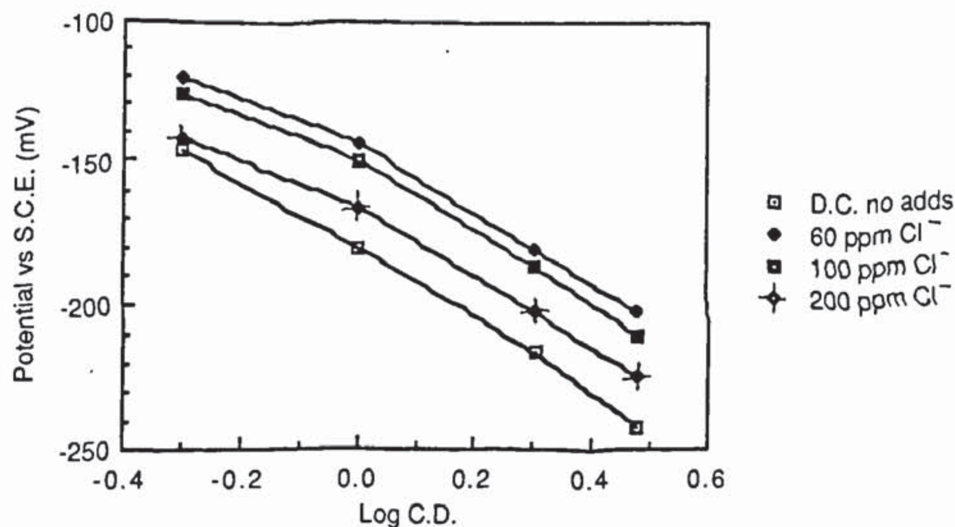

The effect of pulsed reverse current on the polarisation behaviour was then examined using the same additive concentrations as described for figures 38 and 39. Figures 40 and 41 show the results obtained with MPS and SSP respectively. It can be seen from these figures that the use of pulsed reverse current had a large effect on the polarisation slope and that similar effects were obtained with MPS and SSP. Significant deviation from Tafel behaviour occurred when pulsed reverse current was applied to these solutions. It appeared that at higher current densities, polarisation of the cathode surface occurred which in turn suggests that low current density areas were depolarised. This tended to encourage the deposition of metal at low current density and so should give better metal distribution. Chloride concentrations of 100 to 200 ppm were necessary for this effect to be maximised.

Figure 40 The Effect of Combined Additives on Electrolyte Polarisation Characteristics at Three Different Chloride Concentrations: Pulsed Reverse Current - 40 ppm MPS, 75 ppm Oxilube 50,000

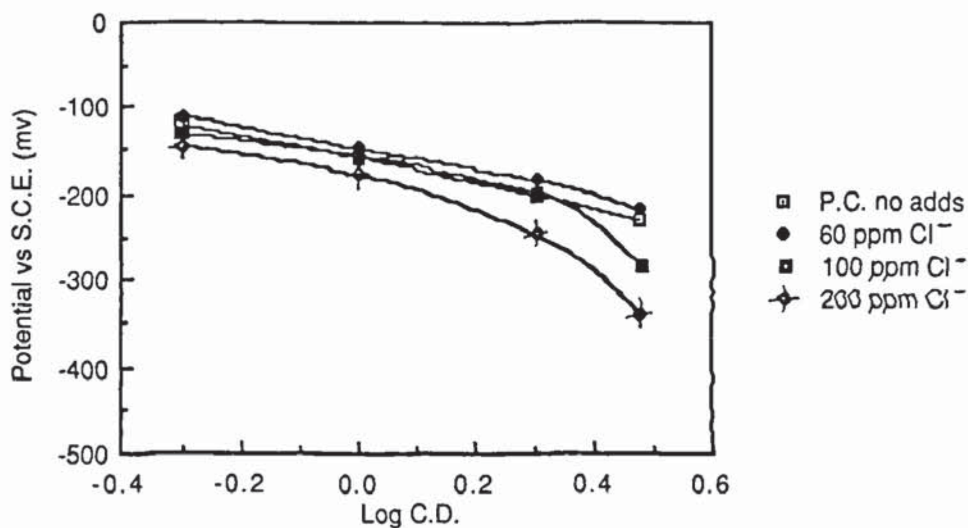

Figure 41 The Effect of Combined Additives on Electrolyte Polarisation Characteristics at Three Different Chloride Concentrations: Pulsed Reverse Current - 40 ppm SSP, 75 ppm Oxilube 50,000

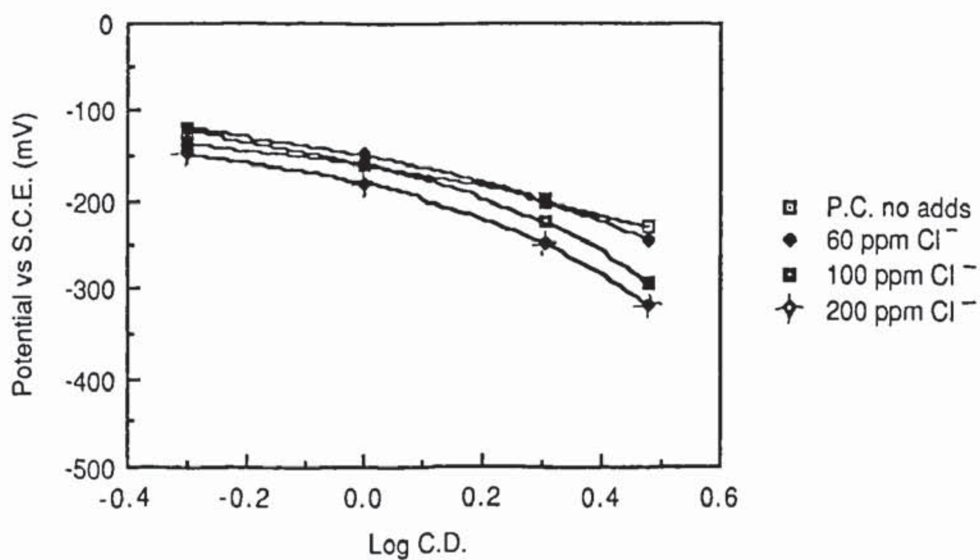

11.1.4. The Effect of Varying Polyether Concentration on Electrolyte Polarisation Characteristics.

The effect on the polarisation characteristics of electrolytes containing concentrations of Oxilube 50,000 ranging from 0.75 to 75 ppm was studied using direct current . These results are shown in figure 42.

Figure 42. The Effect on Electrolyte Polarisation Characteristics of Varying Concentration of Oxilube Using Direct Current. (Cl^- 100 ppm.)

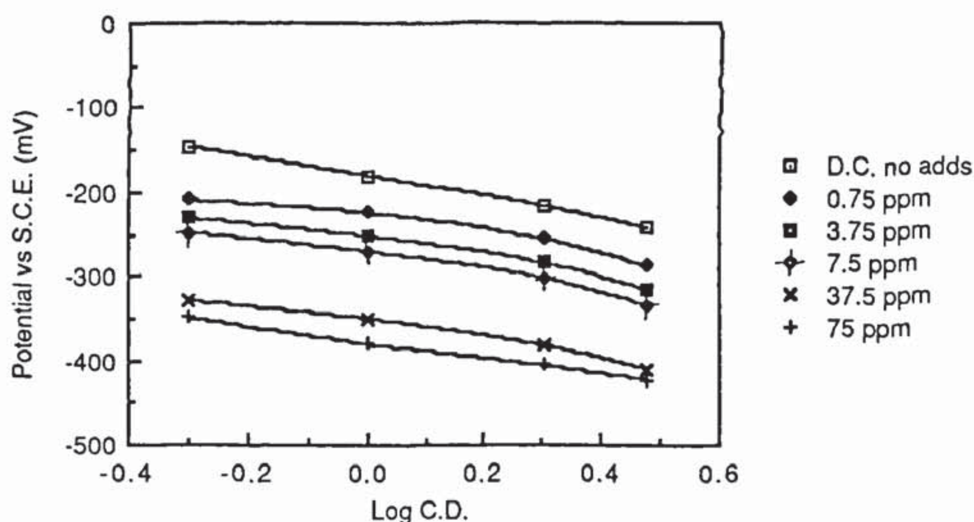

It can be seen from the results illustrated in this figure that even very small additions of the polyether had an appreciable effect on the deposition potentials recorded. The effect of polyether concentration increased rapidly up to a concentration of 37.5 ppm and above this concentration, there was little effect on the deposition potential. This suggested that around this concentration, there was sufficient polymer present in the solution to reach adsorption equilibrium. Thus, the optimum concentration of polyether was probably between 30 and 75 ppm. Concentrations up to 750 ppm appeared to produce essentially the same results as 75ppm.

11.1.5. The Effect of Direct and Pulse Reverse current on Electrolyte Polarisation Characteristics: Electrolyte Containing Polyether Plus Varying Concentration of MPS.

Using an electrolyte containing 100 ppm of chloride ion and 75 ppm of Oxilube 50,000, the effect of varying the concentration of MPS using both direct and pulsed reverse current was studied. The results are shown in figures 43 and 44.

Figure 43. The Effect of Varying MPS Concentration on Electrolyte Polarisation Characteristics - Direct Current.
Electrolyte Containing 75 ppm of Oxilube 50,000.

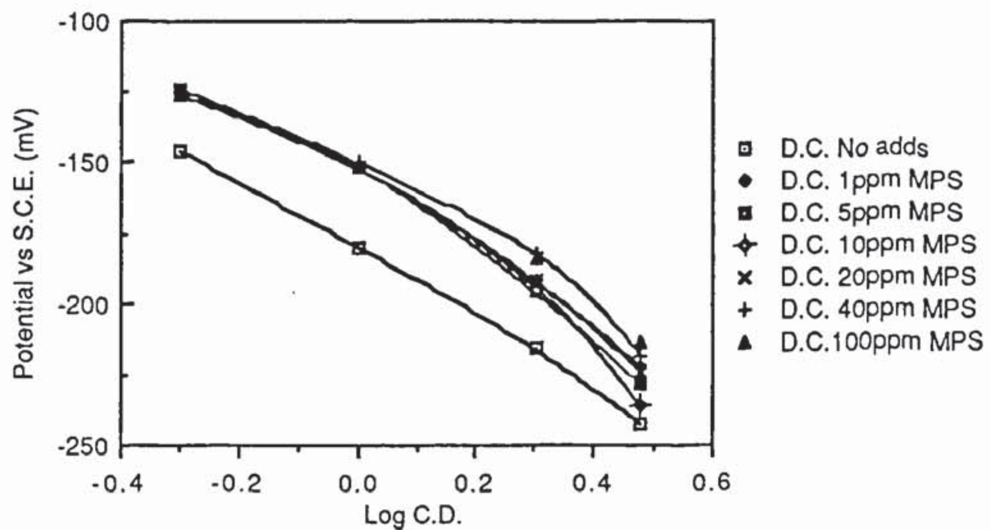

It can be seen from figure 43 that over the whole concentration range studied, varying the MPS concentration had little effect on the polarisation curves although at concentrations of 40 ppm and above, there was slightly more depolarisation at higher current densities than at lower concentrations.

Figure 44. The Effect of Varying MPS Concentration on Electrolyte Polarisation Characteristics - Pulsed Reverse Current. Electrolyte Containing 75 ppm of Oxilube 50,000.

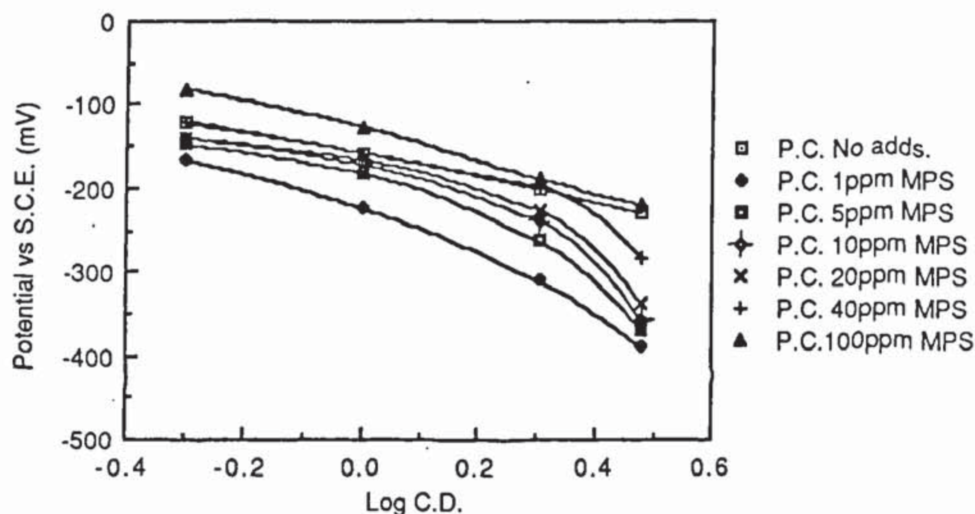

The effects of varying the concentration of MPS with pulsed reverse current can clearly be seen in figure 44. At the lowest concentrations, pulsed current reduced the depolarising effect of the MPS throughout the current density range. At concentrations of 10 to 40 ppm, the depolarising effect was reduced at progressively higher current densities until at 100 ppm, the depolarising effect of the MPS appeared not to be affected. Thus it was concluded that the most effective concentration range for MPS was between 10 and 40 ppm.

11.1.6. The Effect of Polyether Molecular Weight on the Polarisation Characteristics with Direct Current and Pulsed Reverse Current.

The Oxilube which was used for the tests is available in several molecular weight ranges. The effect of changing the molecular weight of the Oxilube was investigated and the results are shown in figures 45, 46 and 47.

Three polymers having molecular weights of 18,000, 50,000 and 92,000 were examined at a concentration of 75 ppm. These additives were studied singly using direct current, and in conjunction with 20 ppm of MPS with both direct and pulsed reverse current.

Figure 45. The Effect of Molecular Weight of Polyether on Electrolyte Polarisation Characteristics: Direct Current.

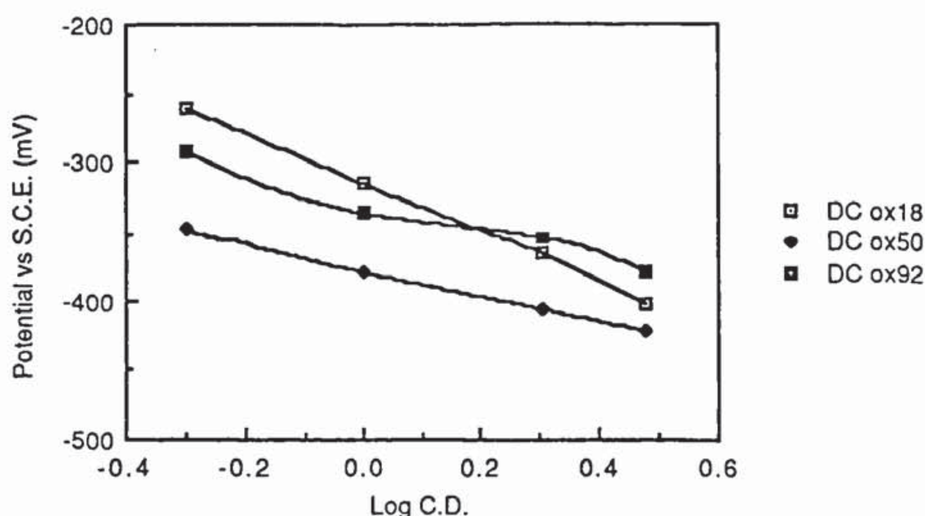

It can be seen from figure 45 that the molecular weight of 50,000 produced the highest deposition potentials. It may be expected that at higher molecular weights, the surface coverage would increase which would cause the deposition potential to become more negative for a given current density. However, beyond a certain molecular weight, steric factors may prevent adequate coverage. This was observed with the high molecular weight (92,000) polymer. It was also noted that deposits from the electrolyte with the 92,000 molecular weight polymer gave very uneven nodular deposits. It was therefore concluded that polymers of this type with molecular weights in excess of around 50,000 were unsuitable.

Figure 46. The Effect of Molecular Weight of Polyether on Electrolyte Polarisation Characteristics: Direct Current

Electrolyte Containing MPS (20 ppm) and Oxilube (75 ppm)

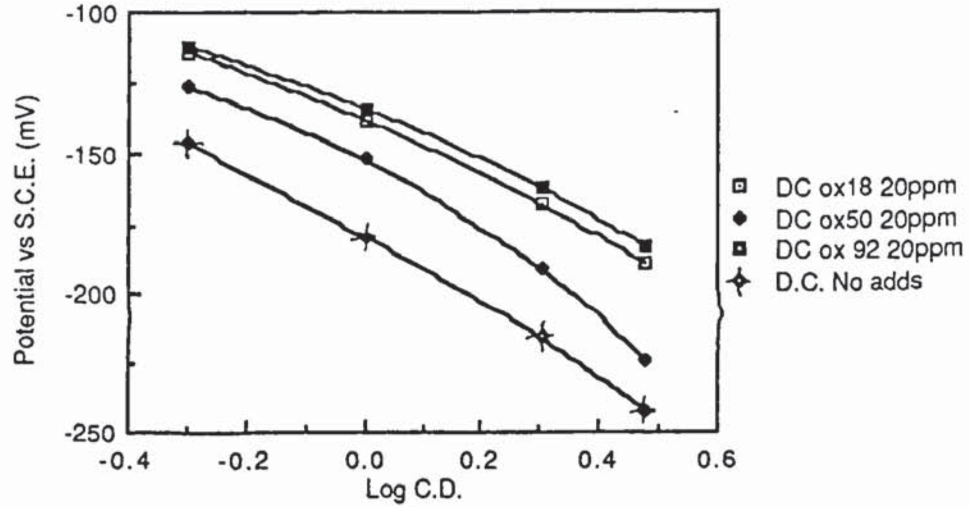

It can be seen from the results in figure 46 that using direct current for a solution containing 20 ppm of MPS, the electrolyte containing the polymer with a molecular weight of 50,000 gave the most negative deposition potentials and also produced a slope which was slightly greater than using higher or lower molecular weights.

Figure 47 illustrates the results obtained using an electrolyte containing 20 ppm MPS with the three different molecular weight ranges using pulsed reverse current.

Figure 47. The Effect of Molecular Weight of Polyether on Electrolyte Polarisation Characteristics: Pulsed Reverse Current.

Electrolyte Containing MPS (20 ppm) and Oxilube (75 ppm)

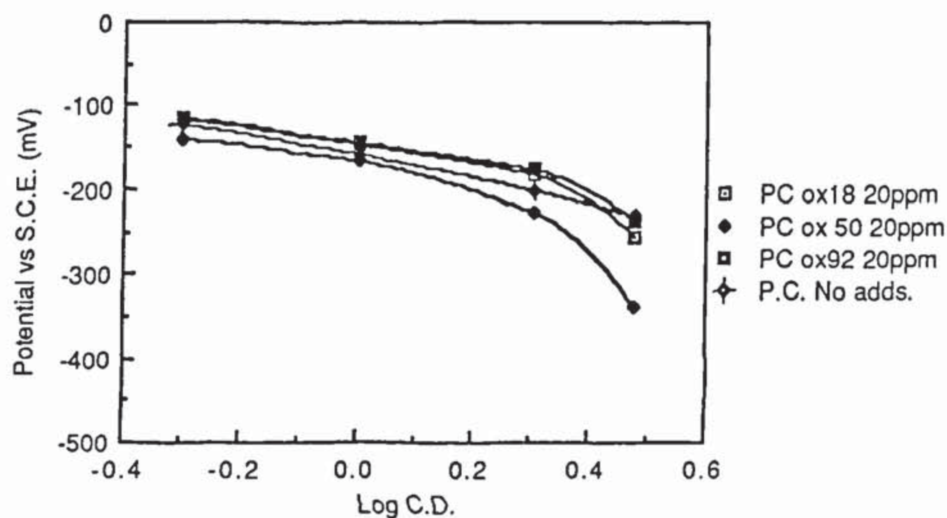

It can be seen from these results that the greatest effect on the polarisation slopes was obtained with the 50,000 molecular weight polymer. This indicated that from the viewpoint of throwing power, the 50,000 molecular weight polymer was the most suitable of the three molecular weights studied.

11.2. Results of Rest Potential Studies.

Table 18. The Effect of Additions of Polyether on Rest Potentials and Exchange Current Densities.

	Additions.	Rest Potential (mV)	$J_0 \times 10^4$ (A/cm^2)
1)	No Additions (100 ppm Cl^-)	-38	6.96
2)	0.75 ppm Ox 50,000 (100 ppm Cl^-)	-78	2.95
3)	3.25 ppm Ox 50,000 (100 ppm Cl-)	-92	2.91
4)	7.5 ppm Ox 50,000 (100 ppm Cl-)	-100	2.36
5)	32.5 ppm Ox 50,000 (100 ppm Cl-)	-100	0.35
6)	75 ppm Ox 50,000 (100 ppm Cl-)	-100	0.13

These results illustrate that the addition of Oxilube to the electrolyte caused the rest potential to become more negative up to a concentration of 7.5 ppm. This was probably due to the surface blocking effect of the polymer chains. The exchange current densities which were calculated by Tafel extrapolation also showed a decrease with increasing polymer concentration due to this effect.

The effect on the rest potential of additions of MPS and SSP are shown in the next table :-

Table 19. The Effect of Sulphopropyl Sulphides on Rest Potentials and Exchange Current Densities.

	Additions	Rest Potential (mV)	$J_0 \times 10^4$ (A/cm^2)
1)	No Additions (60 ppm Cl^-)	-38	6.96
2)	40 ppm MPS (60 ppm Cl^-)	-18	19.60
3)	40 ppm SSP (60 ppm Cl^-)	-18	27.60

It can be seen from these results that the addition of both MPS and SSP caused the rest potential to move to less negative values. Calculation of exchange current densities showed an increase. This was due to the catalytic effect of these compounds on the reduction and oxidation of copper.

Table 20 shows the effect of the combined additives (Sulphopropyl sulphides + Polyether) on the rest potentials and exchange current densities.

Table 20. The Effect of Combined Additives on the Rest Potentials and Exchange Current Densities.

	Additions	Rest Potential (mV)	$J_0 \times 10^4$ (A/cm^2)
1)	No Additions (60 ppm Cl^-)	-38	6.96
2)	75ppm Ox + 40ppm MPS (60 ppm Cl^-)	-34	10.60
3)	75ppm Ox + 40ppm SSP (60 ppm Cl^-)	-36	8.70

In combination, the additives produced an increase in the exchange current density as compared to an electrolyte with no additives. This suggests that the sulpopropyl sulphide was preferentially adsorbed compared to the polyethers.

To summarise the results of the polarisation studies, it appeared from the data obtained that electrolytes containing both Polyether and sulphopropyl sulphides, in the presence of chloride ion, could give a much better throwing power at low current densities with pulsed current than with direct current. To test this hypothesis, Hull cell panels were plated at 2A cell current using both pulsed and direct current. In the case of pulsed reverse current, 2A was the time averaged overall current. Thickness distribution profiles of the panels were measured using a coulometric method and the results are shown in figure 48.

It can be seen from the thickness distribution displayed in this figure that a very different metal distribution was obtained by the use of pulsed reverse current with the electrolyte containing additives, especially at low current densities where much more metal was deposited than when direct current was used.Thus it may be expected that on items such as printed circuit boards that an improvement in the "hole throwing power" would result.

Figure 48. The Effect of Pulsed Reverse Current on The Metal Distribution on a Hull Cell Panel.

(Electrolyte containing 40ppm MPS, 75ppm Ox, 100ppm Cl^-)

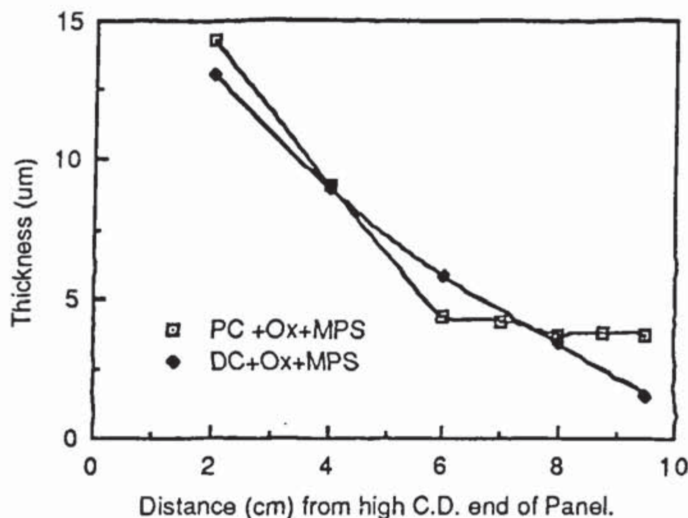

11.3. Throwing Power Studies.

Figures 49 and 50 show the effect of various additive combinations on the hole/land thickness ratio of various sizes of holes. Figure 49 shows the ratio obtained using direct current and figure 50 the effect of pulsed reverse current 10 ms cathodic, 0.5 ms anodic and an anodic / cathodic peak current density ratio of 3:1. It can be seen that with direct current, the best throwing power was obtained in the additive free electrolyte. In the case of pulsed reverse current, the throwing power was improved somewhat with the addition of S.S.P. with the smaller hole sizes but a very large improvement in the "Hole throwing power" was obtained by using a combination of polyether and S.S.P.. Thus in order to maximise throwing power, a combination of additives is required.

The remainder of the throwing power tests were carried out using an electrolyte containing both S.S.P. and Oxilube at 20 p.p.m. and 75 p.p.m. respectively. Figure 51 shows the effect of varying anodic / cathodic current density ratio on the hole / land ratio for various size holes using 10 ms cathodic and 0.5 ms anodic. It can be seen from the results displayed in this figure that hole throwing power was maximised in holes of 1.2 mm in diameter and above at an anodic / cathodic current density ratio of 2:1 whereas smaller holes achieved maximum hole throwing power at a ratio of 3:1.

Figure 52 shows the effect of varying anodic / cathodic current density ratio on the hole / land ratio for various size holes using 10 ms cathodic and 1 ms anodic. In this case, hole throwing power is maximised at an anodic / cathodic current density ratio of 2:1 irrespective of hole size. However, the hole throwing power obtained in the 0.6 mm holes remains below 60% in all cases. In most cases using 10 ms : 1 ms, results were inferior to using 10ms : 0.5 ms.

Figure 49. Hole/Land Thickness Ratio Obtained using Different Additive Combinations with Direct Current.

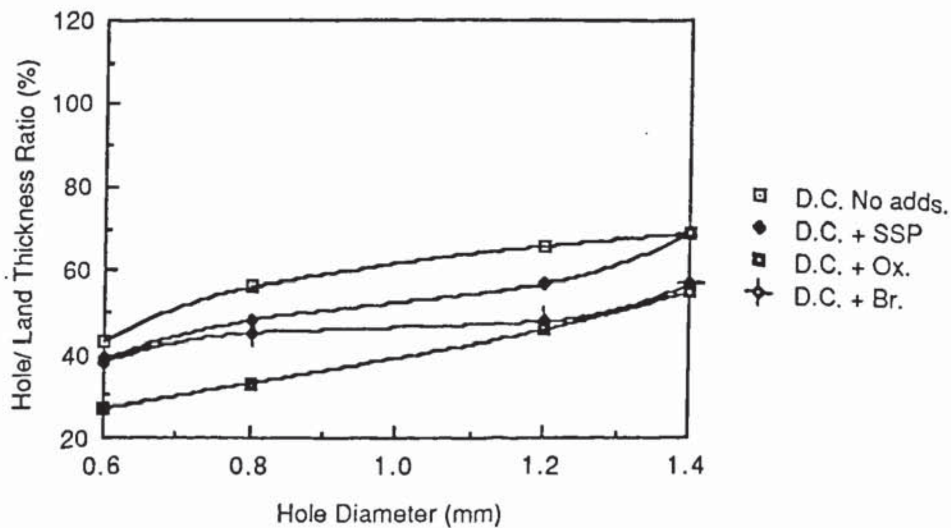

Figure 50. Hole/Land Thickness Ratio Obtained using Different Additive Combinations with Pulsed Reverse Current.

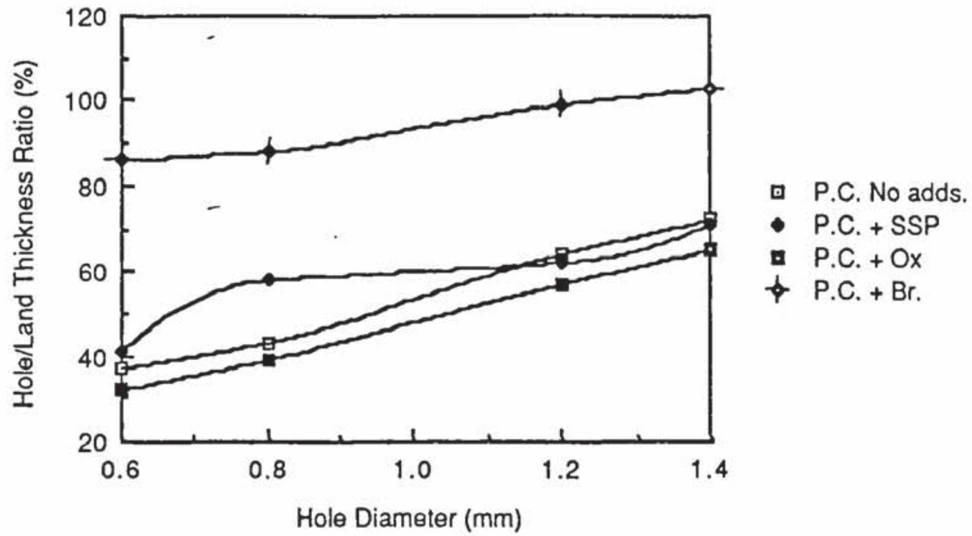

Figure 51. Hole/Land Thickness Ratios Obtained using 10 ms Cathodic, 0.5 ms Anodic Pulse Times. Electrolyte Containing SSP and Oxilube.

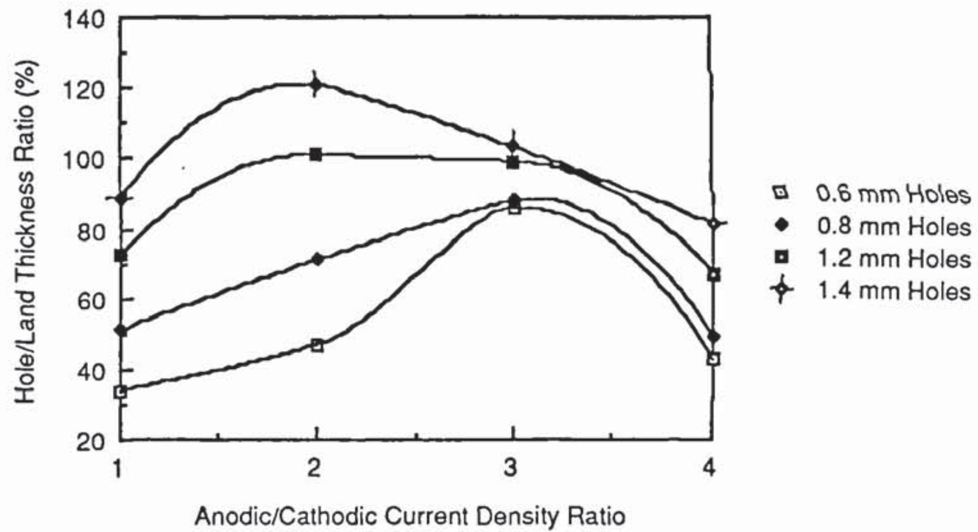

Figure 52. Hole/Land Thickness Ratios Obtained using 10 ms Cathodic, 1.0 ms Anodic Pulse Times. Electrolyte Containing SSP and Oxilube.

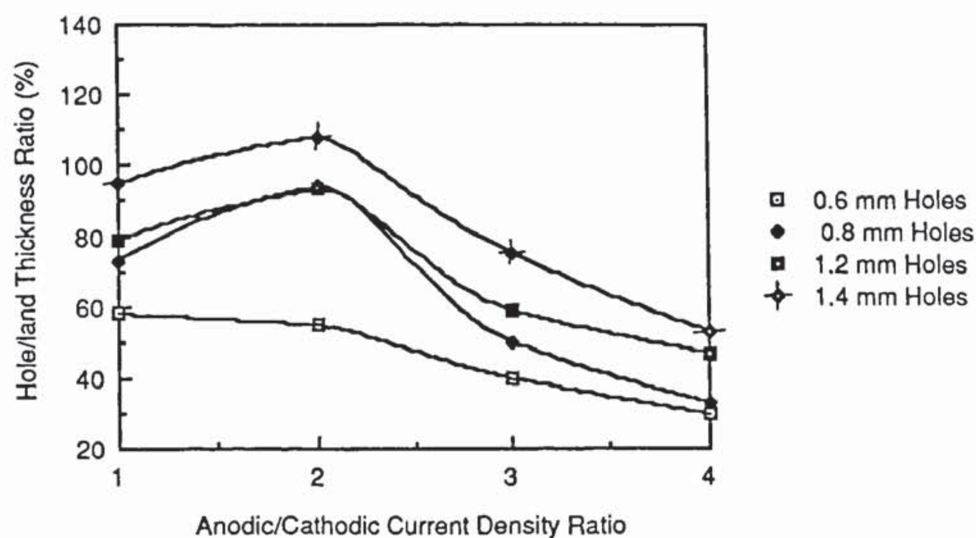

Some experiments were carried out using 10 ms cathodic and 2 ms reverse at anodic / cathodic current density ratios of 1:1 and 2:1. In all cases throwing power was very poor and an etched surface was produced with some apparent surface oxidation. The results of these experiments are listed in table 21.

Table 21. Hole / Land Thickness Ratios 10ms Cathodic, 2ms Anodic.

Anodic / Cathodic Current density ratio	Hole Diameter (mm)	Hole / Land Thickness ratio (%)
1:1	0.6	32
1:1	0.8	46
1:1	1.2	62
1:1	1.4	75
2:1	0.6	7
2:1	0.8	12
2:1	1.2	19
2:1	1.4	43

From the results of these tests using a pulse time of 10 ms cathodic and varying the length of the anodic pulse, it was concluded that 0.5 ms anodic at an anodic / cathodic peak current density ratio of 3:1 gave the best results. This programme was used to plate test specimens in a commercial bright acid copper electrolyte (P.C. 81 from Schloetter inc.). The results of these tests are displayed in figure 53. It can be seen from this figure that similar results were obtained in this case as from the laboratory prepared electrolyte . To maximise the throwing power in the 0.6 mm holes, an anodic / cathodic current density ratio of 3:1 is required. Figure 54 shows the results obtained from the commercial electrolyte using a reverse time of 1 ms. Again, results are similar to those obtained in the laboratory prepared electrolyte using the same plating conditions.

Having established that for a 10 ms cathodic pulse the optimum anodic time was 0.5 ms, test panels were plated maintaining the same anodic / cathodic time ratio but varying the length of the cathodic pulse. Times of 0.5:10, 1:20, 2.5:50 and 5:100 ms were tested at an anodic / cathodic current density ratio of 3:1. The results of these tests are plotted in figure 55 as hole diameter vs hole / land thickness ratio. From these results, it can be seen that in all cases, the hole throwing power was much better than that obtained by using direct current at the same average current density. Best overall throwing power results were obtained using 20 ms cathodic and 1 ms anodic.

Figure 53. Hole/Land Thickness Ratio Obtained using 10 ms Cathodic and 0.5 ms Anodic Pulse Times in P.C.81 Bright Acid Copper.

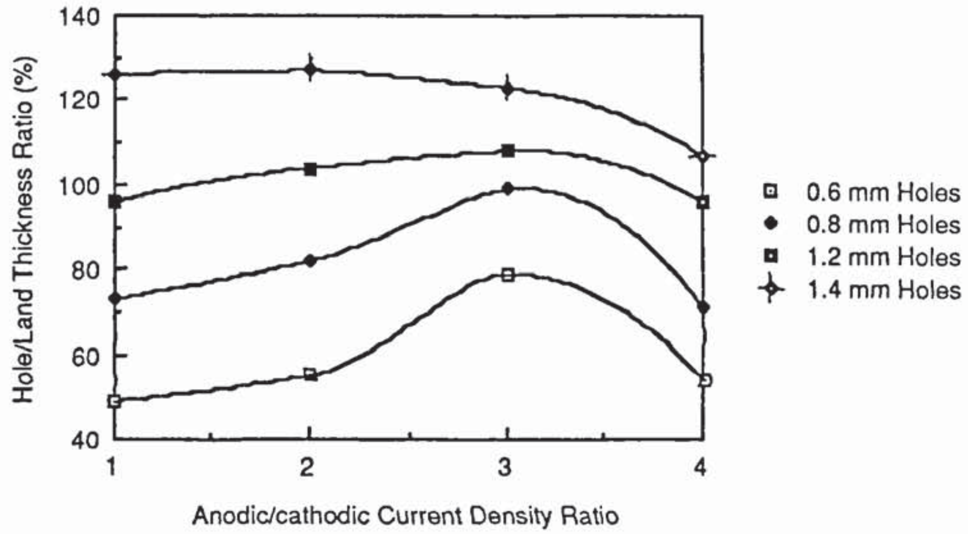

Figure 54. Hole/Land Thickness Ratio Obtained using 10 ms Cathodic and 1.0 ms Anodic Pulse Times in P.C.81 Bright Acid Copper.

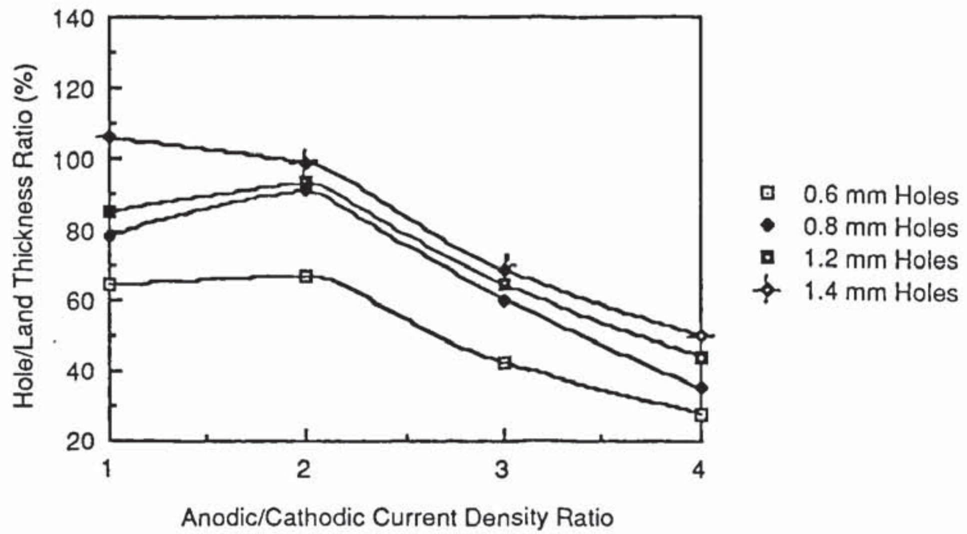

Figure 55. Hole/Land Thickness Ratios Obtained Using Different Cathodic Pulse Times.

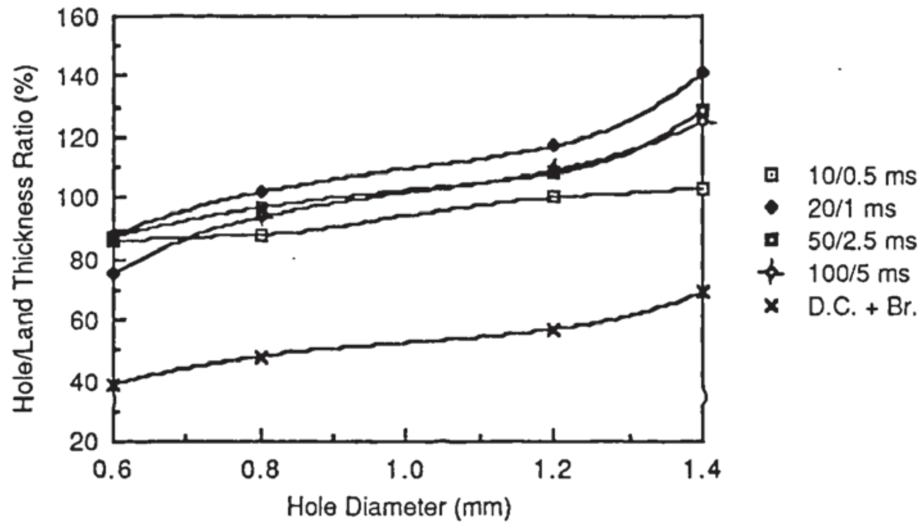

11.4. Metal Distribution on Boards Produced Under Commercial Conditions.

In order to assess the throwing power of boards plated under commercial conditions, a series of boards (3.2 mm thick) with a standard test pattern were plated using direct current and pulsed reverse current. The boards were then sectioned in four specific areas to determine the effect of pulsed reverse current on the "hole throwing power" of different pad configurations. The areas sectioned for the tests were as follows :-

Series 1. - Isolated pads with 0.8 mm holes at the centre of the test boards.

Series 2. - Isolated pads with 0.8 mm holes at a corner of the board.

Series 3. - 0.8 mm holes with isolated pads on one side and a ground plane on the other, situated towards the edge of the board.

Series 4. - 0.5 mm holes on isolated pads near the edge of the board.

Figure 56 shows the hole/land thickness ratios obtained using a cathodic pulse time of 10 ms and a reverse pulse time of 0.5 ms. It can be seen from the results displayed in this figure that better metal distribution can be obtained by the use of pulsed reverse current at an average current density of 3 A/dm^2 than with direct current at a current density of 2 A/dm^2.

Figure 57 shows the results obtained on commercially plated boards using an anodic pulse time of 1ms. Again, it can be seen that a substantial improvement in the hole/land thickness ratio could be obtained.

Figure 56. Hole/Land thickness Ratios Obtained on Commercially Plated Boards. (10 ms Cathodic 0.5 ms Anodic.)

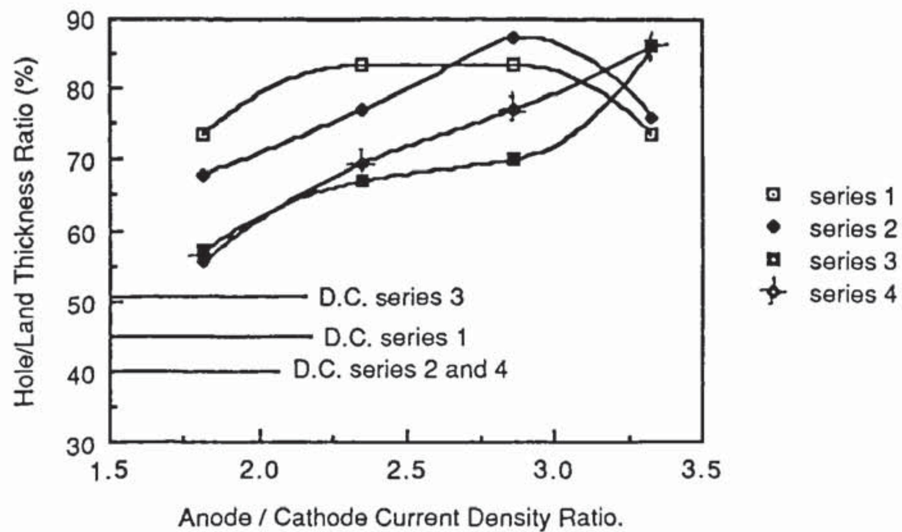

Figure 57. Hole/Land thickness Ratios Obtained on Commercially Plated Boards.

(10 ms Cathodic 1.0 ms Anodic.)

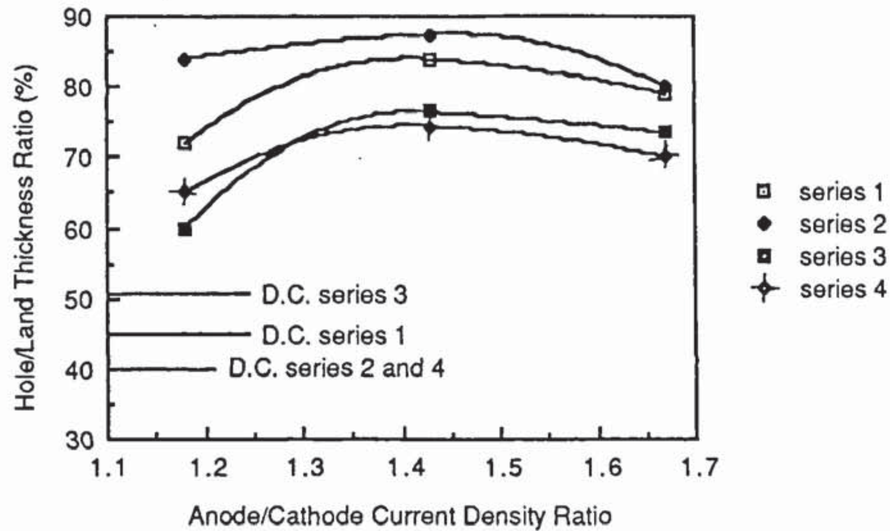

In addition to providing information on the hole throwing power of the electrolytes, the commercial test boards also provided some data on the surface distribution of metal. This was achieved by determining the ratio of metal thickness on large gound planes to the thickness obtained on isolated pads. the results of these measurements are displayed in figure 58.

It can be seen from these results that a more even surface distribution can be obtained by the use of pulsed reverse current than by the use of direct current.

Figure 58. Ground Plane/Isolated Pad Ratio Using Pulsed Reverse and Direct Current on Commercially Produced Boards.

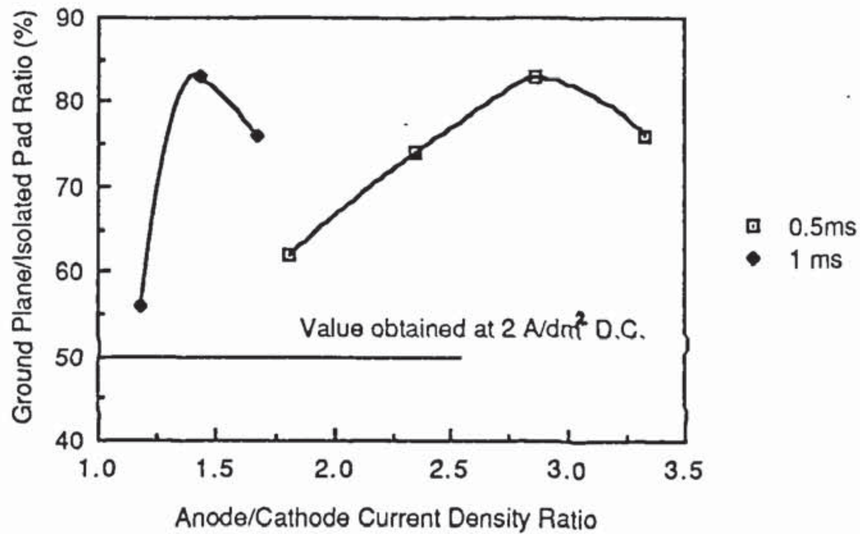

11.5. Surface Topography Studies.

Figure 59a shows the surface topography of a deposit plated from an additive free electrolyte using direct current. Figure 59b shows the effect of adding 100 ppm of Oxilube. The visible surface texture appears to be refined but this can be misleading as surface topography does not necessarily reflect the true grain size which can only be revealed by T.E.M.. When S.S.P. and oxilube are present in combination, a bright deposit results which has no easily resolvable surface features.

Figure 60a shows the surface topography of a deposit plated from an additive free electrolyte using pulsed reverse current 10ms cathodic, 0.5 ms anodic and a 3:1 anodic / cathodic current density ratio. In this photograph, several well defined grains are visible on the surface. These grains have features which seem to indicate twinning and so may in fact represent single crystals and not polycrystalline grains. Figure 60b shows the effect of adding Oxilube to this system using the same pulse parameters. Again, the surface grains are well defined and if monocrystalline indicate a grain refining effect. Figure 60 c shows the effect of a combination of Oxilube and S.S.P.. Here, a much finer surface texture is obtained and individual grains are no longer visible as well defined crystals. T.E. M. must be used to determine the actual effect on grain size.

Figure 61 shows the effect of changing the anodic/cathodic pulse current density ratio while keeping other pulse parameters constant (10 ms cathodic, 1 ms anodic). It can be seen that as the anodic pulse current density is increased, the texture of the surface becomes more clearly defined and the effects of copper removal during the anodic pulse can be seen. At a ratio of 4:1, the surface topography takes the form of "plates" of copper. At an anodic time of 2 ms and an anodic/cathodic current density ratio of 2:1, the deposit became dendritic in nature as can be seen from figure 62.

Figure 59. Surface Topography of Deposits Produced by Direct Current.

59a) Additive Free Electrolyte.

59b) Electrolyte + 75 ppm Oxilube 50,000.

Figure 60. Surface Topography of Deposits produced By Pulsed Reverse Current. Cathodic time 10 ms, Anodic time 0.5 ms Anodic/Cathodic Current Density Ratio 3:1.

60a) Additive Free Electrolyte

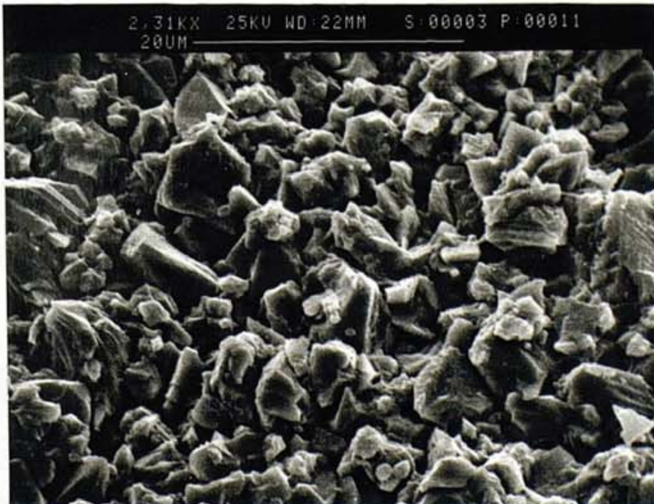

60b) Electrolyte + 75 ppm Oxilube 50,000

60c) Electrolyte + 75 ppm Oxilube + 20 ppm S.S.P.

Figure 61. Surface Topography of Deposits Produced at Various Anodic/Cathodic Current Density Ratios. (10ms Cathodic, 1 ms Anodic)

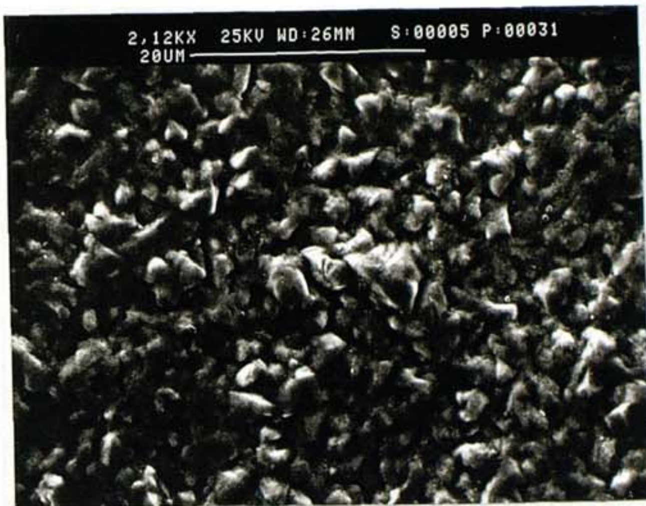

61a) 2:1 Ratio

61b) 3:1 Ratio

61c) 4:1 Ratio.

Figure 62. Surface Topography of Deposit Produced Using Cathodic Pulse Time 10 ms, Anodic Pulse Time 2 ms

11.6. Transmission Electron Microscopy Studies.

Figure 63a shows the typical grain structure obtained from deposits produced by direct current. Grains are variable in size and twinning is evident in a large number of grains. The average grain size is 1.5 - 2.5 µm. The effect of adding 100 ppm of Oxilube is shown in figure 63b. the grain size in this case is very variable and consists of some very small grains surrounding larger grains. These larger grains have many growth faults and imperfections. When a combination of S.S.P. and Oxilube is used, the structure is as shown in figure 63c. Here the grain size is fairly uniform and twins are present. The average grain size is up to 4 µm.

Figure 64 shows the results obtained using pulsed reverse current 10 ms cathodic and 0.5 ms anodic and a peak anodic / cathodic current density ratio of 3:1. Figure 64 a shows the grain structure obtained from the additive free electrolyte. Grains are twinned and much larger in size than those obtained by deposition with direct current. Average grain size was 15 - 20 µm. It is interesting to note that the grain size measured by

T.E.M. corresponds to the size of the surface "grains" observed by S.E.M. This suggests that these surface topographical features were therefore monocrystalline grains. Figure 64b shows the effect of adding 100 ppm of Oxilube. Here, the grains are smaller than those obtained in the additive free system and have an average grain size of 2 - 4 μm. Again the observed grains on the surface of the deposit correspond to the grain size determined by T.E.M.. Figure 64c shows the effect of a combination of S.S.P. and Oxilube. This combination of additives with the use of pulsed reverse current produces still further grain refinement giving an average grain size of 1 -2 μm.

Figure 63. T.E.M. Photographs Showing Grain Structure of Copper Deposits Produced By Direct Current.

5 μm

63a) Additive Free Electrolyte.

5 μm

63b) Electrolyte + 75 ppm Oxilube 50,000

5 μm

63c) Electrolyte + 75 ppm Oxilube + 20 ppm S.S.P.

Figure 64. T.E.M. Photographs Showing Grain Structure of Copper Deposits Produced By Pulsed Reverse Current.(10:0.5ms, 3:1)

8·3 μm

64a) Additive Free Electrolyte

5 μm

64b) Electrolyte + 75 ppm Oxilube 50,000

64c) Electrolyte + 75 ppm Oxilube + 20 ppm S.S.P.

11.7. Hardness Values.

Hardness values were obtained for deposits plated under the same conditions as for the T.E.M. studies. The results of these measurements are shown in table 22. Each reading quoted is an average of 10.

Table 22. Hardness of Copper deposits.

Type of Deposit.	Hardness (Hv_{50})
D.C. No Additions	128
D.C. + Oxilube	143
D.C. + Oxilube + SSP	112
P.C. No Additions	89
P.C. + Oxilube	116
P.C. + Oxilube + SSP	125

Chapter 12.

Discussion of Results - Copper.

12.1 Introduction.

In order to consider the overall effect of pulsed reverse current on "hole throwing power", it is necessary to consider the effect of this on an additive free electrolyte and also the effect of pulsed reverse current on the adsorption characteristics of the organic additives. The net effect is likely to be a combination of these effects. In this discussion, the effects of concentration overpotential caused by depletion of copper in the holes is neglected and only the effects of activation overpotential are considered. Calculations of the fluid dynamics involved in the plating of high aspect ratio through holes have been carried out by Fisher et al (158) and also by Landau et al (159). These confirm that the effects of concentration overpotential are very small.

12.2 The Effect Of Pulsed Reverse Current on an Additive Free Acid Copper Electrolyte.

If the effects of concentration overpotential are neglected, the overall throwing power of the electrolyte depends upon the primary and secondary current density distributions. Primary distribution depends only upon cell geometry factors and secondary distribution takes into account the effects of activation overpotential. Ibl (160) defined a dimensionless variable (the Wagner number) the magnitude of which was indicative of the throwing power of the electrolyte. This was defined as follows :-

$$W_a = \frac{d\eta}{dj} \cdot \frac{\kappa}{L} \qquad (74)$$

Where :-

W_a = Wagner number

j = Current Density

L = The characteristic length of the electrode

η = Electrode potential

κ = Specific electrical conductivity of electrolyte.

In this equation, the term which describes the effect of secondary current distribution is the rate of change of potential with current ($d\eta/dj$). By applying Ohm's law, for any fixed potential or current, this term is simply the electrode resistance. For a given cell geometry and conductivity, the higher the electrode resistance, the better the throwing power. The electrode resistance is not a constant value but depends upon the level of the applied overpotential. As applied overpotential is increased, the electrode resistance falls so the effects of secondary current distribution are reduced and the overall distribution tends towards a primary distribution.

When plating with pulsed reverse current, because metal is removed during the anodic pulse, a correspondingly higher overpotential needs to be applied during the cathodic pulse in order to maintain the same plating rate as for an equivalent direct current. This means that during the deposition phase, the current distribution is less uniform than for a corresponding direct current. Thus it may be expected that in an additive free electrolyte, pulsed reverse current would produce a deterioration in throwing power. However, in addition to considering the situation during the cathodic phase, we must

consider the effect of the anodic pulse. During this phase, the applied current density is three times that applied during the cathodic pulse so the current density distribution would be less uniform during dissolution than during the cathodic pulse. This would tend to increase the overall deposit uniformity provided that the efficiency of the dissolution process were 100% over the entire electrode surface. This possibility was investigated by White and Galasco [148], they found that at high anodic pulse current densities, passivity and oxidation of the surface occurred causing a deterioration in throwing power.

The net effect of these processes can be seen by comparing the hole throwing powers determined from the additive free electrolyte using direct and pulsed reverse current (figures 49 and 50 respectively). Better hole throwing power was obtained with direct current than with pulsed reverse current, particularly in the smaller holes.

12.3 Factors Affecting the Incorporation of Organic Additives in Deposits Plated from Acid Copper Electrolytes.

The mechanisms of incorporation of organic additives into nickel deposits has been discussed in some detail by Edwards [131-136]. He identified two general cases for the incorporation of additives where incorporation is controlled solely by diffusion and where a combination of adsorption and diffusion occurs. Incorporation solely by diffusion is rarely encountered and only occurs if irreversible adsorption occurs on the cathode surface. Usually the incorporation of organic additives is controlled by an adsorption/diffusion mechanism. Research into the adsorption characteristics of polyethers and sulphopropyl sulphides has indicated that in the case of these additives, the rate of incorporation at the cathode is negligible and so the surface effect of these additives is controlled entirely by adsorption. Current theories concerning the

mechanism of adsorption of these organic compounds are as follows :-

12.3.1. Adsorption of Polyether Molecules.

The adsorption behaviour of polypropylene glycol has been studied using differential capacitance methods by Stoychev et. al.[161,162]. The results obtained showed that in a support electrolyte consisting of 1N H_2SO_4, the polypropylene glycol was very weakly adsorbed. However, as the results in figure 42 show, the presence of a polyether in the acid copper electrolyte has a very strong influence on the deposition potentials which are shifted cathodically by up to 200 mV. This suggests a stronger interaction. An explanation for this was provided by Yokoi et. al. [163] who suggested that the polyether molecules could form complexes with copper (I) ions and be adsorbed on the surface as a cationic polyelectrolyte. In the absence of chloride ion, the cuprous ions are adsorbed on the cathode surface and reduced to copper metal with little shift in deposition potential. It was proposed by Yokoi et. al. [163] that chloride ions could become specifically adsorbed on the cathode and interact with the chelated cuprous ions effectively binding the polyether molecule to the cathode surface. This process would effectively raise the deposition potential since incoming copper ions would have to pass the barrier of adsorbed polyether. Figure 65 illustrates this proposed mechanism which explains the observed influence of the chloride ion on the adsorption behaviour of the polyether observed in the results section. Because the polyether is bound to the surface via a bond between chelated cuprous ions and adsorbed chloride ions, it is unlikely to become incorporated into the deposit. Thus the surface coverage is likely to be governed solely by adsorption and diffusion can be ignored. This explains the ability of the polyether to suppress deposition over a wide range of potentials. Above a certain molecular weight, steric factors may prevent even surface coverage by the polyether. This was observed when using the highest

molecular weight polymer (Oxilube 92,000). In this case, nodular deposition occurred due to this factor because deposition would be expected to occur at a higher rate in areas where the polymer is not adsorbed. A log/log plot of potential vs Oxilube concentration (see Fig 66) indicates that at a temperature of 22 ^{o}C, maximum surface coverage is obtained at a concentration of around 75 ppm since no appreciable change in deposition potential was obtained at higher concentrations.

Figure 65 . Mechanism Proposed by Yokoi et al (163) for the Adsorption of Polyether Molecules.

Figure 66. Log Potential vs Log Oxilube Concentration at 2A/dm^{2},22°C.

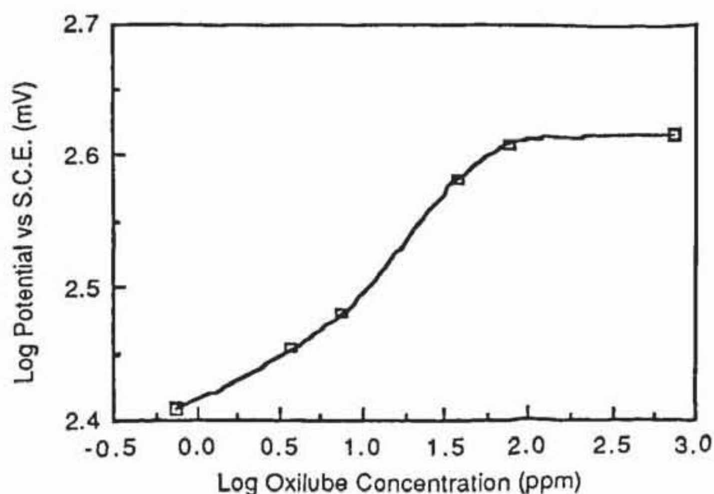

12.3.2. Adsorption of the Sulphopropyl Sulphide.

The adsorption of an organic disulphide (composition unspecified) on a copper surface has been studied by Stoychev et. al. (161,162). It was found that in a solution of 1N H_2SO_4, The disulphide was strongly adsorbed on the copper surface. An interesting finding from this work was that the degree of adsorption had an inverse relationship with concentration. This was proposed to be caused by the anionic nature of the disulphide causing mutual repulsion thus preventing increased adsorption with increasing concentration. This observation provides an explanation for the results observed in figure 43 where a concentration of 1ppm of the added MPS in the presence of polyether produced virtually the same effect on the deposition potentials as 100 ppm. In an electrolyte containing polyether molecules, the effect of adding a sulphopropyl sulphide is to cause the deposition potentials to shift anodically to around the same values as for a polyether free system. It may do this either by being preferentially adsorbed on the surface and excluding the polymer film, or by being specifically adsorbed on the surface and catalysing the deposition of copper. The fact that the polyether and sulphopropyl sulphide work synergistically together in brightener formulations suggests that the latter case is the most likely. This is further supported by the proposed mechanism of adsorption of the polyether by cuprous ions interacting with specifically adsorbed chloride ions. Because the chloride ions are small, they are not likely to be displaced by the added sulphopropyl anions. The actual mechanism of catalysis has not yet been established but it is probable that the catalysis mechanism is a fully reversible process because the system appears to be almost totally under adsorption control. If the catalysis mechanism were irreversible, the sulphopropyl sulphide would be comsumed at the cathode surface and diffusion control would take over at high current densities. Some evidence for the adsorption control of the sulphopropyl sulphide is provide in fig 43 where it would be expected that at a

concentration of only 1 ppm, diffusion limitations would begin to be apparent at the higher current densities and the deposition potential would shift to more negative values. A second piece of evidence is the fact that in practice, the consumption of these addition agents is very low and the sulphur content of the copper deposited from electrolytes containing these additives is virtually undetectable. As an example, a foil of copper was produced from an electrolyte containing 40 ppm of MPS and 75 ppm of Oxilube 50,000 with 100 ppm Cl^-. The foil was analysed for sulphur using proton induced X-ray emission analysis which can detect levels of sulphur down to 0.01%. No sulphur was detected in the deposit using this method. Finally, it has been reported by Kardos (164) that levelling can be induced in copper deposits from an acid electrolyte containing only polyether and chloride if the article to be plated is first immersed in a solution containing a sulphopropyl sulphide. This "surface catalysed levelling" is due to the catalytic effect of the sulphopropyl sulphide and was found to persist for over 30 minutes of plating. Thus it was concluded that the sulphopropyl sulphide was not consumed but remained adsorbed on the surface of the growing deposit. A possible mechanism for the catalytic effect of the sulphopropyl sulphide molecule is shown in figures 67a and 67b . In these figures, MPS is shown for the sake of clarity. SSP may be considered to behave in a similar manner. Solid lines on the diagrams represent chemical bonds and dotted lines indicate complex formation. The broken line between the sulphonate group and a chelated copper (I) ion represents a possible charge interaction.

Figure 67a. Proposed Mechanism for Adsorption and Complex Formation of Sulphopropyl Sulphide.

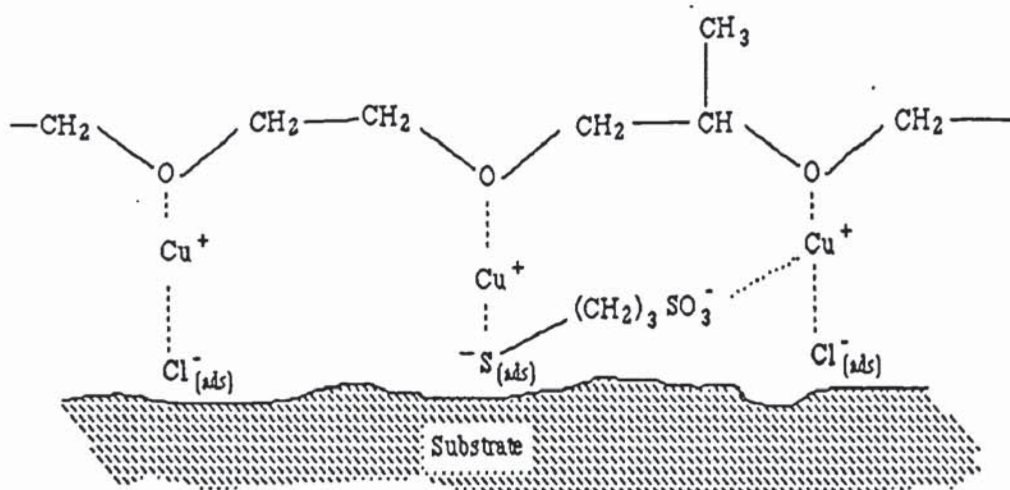

Figure 67b Final Stage of Reduction.

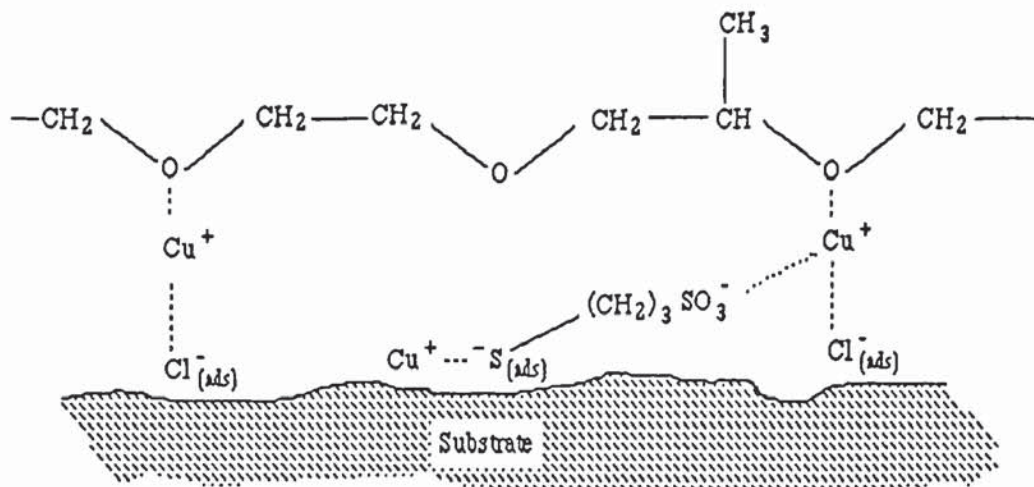

12.3.3. Adsorption of Chloride Ions.

In an additive free system, when chloride ions are added to the base electrolyte, a depolarisation effect occurs. This has been reported by Stoichev and Rashov [165]. The depolarisation effect was reported to increase in a linear fashion with increasing chloride concentration and the addition of 100 ppm of chloride to an additive free electrolyte resulted in a depolarisation of approximately 25 mV. In the presence of polyether however, this depolarisation effect is overridden by the increased polarisation effect of the polyether when in combination with chloride ions.

12.4. The Effect of Pulsed Reverse Current on the Adsorption of Organic Additives.

From the experimental data obtained in the study of the polarisation behaviour of acid copper electrolytes containing organic additives, it appears that the adsorption of the polyether is not much affected by the application of pulsed reverse current but in the case of the sulphopropyl sulphide, progressive desorption tends to occur as the average current density is increased. This shifts the deposition potentials to more cathodic values due to the polarisation effect of the polyether. Thus low current density areas are depolarised relative to high current density areas which gives a more even deposition. The effect of pulsed reverse current on the adsorption behaviour of the additives used in the study can be explained as follows :-

12.4.1. The Effect of Pulsed reverse Current on the Adsorption of Polyethers.

As discussed earlier, the polyether molecules are not specifically adsorbed on the copper surface but form complex polycations with copper (I) ions and are bound to the

cathode surface by specifically adsorbed chloride ions. During the anodic pulse, oxidation of copper from the cathode surface occurs. As the anodic pulses are relatively short, much of this copper will only be oxidised to copper (I). Because of the ability of the polyether layer to chelate this species, it may be expected that the polyether film would trap much of the copper (I) formed during the anodic pulse. This process would not be expected to cause desorption since the polyether film would remain attached via chloride ions. During the following cathodic pulse, the concentration of copper (I) ions built up during the anodic pulse would be reduced again to copper metal. The net effect of this would be that the adsorption of the polyether would be relatively unaffected by the use of pulsed reverse current.

12.4.2. The Effect of Pulsed Reverse Current on the Adsorption of Sulphopropyl Sulphides.

Unlike the adsorption of the polyether, it is likely that the sulphopropyl sulphides are specifically adsorbed. The active sulphide or disulphide group has a high affinity for copper and differential capacitance measurements have shown that these species are adsorbed strongly on copper surfaces immersed in a sulphuric acid (1N) electrolyte.[161,162] These species also have a strong catalytic effect on the deposition of copper. The mechanism of catalysis has not been fully established, but probably involves the active sulphide or disulphide groups as illustrated in figures 67a and 67b. Because reduction and oxidation are reversible, and the catalyst presumably lowers the activation energy for this process, it is probable that oxidation of copper is catalysed by sulphopropyl sulphides as well as reduction. Thus during the anodic pulse, copper would be preferentially oxidised from the copper atoms in the lattice attached to the sulphopropyl sulphide molecules. This would tend to cause the sulphopropyl sulphide to desorb from the surface attached to a copper (I) ion. During the cathodic pulse, this

desorption process would tend to be reversed and if the cathodic pulse were long enough, the catalytic effect of the sulphopropyl sulphide would be resumed. The speed at which the catalytic effect of the sulphopropyl sulphide molecule is re-established depends upon the rate of resorption and this in turn depends upon the bulk solution concentration of the sulphopropyl sulphide. This explains the results observed in figure 44. At a concentration of 1ppm of MPS, the rate of resorption is low so even the lowest applied pulsed reverse current densities had a significant effect on the deposition potentials and at a current density of 3 A/dm^2, the potential was virtually the same as an electrolyte with no MPS added. As the concentration of MPS was increased, so the current density at which the effect of the desorption of MPS was evident also increased. This is proposed to be due to an increased rate of resorption. Finally, at a concentration of 100 ppm MPS, the rate of resorption was sufficiently high to prevent the polarisation effect being observed in the current density range studied.

However, the results of the T.E.M. studies have shown that the addition of S.S.P. to an electrolyte containing polyether produces grain refinement when pulsed current is applied. This indicates that the S.S.P. molecule remains surface active although its catalytic activity is lost. A possible explanation for these observations is that after desorption of the S.S.P. molecule attached to a copper (I) ion, this species could then be chelated by the polyether molecules adsorbed on the surface as shown in figure 68 . This process would render the sulphopropyl sulphide catalytically inactive and increase the adsorption coefficient of the polyether by adsorption of the sulponate group which would explain the grain refining effect shown by the T.E.M. photographs.

Another possible explanation for the loss of catalytic activity of the sulphopropyl sulphide could be that it is oxidised to another species during the anodic pulse. Disulphides can be oxidised by powerful oxidants either with or without cleavage of the

S-S bond. If the oxidation process proceeds without cleavage, the intermediate products are sulphones and disulphones. If bond cleavage occurs, the intermediate products are sulphinic acids (166). In both cases, the end product when oxidation is complete is a sulphonic acid. The end product is arrived at by the progressive addition of oxygen to the sulphur atoms. This process would only be expected to occur at an electrode if the electrode potential were sufficiently anodic to allow discharge of oxygen. Polarographic studies showed that up to an applied overpotential of +0.5 V, no oxidation of S.S.P. occurred at a dropping mercury electrode. Although the oxidation potential of S.S.P. at a copper electrode will differ significantly, it is probable that S.S.P. is not oxidised at the anodic potentials which are applied during pulsed reverse plating using the conditions employed in the experimental work. Thus the most likely explanation of the effects of the sulphopropyl sulphide under the influence of pulsed reverse current is provided by the desorption/chelation theory outlined above.

Figure 68. Proposed Mechanism for Adsorption of Sulphopropyl Sulphide with Pulsed Reverse Current.

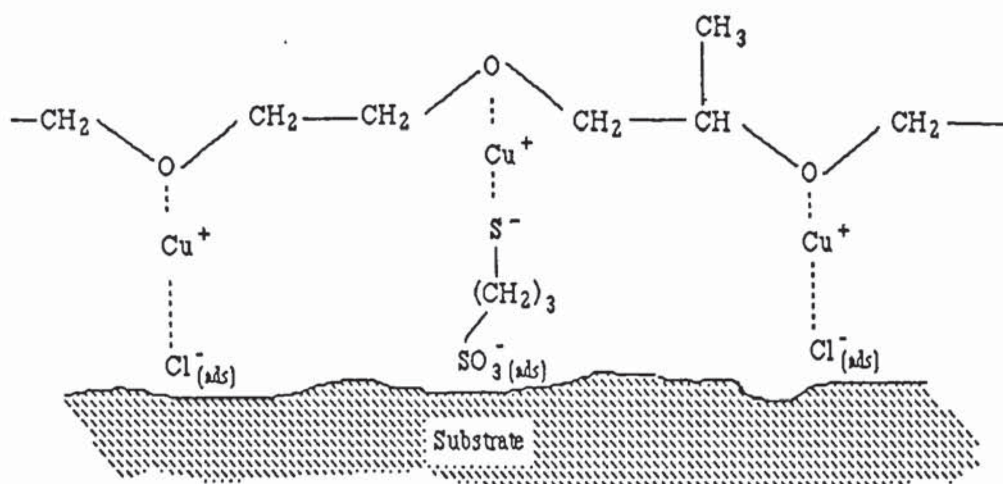

12.5. The Effect of Additives on the Structure of Deposits.

The results of the T.E.M. studies have shown that in an additive free electrolyte, the grain size of copper electrodeposits is increased by an order of magnitude by the use of pulsed reverse current. A possible explanation for this could be that during the anodic pulse, copper atoms may be removed preferentially from high energy sites which are most probably lattice misfits. Also, adsorbed ions of other species may be desorbed from growth sites. The net effect of this would be an activation of growth sites so that fresh nucleation would tend to occur at existing growth sites rather than forming new ones, thus causing grain growth.

When polyether is added to the electrolyte, an overall grain refinement is produced using pulsed reverse current. This is most probably due to the blocking of growth sites by adsorption of the polyether. In the case of direct current, the polyether is adsorbed strongly in some areas giving very small grains but in other areas, grains grow much larger but with many imperfections. Probably, the high molecular weight of the polyether used in the experiments prevented even adsorption under conditions of direct current plating. This was observed to cause "step" plating of the test panel plated with direct current.

When S.S.P. was added to the electrolyte containing polyether, the use of pulsed reverse current produced a further reduction in the grain size. The polarisation studies on the behaviour of acid copper electrolytes containing these additives suggested that pulsed reverse current produced desorption of the sulphopropyl sulphide. The T.E.M. evidence suggests that although the catalytic form of the sulphopropyl sulphide may be desorbed, the molecule remains surface active and so must be adsorbed in some form. When plating is carried out using direct current, an electrolyte containing S.S.P. and

polyether produces a bright deposit. T.E.M. results show that this deposit consists of fairly uniform grains of slightly larger size than those obtained from an additive free electrolyte. Thus, in this case, the S.S.P. causes grain growth rather than grain refinement suggesting that a different mechanism is occurring here. Since different grain sizes and structures are obtained by using direct and pulsed reverse current, it is evident that the physical and mechanical properties of the deposits will vary. The hardness values reported in the experimental results section show a correlation with the grain size of the deposits with the largest grain sizes producing the softest deposits. The changes in grain size may also affect the ductility of the deposits which is very important for the production of deposits for use on printed circuit boards and warrants further investigation.

12.6. Factors Affecting the Chemical Stability of Additives in Acid Copper Electrolytes.

12.6.1. The Sulphopropyl Sulphides.

The two sulphopropyl sulphides used in the experiments had the following structures :-

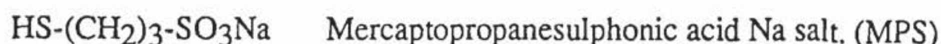

$HS-(CH_2)_3-SO_3Na$ Mercaptopropanesulphonic acid Na salt. (MPS)

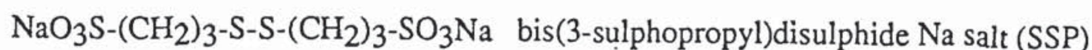

$NaO_3S-(CH_2)_3-S-S-(CH_2)_3-SO_3Na$ bis(3-sulphopropyl)disulphide Na salt (SSP)

The SSP is the disulphide of the MPS and the two species are interchangeable by oxidation and reduction in the following manner :-

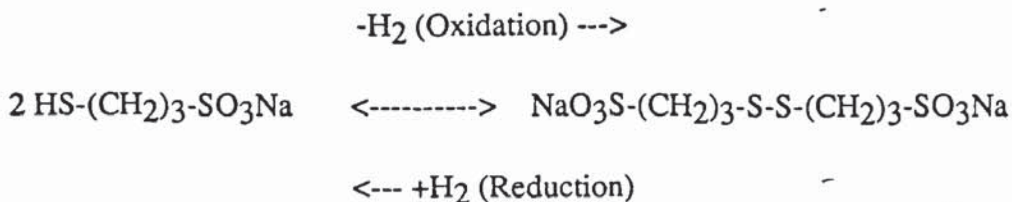

It is quite possible that when SSP is used as an additive, it is reduced at the cathode to MPS. This is a possible explanation for why the results obtained with the two different additives are so similar. Also, this may explain why equivalent weight percentages of MPS and SSP give similar brightening activities even though their molecular weights are considerably different. However, the acid stability of the MPS is not likely to be as good as SSP because the active mercapto group can undergo acid hydrolysis more rapidly than the disulphide group :-

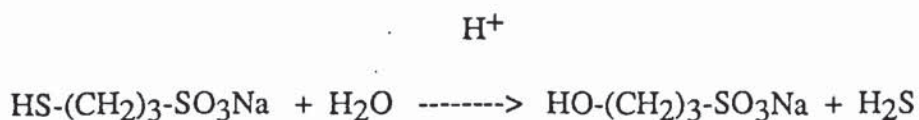

However, this reaction is slow at room temperature and the MPS present in the solutions was only decomposed over a period of weeks thus the validity of the results should not be affected too much by decomposition of MPS. From a commercial point of view, stability of the sulphur containing compounds is very important which explains why in most of the patents (125-129) the disulphide (SSP) rather than the sulphide is patented. Thus for any commercial application, only the disulphide would be suitable.

12.6.2. The Polyethers.

Polyethers generally have quite good acid stability. High molecular weight polymers have some susceptibility to acid hydrolysis which can cause chain scission and lead to a lowering of the average molecular weight. For example, with polyethylene glycol :-

$$HO\text{-}(CH_2\text{-}CH_2\text{-}O\text{-})_n\text{-}H + H_2O \xrightarrow{H^+} HO\text{-}(CH_2\text{-}CH_2\text{-}O\text{-})_m\text{-}H + HO\text{-}(CH_2\text{-}CH_2\text{-}O\text{-})_p\text{-}H$$

Where n is an integer representing the number of ethylene oxide units in the original polymer and m and p represent the number of ethylene oxide units in the fragments after acid hydrolysis. It should be noted here that n=m+p to balance the equation.It is reasonable to consider that this hydrolysis effect is too slow to affect the experimental results obtained.

When the effect of molecular weight on the polarisation characteristics was studied, this was done at the same weight percentage for all tests. This would mean that since the molecular weight varied, the molecular concentration in solution would also vary. However, the concentration of polymer used was close to the top of the curve shown in figure 66 so the rate of polymer inclusion should have been under adsorption control. Thus the differences in molecular concentration could be considered to be negligible.

Chapter 13

Conclusions - Copper.

1) A combination of organic additives has been found which has been shown to be effective in changing polarisation characteristics such that metal distribution can be improved over a range of current densities when a pulsed current source is employed. A Theory has been proposed to account for this phenomenon. Subsequent laboratory and industrial trials have shown that the "hole throwing power" of electrolytes can be improved by the use of pulsed reverse current if the plating bath contains appropriate organic compounds.

2) When polyethers are added to acid copper electrolytes, the deposition potentials for a given current density are more negative than the corresponding deposition potentials in the absence of this additive. This phenomenon is believed to be due to a surface blocking effect caused by the adsorption of the polyether on the cathode surface. This surface blocking effect increases with increasing molecular weight of the polymer until above a certain molecular weight, the polymer becomes too weakly adsorbed to be effective. The maximum effective molecular weight of polyether was determined experimentally to be around 50,000. The addition of these polyethers also causes a shift in the rest potential to more negative values and a reduction in the exchange current density. Chloride ions appear to play some part in the adsorption mechanism and increasing the chloride ion concentration tends to cause the rest potential to become more negative.

3) When sulphopropyl sulphides are added to acid copper, the deposition potentials for a given current density are less negative than the corresponding deposition potentials in the absence of this additive. This is due to a catalytic effect of the active sulphur containing groups. Thus the addition of these additives causes a shift in the rest potential to less negative values and an increase in the exchange current density.

4) In additive free solutions and when either polyethers or sulphopropyl sulphides are present singly, A plot of log current density versus potential gives a straight line over the current density range studied in the experiments. This straight line behaviour was noted using both pulsed reverse and direct current. This implies that :-

> i) The system was essentially under activation control i.e. concentration polarisation was negligible.
>
> ii) The system obeyed Tafel kinetics.

5) When both additives were present, the rest potential and calculated exchange current densities were close to those obtained from solutions containing only the sulphopropyl sulphide. It was concluded from this that the sulphopropyl sulphide was preferentially adsorbed.

6) When both additives were present, a plot of log current density versus potential gave a straight line using direct current but a significant change in slope at higher current densities with pulsed reverse current. It was therefore concluded that pulsed reverse current altered the adsorption mechanism of the sulphopropyl sulphide at higher current densities.

7) From the experimental results, it was determined that on the basis of the magnitude of the change of slope of the polarisation curve when pulsed reverse current was used, the most effective concentration ranges of the additives were as follows :-

i) Mercaptopropane sulphonic acid - 10 - 40 p.p.m.
(or its disulphide)

ii) Polyalkylene glycol (25% propylene oxide) - 70 p.p.m. - 1g/l
Molecular weight 50,000

iii) Chloride ion - 100 - 200 p.p.m.

8) The hole throwing power obtained on printed circuit boards can be enhanced substantially by the use of pulsed reverse current when the electrolyte contains a suitable combination of sulphopropyl sulphides, polyethers and chloride ions.

9) Optimum conditions of pulsing were obtained at a anodic / cathodic time ratio of 1:20 and an anodic / cathodic current density ratio of 3:1 for both the laboratory prepared electrolyte and the commercial electrolyte. At lower time ratios or higher current density ratios, peak cathodic current densities increase to a point where a deterioration in throwing power occurs. These parameters have been obtained for an average deposition rate corresponding to 3 A/dm^2 direct current.

10) The use of pulsed reverse current on an additive free electrolyte causes and increase in the average grain size from 1.5 - 2.5 μm with direct current to 15 - 20 μm with pulsed reverse current. This is due to the activation of growth sites during the anodic pulse.

11) When S.S.P. is added to an electrolyte containing polyether, grain growth occurs with direct current and grain refinement with pulsed reverse current. This is due to a change in the adsorption mechanism of the sulphopropyl sulphide as described in the discussion.

Chapter 14.

Concluding Comments on General Aspects of Plating with Pulsed Current.

14.1. Introduction.

The sections covering the research work studying the effects of pulsed current on the electrodeposition of chromium and copper have dealt with specific applications of pulsed current to an electrochemical system. However, studying the published literature in conjunction with the experimental results obtained in this thesis enables several general conclusions to be drawn concerning the effects of pulsed current when applied in a practical situation. These will be presented in this chapter.

14.2. Effect of Pulsed Current on Current Density Distribution.

Primary current density distribution is independent of electrochemical parameters and so is not influenced by the shape of the applied waveform. Thus pulsed current has no influence on primary current density distribution.

Secondary current distribution depends upon the level of applied overpotential. As the activation overpotential increases, the electrode resistance falls because more ions have the necessary activation energy for reduction. This causes the overall current density distribution to approach a primary distribution. In order to maintain the same average rate of deposition as direct current, the peak cathodic overpotential is always higher when pulsed current is employed. This means that with pulsed current, the effects of

secondary current distribution are less than when direct current is used. If the system is such that the effects of mass transport are negligible (as in acid electrolytes with high cathodic efficiency), then the use of pulsed current produces a more uneven current density distribution than direct current.

In electrolytes where the cathodic efficiency is significantly less than 100%, the use of pulsed current may change the relative efficiencies of metal deposition and hydrogen discharge and may under suitable conditions produce an increase in throwing power. As the research work presented in this thesis has shown, Electrolytes containing organic additives may undergo changes in the deposition mechanism when pulsed current is used which produce changes in the uniformity of deposition which can be beneficial in improving throwing power.

Tertiary current distribution is only significantly affected by pulsed current when the system is operated close to the pulse limiting current density. In practical applications, this is unlikely because of the high pulse current densities required. Thus in practical applications, tertiary current distribution in deposition with pulsed current is similar to that obtained with direct current.

14.3. Effect of Pulsed Current on Maximum Rate of Deposition.

If Pulses of a high frequency are applied to a plating system, the diffusion layer has no time to disperse between pulses. In this case, the diffusion system consists of a stationary layer where the concentration gradient depends only on the average applied current density, and a pulsating layer where the concentration gradient varies with time. The total thickness of the diffusion layer is equivalent to that obtained using the same average current density with direct current. Because of this, the use of pulsed current in

practical applications has little influence on the limiting current density. However, having stated that pulse plating cannot increase the limiting current density of a plating electrolyte, it must be emphasised that the maximum current density at which a plating electrolyte can be operated is usually only 10 to 20% of the theoretical limiting current density. This is because mass transport effects produce "burning" at higher current densities. Clearly, there is room for improvement and it has been claimed that higher plating rates can sometimes be achieved with pulsed current due to improved deposit properties. This effect is attributed to the effect of pulsed current on the process of electrocrystallisation rather than an enhancement of the rate of mass transport.

14.4. Effect of Pulsed Current on Power Consumption.

When pulsed current is applied to any electrochemical system, for an equivalent rate of deposition to direct current, the applied overpotential during the pulses is higher than for direct current. Thus the cell voltage is always higher when pulsed current is used than with direct current. Since power consumption is the product of the average current and the cell voltage, power consumption is always increased when pulsed current is used. This is not usually a problem but in high power applications, (for example in the deposition of chromium), electrolyte overheating can result because of this phenomenon.

14.5. Effect of Pulsed Current on Deposit Properties.

The effect of pulsed current on deposit properties is specific to the electrochemical system to which it is applied and so it is not possible to generalise on these effects. For instance, pulsed current causes grain refinement and increase in hardness of nickel deposits from a Watt's electrolyte [78], but grain growth in the case of gold deposition

from a gold/cobalt alloy electrolyte (74). In cases where grain refinement occurs, these effects are usually much smaller than the grain refining effects of organic additives.

14.6. Other Aspects of Deposition with Pulsed Current.

The research presented in this thesis has shown the specific nature of the effects of pulsed current on two very different electrochemical systems. In the case of chromium deposition, the chemistry of the deposition reaction has been shown to be affected by the application of unipolar current pulses. This can lead to co-deposition of hydride phases depending upon the frequency of the applied pulses. The electrocrystallisation process is also changed by the use of pulsed current causing a change in deposit orientation. In the case of deposition of copper from acid electrolytes containing organic additives, the use of pulsed reverse current has been shown to change the adsorption properties of the organic additives so that an enhanced throwing power can be obtained. This process has been shown to be effective commercially for plating high aspect ratio holes in printed circuit boards.

Research on the use of pulsed current in association with electrolytes containing organic additives has been neglected until now but may yield many useful commercial applications.

Chapter 15.

Suggestions for Further Work.

15.1. Chromium.

The ability of pulsed current to produce crack free deposits of a similar hardness to deposits produced by direct current has been demonstrated in the present work. Potentiodynamic scans have indicated that an improvement in corrosion resistance properties could be obtained from these crack free deposits. However, the coatings obtained are brittle and macro-cracking of the coating would lead to localised corrosive attack in use. Further work is required to assess the effect of grinding operations and heat treatment on the corrosion resistance of pulse plated chromium deposits and to determine whether a significant increase in corrosion protection is obtained in practice. More information could be obtained both from potentiodynamic scans and salt spray testing of samples subjected to grinding and heat treatment operations.

In addition, further work is required to assess the wear resistance of pulse plated chromium deposits. This is important because the primary reason for the application of hard chromium deposits is to give good wear resistance properties. A project involving the Falex test has just been commenced at Aston University to evaluate wear behaviour of chromium electrodeposits produced from several electrolytes.

The results of the work studying the effect of varying frequency on the composition of chromium deposits suggested a hypothesis to explain the formation of hydride phases in the deposits. More work could be undertaken to confirm this hypothesis. It would be of interest to determine the effects of temperature, current density and electrolyte

composition over the range of frequencies where hydrides are co- deposited. In the present work, these factors were held constant to minimise the number of variables.

Finally, determination of the covering power of chromium electrolytes has shown that this is very substrate sensitive. No satisfactory hypothesis for this phenomenon could be provided on the basis of the experimental results presented in chapter 8. This warrants further work.

15.2. Copper.

The current research has shown the ability of pulsed reverse current to influence the adsorption mechanism of organic additives used as brighteners in acid copper electrolytes. The resultant change in the polarisation characteristics of the electrolyte leads to a much improved "hole throwing power" on printed circuit boards. This has been shown to be effective both in laboratory trials and in commercial practice. A mechanism has been proposed to explain this phenomenon. However, in the production of printed circuit boards, the physical properties of the electrodeposited copper are of paramount importance because of the stresses applied to the deposit when components are soldered to the boards. Thus the ductility of the deposit is very important. The use of pulsed reverse current to improve hole throwing power also changes the grain size of the deposits. This has been demonstrated in the present work by the use of transmission electron microscopy. Because of this observation, further work is required to determine the effect of pulsed reverse current on deposit properties such as ductility and tensile strength.

Further work is also required to determine the effect of pulsed reverse current on the consumption of the additives used in the plating electrolytes. It is important to know

this so that the electrolytes can be maintained at the correct additive levels. Investigation of the possible formation of additive breakdown products is required because in the long term, these can adversely affect the deposit properties. The effect of levelling agents has not been studied in the current work. These compounds usually act as polarising agents and thus influence the polarisation characteristics of an electrolyte. this may explain differences in the behaviour of different commercial brightener systems when used in conjunction with pulsed reverse current. A study of the effect of pulsed and pulsed reverse current on the adsorption of diffusion controlled inhibitors would provide useful data.

15.3. Other Work.

It would be of considerable interest to investigate the effects of modulated current on brightener mechanisms. This area of research has up to now been unexploited and may yield some interesting applications. The current research has shown how a combination of organic additives may improve "hole throwing power" when pulsed reverse current is used but other combinations of additives could produce even more dramatic effects.

It was indicated early in the thesis that some work was undertaken on nickel. Deposition of this metal from electrolytes with and without addition agents warrants further study. The utilisation of pulsed current in electroforming is known to have some benefits but the effects of pulsed reverse current on stress certainly justifies more research. Interest has been expressed from a commercial source on the use of pulsed current for the production of electroformed mesh products from electrolytes containing organic addiuves. In view of the results achieved with copper in the present work, this would seem to be a very worthwhile area for future research.

References.

1. Coehn, A., German patent 75482 (1893).

2. Puippe, J. Cl. and Leaman, F. "Theory and Practice of Pulse Plating." A.E.S.F. publication (1986).

3. Puippe, J. Cl., Ibl, N., Hosokawa, K. and Angerer, H. "Influence of Pulse Parameters on Properties of Deposits." Proc. A.E.S.F. International Pulse Plating Symposium Boston, April 19-20(1979).

4. Puippe, J. Cl. and Ibl, N., "Limitation of Useful Range of Conditions in Pulse Plating Due To Capacity Effects." Proc. A.E.S.F. International Pulse Plating Symposium Rosemont, Illinois October 6-7 (1981).

5. Puippe, J. Cl. and Ibl, N., "Influence of Charge and Discharge of the Electric Double Layer in Pulse Plating." J. Appl. Electrochem. **10.** 775-784 (1980).

6. Ibl, N., "Some Theoretical Aspects of Pulse Electrolysis." Surface Technology **10.** 81-104 (1980).

7. Maksimovic, M.D. and Zecevic, S.K., "Influence of the Double Layer in Periodically Changing Rate Metal Deposition." Surface and Coatings Technology **30.** 405-413 (1987).

8. Maksimovic, M.D. and Dimitrijevic, Z.S., "Fundamental Aspects of Pulsating Current Metal Deposition V: The Determination of the Optimal Frequency Range." Surface Technology **17.** 3-9 (1982).

9. Yeager, E., Bockris, J. O'M. and Sarangapani, S., "A Comprehensive Treatise of Electrochemistry Volume 6 - Electrodics : Transport." Plenum Publications. New York. (1983).

10. Cheh, H.Y., "Electrodeposition of Gold by Pulsed Current." J. Electrochem. Soc. **118.** 551-557 (1971).

11. Datta, M. and Landolt, D., "Experimental Investigation of Mass Transport in Pulse Plating." Surface Technology **25.** 97-110 (1985).

12. Viswanthan, K., Farrell-Epstein, M.A. and Cheh, H.Y., "The Application of Pulsed Current Electrolysis to a Rotating Disk Electrode I : Mass Transfer." J. Electrochem. Soc. **125.** 1772-1776 (1978).

13. Vetter, K.J., "Electrochemical Kinetics." Academic Press. New York. 1967.

14. Rosebrugh, T.R. and Miller, W.C., "Mathematical Theory of the Changes of Concentration at the Electrode Brought About by Diffusion and Chemical Reaction." J. Phys. Chem. **14.** 816-884 (1910).

15. Siver, Y.G., "Non Stationary Electrode Processes in Stirred Media." Russ. J. Phys Chem. **34.** 273-277 (1960).

16. Hale, J.M., "Transients in Convective Systems I : Theory of Galvanostatic and Galvanostatic with Current Reversal Transients at a Rotating Disc Electrode." J. Electroanal. Chem. **6.** 187-197 (1963).

17. Chin, D.T., "Mass Transfer and Current-Potential Relation in Pulse Electrolysis." J. Electrochem. Soc. **130.** 1657-1667 (1983).

18. Popov, K.I., Maksimovic, M.D.and Djokic, D., "Fundamental Apsects of Pulsating Current Metal Electrodeposition III : Maximum Practical Deposition Rate." Surface Technology **14.** 323-333 (1981).

19. Puippe, J.Cl., Dissertation ETH 6255 Zurich (1978). (As referenced in "Theory and Practice of Pulse Plating." A.E.S.F. publication (1986).)

20. Despic, A.and Popov, K.I., "Time Optimal Electrodeposition of Metals with a Pulsating Current." J. Appl. Electrochem. **3.** 161-168 (1973).

21. Popov, K.I., Maksimovic, M.D. and Ocokoljic, B.M., "Fundamental Apsects of Pulsating Current Metal Electrodeposition I : The Effect of the Pulsating Current on the Surface Roughness and the Porosity of Metal Deposits." Surface Technology **11.** 99-109 (1980).

22. Puippe, J. Cl.and Leaman, F., "Theory and Practice of Pulse Plating." A.E.S.F. Publication. Chapter by D. Landolt 69-71 (1986).

23. Viswanthan, K., Farrell-Epstein, M.A. and Cheh, H.Y., "Simultaneous Discharge of Two Reacting Species Under Pulsed Conditions." J. Electrochem. Soc. **127.** 2383-2385 (1980).

24. Verbrugge, M.W. and Tobias, C.W., "A Mathematical Model for the Periodic Electrodeposition of Multicomponent Alloys." J. Electrochem. Soc. **132.** 1298-1307 (1985).

25. Ibl, N., "Current Distribution in Pulse Plating." Proc. A.E.S.F. International Pulse Plating Symposium Rosemont, Illinois October 6-7 (1981).

26. Hoar, T.P., "Polarisation." Plating." **60.** 35-42 (1974).

27. Popov, K.I.and Maksimovic, M.D., "Fundamental Apsects of Pulsating Current Metal Electrodeposition IV : Tafel Equation in the Deposition of Metals by a Pulsating Current." Surface Technology **15.** 161-165 (1982).

28. Andriacos, P.C., Cheh, H.Y. and Linford, H.B., "Application of Pulsed Plating Techniques to Metal Deposition Part IV - Microthrowing Power of Gold Deposition." Plating and Surface Finishing. **64.** 44-48 (1977) .

29. Popov, K.I. and Maksimovic, M.D., "Fundamental Apsects of Pulsating Current Metal Electrodeposition VIII : The Effect of Pause to Pulse Ratio on Microthrowing Power of Metal Deposition." Surface Technology **22.** 155-158 (1984).

30. Popov, K.I., Totovski, D.C. and Maksimovic, M.D., "Fundamental Apsects of Pulsating Current Metal Electrodeposition VII : The Comparison of Current Density Distributions in Pulsating Current and Periodic Reverse Current Electrodeposition of Metals." Surface Technology **19,** 181-185 (1983).

31. Puippe, J.Cl. and Ibl, N., "The Morphology of Pulse Plated Deposits." Plating and Surface Finishing. **67.** 69-72 Jun. (1980).

32. Ozerov, A.M., Litvishko, N.P., Vavilina, I.N., Chetvertnov, P.M. and Zhak, Y.E., "Electrolysis by Pulsating Current." J. Appl. Chem. U.S.S.R. **40.** 1101-1103 (1967).

33. Cheh, H.Y., "The Limiting Rate of Deposition by P.R. Plating." J. Electrochem. Soc. **118.** 1132 - 1134 (1971).

34. Popov, K.I., Keca, D.N. and Vidojkovic, S.I., "Mathematical Model and Digital Simulation of Pulsating Overpotential Copper Electrodeposition." J. Appl. Electrochem. **6.** 365-370 (1976).

35. Popov, K.I., Maksimovic, M.D., Adzic, R.R. and Ostojic, G.R., "A Computer Simulation of Copper Deposition by Pulsating Overpotential." J. Appl. Electrochem. **8.** 75-79 (1978).

36. Jernsted, G.W., U.S. Patent No. 2,451,340 (1948).

37. Jernsted, G.W., U.S. Patent No. 2,451,341 (1948).

38. Jernsted, G.W., U.S. Patent No. 2,678,909 (1954).

39. Jernsted, G.W., U.S. Patent No. 2,690,997 (1954).

40. Dini, J.W., "Periodic Reverse Plating." Metal Finishing. **61**(7). 52-58 (1963).

41. Bayerns, P., "Electroplating With Modulated Current." Trans. Inst. Metal Finishing. **31.** 429-452 (1954).

42. Hickling, A.and Rothbaum, P., "Cyclic Electrolysis." Trans. Inst. Metal Finishing. **34.** 199-221 (1957).

43. Garte, S.M., "Effect of Substrate Roughness on the Porosity of Gold Electrodeposits." Plating. **53.** 1335-1339 (1966).

44. Garte, S.M., "Porosity of Gold Electrodeposits : Effect of Substrate Surface Structure." Plating. **55.** 946-951 (1968).

45. Nobel, F.I., Ostrow, B.D. and Thompson, D.W., "Porosity Testing of Gold Electrodeposits." Plating. **52.** 1001-1008 (1965).

46. Leeds, J.M. and Clarke, M., "The Effects of Plating Conditions on Porosity in Gold Deposits." Trans. Inst. Metal Finishing. **46.** 1-11 (1968).

47. Sard, R., Okinaka, Y. and Rushton, J.R., "Some Properties of Electroless Gold Deposits." Plating. **58**(9). 893-900 (1971).

48. Leaman, F.H.and Kownacki, B.A., "Pulsed Versus Direct Current for Continuous Plating of Contacts." Proc. A.E.S.F. International Pulse Plating Symposium Boston, April 19-20(1979).

49. Wang, Y.Y., Tung, C.S.and Wan, C.C., "Application of Pulsed Current to Gold Plating." Metal Finishing. **67**(9). 21-25 (1980).

50. Rehrig, D.L., "Effect of Deposition Method on Porosity in Thin Gold Films." Plating. **61**(1). 43-46 (1974).

51. Fallot, J.F., "Pure Gold : A Comparison of Pulse Plating Versus D.C.." Proc. A.E.S.F. International Pulse Plating Symposium. Washington D.C. October 28-29 (1986).

52. Popov, K.I., Keca, D.N.and Vuksanovic, B.I., "The Effect of the Overpotential of Deposition on the Porosity of Metal Deposits." J. Appl. Electrochem. **7.** 185-188 (1977).

53. Popov, K.I., Keca, D.N.and Draskovic, D.A., "The Effect of Pulsating Potential Electrolysis on the Porosity of Metal Deposits." J. Appl. Electrochem. **6.** 155-157 (1976).

54. Sullivan, W., "Electroplating Cobalt with a High Current Capacity Pulse Plating System." Plating. **62**(2) 139-141 (1975).

55. Cheh, H.Y., Andriacos, P.C. and Linford, H.B., "Application of Pulsed Plating Techniques to Metal Deposition Part III - Macrothrowing Power of Cu, Ag and Au Deposition." Plating and Surface Finishing. **64**(7). 42-44 (1977).

56. Paatsch, W., "Investigation of Hydrogen Embrittlement of High Tensile Strength Steel During Electrodeposition Processes. Part I - Hydrogen Permeation Experiments." Metalloberflache. **33.** 546 (1979).

57. Paatsch, W., "Investigation of Hydrogen Embrittlement of High Tensile Strength Steel During Electrodeposition Processes. Part II - Tensile Tests." Metalloberflache. **34.** 174 (1980).

58. Kleinekathofer, W., Muramaki, T. and Raub, C.J., "Deposition of Nickel by Pulse Plating." Proc. A.E.S.F. International Pulse Plating Symposium Boston, April 19-20(1979).

59. Kleinekathofer, W. and Raub, C.J., "Electrodeposition of Nickel by the use of Pulsed Current." Surface Technology. **7.** 23-34 (1978).

60. Faust, G.L., Schaer, G.R. and Semones, D.E., "Electroplating Chromium Directly on Aluminium." Plating. **48**(6). 605-612 (1961).

61. Knodler, A., "Electrodeposition of Chromium from Chromic Acid Solutions by Pulse Plating." Proc. A.E.S.F. International Pulse Plating Symposium Boston, April 19-20 (1979).

62. Locarnini, J.M. and Ibl, N., "Pulse Plating of Palladium." Proc. A.E.S.F. International Pulse Plating Symposium Rosemont, Illinois October 6-7 (1981).

63. Munier, G.B., "Polymer Codeposited with Gold During Electroplating." Plating. **56.** 1151-1157 (1969).

64. Eisenmann, E.T., "The Precipitation of $KCo[Au(CN_2)]_3$ and similar Cyanaurate Complexes." J. Electrochem.Soc. **124.** 1957-1958 (1977)

65. Okinaka, Y., Koch, F.B., Wolowodiuk,C.and Blessington, D.R., " 'Polymer' Inclusions in Cobalt Hardened Electroplated Gold." J. Electrochem. Soc. **125.** 1745 -1750 (1978).

66. Leidheiser, H., Verles, A., Varsanyi, M.L.and Czako-Nagy, I., "The Chemical State of Cobalt in Cobalt Hardened Gold Electrodeposits." J. Electrochem Soc. **126.** 391-394 (1979).

67. Knodler, A., "Electrodeposition of Gold Alloys From Acid Solutions by Pulse Plating." Proc. A.E.S.F. International Pulse Plating Symposium Boston, April 19-20(1979).

68. Reid, F.H., Metaloberflache. **30.** 453 (1976) (As referenced by Fluhmann et al. in "Effect of Pulsed Current Plating on Gold-Cobalt Electrodeposition." Proc. A.E.S.F. International Pulse Plating Symposium Boston, April 19-20(1979).)

69. Branik, M. and Schnabl, H., "Properties of Hard Gold Deposited by Pulse Current for Connector Application." Proc. A.E.S.F. International Pulse Plating Symposium Boston, April 19-20(1979).

70. Fluhmann, W., Mausli, P.A., Reid, F.H. and Steinemann, S., "Effect of Pulsed Current Plating on Gold-Cobalt Electrodeposition." Proc. A.E.S.F. International Pulse Plating Symposium Boston, April 19-20(1979).

71. Stimetz, C.J.and Hren, J.J., "Pulse Plating of Hard Gold Electrodeposits." Proc. A.E.S.F. International Pulse Plating Symposium Boston, April 19-20(1979).

72. Leaman, F.H. and Kownacki, A., "Pulsed Versus Direct Current for Continuous Plating Contacts for Electrical Connectors with Nickel Underplating and Cobalt Hardened Gold." Proc. A.E.S.F. International Pulse Plating Symposium Boston, April 19-20(1979).

73. Antler, M., " Structure of Polymer Codeposited in Gold Electrolytes." Plating. **60.** 468 -475 (1973).

74. Fluhmann, W, Reid, F.H., Mausli, P.A. and Steinemann, S.G., "Effect of Pulsed Current on the Structure and Properties of Gold - Cobalt Electrodeposits." Plating and Surface Finishing. **67**(6). 62-65 (1980).

75. Holmbom, L.G. and Jacobson, B.E., "Influence of Bath Temperature and Pulse Plating Frequency on Growth Morphology of Electrodeposited Gold." Proc. A.E.S.F. International Pulse Plating Symposium. Washington D.C. October 28-29 (1986).

76. Hayashi, T., Kitanishi, H. and Fukumoto, Y., "Morphology and Crystallographic Features of Silver Deposits in the Pulsed Current Electrolysis." Proc. A.E.S.F. International Pulse Plating Symposium Rosemont, Illinois October 6-7 (1981).

77. Fukumoto, Y., Kawashima, Y. and Hayashi, T., Proc. A.E.S. 71st Annual Technical Conference (1984). (As referenced by J.Cl Puippe in "Theory and Practice of Pulse Plating." A.E.S.F. publication.)

78. Sutter, B., Mortier, F., Laroche, M.A., Reby, J. and Vasseur, G., Interfinish 84 (October 21-26, 1984) (As referenced by B. Sutter in "Theory and Practice of Pulse Plating." A.E.S.F. publication.)

79. Kendrick, J., "The Effects of Alternating Current on the Properties of Nickel Deposits from an All-Chloride Solution." Trans. Inst. Metal Finishing **44.** 78-83 (1966)

80. Crossley, J.A., Kendrick, J. and Mitchell, W.I., "The Structure of Nickel Deposited from an All-Chloride Solution by Square Wave Alternating Current." Trans. Inst. Metal Finishing. **45.** 58-63 (1967).

81. Reby, J., Vasseur, G. and Sutter, B., "Chromage Dur en Courant Periodiquement Inverse." Proc. Interfinish 88, Paris. **2.**(October 4-7 1988).

82. Colombini, C., "Use of Pulse Rectifiers with Periodic Reversing Polarity in Hard Chromium Plating." Proc. Interfinish 88, Paris. **2.**(October 4-7 1988).

83. Dini, J.W. and Johnson, H.R., Gold Bulletin. **13.** 31 (1980). (As referenced by A. Knodler in "Theory and Practice of Pulse Plating." A.E.S.F. publication.)

84. Gore, G. "On the Properties of Electrodeposited Antimony." Trans. Royal Society (London) Part 1, 185-192 (1858).

85. Mills, E.J., "On Electrostriction." Proc. Royal Society , **26.** 504-512 (1877).

86. Weil, R., "The Origins of Stress in Electrodeposits. Part I." Plating **57.** 1231-1237 (1970).

87. Weil, R., "The Origins of Stress in Electrodeposits. Part II." Plating **58.** 50-56 (1971).

88. Weil, R., "The Origins of Stress in Electrodeposits. Part III." Plating **58.** 137-146 (1971).

89. Hart, A.C., Wearmouth, W.R. and Warner, A.C., "The Anodic Behaviour of Nickel in Nickel Sulphamate Electroplating Solutions." Trans. Inst. Metal Finishing. **54.** 56-60 (1976).

90. Knapp, B.B., "Notes on Nickel Plating from Sulphamate Solutions." Plating **58.** 1187-1193 (1971).

91. Bidmead, G.F., "The Effect of Current Surging on the Electrodeposition of Microcracked Chromium." Trans. Inst. Metal Finishing. **53.** 127-132 (1975).

92. Lashmore, D.S. and Oberle, R., "Electrodeposition of Artificially Layered Materials." Proc. A.E.S.F. International Pulse Plating Symposium. Washington D.C. October 28-29 (1986).

93. Celis, J.P., Roos, J.R., Blanpain, B. and Gilles, M., "Pulse Electrodeposition of Compositionally Modulated Multilayers." Proc. Interfinish 88, Paris. **2.**(October 4-7 1988).

94. Lashmore, D.S. and Weinroth, J., "Pulsed Electrodeposition of Nickel Phosphorus Metallic Glass Alloys." Proc. A.E.S.F. International Pulse Plating Symposium Rosemont, Illinois October 6-7 (1981).

95. Lashmore, D.S., Weisserhaus, I. and Pratt, K., "Electrodeposition of Nickel-Chromium Alloys." Plating and Surface Finishing **73**(3). 48-55 (1986).

96. Tannenberger, H. and Schnidler,K., "Control of the Composition of Palladium-Nickel Deposits by Pulse Plating." Proc. A.E.S.F. International Pulse Plating Symposium. Washington D.C. October 28-29 (1986).

97. Fukumoto, Y., Kawashima, Y., Aoki, I. and Hayashi, T., "Composition of Pulse Plated Gold-Nickel and Palladium Nickel." Proc. A.E.S.F. International Pulse Plating Symposium. Washington D.C. October 28-29 (1986).

98. Dossenbach, O. and Sturtznegger, B., "Pulsed Current Electrodeposition of Palladium-Silver Alloys." Proc. A.E.S.F. International Pulse Plating Symposium. Washington D.C. October 28-29 (1986).

99. Cherkaoui, M., Chassaing, E. and Vu Quang, K., "Investigation of Nickel Molybdenum Alloy Coatings Obtained by Pulse Plating." Proc. A.E.S.F. International Pulse Plating Symposium. Washington D.C. October 28-29 (1986).

100. Lowenheim, F.A., "Modern Electroplating." Third Edition Published by John Wiley and Sons. (1974).

101. Dennis, J.K. and Such, T.E., "Nickel and Chromium Plating." Second edition, Butterworths press.

102. Smart, D., Such, T.E., Wake, S.J., "A Novel Trivalent Chromium Electroplating Bath." Trans. Inst. Metal Finishing. **61**. 105-110 (1983).

103. Fink, C.G., U.S. patent No 1,581,188 (1926).

104. Leibrich, E., German patent No 448,526 (1927).

105. Fink, C.G., U.S. patent No 1,844,751 (1932).

106. Jones, A.R. "Microcracks in Hard Chromium Deposits." Proc. Interfinish 88, Paris. **2.**(October 4-7 1988).

107. Kasper, C., J. Res. Nat. Bureau Stand. **9.** 353(1932); **11.** 515(1933); **14.** 693(1935). (As referenced by J.K. Dennis in "Nickel and Chromium Plating" see ref. 101.)

108. Ogburn, F. and Brenner, A., Trans. Electrochem. Soc. **96.** 347 (1949).

109. Silverman, L. "The Analysis of Chrome Plating Solutions." Metal Finishing. **48.** No.2. 46-54 (1950).

110. Rogers, R.R., "Studies in the Theory of Chromium Electrodeposition." Trans. Electrochem Soc. **68.** 391-415 (1935).

111. Snavely, C.A., " The Mechanism of Chromium Plating." Trans. Electrochem. Soc. **92.** 537-577 (1948).

112. Snavely, C.A. and Faust, C.L., "Studies on the Structure of Hard Chromium Plate." J. Electrochem. Soc. **97.** 99-108 (1950).

113. Williams, C. and Hammond, R.A.F. "The Effect of Chromium Plating on the Fatigue Strength of Steel." Trans. Inst. Metal Finishing. **32.** 85-106 (1965).

114. Dennis, J.K., " The Effect of the Underlying Metal on the Internal Stress and Formation of Microcracks in Electrodeposited Chromium." Trans. Inst. Metal Finishing. **43.** 84-96 (1965).

115. Knodler, A. "Der Einfluss der Welligkeit des Gleichstromes auf die Galvanische Abscheidung von Metallen." (The Influence of D.C. Ripple on the Electrodeposition of Metals) Galvanotechnik **61.** (4) 290-302 (1970).

116. Saiddington, J.C. and Hoey, G.R., "Crack Free Chromium from Conventional Plating Baths." Plating. **61.** 923-934 (1974).

117. Saiddington, J.C. "Effect of Plating Interruptions on the Surface Appearance of Electrodeposited Chromium." Plating & Surface Finishing. **65.** 45-49 Jan. (1978).

118. Nesnidal, V.L. "Pulse Hard Chrome Plating with Single Phase Square-wave Rectification." Proc. A.E.S.F. International Pulse Plating Symposium Boston, April 19-20(1979).

119. Haring, H.E. and Blum, W. " Current Distribution and Throwing Power in Electrodeposition." Trans. Electrochem. Soc. **44.** 313-345 (1923).

120. Graham, A.K. "A Study of the Influence of Variables on the Structure of Electrodeposited Copper." Trans. Electrochem.Soc. **52.** 157-175 (1927).

121. Phillips, W.M. and Clifton, F.L. U.S. patent No 2,563,360 (1951).

122. Slunder, C.J., Bearse, A.E. and Faust, C.L. "Ductile, Mirror-Bright Copper Plate from Acid Sulphate Baths." Plating. **37.** 1040-1060 (1950).

123. Safranek, W.H., Combs, E.L. and Faust, C.L. " Ductile, Mirror-Bright Copper Plate from Acid Sulphate Baths. Part II - Pilot Plant Operation and Application." Plating. **37.** 1149-1161 (1950).

124. The "Sulfast" Acid Copper System. Described in the Canning Handbook. 18th Edition.

125. Combs, D.J., "Aqueous Acid Copper Electroplating Bath for Bright, Smooth Copper Electroplates." O.M.I. International Corporation. U.S. Patent no. 501211. 10/June/1983.

126. Watson, A.A., "Acid Copper Electroplating Baths Containing Brightening and Levelling Additives." M&T Chemicals Inc. U.S. Patent no. 277057 24/June/1981.

127. Ohme, R., Hoerig, L., Vieweger, U., Strobel G. and Weizorek, G. "Electrodeposition of Bright Copper." V.E.B. Lokomotivbau-Electrotechnishe Werke. German Patent no. 2025538 21/October/1971.

128. Yoshikata, T and Mitsui, T. "Acidic Copper Electroplating Bath Containing Brighteners." Okuno Chemical Industry Co. Ltd.. Japanese Patent no. 49/107933 14/October/1974.

129. Eckles, W.E. and Starinshak, T.W. "Acid Copper Plating and Additive Composition Thereto." R.O. Hull and Co. Inc. U.S. Patent no. 4038161 26/July/1977.

130. Watson, S.A. and Edwards, J. "An Investigation of the Mechanism of Levelling in Electrodeposition." Trans. Inst Metal Finishing. **34.** 167-198 (1957).

131. Edwards, J. "Radiotracer Study of Addition Agent Behaviour: 4- Mechanism of Incorporation." Trans. Inst. Metal Finishing **41.** 140-146 (1964).

132. Edwards, J. "Radiotracer Study of Addition Agent Behaviour: 1- Incorporation of Sulphur and Carbon in Nickel Deposited from Solutions Containing Thiourea." Trans. Inst. Metal Finishing **39.** 33-44 (1962).

133. Edwards, J. "Radiotracer Study of Addition Agent Behaviour: 2- Adsorption on Metal Surfaces from Solutions Containing Thiourea." Trans. Inst. Metal Finishing **39.** 45-51 (1962).

134. Edwards, J. "Radiotracer Study of Addition Agent Behaviour: 3- Incorporation of Sulphur in Nickel Deposited from Solutions Containing p-Toluenesulphonamide and Saccharin." Trans. Inst. Metal Finishing **39.** 52-55 (1962).

135. Edwards, J. and Levett, M.J. Radiotracer Study of Addition Agent Behaviour: 5- Further Results for Thiourea, p-Toluenesulphonamide and Saccharin." Trans. Inst. Metal Finishing **41.** 147-156 (1964).

136. Edwards, J. and Levett, M.J. "Radiotracer Study of Addition Agent Behaviour: 6- Coumarin and Melilotic Acid." Trans. Inst. Metal Finishing **41.** 157-168 (1964).

137. Stoychev, D.S., Vitanova, I., Rashkov, S.T. and Vitanov, T. "Adsorption of Substances Acting as Brighteners in the Electrolytic Deposition of Copper." Surface Technology **7.** 427-432 (1978).

138. Mirkova, L., Rashov, S.T. and Nanev, C.H.R. "The Levelling Mechanism During Bright Acid Copper Plating." Surface Technology **15.** 181-190 (1982).

139. Reid, J.D. and David, A.P. " Effects of Polyethylene Glycol on the Electrochemical Characteristics of Copper Cathodes in an Acid Copper Medium." Plating & Surface Finishing. **74.** 66-70 Jan.(1987).

140. Safranek, W.H. Technical Report on the Properties of Electrodeposited Copper. The Copper Development Assoc. (1970).

141. Cuthbertson, J.W. "The Structure of Heavy Electrodeposits of Copper and Nickel." Trans. Electrochem. Soc. **77.** 157-176 (1940).

142. Wood, W.A. "The Influence of Crystal Orientation of the Cathode on That of an Electrodeposited Layer." Proc. Phys. Soc. (London) **43.** 138-141 (1931).

143. Kushner, J.B. "Relationship Between Deposit Thickness and Current Density During the Early Stages of Deposition." J. Electrochem. Soc. **112.** 413-417 (1965).

144. Lamb, V.A. "Electroplating With Current Pulses in the Microsecond Range." Plating. **56.** 909-913 (1969).

145. Cheh, H.Y., Linford, H.B. and Wan, C.C. "Application of pulsed Plating Techniques to Metal Deposition. Part II - Pulsed Plating of Copper." Plating & Surface Finishing. **64.** 66-67 May (1977).

146. Mattson, B.E. and Bockris, J. O'M. "Galvanostatic Studies of the Kinetics of Deposition and Dissolution in the Copper + Copper Sulphate System." Trans. Faraday. Soc. **55.** 1586-1601 (1959).

147. Vilambi, N.R.K. and Chin, D.T. "Selective Pulse Plating from an Acid Copper Sulphate Bath." Plating & Surface Finishing. **75.** 67-73 Jan.(1988).

148. White, J.R. and Galasco, R.T. "Influence of Pulse plating on Surface Distribution and Metallurgy of Copper Deposits." Plating & Surface Finishing. **75.** 122-126 May.(1988).

149. Mann, J. "Periodic Reverse Current Process in Electroplating Using Acid Copper Electrolysis." Trans. Inst. Metal Finishing. **56.** 70-74 (1978).

150. Cavallotti, P.L., Colombo, D., Galbiati, E., Piotti, A. and Kruger, F. "Preferred Orientation and Morphology of Pulse Plated Copper and Cobalt." Plating & Surface Finishing. **75.** 78-82 April. (1988).

151. Farr, J.P.G. and Ashiru, O.A. "Electrode Impedance and the Effects of Additives on the Electrodeposition of Silver." Trans. Inst. Metal Finishing **64** 137-141 (1986).

152. Brenner, A. and Senderoff, S. "A Spiral Contractometer for Measuring Stress in Electrodeposits." J. Res. Nat. Bureau of Standards **42** R.P.1953 89-104 (1949).

153. Hoar, T.P. and Arrowsmith, D.J. "Stress in Nickel Deposits." Trans. Inst. Metal Finishing. **36** 1-6 (1958).

154. W.Canning in Association with Spon. The Canning Handbook: Surface Finishing Technology. 23rd edition (1982).

155. Montgomery, A., "Pulse Plating of Electrolytic Copper." Circuit World 2(15) 33-35 (1989).

156. Joint Committee on Powder Diffraction Standards. "Powder Diffraction File." Continuously Updated (Microfiche).

157. Cullity, B.D. "Elements of X-ray Diffraction." Second edition (1978) Addison-Wesley Publishing.

158. Fisher, G.L., Sonnenberg, W. and Bernards, R. "Electroplating High Aspect Ratio Through Holes in Thick Printed Circuit Boards." Proc. I.M.F. Annual Technical Conference, 11th April 1989.

159. Landau, U. and Lanzi, O. "Analysis of Mass Transport and Ohmic Limitations in Through Hole Plating." J. Electrochem Soc. **135(8)** 1922 (1988).

160. Ibl. N. I.U.P.A.C. Information Bulletin No 59, (1977).

161. Stoychev, D.S., Vitanov, I., Rashkov, S. and Vitanov,T. "Adsorption of Substances Acting as Brighteners in the Electrolytic Deposition of Copper." Surface Technology **7** 427-432 (1978).

162. Stoychev, D.S., Vitanov, I., Vitanov, T. and Rashkov, S. "Adsorption Behaviour of Some Brightening Agents Used in Electrolytic Copper Deposition from Acid Solutions." Compt. Rand. Acad. Bulg. Sci. **11(32)** 1515-1518 (1979).

163. Yokoi, M., Konishi, S. and Hayashi, T. "Adsorption Behaviour of Polyoxyethyleneglycol on the Copper Surface in an Acid Copper Sulphate Bath." Denki Kagaku **52** 218-223 (1984).

164. Kardos, O. "Current Distribution on Microprofiles - Part III." Plating and Surf. Fin. 4(**61**) 316-325 (1974).

165. Stoychev, D.S. and Rashkov, S. "Effect of Some Addends on the Electrolytic Deposition and Structure of Copper Coatings from Acid Solutions." Compt. Rand. Acad. Bulg. Sci. 2(**26**) 243-246 (1972).

166. Oae, S., "The Organic Chemistry of Sulphur." Plenum Press 1977.